

# THE PROCEEDINGS OF THE PHYSICAL SOCIETY

VOL. 51, PART 1

2 January 1939

No. 283

## CONTENTS

	PAGE
PROF. A. V. HILL. The transformations of energy and the mechanical work of muscles . . . . .	1
E. E. WIDDOWSON. The relation between range and energy for the upper limits of $\beta$ -ray spectra . . . . .	19
A. NUNN MAY. The extinction of discharges in Geiger-Muller counters . . . . .	26
L. F. BATES and G. G. TAYLOR. Ferromagnetic compounds of chromium . . . . .	33
N. F. ASTBURY and L. H. FORD. The precision measurement of capacitance . . . . .	37
J. E. R. CONSTABLE. Transmission of sound between neighbouring rooms in a brick building . . . . .	53
A. K. SEN GUPTA. Rotational analysis of the ultra-violet bands of germanium monoxide . . . . .	62
G. W. BRINDLEY and P. RIDLEY. The characteristic temperature of magnesium oxide . . . . .	69
G. W. BRINDLEY and P. RIDLEY. An x-ray investigation of atomic vibrations in cadmium . . . . .	73
E. V. APPLETON, R. NAISMITH and L. J. INGRAM. The critical-frequency method of measuring upper-atmospheric ionization . . . . .	81
S. CHAPMAN. The atmospheric height distribution of band-absorbed solar radiation . . . . .	93
T. L. ECKERSLEY and G. MILLINGTON. The limiting polarization of medium waves reflected from the ionosphere . . . . .	110
J. H. PIDDINGTON. The origin of radio-wave reflections in the troposphere . . . . .	129
M. V. WILKES. Theoretical ionization curves for the E region . . . . .	138
L. J. COLLIER, W. S. STILES and W. G. A. TAYLOR. The variation with temperature of the electrical resistance of carbon and graphite between 0°C. and 900°C. . . . .	147
R. W. POWELL and F. H. SCHOFIELD. The thermal and electrical conductivities of carbon and graphite to high temperatures . . . . .	153
S. WHITEHEAD and W. HACKETT. Measurement of the specific inductive capacity of diamonds by the method of mixtures . . . . .	173
Reviews of books . . . . .	191

Price to non-Fellows 7/- net; post free 7/5

Annual subscription 35/- post free, payable in advance

Published by

THE PHYSICAL SOCIETY

1 Lowther Gardens, Exhibition Road  
London, S.W.7

Printed at

THE UNIVERSITY PRESS, CAMBRIDGE

**THE PHYSICAL SOCIETY****OFFICERS OF THE SOCIETY, 1938-39:****President:**—A. FERGUSON, M.A., D.Sc., F.Inst.P.**Hon. Secretaries:**W. JEVONS, D.Sc., Ph.D., F.Inst.P. (*Business*).J. H. AWBERY, B.A., B.Sc., F.Inst.P. (*Papers*).

Office of the Society:—1 Lowther Gardens, Exhibition Road, London, S.W.7.

**Hon. Foreign Secretary:**—Prof. O. W. RICHARDSON, M.A., D.Sc., F.R.S.**Hon. Treasurer:**—C. C. PATERSON, O.B.E., D.Sc., M.I.E.E., F.Inst.P.**Hon. Librarian:**—J. H. BRINKWORTH, D.Sc., A.R.C.S., F.Inst.P.**Editor of the Proceedings:**—Capt. C. W. HUME, M.C., B.Sc.,  
284 Regent's Park Road, Finchley, N.3.**Assistant Secretary:**—Miss J. I. DENNIS.

All communications, other than those to the Editor, should be sent to the office of the Society, viz. 1 Lowther Gardens, Exhibition Road, London, S.W.7.

**INSTRUCTIONS TO AUTHORS**

**NOTE.** The acceptance of a paper for publication in the Proceedings rests with the Council, advised by its Editing Committee. The high cost of printing renders it imperative to exclude matter that is not novel and not of importance to the understanding of the paper.

Authors offering original contributions for publication in the Proceedings should observe the following directions; failure to comply with these may cause considerable delay in publication.

**Manuscript.**—A clear and concise style should be adopted, and the utmost brevity consistent with effective presentation of the original subject-matter should be used. The copy should be easily legible, preferably typewritten and double-spaced. It should receive a careful final revision before communication, since alterations are costly when once the type has been set up. Mathematical expressions should be set out clearly, in the simplest possible notation.

**References.**—In references to published papers the author's initials and name followed by the title of the journal in italics, volume, page and year should be given thus: *Proc. Phys. Soc.* 43, 199 (1931). The abbreviations given in the *World List of Scientific Periodicals* should be employed.

**Drawings and tables.**—Diagrams must be carefully drawn in Indian ink on white paper or card. Their size and thickness of line must be sufficient to allow of reduction. *Lettering and numbering should be in pencil*, to allow of printing in a uniform style. The number of diagrams should be kept down to the minimum. Photographs of apparatus are not ordinarily accepted. Data should in general be presented in the form of either curves or tables, but not both. Footlines descriptive of figures, and headlines indicative of contents of tables, should be supplied. *Sheets should not be larger than foolscap*.

**Abstracts.**—Every paper must be accompanied by an abstract in duplicate, brief but sufficient to indicate the scope of the paper and to summarize all novel results.

**Proofs.**—Proofs of accepted papers will be forwarded to authors. They should be returned promptly with errors corrected, but additions to or other deviations from the original copy should be avoided.

**Reprints.**—Fifty copies of printed papers will be supplied gratis. Extra copies may be purchased at cost price.

**Contributions by non-Fellows.**—Papers by non-Fellows must be communicated to the Society through a Fellow.

**Republication.**—Permission to reproduce papers or illustrations contained therein may be granted by the Council on application to the Hon. Secretaries.

ELECTRICAL MEASURING  
INSTRUMENTS  
OF THE HIGHER GRADES

TURNER

ERNEST TURNER  
ELECTRICAL INSTRUMENTS  
LIMITED  
CHILTERN WORKS  
HIGH WYCOMBE  
BUCKS.

Telephone: High Wycombe 301  
Telegrams: Gorgeous, High Wycombe

AN IMPORTANT NEW BOOK

**ULTRASONICS**

AND THEIR SCIENTIFIC AND TECHNICAL APPLICATIONS

**By Dr. LUDWIG BERGMANN***Professor of Physics in the University of Breslau*

The subject of ultrasonics (or supersonics)—the study of material vibrations of a frequency of 20,000 to 2,000,000 per second—is one of great interest, with many applications in various branches of science and technology. Until the publication of this book the literature of the subject was scattered through some hundreds of issues of scientific and technical journals.

Dr. Bergmann's book, though very comprehensive, is not too heavy or detailed, and provides just such an account as was needed of the present situation in ultrasonic research and its applications. In all cases references are given to the original source, and the bibliography has been brought right up to date. The English translation is by Dr. H. Stafford Hatfield.

*With numerous illustrations and text figures. Price 16s. net.*

G. BELL AND SONS, LTD., PORTUGAL STREET, LONDON, W.C.2

**TELCON METALS**

MAGNETIC  
ALLOYS

RESISTANCE  
ALLOYS

MUMETAL	Highest permeability alloy commercially produced.
RADIOMETAL	Lowloss alloy with high incremental permeability.
RHOMETAL	Magnetic alloy suitable for higher audio and carrier frequency apparatus.
2129 ALLOY	High permeability alloy giving effective magnetic screening with economy.
PYROMIC	High grade nickel-chromium alloy for resistances at high temperatures.
CALOMIC	Nickel-chromium-iron electrical resistance alloy.

TELCON ALLOYS are produced under close metallurgical supervision and have guaranteed characteristics. Brochure and full technical data on request.

**THE TELEGRAPH CONSTRUCTION & MAINTENANCE CO. LTD.**

Works: TELCON WORKS, GREENWICH, S.E.10

Telephone: GREENWICH 1040

Head Office: 22 OLD BROAD ST., E.C.2

Telephone: LONDON WALL 3141

# THE PROCEEDINGS OF THE PHYSICAL SOCIETY

---

VOL. 51, PART I

1 January 1939

No. 283

---

## THE TRANSFORMATIONS OF ENERGY AND THE MECHANICAL WORK OF MUSCLES

*The twenty-third Guthrie Lecture, delivered 11 November 1938*

BY PROF. A. V. HILL, F.R.S.

IT gave me unusual pleasure to accept the invitation of the Physical Society to deliver this 23rd annual Guthrie Lecture. A personal pleasure, since the invitation, and the honour it signifies, were one more—and a very special—sign of the friendliness which I have so often experienced from your Society and its members: a scientific pleasure, since it gave one the opportunity of presenting in physical terms, for your consideration and criticism, some new and strikingly simple relations which have lately appeared in an old and apparently complicated subject. It will not seem to you strange that the discovery of those simple relations was preceded by a considerable improvement in experimental method and a long time spent in that improvement (figure 4 below); or that the apparent complexity was really due to an imperfect knowledge of the facts. That is the way in scientific progress. It is encouraging, however, to find once more, even in such uncompromising material as our own bodies are made of, that physical simplicity may be found if only we search for it patiently, with instruments and methods sufficiently well adjusted to the purpose.

A philosopher once remarked that the chief occupation of mankind is moving things about: he might have added, "or holding things in place". Both occupations are functions of the muscular system, both require the continual transformation of energy. In the dynamic process of moving things chemical energy is transformed partly into mechanical work, partly into heat: in the static process of holding things in place chemical energy is transformed only into heat. Muscle is by far the most important agent in the animal body for transforming energy: we shall discuss to-day the mechanical work which a muscle performs and the energy which it uses; and we shall see that the study of these can throw considerable light on the nature of the biological mechanism.

There are many kinds of muscle, the voluntary muscles which move the limbs and other parts of the body, the heart which circulates the blood, the involuntary muscles which perform a variety of functions—for instance in digestion or excretion

—and are outside the conscious control of the animal. All of these muscles consist, as to 80 per cent of water, as to the remainder chiefly of protein, but also of salts, carbohydrates and various chemical substances. Much has been learnt in recent years about the chemical processes occurring in muscle and the enzymes which catalyse them; but the story is complex and as yet by no means clear, and its details are, for the present purpose, irrelevant. All we need to know is that muscle is liberally supplied with oxygen by diffusion from its blood vessels, that it contains an ample supply of fuel for oxidation, and that a variety of chemical reactions are known to occur in it during activity to provide energy for the work it does and the heat it gives out.

The mechanical activity of muscle resulting from stimulation, namely, shortening or the development of an external force, is probably associated with alterations in the mutual relations of an ordered array of protein molecules. A comparison of the molecular patterns of resting and of active muscle, by modern physical methods, should throw much light on the mechanism of muscle. That remains, however, largely a matter for future achievement: though research may be guided by the relationships which we are later to discuss.

The anatomical unit of voluntary muscle is the single fibre, a long thin cylinder about  $50\mu.$  in diameter, to which comes a nerve fibre conveying impulses which cause it to contract. With the nature of those impulses we are not now concerned: it is sufficient that their action can be imitated electrically, in all significant respects, by short pulses of current, for instance by condenser discharges, applied directly to the muscle. When a muscle fibre is stimulated by a single shock it contracts and relaxes again: with a succession of shocks at a sufficient but not too high a frequency, it remains contracting until the succession of shocks, the stimulus, ends. A contracting muscle shortens and does work if its load is not too great: otherwise its tension rises and remains up until the stimulus ends.

At rest a muscle uses oxygen and gives out heat at a very low rate depending on its temperature. During activity it uses energy at a high rate, part of the energy appearing as work if the mechanical conditions allow, the larger fraction, however, as in other engines, as heat. The rate at which energy is liberated is not constant, but depends on how fast the muscle is shortening and on how much work it is doing: in fact, as we shall see, the rate of energy liberation depends on the load.

The work done by a stimulated muscle is due entirely to its capacity for shortening under a load. A change of volume does occur, but this is so small that it has no significant mechanical effect. A very important characteristic of muscle is the way in which the speed of shortening, and the rate of doing work, depend on the load. When the load is great the speed of shortening is low, when the load is small the speed of shortening is high, with zero load the muscle attains a certain limiting speed which will be referred to later. When a muscle contracts at constant length it exerts a certain force which is known as the isometric tension: with loads greater than this it lengthens, faster the greater the load, until at a certain limiting load it "gives" or "relaxes", just like a wire stressed beyond its elastic limit.

Consider a contraction steadily maintained by a series of shocks of frequency

high enough to give complete fusion of the individual responses. Let us vary the load and determine experimentally, in different contractions, how the speed of shortening depends on the load. It is very important, for simplicity in interpreting the results, that the load should be constant, that it should demand a constant force in the muscle to overcome it, whatever the velocity of acceleration. This is because the contractile part of the muscle, as we shall see, has in series with it an elastic part which instantly alters its length if the load on it changes. Constancy of load requires that the lever system used for applying the load should be without friction and without inertia. Friction can be sufficiently avoided by the use of miniature ball-bearings (R.M.B.): inertia by the use of the classical isotonic lever, consisting

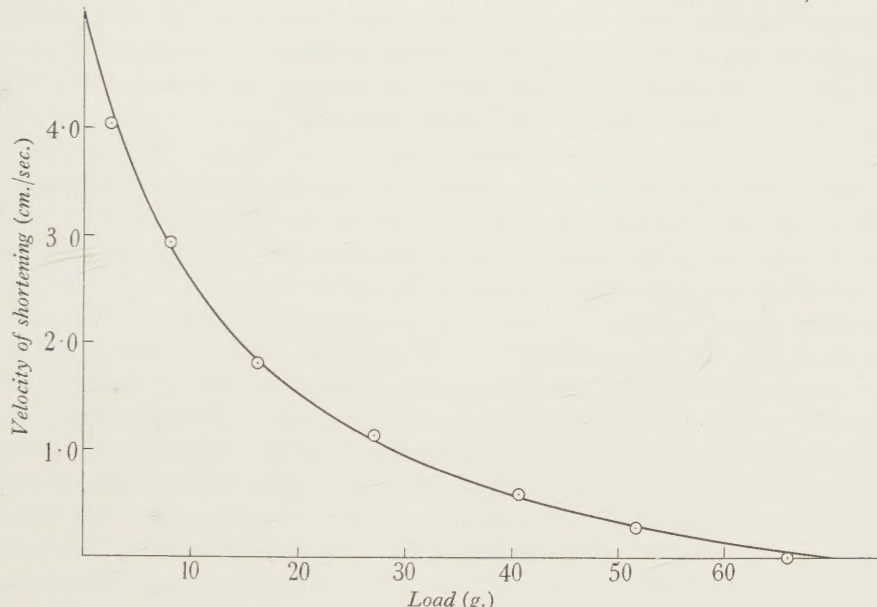


Figure 1. Relation between speed of shortening and load in isotonic contraction of frog's muscle at  $0^{\circ}\text{C}$ . Circles, observed points; curve calculated from the characteristic equation

$$(P+a)(v+b)=(P_0+a)b,$$

where  $P$  is load,  $v$  is velocity,  $P_0$  is isometric tension and  $a$  and  $b$  are constants.

of a thin metal strip with a load hung very close to the axis. At the speeds with which we are concerned the work done by a muscle shortening against an isotonic load of this kind is all used in lifting the load, no significant part of it appears as kinetic energy in the lever system.

In a given contraction, if the load is constant the speed of shortening is constant also (see figure 8 below): this is not true if the muscle shortens more than a certain distance, but that need not be exceeded, and we want to avoid complications. The speed is simply measured from the slope of a record on a drum. The relation between load and speed of shortening is shown in figure 1. It seems natural enough at first that the speed should be greater the less the load. This is not so simple, however, when we come to analyse it. We are apt to think in terms of our muscular sense, and nearly always in ordinary life a greater load is associated with a greater inertia.

If a contracting muscle behaved like a long stretched spring, an analogy which jumps to the mind at once, it would naturally give a greater velocity to a smaller mass: the acceleration, however, not the velocity, would then at first be constant. In the actual experiment, moreover, the load is without appreciable inertia, and the simple analogy of the stretched spring fails. If we wish to stick to the spring as a model it must be one possessing viscosity, a damped spring in which that part of its tension which is not overcoming external force is used in overcoming internal resistance. Then, with a greater external load, less force would be available internally for producing a change of form, and the velocity of shortening would be less.

This modified analogy of the damped elastic body has dominated current views of muscles for some time. In its simplest form it required that the velocity of shortening should increase linearly as the load decreased. Let  $P_0$  be the tension of the spring, the maximum force exerted at zero speed,  $kv$  the viscous resistance to shortening with velocity  $v$ , and  $P$  the load: then

$$P_0 = P + kv.$$

This linear relation is not the one which is found experimentally. Presumably in the rather complex heterogeneous system of muscle the viscous resistance was not simply proportional to the velocity, but to some function of it: for example, as we shall see, to  $v/(v+b)$ , where  $b$  is a constant.  $v/(v+b)$  increases with, but not as fast as, the velocity. Again, the viscosity, if it be viscosity, is present only to a very minor degree in resting muscle, as is easily found by stretching and releasing it. Presumably the "viscosity", like the tension, was a property of the active state: stimulation produced in the muscle a new elastic system, of shorter natural length, and one endowed with considerable hysteresis. Strong evidence indeed existed, for example changes of double refraction, of a molecular pattern in muscle, which altered in activity, and the hysteresis observed might be due to the time taken by the molecules in forming new patterns when the muscle shortened and its external form was changed. Until the new pattern was complete the external force was not fully developed: in changing form at a constant speed, the force was diminished by a constant amount proportional to  $v/(v+b)$ .

This then was the picture. In the resting state a muscle is an elastic and slightly viscous body, with a natural length  $l_r$ . In the active state it suddenly becomes a new elastic and highly viscous body, with a natural length  $l_a$  considerably less than  $l_r$ . It develops a force therefore and tends to shorten. The active state is due to a kind of crystalline pattern in the protein molecules tending towards a shorter length, and the apparent viscosity is the result of the time lag of the molecules in finding new places when the external shape of the muscle alters: until they find new places the full external force cannot be developed. This view of the matter must, I think, be replaced by quite a different and a more exact one, based on considerations of energy regulation, which we will discuss. It is possible, however, that in some respects, and for the case of some muscles, we may have to return to it.

The experimental relation between load and speed is rather exact and can be expressed by a simple equation

$$(P+a)(v+b) = \text{a constant},$$

where  $P$  is load,  $v$  is velocity of shortening, and  $a$  and  $b$  are constants to which we will refer later. The curve is a rectangular hyperbola with axes at  $P = -a$ ,  $v = -b$ . If  $P_0$  be the isometric tension, for which  $v = 0$ , the equation becomes

$$(P+a)(v+b) = (P_0+a)b.$$

This can be written

$$P_0 = P + (P_0 + a) \frac{v}{v+b},$$

which, by analogy with the equation,

$$P_0 = P + kv,$$

suggests, on the hypothesis of the damped spring, that the internal resistance is proportional not to the velocity but to  $v/(v+b)$  as referred to earlier. We shall see, however, that quite a different explanation of the characteristic equation can be given, one based on the manner in which the energy output of the muscle is regulated. This explanation has the convincing evidence in its favour that the constants  $a$  and  $b$  can be determined independently by measuring the heat of shortening and the rate of energy liberation with a thermopile and galvanometer, and the values so determined prove to be the same as those found by fitting the equation to the purely mechanical observations of load and speed.

Let us then turn to the heat-measurements. Figure 2 is a drawing of the thermopile which has made these particular measurements possible. It is a masterpiece of Mr A. C. Downing's skill. Its particular virtue is its thinness, giving it extreme quickness in taking up the temperature of the muscle and an almost negligible heat capacity. Quickness is necessary since the processes which we wish to follow are very rapid. The thermopile has to lie directly in contact with the muscle, so must be effectively insulated: after soaking in salt solution for hours its mica and bakelite, only  $18\mu$ . thick on each face, still maintain a resistance of many megohms between muscle and circuit. It has 42 couples of constantan-manganin,  $15\mu$ . thick, in a length of 14 mm., and it gives 1.56 mv. per  $1^\circ$  C. It has a special provision of dummy couples at each end, so that when the muscle shortens, or relaxes, no part of it shall come on to the active thermopile which has not previously been subject to the same thermal conditions, particularly of heat loss by conduction, as exist, in the part of the muscle already on the thermopile. It must be remembered that a muscle is always producing heat, and a difference of thermal conduction means a difference of temperature in the part affected. By these dummy couples serious errors are avoided: indeed this simple trick of protecting the active part of the thermopile from muscle of a different temperature coming on to it during shortening has been the chief factor in obtaining the present apparently rather accurate results. The thinness of the thermopile has given the necessary speed of response—80 per cent of the full e.m.f. is produced within 12 msec. of the rise of temperature causing it—and the protection of its active elements against temperature differences in the muscle moving over them has made the results reliable.

If, however, justice is to be done to a rapid thermopile it must be connected to a rapid galvanometer, one with a natural period, say, of 50 msec. or less. Now no galvanometer with such a period has—or can have—anything like the required

sensitivity: about 20 times the deflexion is required. The obvious suggestion of amplification by thermionic valves can be put aside, since the temperature changes are small and we have to read to something less than  $0.1 \mu\text{v}$ .: no existing method of amplification is steady to that degree. A more sensitive thermopile, with a much larger number of couples, might conceivably be built, not by soldering where the limit has already been nearly reached, but perhaps by electrodeposition, or sputtering, of the active metals: a twentyfold increase of sensitivity, however, in

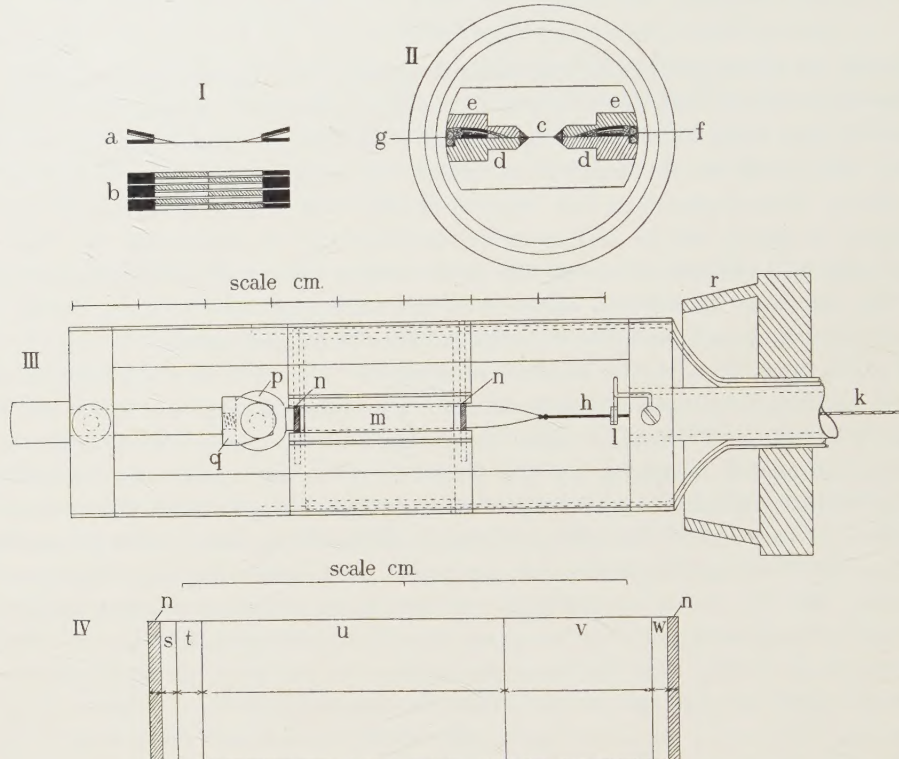


Figure 2. Thermopile for muscle heat. I (a) end view and I (b) side view of element, unmounted. II, end view of element mounted: hot junctions in middle of groove. III, complete instrument with pair of muscles, *m*, clamped at *p* and connected by thread and chain (*h*, *k*) to recording lever: *n*, stimulating electrodes. IV, enlarged view of portion of element in groove: *u*, 42 insulated couples, protected by *v*, 20, and *t*, 3 insulated dummies.

this way, is not at present within sight. A resistance thermometer can be shown to be much less effective than a thermopile. The only thing to do is to choose a galvanometer of suitable period and then to magnify its deflexion.

Fortunately this can be done by photoelectric means, the light returning from the mirror of the primary galvanometer  $G_1$  falling upon a differential photo-cell and producing a current which deflects a secondary galvanometer  $G_2$ , figure 3. An adjustable fraction of the current from the photo-cell is fed back into  $G_1$  in order to make it quicker and more stable: by this the sensitivity can be set to any value required; and any unnecessary sensitivity is not wasted but used to improve the

speed and steadiness of the system. The method works well and provides the sensitivity required. The deflexion resulting from a sudden rise of temperature of the muscle is nearly complete in 50 msec., figure 4.

Hitherto photographic recording has been used. With the unlimited amplification, however, which is possible with a differential photo-cell the secondary galvanometer can be of the pointer type, and a system is being constructed by which the

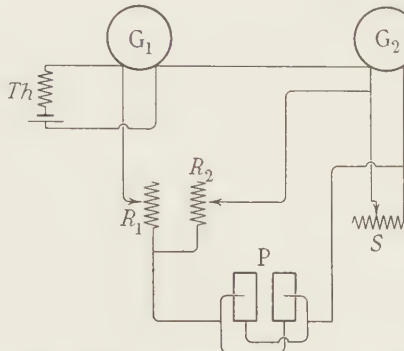


Figure 3. Circuit of coupled galvanometers.  $Th$ , thermopile, connected to primary galvanometer, throwing light on to differential photo-cell  $P$ .  $R_1, R_2$ , resistances for adjusting feed-back to  $G_1$ .  $G_2$ , secondary galvanometer, magnifying movement of  $G_1$ .  $S$ , shunt to  $G_2$ , for adjusting damping.

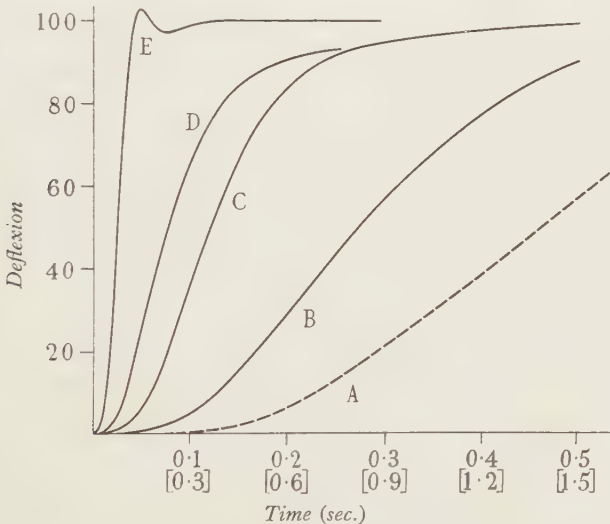


Figure 4. To illustrate speed of recording muscle heat, after short or instantaneous heating.  
A, 1920 (lower time scale); B, 1933; C, 1933; D, 1937; E, 1938.

movements of the primary galvanometer will be recorded, after amplification, on a smoked revolving drum. This arrangement may be useful whenever small e.m.f.s. too small for ordinary amplification, have to be recorded at high speed.

In figure 5 (A) the lines  $A$ ,  $E$  and  $K$  are heat deflexions produced by a muscle contracting isometrically—i.e. without shortening. The rate of heat production is greater at first and in a second or two becomes nearly constant. The deflexions  $L$ ,

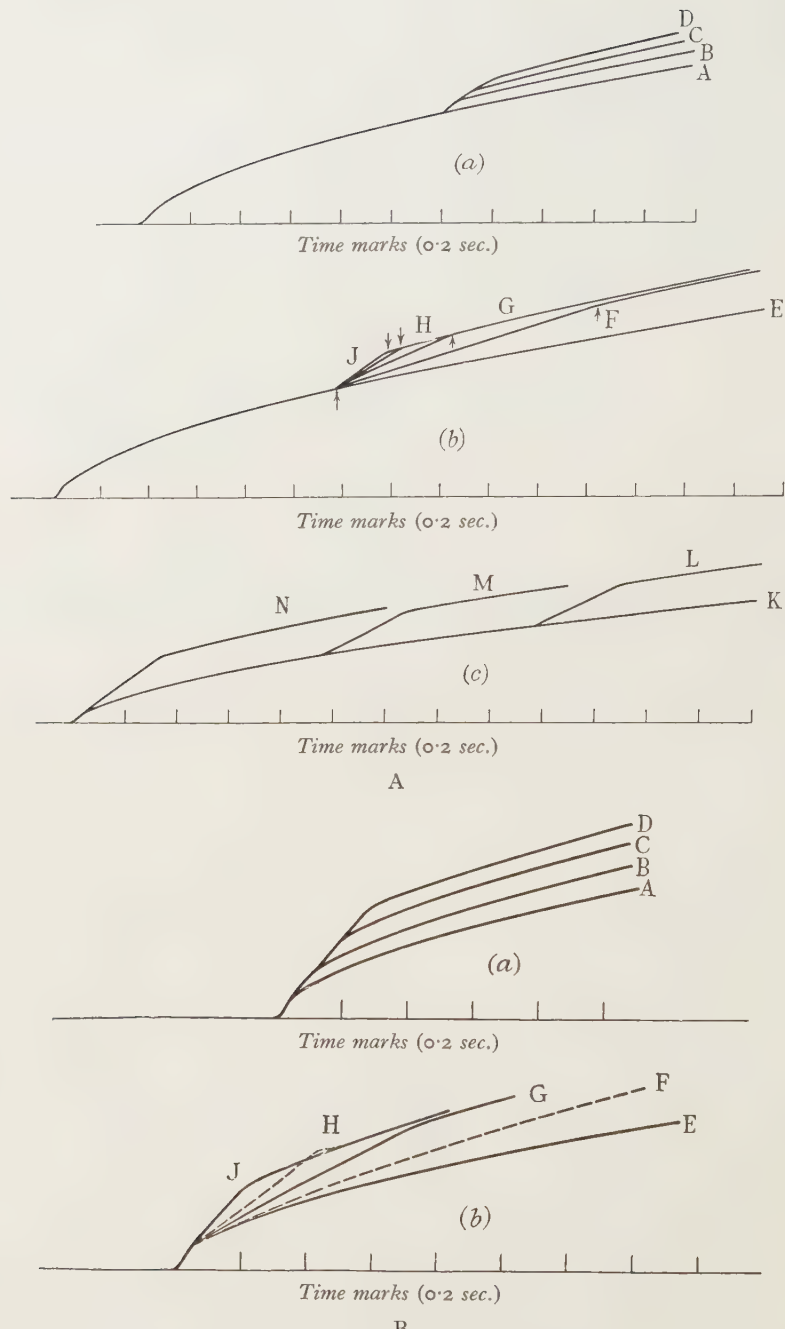


Figure 5. Heat deflexions during isometric and isotonic contractions. (A) *A*, *E*, *K*, isometric *N*, *M* and *L*, release of 9.1 mm. under small load, at start, at 0.9 sec. and at 1.8 sec. *B*, *C* and *D*, shortening under small load through 2, 3½ and 5 mm. *J*, *H*, *G* and *F*, shortening 5.2 mm. against 3, 6, 14 and 25 g. load. (B) *A* and *E*, isometric. *B*, *C* and *D*, shortening under small load through 3.4, 6.5 and 9.6 mm. *J*, *H*, *G* and *F*, shortening 6.5 mm. under loads of 2, 13, 24 and 32 g.

$M$  and  $N$  were given when the muscle was allowed to shorten rapidly 9 mm. under a small load of 3 g. The beginning and the end of shortening are clearly shown by the angles in the curves. Extra heat is produced when shortening is permitted, and the amount of it is the same whenever the shortening occurs. The deflexions  $B$ ,  $C$  and  $D$  were produced by shortening under a small load through various distances, 2,  $3\frac{1}{2}$  and 5 mm. Careful measurement in such cases shows that the extra heat is directly proportional to the amount of shortening. The deflexions  $J$ ,  $H$ ,  $G$  and  $F$  were due to shortening 5·2 mm. against various loads, 3, 6, 14 and 25 g. The greater the load the slower the shortening and the appearance of the extra heat, but careful measurement now shows that the total extra heat is the same whatever the load. With a greater load, of course, correspondingly more work is performed: but the extra heat for shortening is the same. A similar set of effects if shown in figure 5 (B), for shortening at the start. We see, therefore, that the process of shortening as such causes an extra liberation of heat, that this heat is proportional to the amount of shortening, and that it is independent (*a*) of the moment at which shortening occurs; (*b*) of the load, the work done, or the speed of shortening; and (*c*) as has been found in experiments made on the same muscle at different temperatures, after allowing for the alteration of force exerted, of the temperature.

Let  $x$  be the distance which a muscle shortens; then the shortening heat, expressed in dynamical units, is  $ax$ .  $a$  is found to bear a very constant relation to  $P_0$ , the maximum force which the muscle can exert in an isometric contraction: the mean value of  $a P_0$  is 0·25. It is as though the shortening of the muscle were resisted by a constant frictional force equal to one-quarter of the isometric tension, the work done against this resistance being degraded into heat. The maximum force of frog's muscle is about 2 kg./cm.<sup>2</sup> of fibre cross-section, so the apparent resistance is about 500 g. In human muscle the maximum force is several times as great, so the apparent resistance to shortening is probably 1 or 2 kg./cm.<sup>2</sup>, a fairly considerable quantity. The shortening heat may require delicate thermal methods for its detection and measurement, but if we express it in dynamical units we see how important it really is.

When a muscle shortens, then, it gives extra heat  $ax$ , but it also does work  $Px$ , where  $P$  is the load. The total extra energy therefore is  $(P+a)x$ . For very slow shortenings  $P$  may be nearly equal to  $P_0$ , the isometric tension, so the work may be nearly four times the shortening heat. For rapid shortenings  $P$  must be small, and the work becomes small compared with the shortening heat. The rate at which extra energy is liberated in shortening is  $(P+a) dx/dt$  or  $(P+a)v$ , and a very simple and striking relation is found experimentally to exist between this and the load, as shown in figure 6. The rate of extra energy liberation is a linear function of the load,  $(P+a)v = b(P_0 - P)$ , where  $b$  is a constant of the dimensions of a velocity, and in frog's muscle at 0° C. is about  $\frac{1}{3}$  of the muscle's length per second. Unlike  $a/P_0$ ,  $b$  is considerably affected by temperature, being about doubled by a rise of 10° C.

Now the equation  $(P+a)v = b(P_0 - P)$  may be written,

$$(P+a)(v+b) = (P_0+a)b,$$

and this is the very equation which we found earlier to describe the relation experimentally observed between load and speed. The constants  $a$  and  $b$  are the same whether we determine them directly by measurements of heat and work, or indirectly by fitting the equation to the experiments on load and speed. Thus the form of the relation, given in figure 1, between speed of shortening and load requires no special hypothesis of viscosity or hysteresis to explain it: it is an inevitable consequence of the two facts, independently found by measurement of heat and work, (*a*) that shortening as such is accompanied by a proportional liberation of heat, which is independent of all other conditions; and (*b*) that the rate at which energy is liberated decreases linearly with the load on the muscle, as the load is increased.

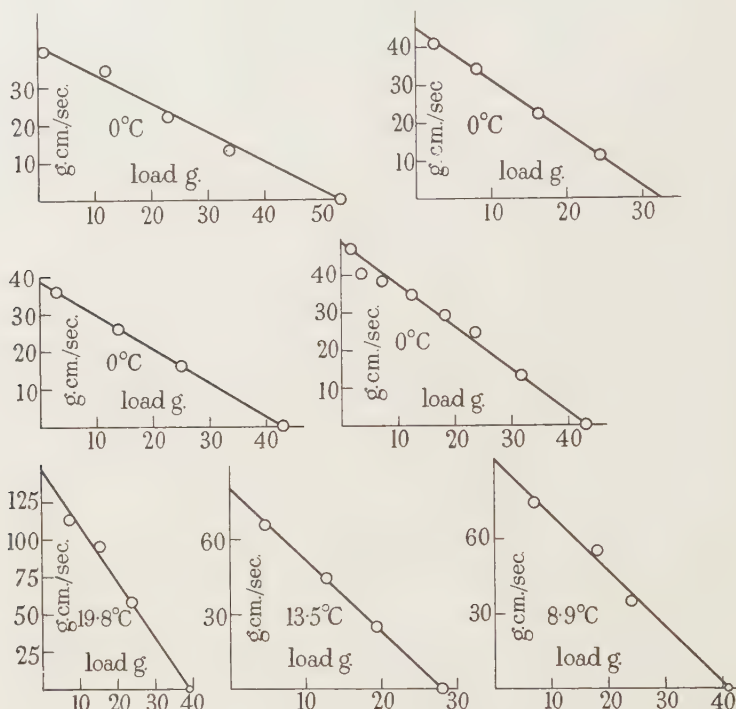


Figure 6. To show rate of total energy liberation (in excess of isometric) as function of load during muscular shortening. Seven consecutive experiments.

Reasonable and attractive, therefore, as the viscosity hypothesis appeared it is found to be completely unnecessary, and we are left with the problem of explaining (if we can) (*a*) the heat of shortening and (*b*) the decrease of total energy rate with increasing load on the muscle. We will return to that later.

We have dealt so far with the case of a muscle shortening under a load less than the isometric tension. What happens when the load is greater? The equation  $(P+a)v = b(P_0 - P)$  suggests that if  $P$  is greater than  $P_0$  then  $v$  will be negative: this is correct (see figure 7). If  $P$  is not too great the muscle lengthens slowly and the

work done by the falling load does not reappear as heat. The extra energy rate ( $P+a$ )  $v$  becomes negative, and the total energy *given out* by the muscle is less than in an isometric contraction (figure 7 B: curve D). If  $P$  is too great the extra energy rate ( $P+a$ )  $v$  should become large and negative, and so might reduce the *total* energy rate too nearly to that of the resting muscle: the contractile state, depending

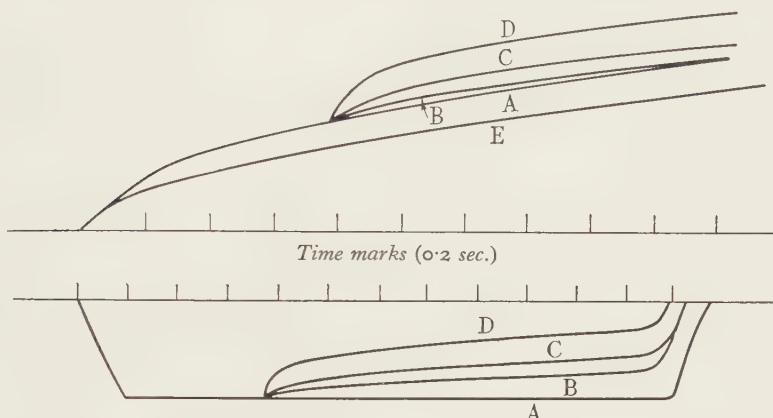


Figure 7 (A). Upper, heat deflexions; lower, mechanical records; during isometric contractions and during lengthening under various loads. E, isometric (long), 40 g. A, shortening under 2.5 g., then isometric (short). B, C, D, lengthening under 52, 57 and 63 g.

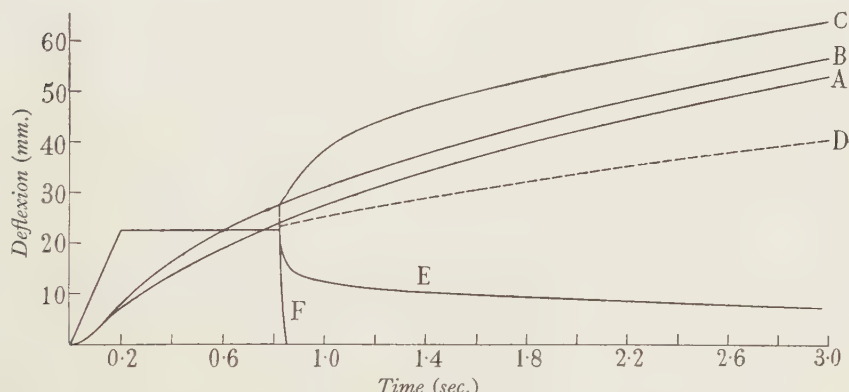


Figure 7 (B). Heat deflexions: A, isometric (long); B, isotonic, small load, then isometric (short); C, isotonic, small load, then lengthening under 59 g. D, net energy liberated during lengthening, i.e. (heat)-(work). E, mechanical record: note give, then slow lengthening. F, sudden give under 68 g.

on a continual liberation of energy, might no longer be maintained. This is what we find: with too great a load the muscle gives, just as it does in relaxation when the stimulus ends, and the work of the load is turned into heat. For technical reasons the experiments on lengthening are very difficult, and at present an exact quantitative parallel cannot be drawn: qualitatively, however, the relations which have been established for shortening muscle seem to apply, with the necessary change of sign,

to lengthening muscle, showing that the processes involved are, to that extent at least, reversible. Had viscosity really been the basis of the relation between load and speed that reversibility could not have been found.

We have considered so far the case of a contraction continuously maintained: it is interesting to see what happens when the stimulus ends and the muscle relaxes. In figure 8, *A* is the heat record of an isometric contraction due to a stimulus of 0.6 sec. duration. *B* is the heat record and *b* the mechanical record of an isotonic contraction due to the same stimulus in which 39 g. was raised and held up, so that in relaxation no work was done on the muscle. *C* and *c* are the heat and mechanical

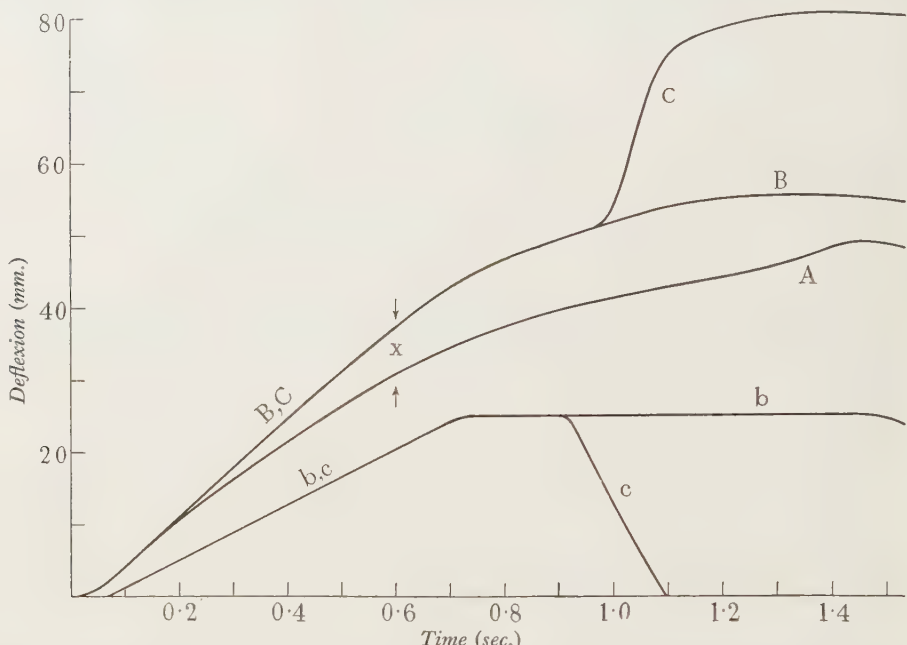


Figure 8. To show heat deflexion during absorption of mechanical energy in relaxation. 0.6 sec. stimulus. *A*, isometric. *B*, isotonic, 39 g. load, all but  $3\frac{1}{2}$  g. held up in relaxation. *C*, isotonic, 39 g. load, bearing on muscle in relaxation. *b* and *c* corresponding mechanical records.

records of the same isotonic contraction in which the load was not held up but allowed to bear on the muscle during relaxation. The work done by the muscle in contraction was turned into heat in relaxation, and the excess of *C* over *B* is found in fact to be equal to the work. In this particular case the work was 30 per cent of the whole energy given out by the muscle. Apparently the process of relaxation is entirely irreversible: the muscle just gives under the load, as a wire gives under a tension beyond its elastic limit, and the work of the load is turned direct into heat.

It will occur at once to an engineer that the observed relation between load and speed, figure 1, implies the existence of an optimum load, one with which the power output of the muscle is greatest. The rate of doing work is  $Pv$ . Using the characteristic equation this becomes  $bP(P_0 - P)/(P + a)$  which can be shown to be a maximum

when  $P/a = \sqrt{(1+P_0/a) - 1}$ . In the frog  $P_0/a = 4$ , so that  $P/P_0 = 0.31$ : that is, the maximum power output occurs with a load about  $\frac{3}{10}$  of the maximum force which the muscle can exert. It is possible that in other muscles  $P_0/a$  will not be exactly 4, but it can be shown that for variation of  $P_0/a$  from 3 to 7 the optimum value of  $P/P_0$  changes only from 0.34 to 0.27. Thus in any practical case the optimum load is about  $\frac{3}{10}$  of the maximum. It would be very interesting to find out whether tools and devices by which work is done, such as spades and oars, have been designed empirically for a load which is near the optimum in this respect.

Maximum horse power, however, is only one factor in a motor: economy is equally important. In muscle the limit to a maintained energy output is set by the oxygen supply through the lungs and circulating blood: if the power expended is greater than corresponds to the maximum oxygen supply, fatigue and exhaustion set in. Hence it is interesting to inquire what load gives the greatest efficiency, the greatest ratio of work to energy. The dominant factors now are these: (a) apart altogether from shortening and doing mechanical work, the mere maintenance of a contraction requires energy, as is seen in the isometric heat deflexions of figure 5; (b) a greater load gives correspondingly greater work, but it results in a slower shortening which has to be maintained longer.

These factors act in opposite directions, and a balance must be struck between them. If the load is small the shortening is quick and little energy is then required to maintain the contraction; but little work is done. If the load is great the work is great too; but much energy is required to keep up the contraction throughout the long shortening involved. If we suppose, for simplicity, what is only a rough approximation, that the energy required to maintain a contraction is proportional to its duration; and if we assume that the stimulus is cut short so that the energy supply for maintenance of contraction is stopped as soon as shortening is complete; then we may write down the following equations:

$$\text{Work} = Px,$$

$$\text{Heat} = ax + kt,$$

where  $ax$  is shortening heat and  $kt$  is the energy required to maintain the contraction for time  $t$ .

Hence the efficiency  $E = (\text{work})/(\text{total energy})$

$$= Px / [(P+a)x + kt]$$

$$= Pv / [(P+a)v + k].$$

With the aid of the characteristic equation we can eliminate  $v$ , and obtain

$$E = 1 - \frac{(P_0+a)a}{P_0+a+K} \frac{1}{P+a} - \frac{(P_0+K)K}{P_0+a+K} \frac{1}{P+K-P},$$

where  $K = k/b$ .  $E$  is a maximum when

$$(P+a)/(P_0+K-P) = \sqrt{\left(\frac{P_0+a}{P_0+K}\right) \left(\frac{a}{K}\right)}.$$

Now in frog's muscle at 0° C. all the quantities involved are approximately known.

In the earlier stages of an isometric contraction  $k$  may be taken as about 180 g.-cm. of energy per g. of muscle per sec., or for a 1-cm. cube of muscle about 189 g.-cm. per sec.  $b$  is about  $\frac{1}{3}$  of the muscle-length per sec., i.e. 0.33 cm./sec. Hence  $K = k/b = 567$  g. For the same block of muscle  $a = 400$  g. and  $a/P_0 = 0.25$ . Substituting these we find, for the highest efficiency,  $P/P_0 = 0.46$ ; and the calculated value of the highest efficiency works out at 39 per cent. Values of the efficiency are obtained experimentally as high as 37 per cent, and these with loads from 0.4 to 0.5  $P_0$ . The agreement is good enough.

These efficiencies refer only to the initial process. A prolonged recovery process follows contraction, during which about as much energy is given out, as heat, as in the contraction itself. The overall efficiencies, therefore, are only about one-half of those referred to.

Apparently, therefore, the most efficient speed is somewhat less than that at which the greatest power is developed. The load for maximum efficiency is 46 per cent of maximum load: the load for maximum power is 31 per cent. Taking 39 per cent of maximum load, however, as a compromise, the calculated efficiency and the calculated power are both practically undiminished: the maxima involved are rather blunt. It is an amusing sidelight on the excellence of biological engineering that the maximum efficiency and the maximum power of a frog's muscle are so nearly obtained at the same speed. Similar experiments and calculations should be made on other muscles, and if possible on those of man: though, with the latter, very different methods will be required! I suspect that closely analogous results will be obtained.

The maximum speed of shortening also should be referred to: from the characteristic equation it occurs at zero load and is simply  $bP_0/a$ . Since  $P_0/a$  is usually about 4 the maximum speed of shortening is  $4b$ . With this, as in the isometric contraction, all the energy is turned into heat.

Having disposed of the damped elastic theory, involving the supposed viscosity, in favour of that involving energy regulation, we have regarded the muscle as being transformed very rapidly by a stimulus to an active state, in which its behaviour is defined by the characteristic equation with the appropriate constants. We have omitted as yet an important factor which must now be shortly considered, an undamped and inert series elasticity. If a muscle contracting isometrically, figure 9, be suddenly released, the tension will drop to zero if the release be of sufficient extent, and then will develop again only gradually, along a curve which is similar to that of the initial development of tension when the stimulus began. If, however, the release be less, not more (say) than 10 per cent of the muscle's length, the tension will not drop to zero but to some intermediate value from which it will redevelop as before. The muscle clearly consists of two parts in series, a purely contractile part governed by the characteristic equation, and a purely elastic part governed by ordinary elastic rules.

Consider now the form of the isometric contraction—which, so far as the contractile portion  $C$  of the muscle is concerned, is not isometric at all, since it has to stretch the elastic portion  $E$  in producing an external tension. The development of the contractile state, when the stimulus is applied, we regard as instantaneous:

it is certainly very quick.  $C$  finds  $E$  at first at zero tension, and begins to shorten rapidly and to stretch it out: the tension of  $E$ , however, rises as it is stretched, so the load on  $C$  increases and its speed of shortening correspondingly diminishes. Thus the development of tension proceeds at a continually decreasing rate, governed by the characteristic equation and the amount of series elasticity. The force  $P$  is related to the time  $t$  by an equation

$$-\log_e (1 - P/P_0) - \frac{P/P_0}{1 + a/P_0} = \frac{tb/c}{1 + a/P_0},$$

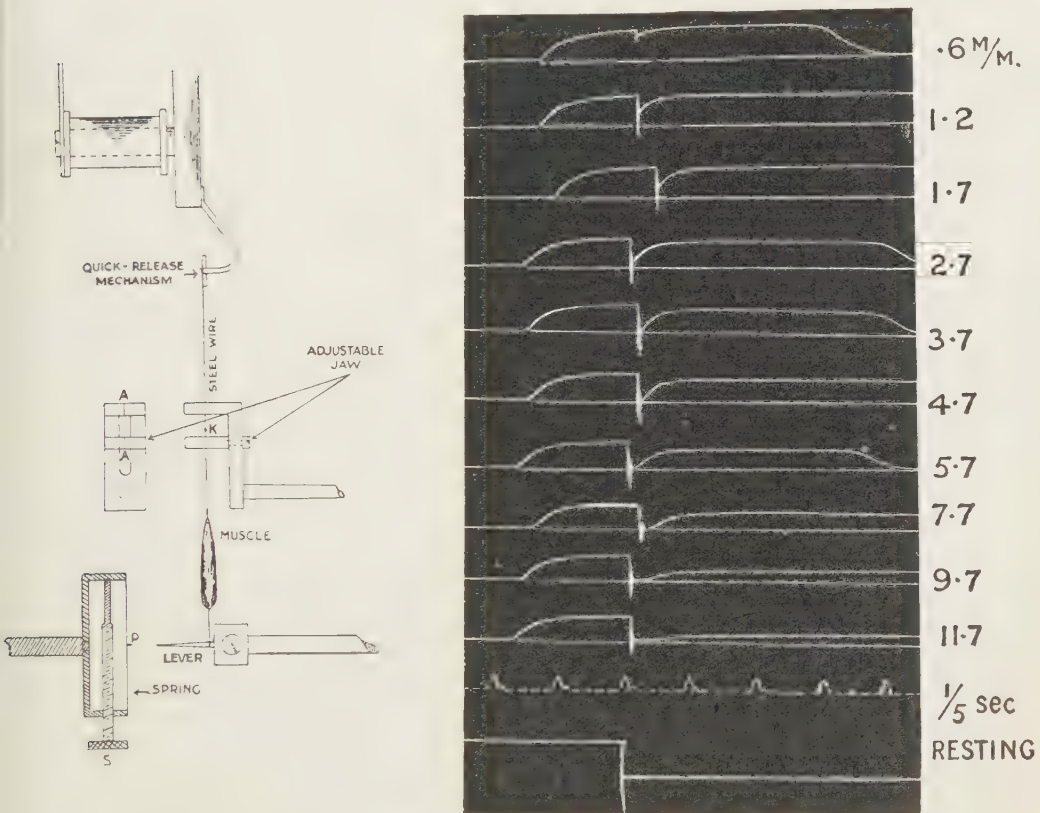


Figure 9. To illustrate method and result of quick release during isometric tetanus. Left, instrument. Right, tension records on moving drum. Note that for release less than 3.7 mm. the tension does not drop to zero: for more than 3.7 mm. it remains at zero for a finite time before it begins to redevelop.

where  $c$  is the amount of stretch of the elastic component under the full isometric tension. This equation, with the known values of  $a/P_0$ ,  $b$  and  $c$ , gives curves, figure 10, which closely represents those experimentally observed. There can be no doubt that the time taken for the tension to develop in an isometric contraction does not represent—as used to be thought—a lag in the development of the contractile state; but is occupied chiefly by the contractile portion shortening at a decreasing rate, as the tension in the elastic portion rises.

This series elasticity is of practical importance. Muscles, particularly mammalian skeletal muscles, are very powerful, and if they could exert their full force instantly against the inertia of the limbs damage would very probably result. Even as it is, in athletes, tearing of muscles, tendons and ligaments is not infrequent. With its series elasticity a muscle cannot instantly develop its full force: and while it is developing it the mass accelerated begins to move, and by the time that the muscle would have developed its full force the mass is moving fast enough to cause that force to be appreciably diminished.

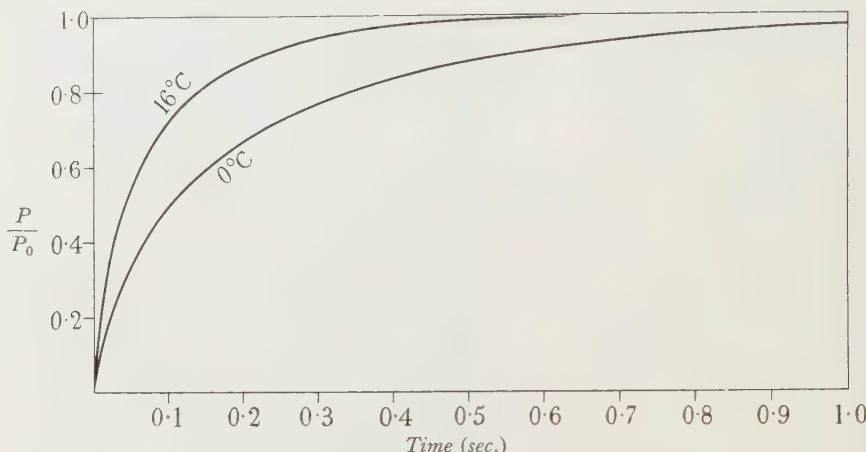


Figure 10. Calculated isometric contractions, assuming a contractile part, governed by the characteristic equation  $(P+a)(v+b)=\text{constant}$ , in series with an elastic part, and the usual values of the constants.

The elasticity acts, moreover, as a buffer against shocks: and it allows the muscle to accumulate a certain amount of potential energy in an isometric contraction and so to shorten suddenly, when required, through a limited distance, at very high speed. This potential energy has two very obvious signs on the heat records. In relaxation from an isometric contraction, the potential energy turns into heat and warms the muscle, like the falling load illustrated in figure 8, but less: a small upward hump *A*, figure 8, appears in the deflexion at the time when the tension is falling most rapidly. At the beginning of activity, on the other hand, all the heat records of isometric contractions, figure 5, show a rapid upstroke at first, much more rapid than the later deflexion. This represents the shortening heat of the contractile part of the muscle rapidly stretching the elastic part. In shortening we find extra heat produced and work done: the extra heat *ax* is apparent at once: the work  $P_0x/2$  appears as heat in relaxation. Since  $P_0/a$  is about 4 the latter should be about twice the former. Both effects can be exaggerated by including a spring in the attachment of the muscle to its recording lever: both can be diminished by making the attachments as rigid, and the tendons as short, as possible.

Let us return to our two chief problems, that of the nature of the shortening heat, that of the mechanism by which the rate of energy liberation is determined by the load. The shortening heat has been written  $ax$  g.-cm., where *a* is constant and

$x$  is distance shortened:  $a$  has necessarily the dimensions of force, and in frog's muscle at  $0^{\circ}\text{C}$ . it is about  $400\text{ g.-wt./cm}^2$  of muscle cross-section; it is natural to think of it as a constant resistance to shortening. It is difficult, however, to believe that if  $a$  were of a frictional nature it would not decrease with a rise of temperature: and experimentally it does not. Further, if it were, there should be a difference  $2a$  between the loads at which a muscle (i) just shortens and (ii) just lengthens:  $2a$  is a rather large quantity, certainly much larger than the difference in question, if it exists. Moreover, there is evidence, not yet quantitative, that the heat of lengthening is negative: so the resistance cannot be of a viscous or frictional character. It is probably best, therefore, not to think of  $a$  as a real force, but simply of  $ax$  as heat set free in shortening  $x$ .

Without a more concrete picture of the mechanism of muscle than we have at present it is probably not useful to speculate very far about the nature of the shortening heat; one or two analogies, however, may be pertinent. Consider the case of surface tension. This has a negative temperature coefficient, so that heat is given out when an area exhibiting surface tension contracts and does work. With an air-benzene surface, for example, the heat given out is calculated as about  $0.04\text{ g.-cm.}$  for each  $1\text{ cm}^2$  by which the area is diminished. We can imagine a  $1\text{-cm. cube}$  made up of 5000 films of substance *A* interleaved with 5000 films of substance *B*. If each interface had the same properties as one of air-benzene, the 10,000 of them together would give a shortening heat of  $10,000 \times 0.04$ , that is  $400\text{ g.-cm./cm.}$ : the same as frog's muscle. If we desired a molecular and not a thermodynamic analogy we might think of chemical affinities, or electrical attractions, satisfied, and heat given out, by the folding up of chains of muscle protein during shortening. When more is known about the spatial pattern of the protein molecules, and of their mutual relationships, it may be obvious why shortening causes a proportional liberation of heat: at present we can only guess.

The control exercised by the load on the rate of energy expenditure may be due to some mechanism as follows. Imagine that the chemical transformations associated with the condition of activity occur by passage through, or perhaps by the catalytic effect of, certain active points in the molecular machinery: and that when the tension in the muscle is high the affinities of more of these points are being satisfied by the attractions they exert on one another, and fewer of them are available to take part in chemical transformation. When the tension is low, less of these affinities are being involved in mutual attraction, and more of them are exposed to, or ready to take part in, chemical reaction. The rate at which chemical transformation would occur, and therefore at which energy would be liberated, would be directly proportional to the number of exposed affinities or catalytic groups, and so would be a linear function of the force exerted by the muscle, increasing as the force diminished. Other such schemes could easily be devised, by which the tension in the muscle fibre determined its rate of energy liberation. It would be impossible, again, to decide between them until we have a clearer idea, both of the spatial pattern of the molecular machinery and of the manner in which chemical energy is transformed in it into work and heat.

Some ten years ago, when Rutherford was President, I was reading a paper to the Royal Society. I had apologized for what I thought was a rather adventurous theory and he—in the cheery way we all remember—interposed “Don’t worry about it, Hill: the physicists can do much worse than that”. If I could I would produce a theory of the mechanisms of which I have spoken to-day and leave the members of the Physical Society to go one better—or one worse! But I do not believe that we have yet a sufficient basis for a theory. Physiology is not yet ripe for overmuch hypothesis. What is wanted still is a more precise and quantitative knowledge of the facts; and we have seen to-day how much more easily facts can be fitted together, once they are accurately known. Twenty-eight years ago, on this very day, on 11 November 1910, Langley, then Professor of Physiology at Cambridge, suggested, in a letter which I still have, that I should “settle down to investigate the variation in the efficiency of the cut-out frog’s muscle as a thermodynamic machine”. One year later, being very young, I wrote at the end of my first paper on that subject, the following grandiloquent sentence, which Langley, who did not usually like such things, allowed me to publish: “A complete investigation of these facts will give us more real insight into the nature of the muscular machine, and therewith of all living tissues, than any theories of contraction ever founded by ingenious minds upon insufficient knowledge.” It was provocative, and I know it provoked an old gentleman who believed that I must be referring to himself: and to-day perhaps I should write it more humbly. But, in spite of its grandiloquence, I still think that it is true, and I should not like now to fall under my own youthful condemnation by proposing a theory of contraction on evidence which is still inadequate.

# THE RELATION BETWEEN RANGE AND ENERGY FOR THE UPPER LIMITS OF $\beta$ -RAY SPECTRA

By E. E. WIDDOWSON, University College, Hull

*Communicated by Prof. L. S. Palmer, 31 May 1938. Read in title 14 October 1938*

**ABSTRACT.** The linear relation  $R = 0.460E_K - 0.226$ , connecting the maximum range  $R$  in g./cm.<sup>2</sup> with the Konopinski-Uhlenbeck upper limit  $E_K$  in Mv. for continuous  $\beta$ -ray spectra, is obtained from experimental results; and those results which show large deviations from it are discussed. The {range, energy} relation for electrons in lead, aluminium and air is obtained from quantum mechanical formulae, and is found to be linear in the region under consideration. Reasons for the differences between the theoretical and empirical relations are suggested.

## § 1. THE RELATION BETWEEN RANGE AND ENERGY FOR KONOPINSKI-UHLENBECK UPPER LIMITS

FEATHER<sup>(1)</sup> obtained the empirical relation  $R = aE + b$  ( $E > 0.7$  Mv.), where  $R$  is the maximum range in g./cm.<sup>2</sup>, and  $E$  is the upper energy limit in Mv., for continuous  $\beta$ -ray spectra;  $a$  and  $b$  being best represented by 0.511 and -0.091 respectively. This relation applies to the upper limits determined directly from the experimental data. Upper limits obtained by extrapolating a Konopinski-Uhlenbeck plot<sup>(2)</sup> are, in general, higher than those obtained directly, and it is of interest to obtain a similar linear relation connecting the maximum range and the Konopinski-Uhlenbeck upper limit.

The table gives results for those radioactive elements, emitting electrons or positrons, for which results have been obtained both for the maximum range, by absorption, and for the extrapolated Konopinski-Uhlenbeck upper limit, by expansion chamber or magnetic focusing. All available results are given except certain widely divergent values generally held to be in error. Figure 1 gives the maximum range plotted against the Konopinski-Uhlenbeck upper limit for the 14 elements listed in the table. In cases where two or more results are given for one element, their mean value has been used.

The points corresponding to nine of the elements lie close to the straight line fitted to them by the method of least squares. Its equation is

$$R = 0.460E_K - 0.226, \quad \dots\dots(1)$$

where  $E_K$  is the Konopinski-Uhlenbeck upper limit in Mv. The dotted line, which is shown for comparison, corresponds to Feather's relation given above, between the maximum range and experimental upper limit, corrected in accordance with more recent determinations<sup>(8)</sup>, thus

$$R = 0.536E - 0.165. \quad \dots\dots(2)$$

The remaining five points, for actinium B, radium C'', mesothorium 2, uranium X<sub>2</sub> and fluorine, which show considerable deviations, may be considered briefly. The Konopinski-Uhlenbeck upper limits for radium C'', mesothorium 2 and uranium X<sub>2</sub>, determined by Lecoin<sup>(4)</sup> with an expansion chamber, are all too low compared with results expected from relation (1). Lecoin states that in the case of uranium X<sub>2</sub> the Konopinski-Uhlenbeck plot was not linear, and no great importance can therefore be attached to this result. The absorption measurements by Sargent<sup>(11)</sup> and Feather<sup>(13)</sup> are in very good agreement with each other, and with the value obtained for the maximum range by applying relation (2) to the experimental upper limit of 2.32 Mv. found by Gray and Ward<sup>(21)</sup>. It is probable that in this

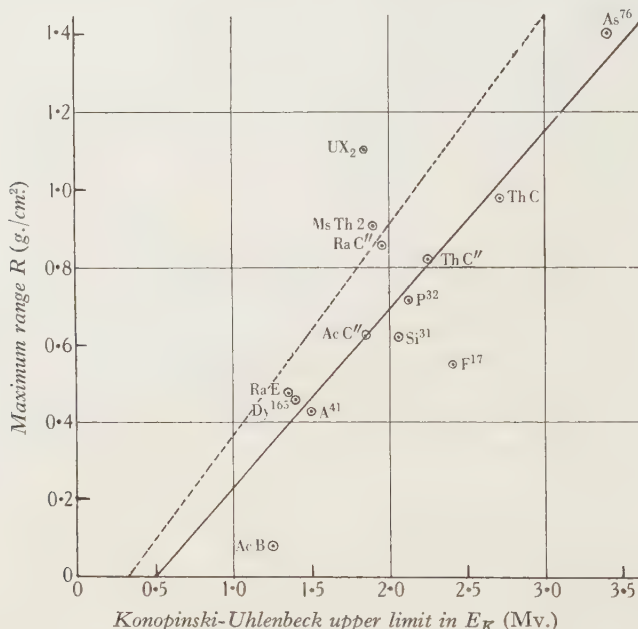


Figure 1. Relationship between range and energy for Konopinski-Uhlenbeck upper limits.

case and in the case of mesothorium 2 and radium C'' the expansion-chamber results are too low, and that the Konopinski-Uhlenbeck upper limits are approximately 2.9 Mv. for uranium X<sub>2</sub>, 2.5 Mv. for mesothorium 2 and 2.4 Mv. for radium C'', as determined from relation (1).

Determinations for actinium B are difficult owing to its short half-life and the overlapping of the  $\beta$ -ray spectra of actinium B and actinium C''. For this element the range is low in comparison with the Konopinski-Uhlenbeck upper limit: it is also low in comparison with the value of 0.23 g./cm<sup>2</sup> expected from the decay constant<sup>(3)</sup>. Even this value is less than that obtained from the expansion-chamber result by relation (1), which is about 0.3 g./cm<sup>2</sup>.

The discrepancy for the point corresponding to F<sup>17</sup> (positron emitter) is probably due to the fact that the value 0.55 g./cm<sup>2</sup>, at which thickness Danysz and Zyw state the positrons to be "completely absorbed"<sup>(14)</sup>, is not strictly comparable with

the 'end point' used by other workers. A similar determination by Zyw for Sc<sup>42</sup><sup>(22)</sup> gives a result correspondingly low compared with the maximum range obtained from the experimental upper limit by means of relation (2). The range for F<sup>17</sup> given by relation (1) is about 0.9 g./cm<sup>2</sup>.

We may conclude that in general the linear relation

$$R = 0.460E_K - 0.226 \quad (E_K > 1.0 \text{ Mv.})$$

between the maximum range and Konopinski-Uhlenbeck upper limit provides a satisfactory representation of the experimental results.

Element	Maximum range (g./cm <sup>2</sup> )	Reference	Konopinski-Uhlenbeck limit (mv.)	Method	Reference
AcB	0.08	(3)	1.25	chamber	(4)
AcC"	0.60-0.65	(5)	1.850	chamber	(4)
RaC"	0.86	(6)	1.95	chamber	(4)
RaE	{ 0.475 0.478	{ (1) (8)	1.36	mean value	(7), (8)
ThC	0.98	(9)	2.70	chamber	(10)
ThC"	{ 0.79 0.84	{ (9) (11)	2.25	chamber	(12)
MsTh <sub>2</sub>	0.91	(13)	1.900	chamber	(4)
UX <sub>2</sub>	{ 1.10 1.11	{ (11) (13)	1.850	chamber	(4)
F <sup>17</sup>	0.55	(14)	2.4	chamber	(15)
Si <sup>31</sup>	{ 0.675 0.571	{ (16) (8)	2.05	chamber	(15)
P <sup>32</sup>	0.720	(16)	{ 2.10 2.15	mag. focusing	(17)
A <sup>41</sup>	0.432	(18)	1.5	chamber	(15)
As <sup>76</sup>	1.400	(8)	3.4	chamber	(19)
Dy <sup>165</sup>	0.46	(5)	1.4	chamber	(20)

The errors estimated by different workers are not strictly comparable, and are therefore not given in the table.

## § 2. THEORETICAL DEDUCTION OF THE RELATION BETWEEN RANGE AND ENERGY

The reason for the linearity of the relation between range and energy can be obtained from a consideration of the general theory of the energy-losses of an electron in its passage through matter. This subject was treated by Bohr and others by classical methods, and has been worked out more recently by Bloch<sup>(23)</sup>, Bethe and Heitler<sup>(24)</sup> and others by the use of quantum mechanics.

Now while in general the energy lost by an electron in traversing unit path varies rapidly with the energy, it is practically constant for energies from 0.7 to 3.2 Mv., and it is between these values that the known upper limits of continuous  $\beta$ -ray spectra lie. For energies below 0.7 Mv. the energy-loss is due almost entirely to inelastic collisions, and the loss per unit path decreases rapidly as the energy increases. The loss due to collisions is a minimum at about 1 Mv., and thereafter increases steadily and very slowly, figure 2. Radiation losses cease to be negligible

after about 1 Mv., but for light elements they constitute less than one-tenth of the total loss for energies even up to 5 Mv. At very high energies radiation losses become enormous, so that the total rate of loss of energy increases rapidly. Curves showing the energy-loss per cm. of path in lead for electrons of energies from  $0.01 \text{ mc}^2$  to  $1000 \text{ mc}^2$  are given by Heitler<sup>(25)</sup>.

The energy-loss due to collisions has been calculated by Bloch<sup>(23)</sup>; the average loss in Mv. per unit ( $\text{g./cm}^2$ ) of path for an electron is given by

$$\left( -\frac{dE}{dx} \right)_{\text{coll.}} = \frac{3}{4} N Z \phi_0 \frac{1}{\rho} \frac{1}{\beta^2} 0.51 \left[ \log T/2 + 2 \log \frac{(T+1)}{IZ} + \frac{1}{(T+1)^2} \right],$$

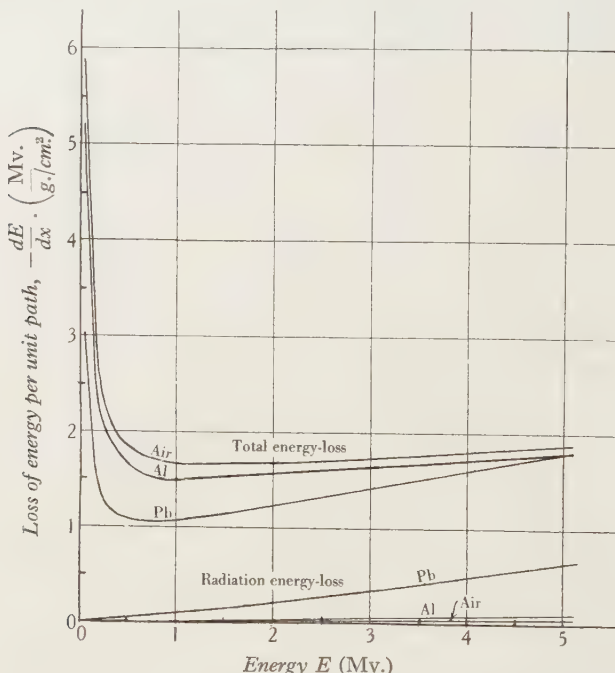


Figure 2. Loss of energy of an electron per unit path in lead, aluminium and air.

where  $E$  is the energy of the electron in Mv.,  $x$  is the length of path in  $\text{g./cm}^2$ ,  $N$  is the number of atoms per  $\text{cm}^3$  of the substance,  $Z$  is the atomic number of the substance,  $\rho$  is the density,  $\phi_0$  is the cross-section of an electron,  $6.57 \times 10^{-25} \text{ cm}^2$ ,  $\beta$  is the ratio of the velocity of the electron to the velocity of light,  $T$  is the kinetic energy  $\div mc^2$ ,  $[1/(1-\beta^2)^{1/2} - 1]$  or  $1.96 E$ , and  $IZ$  is the average ionization energy of the atom,  $I$  having the value  $13.5 \text{ eV}$ .<sup>(23)</sup> This formula is valid so long as  $\beta \gg 1/137$ .

The energy loss due to radiation (Bremsstrahlung) being emitted by the electron as a result of deflection in the field of an atom is given by<sup>(24)</sup>

$$\left( -\frac{dE}{dx} \right)_{\text{rad.}} = \frac{I}{\rho} N \phi_{\text{rad.}} (E + 0.51),$$

where  $\phi_{\text{rad.}}$  is the appropriate cross-section, which reduces to  $16\bar{\phi}/3$  for very small velocities, and to  $4\bar{\phi} \{ \log 2 (1.96E + 1) - 1/3 \}$  for extremely high velocities. Values

for intermediate velocities, with which we are concerned, have been calculated by Bethe and Heitler<sup>(24)</sup>.  $\bar{\phi} = Z^2 r^2 137$ , where  $r$  is the classical electronic radius.

The occurrence of the factor 0.51 and its reciprocal 1.96 is a result of the relationship  $T/mc^2 = 1.96E$ , where  $E$  is in Mv., since  $mc^2 = 0.51$  Mv.

The values of  $(-dE/dx)$ , the total energy loss per unit path, and  $(-dE/dx)_{\text{rad}}$  are given for lead, aluminium and air, in figure 2.

The average range  $R$  of the electron is given by

$$R = \int_0^{E_0} \frac{dE}{(-dE/dx)},$$

and may be obtained by numerical integration from a graph of the reciprocal of  $(-dE/dx)$  plotted against  $E$ . The results for lead, aluminium and air are given in

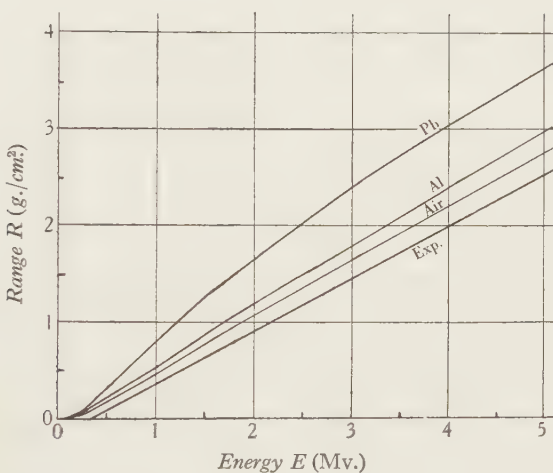


Figure 3. Range of an electron in lead, aluminium and air.

figure 3, together with the empirical linear relationship (2) for experimental upper limits,  $R = 0.536E - 0.165$ . Aluminium has been used for practically all the absorption determinations of upper energy limits, but the theoretical curves for lead and air are given for comparison.

The first point of interest is the approximate linearity of the curves for aluminium and air for energies above 0.7 Mv. For aluminium the calculated values show that the slope nowhere differs by more than 3 per cent from its average value, in the region 0.7 to 3.2 Mv. This fact is striking in view of the multiplicity of operating factors. Since the energy-loss due to collisions alone is a minimum at about 1 Mv., the curves cannot be accurately linear above this energy, for both collision and radiation losses are increasing with  $E$ . Complete linearity would be obtained only over a region where, for example, collision losses decreased with increasing energy and radiation losses increased, so that their sum was constant. Within experimental accuracy, however, the curve is linear over the region concerned, and even up to energies considerably higher than 3.2 Mv.

Secondly, divergences between the empirical and the calculated straight lines for aluminium must be considered, with regard both to the slope and the actual position. The average calculated value of  $1/(-dE/dx)$  between 0.7 and 3.2 Mv. is 0.63, showing about 16 per cent difference from the slope of the empirical line (0.536). The slope of the line fitted by the method of least squares to all available experimental upper limits was found to have a slope of 0.593, which is considerably nearer to the calculated slope. Upper limits of continuous spectra of  $\beta$  ray and positron active elements may be considered together, since although at high energies the energy lost in passing through matter is slightly greater for a positron than for a negative electron owing to annihilation, for energies below 5 Mv. the difference is negligible<sup>(24)</sup>.

With regard to the actual position of the line, the calculated range is from 20 to 25 per cent higher than that found by experiment. It must be borne in mind, however, that the actual superposition of the two lines constitutes a far more stringent test than is usually applied; in most cases the variation of theoretical formulae with certain factors is tested by calculating some expression which should have a constant value. The discrepancy is probably due to two factors. In the first place, owing to scattering, some electrons are eventually deviated through so large an angle that they are not received by the counting apparatus, while others finally reach the counter or ionization chamber, but only after they have traced out paths considerably in excess of the direct path through the absorber. Even for homogeneous  $\beta$  rays the form of the absorption curve is thus very dependent on the experimental arrangement<sup>(26)</sup>, and although the total range of homogeneous  $\beta$  rays appears to be approximately independent of experimental conditions, it is obtained from extrapolation of the absorption curve, which exhibits a tail owing to the straggling introduced by scattering. (The true straggling which also occurs is very small in the region under consideration<sup>(25)</sup>.) Thus although the effective range measured experimentally is a reproducible quantity fairly independent of experimental arrangement<sup>(27)</sup>, it is not identical with the range defined theoretically.

In the second place, similar considerations apply to the maximum range of inhomogeneous  $\beta$  rays from radioactive substances. The form of the absorption curve depends on experimental conditions<sup>(8)</sup>, and again, the effective maximum range for which fairly reproducible results can be obtained is not identical with the maximum range defined theoretically<sup>(1)</sup>. While the experimental maximum range has a definite and consistent meaning, it is an empirical conception, and it will be considerably lower than the actual range of the electrons of highest energy emitted by the source.

According to the present theory the range (g./cm.<sup>2</sup>) of electrons increases with the atomic number of the absorber. Early experimental workers did not find this to be the case: Schonland<sup>(28)</sup> found the range to be independent of the atomic number of the absorber for cathode rays with energy below 0.04 Mv., while according to Schmidt<sup>(29)</sup> and Douglas<sup>(30)</sup> the maximum range in g./cm.<sup>2</sup> of  $\beta$  rays from radium  $E$  is less in heavy than in light elements. Douglas points out, however, that the actual range, which includes the zigzag path through the absorbing material,

increases with atomic weight. Bloch<sup>(23)</sup> shows that in the case of  $\alpha$  particles the dependence of the range on atomic number of the absorber is very satisfactorily represented by the quantum-mechanical results. The apparent discrepancies are again probably due to the difference between the definitions of theoretical and of effective experimental range.

In consideration of the character of the Konopinski-Uhlenbeck upper limit of  $\beta$ -ray spectra, there is little to be gained from a close comparison of the theoretical {range, energy} relation with the empirical relation found in §1 connecting the maximum range and Konopinski-Uhlenbeck upper limit. The most significant result is the fact that the theoretical relation, as well as the empirical relation for both experimental and Konopinski-Uhlenbeck upper limits, is linear over the region which includes the upper limits of  $\beta$ -ray spectra of radioactive elements.

## REFERENCES

- (1) FEATHER, N. *Phys. Rev.* **35**, 1559 (1930).
- (2) KONOPINSKI, E. J. and UHLENBECK, G. E. *Phys. Rev.* **48**, 7 (1935).
- (3) SARGENT, B. W. *Proc. Camb. Phil. Soc.* **29**, 156 (1932).
- (4) LECOIN, M. *J. Phys. Radium*, **9**, 81 (1938).
- (5) BASCHWITZ, A. *J. Phys. Radium*, **9**, 120 (1938).
- (6) DEVONS, S. and NEARY, G. J. *Proc. Camb. Phil. Soc.* **33**, 154 (1937).
- (7) O'CONOR, J. S. *Phys. Rev.* **52**, 303 (1937).
- (8) WIDDOWSON, E. E. and CHAMPION, F. C. *Proc. Phys. Soc.* **50**, 185 (1938).
- (9) CHALMERS, J. A. *Proc. Camb. Phil. Soc.* **25**, 331 (1929).
- (10) RICHARDSON, H. O. W. and LEIGH-SMITH, A. *Proc. Roy. Soc. A*, **162**, 390 (1937).
- (11) SARGENT, B. W. *Proc. Roy. Soc. A*, **139**, 659 (1933).
- (12) CHAMPION, F. C. and ALEXANDER, N. S. *Nature, Lond.*, **137**, 744 (1936).
- (13) FEATHER, N. *Proc. Camb. Phil. Soc.* **34**, 115 (1938).
- (14) DANYSZ, M. and ZYW, M. *Acta Phys. Polon.* **3**, 485 (1934).
- (15) KURIE, F. N. D., RICHARDSON, J. R. and PAXTON, H. C. *Phys. Rev.* **49**, 368 (1936).
- (16) NEWSON, H. W. *Phys. Rev.* **51**, 624 (1937).
- (17) LYMAN, E. M. *Phys. Rev.* **51**, 1 (1937).
- (18) SNELL, A. H. *Phys. Rev.* **49**, 555 (1936).
- (19) BROWN, M. V. and MITCHELL, A. C. G. *Phys. Rev.* **50**, 593 (1936).
- (20) GAERTTNER, E. R., TURIN, J. J. and CRANE, H. R. *Phys. Rev.* **49**, 793 (1936).
- (21) GRAY, J. A. and WARD, A. G. *Canad. J. Res.* **15**, A, 42 (1937).
- (22) ZYW, M. *Acta Phys. Polon.* **3**, 499 (1934).
- (23) BLOCH, F. *Z. Phys.* **81**, 363 (1933); *Ann. Phys., Lpz.*, **16**, 285 (1933).
- (24) BETHE, H. and HEITLER, W. *Proc. Roy. Soc. A*, **146**, 83 (1934).
- (25) HEITLER, W. "Quantum Theory of Radiation" (1936).
- (26) EDDY, C. E. *Proc. Camb. Phil. Soc.* **25**, 50 (1929).
- (27) MADGWICK, E. *Proc. Camb. Phil. Soc.* **23**, 970 (1927).
- (28) SCHONLAND, B. F. J. *Proc. Roy. Soc. A*, **108**, 187 (1925).
- (29) SCHMIDT, H. W. *Phys. Z.* **10**, 929 (1909).
- (30) DOUGLAS, A. V. *Trans. Roy. Soc. Can.* **16**, 113 (1922).

# THE EXTINCTION OF DISCHARGES IN GEIGER-MULLER COUNTERS

By A. NUNN MAY, Ph.D., Halley-Stewart Laboratory,  
King's College, London

*ABSTRACT.* The discharge in Geiger-Muller counters is discussed in terms of the Townsend theory. It consists of a series of electron avalanches, each avalanche being generated from photoelectrons ejected from the outer wall by the previous avalanche. At low currents the average number of photoelectrons per avalanche is small, and if the actual number for some avalanche happens to be zero, the discharge will stop. This accounts for the extinction of the discharge at low currents. The theory gives an exponential decay formula for the probability of the discharge lasting a given time, and the mean life-time increases exponentially with the current. This is in accord with Werner's experiments, and his numerical values are in good agreement with the theory.

## § I. INTRODUCTION

IT has been found by a number of experimenters<sup>(1)</sup> that the discharge in a Geiger-Muller counter can only be continuous if the current is allowed to be greater than a critical value,  $I_{\min}$ . For currents smaller than this the discharge cannot be maintained without some external source of ionization. This fact is the foundation of all methods of using Geiger-Muller tubes as counters. By means of an external resistance, or some valve circuit, the current is kept below  $I_{\min}$  when the discharge sooner or later stops.

This instability at small currents is difficult to explain. Most of the recent workers on the subject ascribe it to the action of the space charge produced by the positive ions<sup>(2)</sup> or to fluctuations in this space charge<sup>(3)</sup>. This type of mechanism may well be important in special cases, such as the counters containing alcohol vapour which Trost<sup>(4)</sup> has investigated, but the following theory based on the essentially discontinuous nature of a small current appears to account for the extinction of the discharge without invoking any space-charge effects.\* Before giving an account of this theory we must describe briefly the mechanism of the discharge in Geiger-Muller counters as it has been elucidated by other workers in terms of the Townsend theory.

The usual form of counter consists of an outer cylinder, of a few centimetres' radius down the axis of which a wire of about  $\frac{1}{10}$  mm. radius is stretched. These are in a vacuum tight enclosure, inside which there is some gas at a pressure of a few centimetres of mercury.† A potential difference  $V$  is applied to the two electrodes,

\* Note added in proof. Since this paper was written the author has seen a paper by von Geel and Kerkum<sup>(5)</sup> who gave a similar theory; their treatment differs, however, in many points from that given here.

† The numerical data in this paper are for counters filled with hydrogen or oxygen.

the outer cylinder being negative. With proper adjustment of the potential  $V$ , any ionization occurring inside the counter leads to a discharge, but if by some means the current in the discharge is kept below  $I_{\min}$  the discharge will soon stop, and the counter is then reset ready for the next count. This is the normal, non-proportional operation of a counter.

## § 2 PROPORTIONAL MULTIPLICATION

If the potential  $V$  is less than the value  $V_0$  at which non-proportional counting starts, then the counter acts proportionally. The electrons generated by the primary ionization are pulled towards the wire by the electric field, and in the strong field in the neighbourhood of the wire they acquire sufficient energy to ionize the gas by collision. The fresh electrons so formed ionize the gas in their turn, and so each primary electron gives rise to an electron avalanche containing in all, say,  $m$  electrons. When all these electrons reach the wire the discharge will stop, unless fresh electrons can be supplied from outside, which does not occur for low potentials. The electron avalanche therefore continues only for a time  $\tau$  about equal to that taken by an electron to reach the wire from the outer wall. In general  $\tau$  will be about  $10^{-6}$  of a second.\*

This type of discharge is often used in detecting small amounts of ionization<sup>(5)</sup>. We are not at the moment concerned with this process except as a part of the normal, non-proportional discharge.

## § 3. THE NON-PROPORTIONAL DISCHARGE

It is found in practice that the multiplication factor  $m$  in the proportional discharge cannot be made much greater than  $10^4$ . Above this figure the discharge continues for a time which is long compared to  $\tau$ . It is now generally admitted that this is due to the emission of photoelectrons from the outer wall of the counter, these being ejected by photons from gas molecules which have been excited by collisions with electrons in the avalanche to states of higher energy than the work function of the cathode<sup>(6)</sup>. Let the number of atoms or molecules so excited by one primary electron be  $sm$ , so that  $s$  is a measure of the ratio of excitation to ionization produced by the electron avalanches. The probability that one of these excited atoms will cause the emission of a photoelectron from the outer cylinder will be  $e\gamma$ , where  $e$  is the probability that the atom will lose its energy by radiation and not, for instance, by colliding with another atom, and  $\gamma$  is the photoelectric yield from the outer wall in electrons per quantum.

Thus the number of photoelectrons generated by each primary electron will be  $e\gamma sm$ , and if

$$e\gamma sm = 1$$

the discharge will be self-maintained. That is, on the average each avalanche of electrons will be followed by another of equal size. The corresponding value of  $m$

\* The positive ions formed by the avalanche in the neighbourhood of the wire move away towards the outer electrode. Their speed is much less than that of the electron and they will take about  $10^{-3}$  sec. to cross the counter.

we will call the normal multiplication,  $M$ , so that

$$M = \frac{I}{e\gamma s}. \quad \dots\dots(1)$$

According to the measurements of Kreuchner<sup>(7)</sup>  $\gamma$  is of the order of  $10^{-5}$  for copper, and photons of about the energy involved here. Since  $e\gamma s$  is probably of the order of 1,  $M$  will be of the order of  $10^5$ . For values of  $m$  less than  $M$  the successive avalanches decrease in size, and the discharge dies away. For values of  $m$  greater than  $M$  the avalanches increase in size, and the discharge grows.

The value of  $V$  at which  $m$  reaches the value  $M$  is  $V_0$ , the starting potential. For values of  $V$  considerably less than  $V_0$ , the tube counts proportionally, since  $m$  is then considerably less than  $M$  and only the first avalanche is of any importance. When  $V$  is nearly equal to  $V_0$ ,  $m$  is nearly equal to  $M$ ; the first few avalanches will then be nearly equal in size, but the slow-moving positive ions formed by them will accumulate near the wire, and their space charge will distort the field, so as to reduce  $m$ . The subsequent avalanches therefore decrease rapidly, and the discharge stops. For values of  $V$  greater than  $V_0$ , the initial multiplication is greater than  $M$  so that the discharge current increases. This causes the rapid development of space charge, and so decreases  $m$ . Finally equilibrium is reached when  $m=M$ , and the current attains a steady value, at which enough positive ions are formed by each avalanche to replace those which have moved away in the time  $\tau$  since the previous avalanche.\*

The conditions for this equilibrium have been studied by Werner<sup>(8)</sup>. His equations give the distribution of space charge, and the current  $I$  corresponding to any given over-voltage ( $V - V_0$ ). In particular  $I$  is proportional to  $(V - V_0)$ . The potential across the counter is therefore given by

$$V = V_0 + kI, \quad \dots\dots(2)$$

where  $k$  is the internal resistance of the counter and is generally of the order of 1 megohm.

The counter is normally used in series with a large resistance  $R$ . The total resistance in the circuit is then  $(R+k)$ , and the current through the counter will be given by

$$I = \frac{U - V_0}{R + k},$$

where  $U$  is the external potential applied to the circuit.

A discharge which satisfies these conditions should continue to burn indefinitely. In fact, however, it will always be extinguished if the current in the discharge is less than the critical value  $I_{\min}$ , or if

$$U - V_0 < (R + k) I_{\min}. \quad \dots\dots(3)$$

\* If  $m \gg M$  then the first few avalanches may form considerably more than the number of positive ions required by the equilibrium conditions. The multiplication will then be much less than  $M$  until this excess space charge has moved across the counter, and in this time the successive avalanches may have decreased to zero. This may be the explanation of the type of discharge observed by Trost<sup>(4)</sup>, in which the discharge was extinguished by the positive ion space charge without the use of a high resistance in series with the counter.

This equation gives the range of applied voltage within which the discharge is still intermittent. The range in which the number of discharges is independent of  $U$  is generally much smaller than this, and since the counter is always used in this region,  $I$  is generally much less than  $I_{\min}$ .

#### § 4. INSTABILITY AT SMALL CURRENTS

To explain this instability we must consider the discharge process in greater detail. Each avalanche of electrons occupies a time of about  $10^{-6}$  sec. Only during the last  $10^{-8}$  sec. of this time are the electrons in the strong field near the wire. Nearly all the excitation of atoms of the gas will therefore occur during the last  $\frac{1}{100}$  the time taken by the avalanche. In this time the photoelectrons necessary to bring about the next avalanche must be generated. Thus the apparently continuous current actually consists of a chain of individual avalanches, the connexion between successive links of the chain being the emission of photoelectrons from the wall. If for any reason this connexion breaks, the discharge will cease. We proceed to calculate the probability of this break.\*

We express the current  $I$  in electrons per sec., a current of  $1 \mu\text{a}$ . being equal to  $6.24 \times 10^{12}$  electrons per sec. The multiplication being  $M$ , the number of photoelectrons emitted by the wall per second is  $I/M$ , since each photoelectron gives rise to  $(M-1)$  others in the discharge. Thus the average number  $\bar{n}$  of photoelectrons ejected during each avalanche is given by

$$\bar{n} = \frac{I}{M} \tau. \quad \dots\dots(4)$$

This is of the order of 10 assuming the value  $10^5$  for  $M$  and  $10^{-6}$  sec. for  $\tau$ ; and for  $I$ ,  $1 \mu\text{a}$ ., which is the order of magnitude given by Werner for counters containing hydrogen.

If the average number of photoelectrons generated by each avalanche is as small as 10, there is a finite probability of the number for some particular avalanche being zero. It is just this which is believed to be responsible for the discharge stopping. The individual photoelectrons are emitted quite independently, so that the probability  $p_0$  of  $n$  being zero for any avalanche is given by

$$p_0 = e^{-\bar{n}}. \quad \dots\dots(5)$$

The probability that  $n$  is at least 1, and therefore that the discharge continues for at least one more avalanche is

$$1 - p_0, \text{ which} = 1 - e^{-\bar{n}}.$$

Similarly the probability that the discharge continues for at least  $N\tau$  sec. is

$$(1 - p_0)^N, \text{ which} = (1 - e^{-\bar{n}})^N. \quad \dots\dots(6)$$

\* This account of the discharge is only strictly correct if all the primary ionization is formed at the same distance from the wire. The error in the life-time predicted by the theory if this is not so will be of the order of  $\tau$ , and may be neglected.

If  $T$  is the mean life-time of the discharge, we can write this probability as

$$e^{-N\tau/T}.$$

Hence,

$$(1 - e^{-n}) = e^{-\tau/T}$$

or

$$\frac{T}{\tau} = 1/\log_e \left( \frac{1}{1 - e^{-n}} \right). \quad \dots\dots(7)$$

If we can assume that  $e^{-n}$  is small, then

$$\begin{aligned} T/\tau &= e^n \\ &= e^{\tau I/M}. \end{aligned} \quad \dots\dots(8)$$

Thus the probability of the discharge surviving for a given time at a current  $I$  is given by an exponential decay formula, in which the mean life  $T$  increases exponentially with  $I$ .

## § 5. COMPARISON WITH EXPERIMENTS

Werner<sup>(3)</sup> has measured the mean life-time of the discharge for various values of  $I$ , and obtained a formula of the type (8) for the variation of  $T$ . His equation is

$$T = t_0 e^{\alpha V'}, \quad \dots\dots(9)$$

where  $V'$  is the over-voltage, which, by equation (2), can be replaced by  $kI$ .

Comparing equations (8) and (9) we obtain

$$\frac{\tau I}{M} = k I \alpha$$

and

$$\tau = t_0$$

$$\text{so that } M = \frac{6.24 \times 10^{12} t_0}{k \alpha}, \quad \dots\dots(10)$$

where  $k$  is expressed in megohms and  $\alpha$  in reciprocal volts.

Werner<sup>(3)</sup> gives the values of  $\alpha$ ,  $k$  and  $t_0$  for counters filled with hydrogen and oxygen, and in the following table these are shown together with values for  $M$  deduced from equation (10). In accordance with the above deduction,  $\tau$  is taken as equal to  $t_0$ .

Gas	Pressure (mm. of mercury)	$\alpha$ (v. <sup>-1</sup> )	$k$ (MΩ.)	$\tau = t_0$ (10 <sup>-7</sup> sec.)	$M$
H <sub>2</sub>	124	2.53	4.5	2.5	1.4 × 10 <sup>5</sup>
O <sub>2</sub>	41	1.57	5.0	6.5	5.2 × 10 <sup>5</sup>

It is an important verification of these views that as Werner has pointed out these values of  $\tau$  are of the order of magnitude we expect for the passage of an electron across the counter, and also the values of  $M$  agree with the estimates we have made

above from the fact that the multiplication in the proportional region cannot be greater than about  $10^4$ , and from the orders of magnitude of  $e$ ,  $\gamma$  and  $s$ . Thus the theory not only predicts the correct formula for the variation of the life-time of the discharge with  $I$ , but without the use of any arbitrary constants gives a satisfactory quantitative agreement with the observations.

### § 6. THE MINIMUM CURRENT

The order of magnitude of  $I_{\min}$  may be deduced from these equations by remembering that  $I_{\min}$  is the limiting current at which there is still a small probability of the discharge breaking down. We can obtain this by making  $T$  large in equation (8).

For instance, if we take  $T$  equal to  $10^{-2}$  or 1 sec. we obtain

$$\frac{T}{\tau} = 10^5 \quad \text{or} \quad 10^7,$$

so that from equation (8)  $\frac{\tau I}{M} = 10 \quad \text{or} \quad 15.$

Thus

$$I_{\min} = \frac{n_{\min} M}{\tau}, \quad \dots\dots(11)$$

where  $n_{\min}$  is the number of photoelectrons per avalanche at which the discharge just becomes stable, and from the above is of the order of 10. From the values of  $M$  and  $\tau$  found above we obtain a value for  $I_{\min}$  of the order of  $1 \mu\text{a}$ . in agreement with observation (3). If we substitute the value of  $M$  from equation (1) in equation (11), we obtain  $I_{\min}$  in terms of the various constants of the counter,

$$I_{\min} = \frac{n_{\min}}{e\gamma s\tau}. \quad \dots\dots(12)$$

The substitution of this value of  $I_{\min}$  in equation (3) will give the range of applied voltages within which the discharge will be intermittent.

In using the counter it is desirable to keep  $R$  as low as possible in order to obtain a quick recovery from each count. At the same time it is desirable to use a large over-voltage, since then the kicks themselves are large and even a partial recovery will give a detectable count. By equation (3) we see that these two conditions together necessitate a large value of  $I_{\min}$ . By equation (12) it will be seen that this can be obtained by reducing each of the factors in the denominator; that is, by reducing the time occupied by each avalanche and the rate of production of photoelectrons by a given current.

In fact it is found that the functioning of a counter is very dependent on such conditions as the presence of impurities in the gas or of surface layers on the outer electrode, which would be expected to change these factors. In this connexion we may mention again the experiments of Trost in which the addition of alcohol vapour to the gas, and varnishing of the outer cylinder, were found to produce a considerable improvement in the working of the counter.

We cannot at the moment embark on any more quantitative discussion of the above equation since the data which would be required are not available. Experiments on the verification of the theory, and its application to the design of counters, are now in progress.

#### § 7. ACKNOWLEDGEMENT

The author wishes to thank Prof. C. D. Ellis for many very helpful discussions during the writing of this paper.

#### REFERENCES

- (1) MOON, P. B. *J. Sci. Instrum.* **14**, 189 (1937); and papers cited there.
- (2) VON HIPPEL. *Z. Phys.* **97**, 455 (1935).
- (3) WERNER, S. *Z. Phys.* **92**, 705 (1934).
- (4) TROST, A. *Z. Phys.* **105**, 399 (1937).
- (5) GEIGER and KLEMPERER. *Z. Phys.* **49**, 753 (1928).
- (6) GREINER. *Z. Phys.* **81**, 543 (1933).
- (7) KREUCHNER, K. H. *Z. Phys.* **97**, 625 (1935).
- (8) WERNER, S. *Z. Phys.* **90**, 384 (1934).
- (9) VON GEEL and KERKUM. *Physica*, **5**, 609 (1938).

# FERROMAGNETIC COMPOUNDS OF CHROMIUM

BY L. F. BATES, Professor of Physics, University College, Nottingham  
AND  
G. G. TAYLOR, B.Sc.

*Received 8 July 1938. Read in title 28 October 1938*

**ABSTRACT.** It is found that when powdered chromium prepared from chromium amalgam is heated with sulphur *in vacuo*, a series of ferromagnetic compounds is formed. The Curie points and specific magnetizations of the prepared specimens are recorded.

## § I. INTRODUCTION

CHROMIUM and manganese belong to the elements of the iron group, but while manganese is well known to form ferromagnetic compounds when heated with diamagnetic elements, for instance, MnP, MnAs, MnSb and MnBi, and gives the ferromagnetic Heusler alloys when alloyed with copper and aluminium, the ferromagnetic behaviour of chromium in combination with other elements has only recently been appreciated. Ochsenfeld<sup>(1)</sup> found that certain combinations of chromium and tellurium are ferromagnetic, and Bates and Baqi<sup>(2)</sup> showed that there is good reason to suppose that chromium combined with hydrogen to form ferromagnetic compounds; a feature of both the hydrogen and tellurium compounds of chromium is that in some instances the magnetization rises to a maximum slightly above room-temperature, although little is known about its variation with applied field. Early this year Nowotny and Årstad<sup>(3)</sup> recorded that CrAs and Cr<sub>2</sub>As<sub>2</sub> are weakly ferromagnetic, but gave no details of their ferromagnetic properties.

Apart from the fact that ferromagnetism is a much more widely spread phenomenon than is generally believed, it seemed from the behaviour of chromium and tellurium that an examination of compounds of chromium and sulphur was likely to lead to interesting results, although Mellor<sup>(4)</sup> records no ferromagnetic sulphides of chromium. Accordingly a series of compounds of chromium and sulphur were made from pure chromium, prepared by Bates and Baqi<sup>(2)</sup> by the distillation of chromium amalgam, which had not been heated to temperatures above 400° C. The several specimens were prepared as follows. Weighed quantities of chromium and sulphur in atomic proportions were placed in a large thick-walled pyrex tube, evacuated and sealed. This was first heated to 100° C. and examined, the product consisting in each case of dark grey masses. Complete combination did not occur with specimens containing a high proportion of sulphur. The earlier specimens were next heated to 200° C. and examined, but as little change was observed, this treatment was later omitted, specimens being heated to 300° C. for about 1 hr. and

then examined. The product was generally a dark grey powder containing large nodules, and on heating to 400° C., partial fusion occurred. The specimens were finally heated to 500° C. for 1 hr., the end product consisting of black fused masses and of smaller globules with a highly polished surface and in some cases with a metallic appearance. The tube was opened and the contents were ground to a powder, which sometimes weakly adhered to a magnet. The powder was placed in a pyrex tube, which was evacuated, sealed, and annealed for 5 or 6 hr. at 400° C. No change in appearance was thereupon observed. Test samples were then placed in pyrex tubes, of internal diameter approximately 3 mm. and length about 10 cm., the tubes being half filled. These were then evacuated and sealed, a small hook being formed at one end of each tube to permit examination of the ferromagnetic properties by the method used by Bates and Illsley<sup>(5)</sup> in their experiments on iron amalgams.

When a uniform tube having a cross-section with an internal area of  $\alpha$  is half filled with a powdered specimen and suspended vertically from one arm of a sensitive chemical balance, so that the upper level of the specimen lies midway between the plane pole-tips of an electromagnet while the ends of the tube are remote from the field, then

$$\delta mg = \frac{1}{2}\alpha (k_s) H^2 + \alpha\sigma H,$$

where  $\delta m$  is the apparent decrease in mass on the application of a field  $H$ ,  $k_s$  is the paramagnetic susceptibility of the substance per unit volume and  $\sigma$  the saturation intensity of magnetization of the material. Hence, when ferromagnetism is present the graph of  $\delta mg/\alpha H^2$  against  $1/H$  should be a straight line, whose slope is a measure of  $\sigma$ .

## § 2. EXPERIMENTAL RESULTS

The results for the several specimens are shown in figure 1, and the values of  $\sigma$  per gramme of material and per gramme of chromium-content are given in the table. In the second column of the table are given the initial constitutions of the mixtures of powdered chromium and sulphur from which the specimens were made, while in the third are given the results of the chemical analyses made for us in the Chemistry Department through the kindness of Professor Gulland.

Specimen no.	Atomic ratio S/Cr		$\sigma/g.$ material	$\sigma/g.$ chromium	$\theta_F$
	Initial	Final			
1	0.5	—	0.0175	—	30 — —
2	1.0	0.65	0.134	0.216	30 — —
3	1.5	1.37	0.197	0.327	— 78 90
4	2.0	0.89	0.072	0.111	30 — —
5	Large	1.37	0.0206	0.038	30 — 100

The chemical analysis of specimens 1 and 2 was difficult as they consisted of parts which were soluble in boiling concentrated hydrochloric acid plus potassium chlorate and parts which were not. The insoluble portion in the case of specimen 2

was definitely ferromagnetic and comprised some 14 per cent of the whole; the constitution of the soluble portion only is given in the table.

The Curie points of the specimens were measured by the method devised by Bates, Gibbs and Reddi Pantulu<sup>(6)</sup>. The specimen was packed in a thin-walled pyrex tube about 4·5 cm. long and 3 mm. in internal diameter and suspended horizontally from a vertical pyrex fibre hanging from a fine phosphor-bronze suspension. The pyrex tube was enclosed in a furnace and the period of oscillation  $t$  was ob-

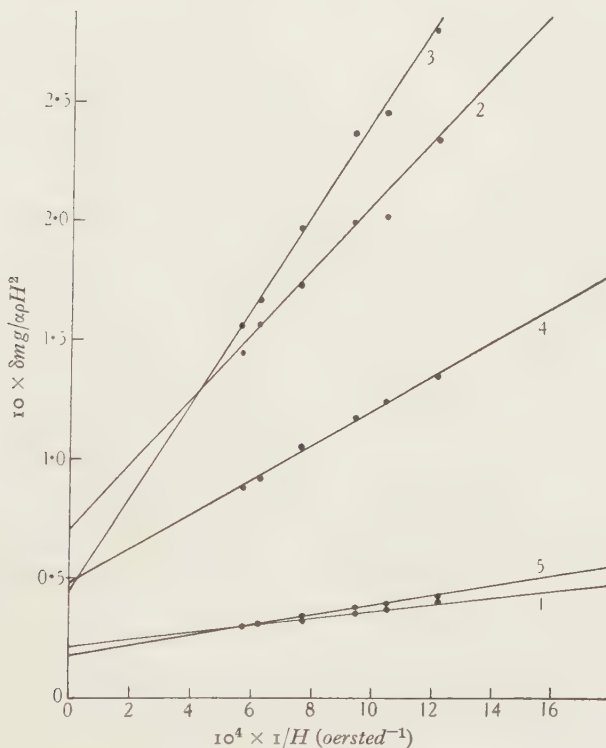


Figure 1. Graphs of magnetic pull as a function of  $1/H$ .

served when the system vibrated in a constant magnetic field at chosen temperatures  $T$ . When  $1/t^2$  was plotted against  $T$  a curve showing a prominent kink at the Curie point was obtained; such curves are shown in figures 2 (a) and 2 (b), and represent the behaviour of the specimens when heated to 400° C. and then allowed to cool slowly, different temperature regions being shown separately in figures 2 (a) and 2 (b) for the sake of clearness. It was found that the magnetization exhibited by the specimen depended markedly upon the quenching of the specimen, the more rapid the cooling the less the intensity of magnetization of the specimen in the applied field.

The above results show that at least two ferromagnetic combinations of chromium and sulphur are possible, with Curie points at 30° and 90° or 100° approximately, but the exact chemical constitution of these combinations is not known.

In view of the importance of chromium in the manufacture of magnetic materials the results are of interest. Jaanus<sup>(7)</sup> has recently given a theoretical study of the magnetic effects of ferromagnetics in dilute concentrations in other materials. It is

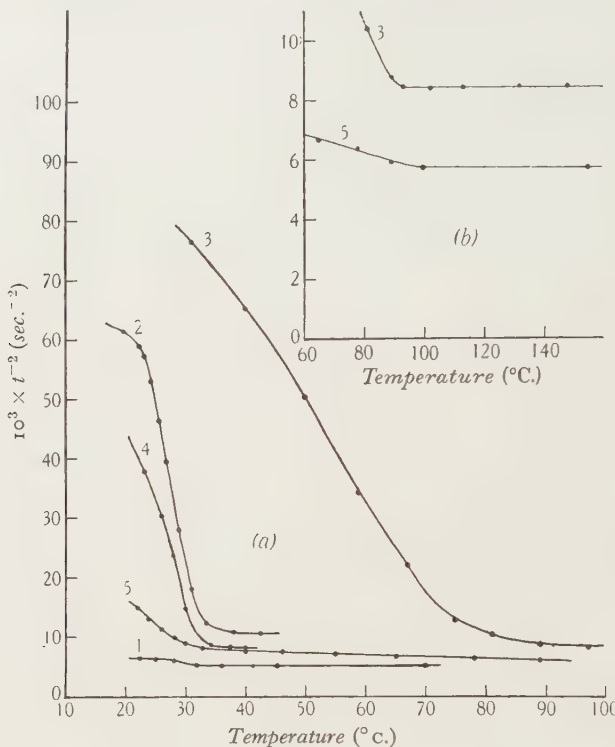


Figure 2. Curves showing variation of magnetization with temperature.

not proposed to discuss his interesting results here, but it is desirable to point out that the results of Bates and Illsley and those of the present communication show that the value of the demagnetization factor 4 assumed by Jaanus is at least twice too large and that the coercive force must be considerably less than 30 oersteds.

### § 3. ACKNOWLEDGEMENT

The experiments described above were carried out with apparatus purchased with a grant to one of us (L. F. B.) from the Government Grants Committee of the Royal Society.

### REFERENCES

- (1) OCHSENFELD, R. *Ann. Phys., Lpz.*, **12**, 353 (1932).
- (2) BATES, L. F. and BAQI, A. *Proc. Phys. Soc.* **48**, 781 (1936).
- (3) NOWOTNY, H. and ÅRSTAD, O. *Z. phys. Chem.* **38**, B, 461 (1938).
- (4) MELLOR, J. W. *A Comprehensive Treatise on Inorganic and Theoretical Chemistry*, **11**, 429 (1931).
- (5) BATES, L. F. and ILLSLEY, P. F. *Proc. Phys. Soc.* **49**, 611 (1937).
- (6) BATES, L. F., GIBBS, R. E. and REDDI PANTULU, D. V. *Proc. Phys. Soc.* **48**, 665 (1936).
- (7) JAANUS, R. *Phys. Z. Sowjet.* **12**, 729 (1938).

# THE PRECISION MEASUREMENT OF CAPACITANCE

By N. F. ASTBURY, M.A., F.I.N.S.T.P.

AND

L. H. FORD, M.Sc., National Physical Laboratory

*Received 12 July 1938. Read in title 28 October 1938*

**ABSTRACT.** The paper describes a method for the measurement of capacitance in terms of mutual inductance and resistance. The circuit is developed from the Carey-Foster bridge, and a combination of two bridge circuits used successively leads to the elimination of small correcting terms. The power factor also of the condenser under test is determined. The values of capacitance and power factor are deduced entirely in terms of two readings of a mutual inductance and two readings of a resistance box. The screening of the bridge, including the mutual inductance, has been carried out in great detail, and the whole circuit is enclosed in an earthed screen within which certain of the components are again screened independently. The effects of stray capacitances within the network and between the network and earth are thus reduced to negligible proportions. The equipment is designed for measurements on capacitances ranging from  $1000 \mu\mu F$ . to  $2 \mu F$ . at frequencies ranging from 50 to 3000 c./sec., and the probable errors are estimated as 5 parts in  $10^5$  on capacitance and 0.00005 on power factor at 1000 c./sec. At higher frequencies and for capacitances outside the stated range, the accuracy may be halved. The circuits are very adaptable and the bridges, as finally constructed, can be used also for the measurement of self-inductance and other quantities.

## § I. INTRODUCTION

IT is perhaps not generally realized that, in the system of electrical measurements used in this country, capacitance is a secondary derived unit. There is, in other words, no primary standard capacitor with which other capacitors can be directly compared, and although, as a matter of practical expediency, capacitors are often calibrated by direct reference to capacitance substandards, the sub-standards themselves have to be measured in terms of the primary standard of mutual inductance at the National Physical Laboratory<sup>(1,2)</sup>, the fundamental standard to which all reactance measurements are ultimately referred. The inductance of this standard is computed from its dimensions, so that the ultimate standard of reference here is the unit of length. The measurement of capacitance is therefore of the type traditionally described as "absolute", although there is in the measurements none of the finality commonly implied by that term. From the viewpoint of the experimenter, absolute measurements are characterized by the special difficulties attendant on correlating quantities of different physical natures, and they demand much more refined technique than the more common electrical measurement which is based on a simple comparison of quantities of the same kind.

The circuit which has been in use at the National Physical Laboratory for the past thirty years for the comparison of capacitance and mutual inductance was developed from Carey Foster's classical network<sup>(3)</sup>, in which capacitance is determined in terms of mutual inductance and resistance. Contributions to the theory and technique of this method have been made by a number of workers<sup>(4, 5, 6, 7, 8)</sup>, but the method required an apprenticeship, and considerable trouble had to be expended to achieve an accuracy of one part in ten thousand in capacitance measurements. With the improvements in the design and manufacture of substandard capacitors which has followed the rapid growth of the communications industry, it became apparent that something more certain in operation than the traditional circuit was required, and it was to meet the demand for more accurate and rapid calibrations that the work described in this paper was carried out.

## § 2. PRINCIPLE OF THE PRESENT METHOD

The Carey Foster circuit as arranged by Heydweiller<sup>(4)</sup> is shown in figure 1. The Wagner earthing arm there shown was added by Dye<sup>(5)</sup>. If  $C$  is the capacitor under test,  $M$  is an adjustable mutual inductance,  $L$  and  $P$  are respectively the total

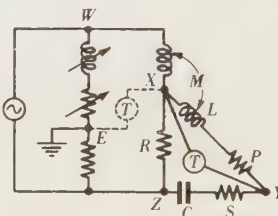


Figure. 1. Carey-Foster bridge (Campbell-Heydweiller).

inductance and resistance of the arm  $XY$ ,  $R$  is the resistance of the arm  $XZ$ , and  $S$  is the resistance in series with  $C$ , then, when balance is established, the values of capacitance  $C$  and power factor  $\gamma$  of the capacitor under test are given by

$$C = M/PR, \quad \dots\dots(2\cdot1)$$

$$\gamma = \omega C [R(L - M)/M - S], \quad \dots\dots(2\cdot2)$$

$\omega/2\pi$  being the frequency of the alternating current supplied to the circuit. These equations do not include the effects of small residual inductances and capacitances, which were first given in full by Butterworth<sup>(6)</sup>. Amongst other things, the measurements call for an accurate knowledge of  $P$ , a resistance which includes a highly inductive copper coil, and of  $L$ , the self-inductance of that coil, each of which quantities depends on  $\omega$ . Additional small correcting terms must therefore be added to the equations to take account of this. The original equations are given in references (6) and (7). They are too complicated to be given in detail here.

The Wagner arm does not eliminate from the circuit the effects of impedance to earth from the junctions of  $C$  and  $S$  and of  $L$  and  $P$ , and spurious values of  $C$

and  $\gamma$  may result in consequence. The actual composition of the Wagner arm made it cumbersome and inelastic while the presence in it of an inductive component which may have a considerable stray magnetic field is undesirable.

The main lines of attack leading to the evolution of the present method were directed to removing the objections outlined above. The first step was the complete elimination of  $S$ . A consideration of equation (2·2) shows that if  $S=0$ , the power-factor balance can be established by adjustment of  $L$ , if this can be effected without alteration of  $M$ . A simple method is to add a variable capacitor in shunt with  $P$ . The effective inductance of the arm then becomes approximately  $L-PK^2$ ; see figure 2. We are then left with only one mid-arm junction in the circuit, that between  $L$  and  $P$ , and the difficulties arising from this are then met by adequate screening.

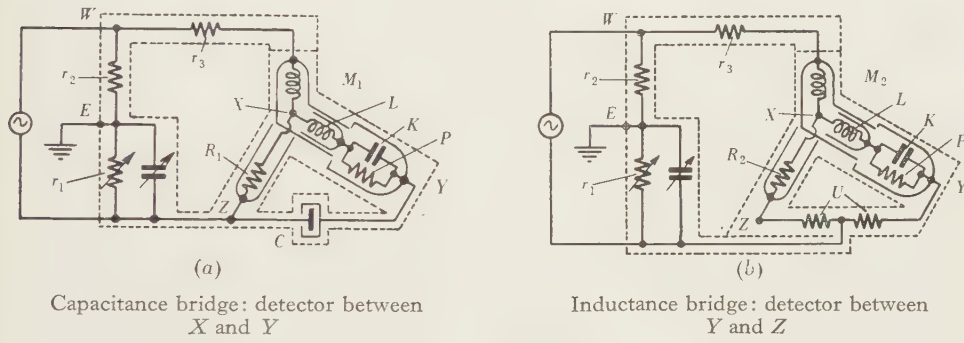


Figure 2. New bridge.

Next, the measurement of the effective resistance and inductance of the arm containing  $L$  and  $P$  must be made simply and accurately at the required frequency. This is done by converting the circuit into a modified Campbell-Heaviside inductance bridge, so that  $L$  may be measured in terms of  $M$  and  $P$  in terms of  $R$ , the latter being made continuously adjustable for this purpose. The simplicity of such a conversion will be apparent from a consideration of figures 2 (a) and 2 (b). In the latter, the resistors  $U$ ,  $U'$  are equal ratio arms. We then have the following equations for  $C$  and  $\gamma$ . Let  $M_1$ ,  $R_1$  be the values of  $M$  and  $R$  required in the capacitance bridge, and  $M_2$ ,  $R_2$  those required in the inductance bridge. Then

$$C = M_1 / R_1 R_2, \quad \dots\dots(2\cdot3)$$

$$\gamma = \omega (2M_2 - M_1) / R_2. \quad \dots\dots(2\cdot4)$$

The properties of the condenser are thus determined completely in terms of the properties of the mutual inductance and the resistance  $R$ . As will be seen later, this statement remains true when the effects of residual inductance and capacitance are taken into account. The practical importance of this is very great, for the properties of  $M$  and  $R$  can, with proper design, be determined with high precision. There is thus at once a great advance on the earlier method, in which a knowledge of the characteristics of several components is required.

The Wagner earthing arm as originally used by Dye<sup>(5)</sup> tended to become unmanageable when  $M$  was small, owing to the fall in impedance of the branch  $WX$ , figure 1. This is easily overcome, at the expense of a slight loss in bridge current, by the addition of a series resistance in this branch. The Wagner balance is then simply effected, with non-inductive components, by applying the principle of the well-known Maxwell inductance bridge. The arrangement is shown in figure 2, where  $r_3$  is the added series resistance.

The screening of the complete circuit must be arranged with a view to localizing and accurately defining the points of action of earth-capacitances, and to reducing to negligible amounts the earth capacitances of the junction of  $L$  and  $P$ , and of the common point  $X$  of the mutual inductance. The latter is especially important, for, although the point  $X$  is brought to earth potential in the capacitance bridge, figure 2a, it cannot be so treated by any simple system in the corresponding inductance bridge, figure 2b. The theoretically desirable screening arrangements are shown in figure 2: a fuller treatment of these and of the practical attempts at realization must be reserved for discussion later in the paper.

### § 3. ANALYSIS OF THE CIRCUITS

In the practical utilization of the circuits broadly described above, consideration must be given to the effects of stray impedance not only as affecting the individual properties of the components of the network, but also as affecting the behaviour of the network as a whole. Thus, in deriving the complete network equations, the resistances must be regarded as possessing finite phase angles, and the mutual inductances as possessing finite phase defects. These can be regarded as characteristic and individual properties of the components and can be measured as such. In addition, the assembly of the components in the network gives rise to a system of mutual impedances and impedances to earth, all of which must be taken into account in establishing the final equations of balance. Fortunately, the effects both of the defects of the components and of the defects of the network are small, and it is therefore permissible to consider each independently. This leads to a considerable simplification of the analysis, which would otherwise become unmanageably involved.

Considering first the circuit independently of the effects of stray mutual impedances and impedances to earth, we define the following quantities; see figure 3.  $\mu_1$  is the mutual impedance operator of the mutual inductor at any setting 1,  $\lambda$  the impedance operator of winding in arm  $XY$ ,  $\eta_1$  the impedance operator of winding in arm  $WX$  at setting 1,  $\xi_1$  the impedance operator of arm  $XZ$  at any setting 1 of the resistor  $R$ ,  $\zeta$  the impedance operator of the combination  $P - K$  in the arm  $XY$ ,  $\rho$  the ratio of impedance operators of the arms  $U$ ,  $U'$ , and  $\kappa$  the impedance operator for the capacitor  $C$  under test.

The fundamental equations of the networks are then best derived by transforming the mutual inductance into a star of impedances from which mutual impedances are absent<sup>(6)</sup>. The results of these transformations are shown in

figures 3 a-b for the capacitance bridge, and figures 3 c-d for the inductance bridge. We then have to consider the four-arm bridges shown in figures 3 b and d, the equations of balance for which are easily seen to be

$$\mu_1 \kappa = \xi_1 (\zeta + \lambda - \mu_1), \quad \dots \dots (3 \cdot 1)$$

$$(\xi_2 + \mu_2) = \rho (\zeta + \lambda - \mu_2). \quad \dots \dots (3 \cdot 2)$$

In practice,  $\rho$  is made as nearly as possible equal to unity. We may write it therefore as  $1 + \theta$ , where  $\theta$  is a complex quantity of the first order of smallness. Thus equation (3.2) becomes

$$(\xi_2 + \mu_2) = (1 + \theta) (\zeta + \lambda - \mu_2). \quad \dots \dots (3 \cdot 3)$$

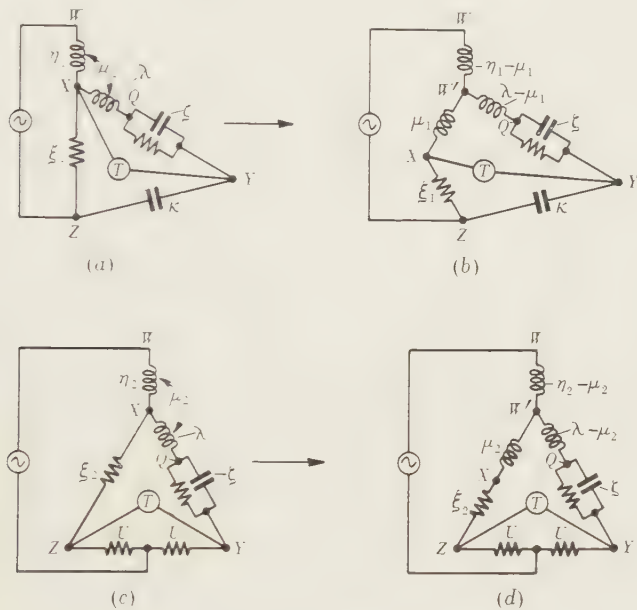


Figure 3. Network transformations.

The ratio arms  $U$ ,  $U'$  can be reversed, and balance can be restored by slight alterations in  $\xi_2$  and  $\mu_2$  to values  $\xi_2'$  and  $\mu_2'$ . We then have

$$(\xi_2' + \mu_2') = (1 - \theta) (\zeta + \lambda - \mu_2'). \quad \dots \dots (3 \cdot 4)$$

Now  $\theta (\mu_2 - \mu_2')$  will be of the second order of smallness and we may therefore, using  $\bar{\xi}_2$  and  $\bar{\mu}_2$  to represent mean values of  $\xi_2$  and  $\mu_2$ , write

$$\bar{\xi}_2 + \bar{\mu}_2 = \zeta + \lambda - \bar{\mu}_2. \quad \dots \dots (3 \cdot 5)$$

Thus  $\theta$  is eliminated from the equations.

Substituting for  $\zeta + \lambda$  from equation (3.5) in equation (3.1), we get

$$\kappa = \xi_1 (\bar{\xi}_2 + 2\bar{\mu}_2 - \mu_1) / \mu_1. \quad \dots \dots (3 \cdot 6)$$

From this equation the effective capacitance  $C$  and power factor,  $\gamma$  of the capacitor

under test can be calculated. If  $\omega/2\pi$  is the frequency of the alternating current in the networks, we may write

$$\left. \begin{array}{l} \kappa = 1/j\omega C (1 - j\gamma) \\ \mu_1 = j\omega M_1 (1 + \delta_{M_1}) \\ \mu_2 = j\omega M_2 (1 + \delta_{M_2}) \\ \xi_1 = R_1 (1 + j\delta_{R_1}) \\ \xi_2 = R_2 (1 + j\delta_{R_2}) \end{array} \right\}, \quad \dots\dots(3.7)$$

in which the  $M$ s represent mutual inductance, the  $R$ s represent resistance, the  $\delta$ s represent small phase angles, and  $j$  is the operator rotating through a right angle.

These values can now be substituted in equation (3.6). The approximate relationship  $C = M_1/R_1 R_2$  in equation (2.3) can be used in simplifying first-order terms, and further, since neither  $\delta_M$  nor  $\delta_R$  varies to any measurable extent for changes in  $M$  and  $R$  of the order assumed in equations (3.3) and (3.4), the question of mean values of  $\delta_M$  and  $\delta_R$  does not arise. We then find, writing  $\bar{M}_2$  and  $\bar{R}_2$  for the mean values of  $M_2$  and  $R_2$ ,

$$C = M_1 \{1 + \omega (M_1 \delta_{M_1} - 2M_2 \delta_{M_2})/\bar{R}_2\}/R_1 \bar{R}_2, \quad \dots\dots(3.8)$$

$$\gamma = \delta_{M_1} + \delta_{R_1} + \delta_{R_2} + \omega (2\bar{M}_2 - M_1)/\bar{R}_2. \quad \dots\dots(3.9)$$

The expression for  $C$  is still further simplified if we put

$$\omega M \delta_M = \sigma,$$

where  $\sigma$  is the impurity of the mutual inductance. The small correcting term in the bracket in equation (3.8) then becomes  $(\sigma_1 - 2\sigma_2)$ . In general

$$M_1 \doteq 2M_2,$$

and for most variable mutual inductances the law

$$\sigma M = \text{constant}$$

is approximately true. It thus follows that

$$(\sigma_1 - 2\sigma_2) \doteq 0$$

and that in general  $(\sigma_1 - 2\sigma_2)/\bar{R}_2$  will be completely negligible. We then have

$$C = M_1/R_1 \bar{R}_2. \quad \dots\dots(3.10)$$

The method thus automatically eliminates a number of small correcting terms and the final expression for  $C$  is similar to Carey Foster's classical expression for his d.-c. bridge.

The quantities  $\delta_M$ ,  $\delta_R$  are constants of the mutual inductance and the resistance  $R$  and their values can be predetermined for all values of  $M$  and  $R$ . Thus, from the practical viewpoint, the power-factor measurement is based on the two experimentally observed readings of  $M$  and on the value of  $R_2$ . The equation for power factor can in fact be written

$$\gamma = \Delta + \omega (2\bar{M}_2 - M_1)/\bar{R}_2, \quad \dots\dots(3.11)$$

where  $\Delta$  is a tabulated quantity characteristic of the circuit.

The values of  $C$  and  $\gamma$  so determined must be corrected for the residual capacitance and power factor of the leads connecting the condenser to the measuring circuit. This leads balance is easily obtained by disconnecting the condenser and balancing in the normal way. The value of  $M$  for this balance will of course be very small. Some practical aspects of the leads balance are dealt with in later sections of the paper.

The modification of the circuit equations arising from the presence of small stray impedances calls for very involved analysis which cannot be given in full here.\* A brief summary of some of the results of the analysis is given in an appendix, and it is deduced that, with the screening system and technique adopted, the residual stray impedances will introduce uncertainties of the order of 2 parts in  $10^6$  on capacitance values and uncertainties up to  $3 \times 10^{-5}$  on power-factor measurements at 1000 c./sec.

#### § 4. THE CONSTRUCTION OF THE BRIDGES

The facility with which a projected circuit and its associated screening system can be sketched out is often apt to mislead the experimenter into the belief that the practical problem of circuit arrangement and screening is correspondingly simple. This is by no means the case, for the circuit sketched as an open loop must in practice be arranged to have no appreciable magnetic field, and the disposition of leads in astatic pairs which are amenable to simple screening treatment and yet will not possess high capacitance or leakance to the screen, is too often in the end a matter of hopeful compromise. The problem was not made easier in the present instance by the need for assembling the bridges in permanent self-contained units of manageable size. Preliminary experiments brought out the desirability of building the inductometer as a separate instrument, the rest of the circuit forming a screened unit.

The design and construction of the variable mutual inductance have been described in detail elsewhere<sup>(8)</sup>. The screening of the instrument is exactly as shown in figure 2. The fixed, or secondary, winding has an inductance of just over 11 mH. and a resistance of 1 Ω. The adjustable windings provide a maximum mutual inductance of 11.11 mH., variation being provided by three decade dials and a slider, on which changes of 0.01 μH. can be easily read. The calibration of this instrument and the determination of its frequency errors and impurity will be referred to later.

The remainder of the bridge circuit is built up of units supplied by various instrument firms to specification. The resistance  $R$  is a non-reactive resistance box with 5 decade dials and a constant-inductance slidewire, giving a maximum value of 11, 111 Ω. It is mounted in a glass tank containing transformer oil and screened by fine-mesh copper gauze which encloses not only the resistance coils but also the switch dials. The screen is connected to one end of the resistance as shown in figure 2. The resistance  $P$  consists of a number of non-reactive units arranged on

\* A paper dealing with the effects of stray impedances in bridge networks has recently been published by one of the authors<sup>(13)</sup>.

a dial so that resistances of 0, 50, 100, 200, 500, 1000, 2000, 5000, 10,000  $\Omega$ . and infinity can be obtained. This is mounted, oil-immersed and screened, in the same way as the resistance  $R$ , and the switch dial is duplicated so that the capacitance  $K$  can be connected not only across the whole resistance but also across any section. The condenser  $K$  is an adjustable mica condenser of good quality, and of 1  $\mu\text{F}$ . maximum capacitance, with a continuously variable air condenser of 1000  $\mu\mu\text{F}$ . maximum capacitance as a fine adjustment. It was supplied by the makers with its own screen connected to one terminal.

The ratio arms are carried on a panel together with the switchgear for making the changeover from the capacitance to the inductance bridge, and are enclosed in a gauze screen connected to the earthed screens of the system. The Wagner arms are mounted on a separate panel. All the components are separated from each other by earthed screens by placing them in screened compartments in a screened box. These earthed screens are provided by facing the wooden structure of the box with sheets of perforated zinc. This makes a cheap, robust and efficient electrostatic screen without introducing large areas of metal into the system, for it must be remembered that the mutual inductance has to be placed within a reasonable distance of the apparatus and there must be no risk of affecting its properties as a result of this proximity.

The box containing the bridge circuits is about a metre long, 60 cm. wide and 25 cm. deep. The lid is made up of a number of thin aluminium panels through which the operating handles of the various switches and dials pass, and which carry the appropriate engraving. These panels, which complete the earthed screen of the system, are readily removable for inspection and cleaning of switchgear. A section of one panel is hinged and conceals the main terminal system of the bridge, consisting of a number of small screened compartments which are built up from thin aluminium sheet and house all the terminals necessary for the external connexions except those leading to the inductometer and test condenser, which it was considered expedient to place at opposite ends of the box. Besides the supply and detector terminals, each pair of which is in its own screened compartment, a pair of terminals is provided in shunt with the condenser  $K$  and another pair in series with the resistance  $P$ . These four terminals are enclosed in a double-screened compartment, the inner screen, which is insulated from the outer, being connected to the screens of  $P$  and  $K$ , while the outer screen is earthed. The points  $X$ ,  $Y$ ,  $Z$  and the common point of the ratio arms are brought by double leads to terminals and copper cups containing mercury all housed in screened compartments. The current and potential leads thus provided for the four arms of the inductance bridge allow the measurement of the d.-c. resistances of these arms to be made with high precision. The cup and terminal on the leads from the point  $X$  are enclosed in a double-screened compartment, the inner screen being connected to the screen of resistance  $R$  while the outer screen is earthed. All the leads to this terminal system are screened or double-screened to conform with the conditions at the corresponding bridge points. A plan of the layout is shown in figure 4, on which the lettering corresponds to that in figures 2 and 3.

The leads to the test condenser are twinned and separated from each other by earthed screens. The effective capacitance between them is thus kept low, and their series inductance is small. The series resistance of these leads is also made as small as possible by the use of wire of as heavy a gauge as is practicable, since the loss in the leads may affect the measured power factor of the condenser (see below). The leads to the mutual inductance are made in a robust rigid unit conforming to the same screening arrangements as the mutual inductance itself and, in determining the effective properties of the instrument, this leads system is regarded as part of it.

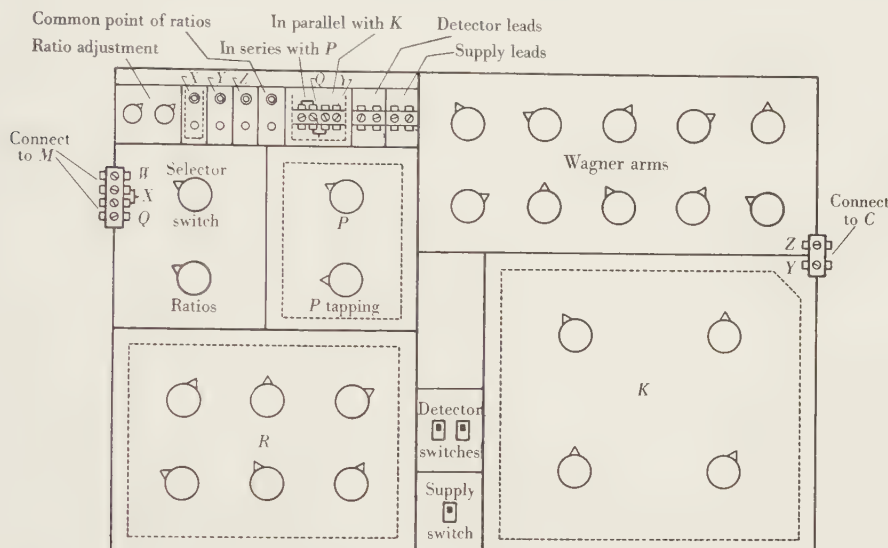


Figure 4. Plan of layout: full lines represent earthed screens, broken lines inner screens.

### § 5. OPERATING TECHNIQUE

The bridge is designed primarily for measurements at frequencies ranging from 50 c./sec. to 3000 c./sec., and the necessary supplies of current are assumed to be available. It may be taken as a general principle that the supply unit should be isolated from the bridge where possible as this makes for a stable system of earth-impedances and a consequent overall stability in the bridge balance points. In the present case, the isolation was effected by the use of a toroidal transformer, wound on a nickel-iron ribbon core and enclosed in an earthed screen, with an earthed screen separating the windings. The capacitance balancing of this transformer, although an attractive refinement, is not essential since a Wagner earthing arm is used. For audio-frequency work a valve amplifier and telephone are used as a detecting system, and these are isolated from the bridge by a transformer similar to that used in the supply circuit. The importance of the use of such a transformer here lies in the fact that it reduces the earth-impedances imposed on the detector

points and so facilitates the simultaneous balancing of the main bridge and the Wagner arm. If the earth-impedances of the detector points are allowed to assume magnitudes comparable with the impedances of the bridge arms, then this simultaneous balancing may prove difficult or even impossible; the balances may become divergent. For power-frequency work, a vibration galvanometer of the Campbell type is used as detector, and as a rule no amplifier is necessary.

Theoretically, the balance points are aperiodic when condensers of very low power factor are under test. In practice, however, circumstances may arise in which a departure from this condition is very marked, owing to the use of the  $P-K$  combination as a means of balancing out part of the self-inductance of the secondary winding of  $M$ . The effective resistance  $P'$  and effective inductance  $L'$  of a condenser  $K$  in shunt with a resistance  $R$  are given by the following equations, in which  $\omega/2\pi$  is the frequency:

$$P' = P/(1 + \omega^2 P^2 K^2), \quad \dots\dots(5.1)$$

$$L' = -KP^2/(1 + \omega^2 P^2 K^2). \quad \dots\dots(5.2)$$

The approximate forms already quoted,

$$P' = P$$

and

$$L' = -KP^2$$

are valid only if

$$\omega^2 P^2 K^2 \ll 1.$$

We may put

$$\omega^2 P^2 K^2 = \omega^2 (L - M)^2 / P^2$$

since

$$L' \approx L - M,$$

and the conditions under which the balance points tend to depart from aperiodicity can be more clearly shown. For the normal working of the bridge,  $M$  is the maximum reading of the inductometer and is therefore nearly equal to  $L$ . When  $P$  has its lowest practical value of 100  $\Omega.$ , the quantity  $\omega^2 (L - M)^2 / P^2$  is of the order of 0.001 at 1000 c./sec. For low values of  $M$ , which in the extreme case include the very small leads readings, the term becomes large and the balance point becomes more dependent on frequency. Since the technique of the method involves the determination of  $P'$  and  $L'$  in situ, no error arises from this, but a practical inconvenience may be caused if the harmonic content of the supply is high, for balance will be obtained only for the frequency  $\omega$ , and a background of harmonics remains in the telephone. Similar conditions may sometimes arise in establishing the Wagner balance, but the use of a simple resistance volume-control in shunt with the telephone is surprisingly effective in establishing good conditions for rapidly working into balance from a fairly large out-of-balance voltage, even when the harmonic content of the supply is as high as 5 per cent.

An examination of equations (5.11) will show that for measurements on condensers of poor power factor at power frequencies, the quantity  $(2M_2 - M_1)$  may be very large, and in fact it may well be that for some conditions the effective inductance of the arm  $ZY$ , even with  $K$  at zero, is too small to satisfy the conditions of balance. In the few cases in which this condition does arise the difficulty can be

met very neatly without the introduction of any extraneous inductive coils by the device of connecting a condenser between a tapping point on the  $P$  resistance and the Wagner earth point. The effect of a capacity  $C_e$  connected in this way and flanked by resistances  $P_1$  and  $P_2$ , is to increase the inductance of the arm by an amount  $C_e P_1 P_2$ .\* The calibration and general quality of this condenser need not be of a high order, and by slightly overadjusting it the power factor balance can be made in the normal way on  $K$ . The successful use of this device depends, of course, on the correct adjustment of the Wagner arms.

When the circuits are switched over to the inductance bridge, all the adjustments in the  $P$  arm remain unaltered and balance is obtained by adjusting  $M$  and  $R$ . The series resistance  $r_3$ , figure 2, in the Wagner arm is best reduced to zero for this arrangement. A switch is provided for reversing the ratio arms, as was indicated in § 3. It is important that this switch shall effect the reversal without altering  $\theta$ , and, in addition,  $\theta$  should be as small as possible to start with. Part of

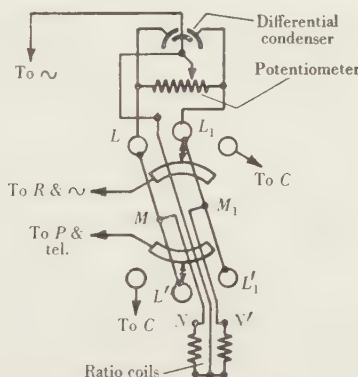


Figure 5. Arrangement of ratio adjustor and reversing switch.

the wiring of the reversing switch is shown in figure 5. The heavy copper leads  $LML'$ ,  $L_1M_1L'_1$ ,  $MN$ , and  $M_1N'$  connect the studs of the switch and the actual coils. Preliminary adjustment was made during assembly to bring  $M$  and  $M_1$  to the mid-points of  $LL'$  and  $L_1L'_1$  respectively, and  $MN$  and  $M_1N'$  were adjusted for equality. The connexions between the switch and coil were thus made equal in resistance within less than  $0.001\Omega$ . for both positions of the switch. In order to reduce  $\theta$ , a small panel is incorporated in the system carrying a potentiometer of about  $500,000\Omega$ . resistance and a differential air condenser of about  $200\mu\mu F$ . capacitance. The connexions of these components to the ratio arms and reversing switch are shown in figure 5. This system can be preset, and equality of resistance and phase angle can be checked by reversal, and once this has been done subsequent reversals can be omitted in a series of measurements.

Reference has already been made to the leads passing to the terminals to which the test condenser is connected. Exigencies of design necessitated that these leads

\* It can be shown that this device does introduce a small error in the determination of  $R_2$ , but at the low frequencies at which this scheme is used, the error does not exceed 2 parts in  $10^5$ .

should be nearly a metre long, and in spite of all available precautions they possess resistance and inductance of such magnitudes that allowances must be made for these quantities in measurements on condensers of large value. If  $r$  and  $l$  are respectively the resistance and inductance of the leads, then at a frequency  $\omega/2\pi$  c./sec. the effective capacitance of the condenser under test is increased by a fraction  $lC\omega^2$  and its power factor by  $rC\omega$ . In the present case, the measured values are  $r=0.030 \Omega.$  and  $l=1.04 \mu\text{H}.$ , so that at 1000 c./sec. the corrections on a  $1-\mu\text{F}.$  condenser are 4 parts in  $10^5$  on capacitance and 0.0002 on power factor. As  $r$  and  $l$  are known to within 5 per cent, the application of these corrections is not likely to introduce any significant errors.

The phase defect of the mutual inductance and the phase angle of  $R$  are found by reference to appropriate standards. Hartshorn<sup>(9)</sup> has described the use of a special standard of mutual inductance, the characteristics of which are determined from radio-frequency measurements, as a method for determining phase defect, while one of the present authors<sup>(10)</sup> has described a series of resistors of calculated phase angles which are used for determining the phase angle of resistances of any magnitude. The phase defect of the specially constructed screened mutual inductance was negligibly small (less than 0.00002 radian) at all settings at a frequency of 1000 c./sec. The phase angle of the resistance  $R$  was determined for a number of settings, and the effects of variation of  $R$  on this phase angle were studied in sufficient detail to enable the phase angle for any combination of the dials to be deduced. The variation with frequency of the magnitudes of  $M$  and  $R$  has also been investigated, the former by assuming the invariability with frequency of a standard air condenser, which is measured on the bridge at various frequencies. This method of measurement, the results of which have been confirmed by tests against condensers ranging in value from 1000 to 10,000  $\mu\mu\text{F}.$ , has the advantage that the effects of certain stray impedances (see appendix) are correctly allowed for. The capacitance between the resistance  $R$  and its screen acts in shunt with the resistance and might therefore be expected to alter the effective resistance for large resistances at audio-frequencies. The comparison of  $R$  with resistors known to be invariable with frequency up to 10,000 c./sec. showed that at a setting of 10,000  $\Omega.$  the change of  $R$  with frequency was only 4 parts in  $10^5$  at 1000 c./sec. It is concluded that the properties of  $M$  and  $R$  are known with sufficient accuracy to permit the use of the bridge at frequencies up to 3000 c./sec.

The absolute calibration of  $M$  is determined by a building-up system, starting from a direct comparison between  $M$  at the setting of 10 mH. and the primary standard of mutual inductance<sup>(8)</sup>. The values of  $R$  are determined by comparison with laboratory standard manganin coils. A set of such standards in pairs of 100, 1000 and 10,000  $\Omega.$  will give, by the use of parallel and series connexions, a range of standard values of 50, 100, 200, 500, 1000, 2000, 5000 and 10,000  $\Omega.$ , and the values of  $R$  and  $P$  are chosen to fall in this series. The calibration of  $M$  is thus obtained in absolute c.g.s. units and the values of  $R$  are obtained in terms of laboratory standards calibrated both in absolute and in international units of resistance<sup>(11)</sup>.

The value of  $C$  is thus obtained either in international units or in absolute units. The former is the value in general use in industry at the present time, but if the recommendations of the International Bureau of Weights and Measures are adopted, the latter will come into use in 1940. The relation, derived from the work mentioned above, is

$$1 \mu\text{F. international} = (1 - 50 \times 10^{-5}) \mu\text{F. absolute.}$$

In carrying out an actual calibration, the values of  $P$  and  $R$  are first chosen to give a convenient reading of  $M$ . Balance is obtained first on the capacitance bridge by adjusting  $M$  and  $K$ , the circuit is then changed over to the inductance bridge, and balance is obtained by adjusting  $M$  and  $R$ , the presetting of the ratio arms for equality of resistance and phase angle having been carried out. The two settings of  $R$  are then compared with the appropriate d.-c. standards. The high quality of the resistance  $R$ , together with the fact that, owing to oil immersion, its thermal stability is of a high order, makes it unnecessary to carry out these d.-c. calibrations for every test. The test condenser is then disconnected and the leads readings are obtained in an exactly similar manner. From these the effective capacitance and power factor of the leads are calculated, and the appropriate corrections are applied. It is found that the leads power-factor correction is less than 0.0001 for capacitances greater than 2000  $\mu\mu\text{F}$ . The leads readings can actually be regarded as circuit constants and it is not generally necessary to determine them on every occasion.

As an overall test of the equipment, a three-dial mica condenser of total capacitance 1  $\mu\text{F}$ . was calibrated throughout its range for capacitance and power factor at 1000 c./sec. A set of values was also obtained by a building-up method<sup>(12)</sup> in which the values of power factor are deduced on the assumption that the power loss of a standard air condenser remains constant for all scale settings, while the capacitance values are related to a single value (0.1  $\mu\text{F}$ ) measured on the new bridge. In the following table are given the maximum and mean deviations between the values obtained by the two methods. The range of capacitance values covered was 0.001 to 1.0  $\mu\text{F}$ . and the table is drawn up in three sections, covering respectively the ranges 0.001 to 0.01  $\mu\text{F}$ ., 0.01 to 0.1  $\mu\text{F}$ . and 0.1 to 1.0  $\mu\text{F}$ .

Table I

Deviation	Capacitance ( $\mu\text{F}$ .)			Power factor		
	0.001 to 0.01	0.01 to 0.1	0.1 to 1.0	0.001 to 0.01	0.01 to 0.1	0.1 to 1.0
Maximum	20 parts in $10^5$	4 parts in $10^5$	10 parts in $10^5$	0.00009	0.00008	0.00008
Mean	8 parts in $10^5$	1 part in $10^5$	6 parts in $10^5$	0.00005	0.00004	0.00003

The conclusion is therefore drawn that the effects of stray impedances have been correctly assumed to be negligible and that the validity of the fundamental equations (3.10) and (3.11) is such that at 1000 c./sec. the probable limits of error on capacitance do not exceed  $\pm 5$  parts in  $10^5$ , and those on power factor do not exceed  $\pm 0.00005$  for capacitances in the range 0.001 to 1  $\mu\text{F}$ .

The values recorded in the above table represent the results of a single series of measurements, taken without any checks. Numerous tests on subsequent occasions have shown that the accuracy estimated above may easily be doubled in any special case.

The bridge has been used successfully at 50 c./sec. and the agreement found on capacitances ranging from 0.01 to 1  $\mu\text{F}$ . was substantially that found above for the measurements made at 1000 c./sec. The performance of the bridge at frequencies higher than 1000 c./sec. has not yet been explored in the same detail, but measurements have been made at a frequency of 3000 c./sec. on capacitances as low as 5000  $\mu\mu\text{F}$ . with results which suggest that the accuracy is not worse than one-half that at 1000 c./sec.

#### § 6. CONCLUSION: GENERAL UTILITY OF THE CIRCUIT

The experience obtained with the bridge has shown it to mark a very great advance on the systems which have preceded it, not only as regards the reliability of the results but also in the speed with which the measurements can be made. Routine tests have been carried out on condensers up to 2  $\mu\text{F}$ . capacitance and the practical upper limit of the measurable capacitance is regarded as 4  $\mu\text{F}$ ., for which  $P=R=50 \Omega$ ., although in special cases capacitances as high as 10  $\mu\text{F}$ . could be measured with a somewhat diminished accuracy.

The circuit was primarily designed as a capacitance test set and it is considered to have fulfilled the original requirements. It is, however, very flexible and can be used for a number of other purposes. Incorporating as it does a Campbell-Heaviside self-inductance bridge, it can obviously be used for measuring self-inductances, and its range as a self-inductance bridge has been extended by the inclusion of additional ratio coils giving ratios of 10/1 and 100/1. The Campbell-Heaviside circuit cannot at this stage be regarded as suitable for high-precision measurements on large inductances at audio-frequencies, and for such measurements power frequencies are to be preferred. Small self-inductances of the order of a few microhenries may also be conveniently measured on the bridge if the inductometer is removed and replaced in the circuit by short-circuiting links, effective variations of self-inductance being obtained by variation of  $K$ . When the inductometer is removed, the bridge can also be used as a series-arm resonance bridge, a self-inductance being inserted in the  $P$  arm while  $P$  itself is set to infinity. The condenser  $K$  and the added inductance can then be put in series, and the bridge so adjusted can be used for the measurement of frequency or of total harmonic content of a supply wave.

#### APPENDIX: THE EFFECT OF STRAY IMPEDANCES<sup>(13)</sup>

*Stray impedances internal to the bridge.* The references are to figure 3. Stray impedances between  $Q$  and  $X$ ,  $X$  and  $W$ ,  $W$  and  $Q$ ,  $W$  and  $Y$ , and  $X$  and  $Y$ , modify the properties of  $M$  and of the  $P$  and  $R$  arms. The characteristics of these

components are determined in situ and therefore include the effects of these impedances.

A small admittance  $\Gamma_1$ , between  $Q$  and  $Z$ , figure 3*b*, leads to a modification of equation (3·6) to

$$\kappa = \frac{\xi_1}{\mu_1} [\xi_2 + 2\mu_2 - \mu_1 + \Gamma_1 \{(\lambda - \mu_1)(\zeta + \kappa) - \zeta(\xi_2 + \lambda)\}]. \quad \dots\dots(A\ 1)$$

If  $\Gamma_1 = j\omega C_1$ , where  $C_1$  is a small capacitance, the above equation can be interpreted for three important practical cases:

- (a)  $\lambda \doteq \mu_1$ ,
- (b)  $\lambda \doteq 2\mu_1$ ,
- (c)  $\lambda \gg \mu_1$  and  $\mu_1 \rightarrow 0$ .

Let  $L$  be the reactive part of  $\lambda$ , so that  $L$  is the self-inductance of the secondary of  $M$ , and let the resistance of the secondary be negligible in comparison with  $R_1$  and  $R_2$  (in practice it does not exceed 1 per cent of these values). Then the errors,  $\Delta C$  and  $\Delta\gamma$ , in  $C$  and  $\gamma$  are as summarized in table 2:

Table 2

Case	$\Delta C/C$	$\Delta\gamma$
$\lambda \doteq \mu_1$	$\omega^2 M_1 C_1$	$\omega C_1 R_2$
$\lambda \doteq 2\mu_1$	○	$\omega C_1 (R_2 - R_1)$
$\lambda \gg \mu_1$ and $\mu_1 \rightarrow 0$	○	$\omega C_1 L / CR_2$

The third case is interesting, for it corresponds to the leads reading, for which  $\gamma$  was found to be 0·007 and  $C$  was 28  $\mu\mu F$ . If the whole of the leads power factor be assumed to be due to  $C_1$ , then  $C_1$  can be estimated from the above result, giving a value of 8  $\mu\mu F$ . This therefore is an upper limit to the probable value of  $C_1$ , from which maximum probable values of  $\omega^2 M_1 C_1$  and  $\omega C_1 R_2$  can be calculated, giving the figures already quoted on p. 43.

*Stray impedances to earth.* Stray impedances to earth from the points  $W$ ,  $Y$  and  $Z$  are dealt with by the Wagner arm in both circuit arrangements. Impedances to earth from  $Q$  and  $X$  (the latter in the inductance bridge) are not dealt with. If admittances  $\Gamma_2$  and  $\Gamma_3$  connect  $Q$  and  $X$  respectively to earth, equation (3·6) must be modified to

$$\mu_1 \kappa = \xi_1 [\xi_2 + 2\mu_2 - \mu_1 - \{\Gamma_2 \zeta (\mu_1 - \mu_2) - \Gamma_3 \xi_2 \mu_2\}]. \quad \dots\dots(A\ 2)$$

Assuming  $\Gamma_2 \doteq \Gamma_3 = j\omega C_2$ , the interpretation for the important cases  $\mu_1 \doteq 2\mu$  and  $\mu_1 \doteq 0$  can be given in simple form. In the first case  $M_2$  can be regarded as being altered by a fraction  $\omega^2 C_2 (2M_2 - L)$  which is almost always negligible since generally  $2M_2$  and  $L$  are of the same order. In the second case the leads power factor is altered by an amount  $\omega M_2 \cdot \omega^2 L C_2 / R_2$ , which is quite negligible for any reasonable value of  $C_2$  at audio-frequencies.

## REFERENCES

- (1) CAMPBELL. *Proc. Roy. Soc. A*, **79**, 428 (1907).
- (2) ASTBURY. *Phil. Mag.* (7), **25**, 290 (1938).
- (3) CAREY FOSTER. *Phil. Mag.* **23**, 121 (1887).
- (4) CAMPBELL and CHILDS. *The Measurement of Inductance, Capacitance and Frequency*, p. 360. (Macmillan, London, 1935.)
- (5) DYE. *Electrician*, **87**, 55 (1921).
- (6) BUTTERWORTH. *Proc. Phys. Soc.* **33**, 312 (1921).
- (7) CURTIS, SPARKS, HARTSHORN and ASTBURY. *Coll. Res. Nat. Phys. Lab., Lond.*, **24**, paper II (1932).
- (8) ASTBURY and FORD. *Phil. Mag.* (7), **25**, 1009 (1938).
- (9) HARTSHORN. *Proc. Phys. Soc.* **38**, 302 (1926).
- (10) ASTBURY. *J. Instn Elect. Engrs*, **76**, no. 460, p. 389 (1935).
- (11) HARTSHORN and ASTBURY. *Philos. Trans. A*, **236**, 442 (1937).  
VIGOUREUX. *Coll. Res. Nat. Phys. Lab., Lond.*, **24**, paper VIII (1937).
- (12) FORD and ASTBURY. *J. Sci. Instrum.* **15**, no. 4 (April 1938).
- (13) ASTBURY. *Phil. Mag.* (7), **26**, 507 (1938).

# TRANSMISSION OF SOUND BETWEEN NEIGHBOURING ROOMS IN A BRICK BUILDING

By J. E. R. CONSTABLE, M.A., PH.D., B.Sc., Physics Department,  
National Physical Laboratory, Teddington, Middlesex

*Received 30 June 1938. Read 28 October 1938*

**ABSTRACT.** A detailed investigation has been made of the mechanism by which sound is transmitted between adjacent rooms in brick buildings. The relative importance of sound transmitted by the intervening partition and by the flanking walls and floors is deduced from measurements of their vibration, and it is shown that indirect transmission by the flanking walls and floors can be markedly greater than direct transmission through the intervening partition. It is shown, for example, that in one pair of average rooms the sound transmitted indirectly was about six times as much as that transmitted directly. A method of predicting the importance of the indirect transmission in any given case is described. It is concluded that in average buildings there is probably no advantage to be gained by installing partitions of special construction having sound-reduction factors greater than 55 or 60 decibels.

## § I. INTRODUCTION

TRANSMISSION of sound through the structure of a building is important both because sound reaches, in this way, parts of a building which are remote from the original noise and also because, as has been mentioned in an earlier paper<sup>(1)</sup>, conduction along the flanking walls and floors limits the insulation obtainable between neighbouring rooms. This form of transmission has been referred to as transmission by indirect paths to distinguish it from direct transmission through an intervening partition.

It is important to study the indirect transmission in an average building so that it can be allowed for in sound-insulation schemes. It is important, also, to ascertain whether the effect can be minimized by varying the construction of the building or by a suitable choice of material.

A few measurements have been made by different workers in various types of building of the attenuation of sound travelling through the building fabric. A. Gastell<sup>(2)</sup> has measured subjectively the transmission of impact sounds in steel-frame buildings and in ordinary brick buildings, and has concluded that transmission by indirect paths is less important in those of the latter type. Berg and Holtsmark<sup>(3)</sup> have made objective measurements in an ordinary brick building of the transmission of audio-frequency vibration originated by a loudspeaker and conclude that sound is attenuated by an average amount of  $\frac{1}{2}$  db./ft. in such buildings. The author made similar measurements<sup>(1)</sup> in a reinforced-concrete building and observed an attenuation of about the same amount for a frequency of 200 c./sec.

In the present paper the chief problem discussed is the effect of indirect transmission upon the sound-insulation between a pair of adjacent rooms. A source of sound in one room generates vibrations in all the boundaries of the room. One of these boundaries, the partition between the rooms, is common to both rooms, and by its vibration will radiate sound directly into the second room. Of the remaining five boundaries, one, the wall opposite the partition, has no direct connexion with the second room; the other four, the flanking walls and floors, are extensions of the corresponding walls and floors in the second room and vibration can be conducted along them from one room to the other. Each wall may be taken to radiate sound energy in amounts proportional to the product of its area and of its mean square

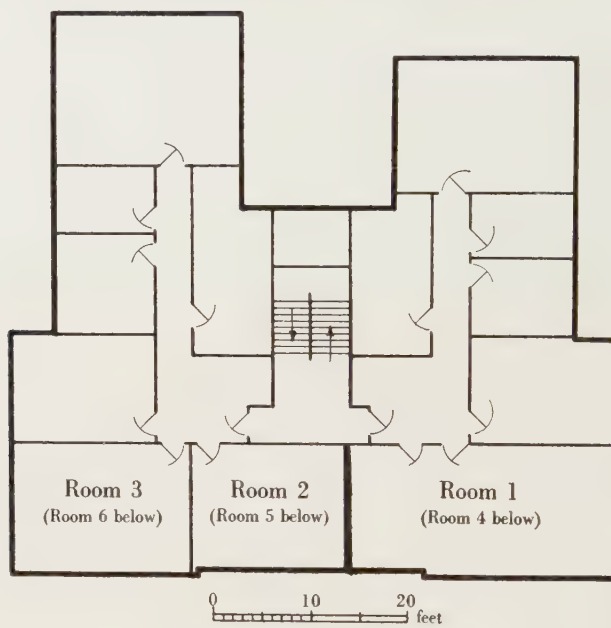


Figure 1.

amplitude of vibration. That radiated by the common partition constitutes the *direct sound* while that radiated by the other surfaces constitutes the *indirect sound*, and it was the purpose of the measurements described below to determine the relative importance of the two paths.

Two buildings have been investigated, the measurements in one being on a more extensive scale than in the other. The first consisted of a modern block of flats built with brick. The building is approximately in the form of a square, is four storeys high, and contains two suites of rooms on each floor. The room-distribution is shown in figure 1, which is a plan of the second floor and is representative of the lay-out on all floors. The outer wall is of cavity construction, consisting of two  $4\frac{1}{2}$ -in. brick leaves separated by 2-in. air space, and the floors are of reinforced concrete  $5\frac{1}{2}$  in. thick covered with a wood floating floor insulated with rubber blocks. The interior walls consist mainly of plastered 3-in. hollow-tile partitions.

A set of six rooms was selected, figure 2, the central rooms of which were divided from the remaining rooms by a plastered 9-in. brick wall on one side and a plastered 3-in. clinker concrete wall on the other. This disposition enabled the transmissions through the two partitions to be compared under identical conditions.

### § 2. DESCRIPTION OF MEASUREMENTS

A warbling note was generated in room 2, figure 2, by a loudspeaker and the intensity of the air-borne sound in each of the rooms was determined. Frequencies of 200, 700 and 2000 c. sec. were used for the measurements. The mean square amplitude of vibration of certain of the walls was also determined, a modified form of loudspeaker movement being used for this purpose. This instrument proved sufficiently sensitive to detect the vibration generated in a wall by a 50-w. loudspeaker working in a room over 100 ft. away.

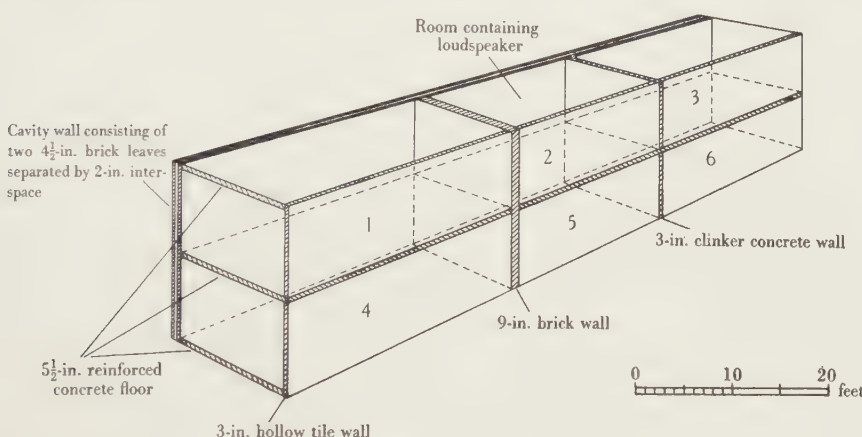


Figure 2.

The measurements of the intensity of the air-borne sound gave the acoustical insulation against transmission vertically, horizontally and diagonally from the room containing the loudspeaker. The vibration measurements enabled the relative amounts of air-borne sound radiated by each of the walls to be calculated.

Careful check measurements were made to confirm that the sound measured had actually been transmitted through the building structure and was not appreciably contributed to by sound leaking through apertures—for example, through gaps round the edge of doors.

### § 3. RESULTS

The results obtained are given in table 1.

It will be seen that, as was to be expected, the 9-in. brick wall is more insulating than the clinker concrete wall, the difference between the average insulations being 6 db. Actually, the difference which would have been expected from laboratory measurements is between 10 and 12 db. The observed effective sound-insulation of each partition is less by at least 5 db. than the figure determined by laboratory

Table 1. Acoustical insulation against horizontal, vertical and diagonal transmission in set of rooms shown in figure 2

Mode of transmission	Acoustical insulation (db.)			Mean acoustical insulation
	At 200 c./sec.	At 700 c./sec.	At 2000 c./sec.	
Horizontal transmission from room 2 to room 1 through 9-in. brick wall weighing 90 lb./ft <sup>2</sup>	40	45	52	46
Horizontal transmission from room 2 to room 3 through 3-in. clinker concrete wall weighing 20 lb./ft <sup>2</sup>	36	40	45	40
Vertical transmission from room 2 to room 5 through 5½-in. reinforced-concrete floor covered with wood floating floor insulated with rubber blocks and weighing 65 lb./ft <sup>2</sup>	38	47	57	47
Diagonal transmission from room 2 to room 4	45	51	61	52
Diagonal transmission from room 2 to room 6	44	52	62	52

measurements for the sound reduction factor. The difference may in part be accounted for by the reverberation of the receiving room, though, as will appear later, there are other reasons for expecting the measured insulation to be lower than the laboratory figure. The total absorption in these rooms was not determined, so that a correction cannot be applied for this factor. By making the reasonable assumption, however, that the room surfaces each had the same average absorption coefficient, we find that the differences between the corrections to be applied to the values obtained for the insulation of the two walls would be about 1 db. only. This is insufficient to account for the fact referred to above, that though the difference between the observed insulations should have been 10 db., it was actually only 6 db. To ascertain whether this effect arose from some unusual behaviour on the part of the partitions themselves, measurements were made of the actual vibration of the brick and clinker concrete walls. The mean differences between the vibration of the brick wall and of the clinker concrete wall are shown in table 2.

Table 2. Amount by which the mean square amplitude of vibration of the brick wall was greater than that of the clinker concrete wall

Frequency (c./sec.)	Difference between mean square amplitude of vibration of walls (db.)
200	9
700	14
2000	15

It will be observed that the average difference between the mean square amplitudes of vibration was 13 db., which differs, by an amount exceeding the experi-

mental error, from the difference between the intensities of the air-borne sound (6 db.) and corresponds more nearly with what would have been expected from laboratory measurements.

It is clear therefore that sound was not transmitted through the intervening partitions only. As check measurements indicated that the additional transmission did not occur by doorways or windows, there is ground for believing that transmission along the flanking wall and floors may have been responsible. To test this point, measurements were made of the vibration of all the walls of rooms 1 and 3. It was not possible to determine the vibration of the structural floor as it was covered with an insulated wood floating floor and the amount of sound transmitted through the gaps between the floor boards was uncertain; the ceiling could not easily be reached and was for this reason not measured. The relative proportions of sound radiated by the partition and by the remaining surfaces of the room were calculated on the assumption (justified by measurements made in other buildings) that the ceiling had the same average amplitude of vibration as the walls, the radiation from the floor being neglected. Neglecting the floor involves only a small error, probably only of the order of 1 db., since its area is only about half that of the walls. The vibration of the windows, which could not be measured since it would be altered by the pressing of a vibration detector against the glass, was assumed to be the same as that of the walls. Actually the area of the windows was only a fraction of that of the walls, so probably no appreciable error is involved. In the calculation allowance had to be made for the fact that the vibration in the flanking walls decreased as the distance from the room containing the loudspeaker increased. A number of measurements had been made at equally spaced points on these walls and the arithmetic mean of the squares of the observed amplitudes was taken as the mean square amplitude of the wall. The contribution of sound energy from the wall was taken as proportional to the product of the area of the wall and the mean square amplitude of vibration. In view of the practical difficulty of determining ceiling vibration, measurements of the indirect transmission to room 5, below room 2, were not made. The results obtained are given in table 3 and show the amounts by which the sound transmitted by indirect paths exceeded that transmitted through the partitions.

Table 3. Calculated contribution of sound transmitted by indirect paths in the set of rooms shown in figure 2

Mode of transmission	Intervening partition	Excess of indirect transmission over direct transmission through partition (db.)		
		At 200 c./sec.	At 700 c./sec.	At 2000 c./sec.
Horizontally from room 2 to room 1	9-in. plastered brick wall	7	8	8
Horizontally from room 2 to room 3	3-in. plastered clinker concrete wall	1	0	1

It will be seen that the indirect paths were definitely predominant in the case of transmission between rooms 1 and 2, but that in the case of transmission between rooms 2 and 3 they were only of an importance comparable with that of the direct transmission. The explanation is to be sought partly in the greater insulating value of the 9-in. brick wall between rooms 1 and 2 and partly in the fact that in room 1 the area of the flanking walls was larger in comparison with the area of the partition than it was in room 3. The figures given for the indirect transmission enable the insulation provided by the partitions alone\* to be deduced from the observed insulation between the rooms.

Using results averaged for all three frequencies, we find that the insulation provided by the brick partition alone is about 55 db. while that provided by the

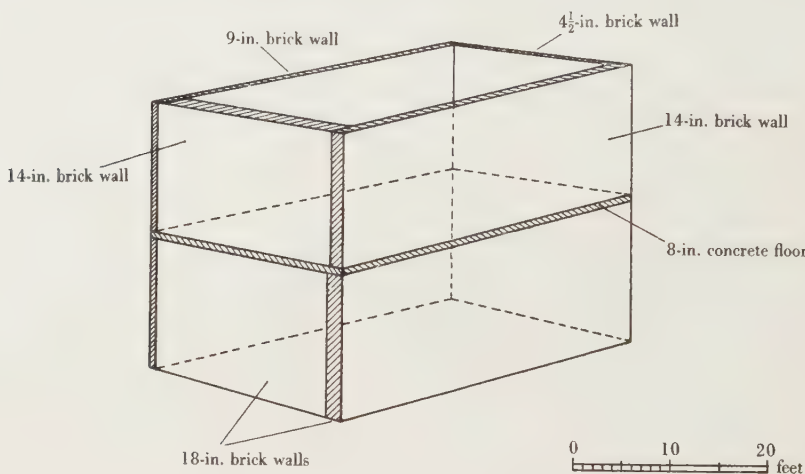


Figure 3.

clinker concrete partition alone is about 43 db. The difference between these insulation figures is 12 db. which is in very satisfactory agreement with the difference, 13 db., obtained by measurements of the actual vibration of the two walls, and also with laboratory measurements.

A similar but less extensive series of measurements was made on a pair of rooms, one vertically above the other, in a 3-storey building built with brick walls and 8-in. reinforced-concrete floors. Each room was bounded on two sides by the exterior brick wall which was 18 in. thick in the case of one room and 14 in. thick in the other. The construction is shown diagrammatically in figure 3. A loudspeaker was operated in one room and measurements of the intensity of the air-borne sound were made in the other, the concrete floor acting as a partition between them. Measurements of the vibration of the walls and floor enabled an estimate to be made of the relative amounts of sound transmitted by direct and indirect paths. The results obtained are given in table 4.

\* This calculation does not include an allowance for the reverberation of the rooms.

Table 4. Transmission of sound between two rooms separated by an 8-in. concrete floor

Frequency of test sound (c./sec.)	200	700	1000
Measured insulation against air-borne sound (db.)	33	45	50
Excess of indirect transmission over direct transmission through floor (db.)	3½	2	2
Decrease of effective insulation of floor due to indirect transmission (db.)	5	4	4

It will be seen that the indirect transmission was markedly greater than the direct transmission. Accordingly any improvement in the insulation provided by the floor alone would have a negligible effect.

#### § 4. DIAGONAL TRANSMISSION

Measurements of the wall vibration were also made to examine the transmission diagonally between rooms 2 and 4, figure 2. From these results it was possible to calculate the difference to be expected between the air-borne sound-intensities in rooms 1 and 4, i.e. the difference between the insulation against horizontal and diagonal transmission. The figure obtained was within 1 db. of the experimentally observed figure, a satisfactory agreement. It has previously been assumed that a measurement of the insulation against diagonal transmission provides an indication of the contribution made, in the case of horizontal or vertical transmission, by the sound transmitted along indirect paths. The results show that this criterion is unreliable; for the insulation against diagonal transmission is, as is shown in table 1, considerably greater than that for horizontal and vertical transmission, yet, as is shown in table 3, indirectly transmitted sound is predominant in at least one room. The reason for this apparent discrepancy lies in the fact that the vibration of the walls is attenuated by several decibels along the length of the flanking walls, this attenuation being more important in the case of diagonal transmission than for horizontal or vertical transmission. Roughly speaking, the wall vibration is halved in intensity for every increase of 6 ft. in the distance from the boundaries of the room containing the loudspeaker. The areas of wall nearest this room contribute most to the indirectly transmitted sound. In the case of horizontal or vertical transmission there is a substantial area of wall, near the room containing the source of sound, which vibrates with about the same amplitude as that part of the flanking wall which bounds the room containing the source of sound. As far as diagonal transmission is concerned, however, there is only a small area, in the corner adjacent to the room containing the source of sound, which vibrates with the maximum amplitude.

### § 5. POSSIBILITY OF PREDICTING MAGNITUDE OF INDIRECT TRANSMISSION

In view of the importance, shown by these measurements, of transmission by indirect paths, a method of calculating the magnitude of the effect when buildings are being designed would be valuable. The results obtained during the measurements in the buildings referred to in this paper throw some light on this point.

It is to be expected that the relative amplitudes of vibration of the walls of the room containing the source of noise will be calculable with sufficient accuracy from the curves relating sound-transmission through solid walls with their weight<sup>(4)</sup>. This is confirmed by measurements made in the buildings referred to in the present paper. The amplitudes of vibration of three of the bounding walls of room 2, figure 2, could be measured readily from outside the room. The vibration of the exterior flanking wall could not be measured, for obvious reasons, on the section of it which formed part of room 2. Measurements of the vibration of this wall in the rooms 1 and 3, close against the partitions dividing these rooms from room 2, showed, however, an amplitude slightly greater than that of the 9-in. brick partition, a result which accords with the weight of the wall. Similarly, measurements of the vibration of the exterior wall of the rooms shown in figure 3 proved that the amplitude was one or two decibels less than that of the floor, a difference to be expected from the relative weights. This behaviour may possibly be explained as follows. Where two walls or a wall and a floor meet they must, obviously, vibrate with the same amplitude. Hence, it is to be expected that, whatever the amplitude of vibration of the walls and floors bounding a room which contains a source of sound may be, the vibration of prolongations of these walls and floors will be influenced by the vibration of the other walls and floors to which they are connected. It is to be expected on this account that the observed attenuation of vibration travelling along a light wall will, in suitable circumstances, suffer a sharp change where the wall comes into contact with a heavier wall or floor. In fact, in rooms remote from that containing the source of sound, the amplitude of vibration of the walls and floors may be expected to tend towards the same average value; the vibration of the heavy elements may be supposed to have been increased by their contact with the light elements and conversely. In actual buildings the majority of the walls and floors usually seem to have weights of the same order, and hence would in any event be expected to vibrate with about the same amplitude; certain of the partitions have a light construction, however, and in the light of the foregoing discussion it is to be expected, as was found experimentally, that their amplitude of vibration will, except where they form part of a room containing a source of sound, be about the same as that of the heavy walls and floors in their neighbourhood.

This circumstance fortunately limits the importance of indirect transmission. However, since the area of the flanking walls and floors in rooms of average shape tends to be large in comparison with that of the partition, it will be seen that when the partition has about the same insulating value as the walls, the contribution of

sound from the latter is likely to exceed that from the partition as, indeed, was shown in the case of the rooms described in this paper.

Normally, partition walls would not be made heavier than the heaviest flanking wall, which is often an exterior wall, and attempts to improve the insulation of the partition wall would be made by adopting double or complex construction rather than by adding to its weight. Without additional weight the partition would not restrict the vibration of the flanking walls attached to it, so that there would seem to be no point in making such partitions much more insulating than the heaviest flanking walls and floors would be if they were treated as partitions. This means that in average buildings there is probably no point in installing partitions of special construction having sound-reduction factors greater than 55 or 60 db., unless steps are taken to reduce the indirect transmission. In certain circumstances increasing the weight of the partition might decrease the vibration of the flanking walls and thus effect an improvement, but this would only be expected to occur if the partition were heavier than any of the flanking walls and floors—a condition which is probably rare.

#### § 6. ACKNOWLEDGEMENTS

The author desires to acknowledge the assistance given by R. Berry, W. C. Copeland, and P. Kinghorn in making the measurements described in this paper. His thanks are due to Dr A. H. Davis and Dr G. H. Aston for helpful discussion and suggestions, and to Dr G. W. C. Kaye, Superintendent of the Physics Department, for encouragement and advice.

#### REFERENCES

- (1) CONSTABLE, J. E. R. *Proc. Phys. Soc.* **50**, 368 (1938).
- (2) GASTELL, A. *Akustische Z.* **1**, 24 (Sept. 1936).
- (3) BERG, R. and HOLTSMARK, J. *Proc. Roy. Norwegian Sci. Soc.* **6**, 22 and **7**, 14.
- (4) CONSTABLE, J. E. R. and ASTON, G. H. *Phil. Mag.* **23**, 161 (1937).

## ROTATIONAL ANALYSIS OF THE ULTRA-VIOLET BANDS OF GERMANIUM MONOXIDE

By A. K. SEN GUPTA, M.Sc., the University College of Science  
and Technology, Calcutta

*Communicated by Prof. P. N. Ghosh, 9 May 1938. Read in title 24 June 1938*

**ABSTRACT.** From measurements on high-dispersion spectrograms, rotational structure analysis is made of the (1, 0), (2, 0) and (0, 3) bands of the ultra-violet band system of germanium monoxide ( $\text{GeO}$ ). The bands are found to be due to a  ${}^1\Sigma \rightarrow {}^1\Sigma$  transition and are thus analogous to the  $A$  bands of  $\text{SnO}$  and  $\text{PbO}$ , as has been suggested in a previous communication. Relevant molecular constants have been obtained for both the states. A few lines due to the less abundant isotopic molecules  ${}^{70}\text{GeO}$  and  ${}^{72}\text{GeO}$  have been observed in the (0, 3) band.

### § I. INTRODUCTION

**S**o far only a single band system lying in the ultra-violet region between  $\lambda 2340$  and  $\lambda 3320$  is known for germanium monoxide,  $\text{GeO}$ . It consists of a large number of bands degraded to the red and appears in the spectrum of an arc between carbon electrodes fed with germanium dioxide or potassium germanium-fluoride or of an uncondensed discharge through the vapour of germanium tetrachloride in an atmosphere of oxygen. Shapiro and his co-workers<sup>(1)</sup> have also secured weak indications of these bands in absorption. The observation of germanium isotope effect in several of the band heads has proved beyond doubt the identity of their emitter.

The vibrational structure analysis of the bands has been carried out satisfactorily by several investigators<sup>(2, 3, 4)</sup> working independently. But no attempt has yet been made to study their rotational structure. Thus the nature of the electronic states involved in the transition remains still uncertain. It has, however, been suggested that since the band system also appears in absorption, its lower state corresponds to the ground state of the molecule and is in all probability a  ${}^1\Sigma$  state as has been found in the case of the monoxides of group IV *b*; while its upper state may be either  ${}^1\Pi$  or  ${}^1\Sigma$  according as it is analogous to the fourth positive and the ultra-violet bands of  $\text{CO}$  and  $\text{SiO}$  respectively or to the  $A$  bands of  $\text{SnO}$  and  $\text{PbO}$ . Jevons and his co-workers are in favour of the first alternative in view of the complex structure of some of the strongest bands from their moderate dispersion spectrograms. They have not, however, overlooked the fact that the complex isotopic nature of germanium might be responsible for such a structure although in reality the bands are due to a  ${}^1\Sigma \rightarrow {}^1\Sigma$  transition.

It was, therefore, thought desirable to undertake a complete rotational structure analysis of these bands with a view to ascertaining definitely the nature of the transition to which the band system is due.

The present paper reports the results of such an analysis carried out for the (1, 0), (2, 0) and (0, 3) bands. Each of these consists of only one *P* and one *R* branch, thus indicating that the band system in question is due to a  ${}^1\Sigma \rightarrow {}^1\Sigma$  transition. In addition to the lines of these two branches a few faint lines due to the isotope effect of germanium have also been recorded in the (0, 3) band.

### § 2. EXPERIMENTAL PROCEDURE

From an inspection of the plates taken previously by the author with a Hilger E 1 quartz spectrograph, it was found that the bands (2, 0), (1, 0), (1, 1), (0, 2) and (0, 3) are fairly intense. Of these (1, 1) and (0, 2) bands are so much superposed by the structure lines of the neighbouring bands that they present a very complicated appearance. Hence the bands (2, 0), (1, 0) and (0, 3) were chosen for a study of their rotational structure.

These bands have been photographed in the first order of a 21-ft. concave grating set up on a Paschen mounting and having 30,000 lines per inch with a 6-in. ruled surface. For light source a carbon arc fed with potassium germanium-fluoride has been used. An effective exposure of about 25 hr. was necessary for obtaining the bands with measurable intensity. Fine-grained photographic plates were used for securing the best definitions of the structure lines and Pfund iron-arc lines were utilized for comparison spectrum.

Measurement of the structure lines was made with a Gaertner comparator (M 1201 a) readable directly to 0.001 mm., and estimable to 0.0001 mm. For each band at least four independent sets of measurements were carried out and reduced to wave-lengths in the usual manner. In no case did the individual wave-lengths data differ from their mean value by more than 0.01 Å. for any particular line. Reductions to vacuum wave-numbers were made with the aid of Kayser's Schwingungszahlen.

### § 3. ANALYSIS OF BAND STRUCTURE

The high-dispersion spectrograms of the three bands investigated reveal that their resolution is complete except for a small region near the heads. Each band is found to consist mainly of two series of lines which are fairly long, owing to the high temperature of the source, and have nearly the same intensity. The two series may, therefore, be associated with the *P* and *R* branches of a band arising from a transition involving similar singlet states. The possibility of one of these series being actually a blend of *P* and *R* branches while the other is a *Q* branch seems improbable from the following considerations. All the three bands, though they have different ( $v'$ ,  $v''$ ) values, show practically identical structure. Further, the lines of (1, 0) and (2, 0) bands are very sharp in the regions in which the rotational isotopic shift would be nearly neutralized by the vibrational isotopic displacement. In other regions they look slightly diffuse. This feature can be attributed to the unresolved isotopic lines under the dispersion employed; their diffuse width, however, corresponds to the calculated spread of the isotopic pattern. On the other hand, a few faint lines due to the less abundant isotopic molecules  ${}^{70}\text{GeO}$  and  ${}^{72}\text{GeO}$  have been

observed in the (o, 3) band. Hence one can conclude that the diffuseness of the lines should not be attributed to unresolved  $\Lambda$ -type doubling. This rules out from consideration a transition involving  $^1\Pi$  states and leads one to assign the band system in question to a  $^1\Sigma \rightarrow ^1\Sigma$  transition.

After the two main series of lines in each band had been sorted out, the next step was the identification of each series and the assignment of quantum numbers to the lines belonging to it. As the bands are degraded to the red, the series of lines starting from their heads should evidently belong to the  $R$  branch. This method of identification was not possible in this case owing partly to incomplete resolution near the heads and partly to the fact that the lines of the two branches appear as close doublets which coalesce into single lines as they approach the head. A little further from the head one can, however, identify the neighbouring lines of the components of the doublets as belonging to either  $R$  branch or  $P$  branch merely from a visual inspection of their relative photographic intensities. Once this had been achieved, it was only a matter of trial to find out the proper combination relationship between them and thereby to arrive at the unique assignment of their  $K$  numbering. Since no lines with low  $K$  values have been observed in these bands, owing to incomplete resolution near the head, it was not possible to secure the further confirmation of the correctness of assignment of the band system to a  $^1\Sigma \rightarrow ^1\Sigma$  transition from the criteria of missing lines.

It is well known that the combination differences,  $\Delta_2 T(K)$ , between the lines of  $R$  and  $P$  branches of a band are given by

$$\Delta_2 T'(K) = R(K) - P(K),$$

$$\Delta_2 T''(K) = R(K-1) - P(K+1).$$

According to the combination principle all the bands having the same upper vibrational state should yield sets of values of  $\Delta_2 T'(K)$  which are numerically identical; and similarly all bands having the same lower vibrational state should give identical sets of values of  $\Delta_2 T''(K)$ . For each of the bands analysed the wave-numbers of the lines with their  $K$  numbering as well as the values of  $\Delta_2 T'(K)$  and  $\Delta_2 T''(K)$  are given in table I.

#### § 4. CALCULATION OF MOLECULAR CONSTANTS

The rotational energy of a molecule in a  $^1\Sigma$  state being given by

$$T(K) = B_v K(K+1) + D_v K^2(K+1)^2 + \dots$$

the combination differences  $\Delta_2 T(K)$  can be expressed as follows:

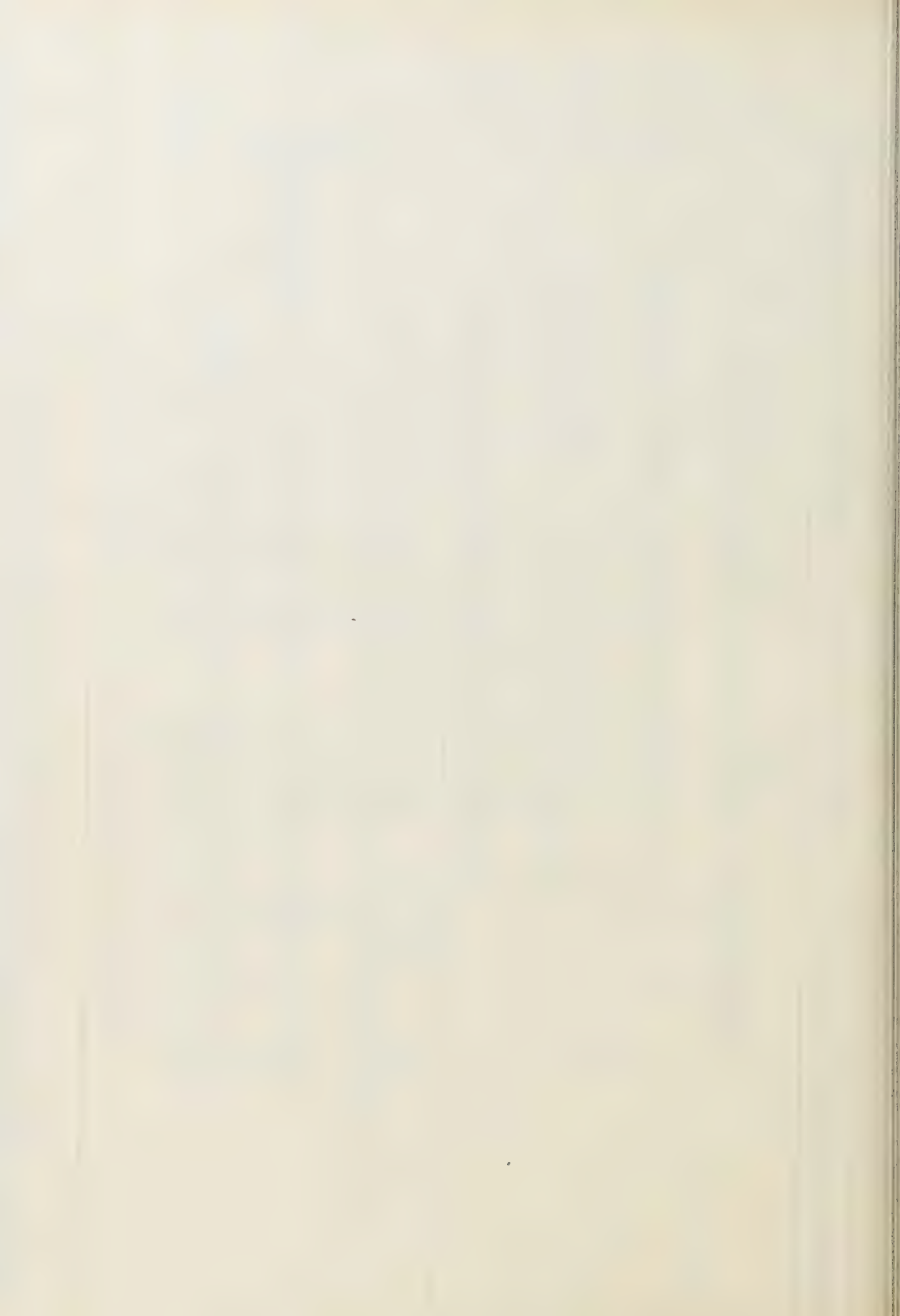
$$\begin{aligned} \Delta_2 T(K) &= T(K+1) - T(K-1) \\ &= 4B_v(K+\frac{1}{2}) + 8D_v(K+\frac{1}{2})^3, \end{aligned}$$

where terms small in comparison with  $8D_v(K+\frac{1}{2})^3$  are dropped. Both  $B_v$  and  $D_v$  depend upon  $v$  according to the relations

$$\begin{aligned} B_v &= B_e - \alpha(v + \frac{1}{2}) \\ &= B_0 - \alpha v \end{aligned}$$

Table I

K	(1, o) band, at $\lambda 2614\cdot65$				(2, o) band, at $\lambda 2571\cdot89$				(o, 3) band, at $\lambda 2881\cdot71$			
	R (K)	P (K)	$\Delta_2 T' (K)$ ( $v' - 1$ )	$\Delta_2 T'' (K)$ ( $v'' = 0$ )	R (K)	P (K)	$\Delta_2 T' (K)$ ( $v' - 2$ )	$\Delta_2 T'' (K)$ ( $v'' = 0$ )	R (K)	P (K)	$\Delta_2 T' (K)$ ( $v' = 0$ )	$\Delta_2 T'' (K)$ ( $v'' = 3$ )
22						38812·28				34637·35		
23						08·70				33·59		
24						05·00				30·10		
25						00·99				26·32		
26						38796·75				22·43		
27							89·02			18·31		
28							85·00			14·02		
29							80·13			09·57		
30							75·41			05·60		
31	38194·68	44·80	49·88	60·73		70·52				00·96		
32	90·87	39·53	51·34	62·73	38818·00	65·57	52·43		34596·36			
33	86·94	33·95	52·99	62·73		59·20	53·86	64·80	34647·15	92·04	55·11	
34	82·76	28·14	54·62	64·26		13·06	55·50	66·73	44·40	87·68	56·72	65·38
35	78·84	22·68	56·16	66·04		08·70	53·20	68·30	40·90	81·77	59·13	66·87
36	74·46	16·72	57·74	68·16		03·70	46·73	56·97				
37	69·86	10·68	59·18	70·12	38799·05	40·40	58·65	70·46	37·35	77·53	59·82	68·75
38	65·06	04·34	60·72	71·93		93·52	33·24	60·28	72·05	33·59	72·15	61·44
39	60·22	38097·93	62·29	73·67		88·69	27·00	61·69	73·85	30·10	66·89	63·21
40	55·29	91·39	63·90	75·57		82·91	19·67	63·24	75·73	26·32	61·11	65·11
41	49·95	84·65	65·30	77·35		77·68	12·06	64·72	77·64	22·43	56·03	66·40
42	44·80	77·94	66·86	78·95		71·59	05·27	66·32	79·35	18·31	50·38	67·93
43	39·53	71·00	68·53	81·01		66·33	38668·33	68·00	81·36	14·02	44·75	69·27
44	33·95	63·79	70·16	83·07		59·60	90·23	69·37	83·30	09·57	38·70	70·87
45	28·14	56·46	71·68	84·96		53·90	83·03	70·87	84·95	05·23	32·72	72·51
46	22·16	48·99	73·17	86·85		47·39	74·65	72·74	87·00	00·27	26·34	73·93
47	16·00	41·29	74·71	88·78		40·91	66·90	74·01	88·60	34595·38	19·95	75·43
48	09·66	33·38	76·28	90·54		34·34	58·79	75·55	90·61	90·29	13·28	77·01
49	03·36	25·46	77·90	92·39		27·48	50·30	77·18	92·36	85·28	06·64	78·64
50	38096·55	17·27	79·28	94·60		20·88	41·98	78·90	94·78	80·08	34499·66	80·42
51	89·60	08·76	80·84	96·27		12·96	32·70	80·26	96·22	74·72	92·71	82·01
52	82·71	00·28	82·43	98·10		06·63	24·66	81·97	98·07	69·21	85·88	83·33
53	75·45	37991·50	83·95	100·04		38698·33	14·89	83·44	100·12	63·70	78·71	84·99
54	68·13	82·67	85·46	101·83		91·34	06·51	84·83	101·42	58·07	71·44	86·63
55	60·56	73·62	86·94	103·63		83·35	38596·91	86·44	103·44	52·06	64·10	87·96
56	53·09	64·50	88·59	105·43		75·70	87·90	87·80	105·36	46·20	56·62	89·58
57	45·35	55·13	90·22	107·24		67·32	77·99	89·33	107·47	40·00	48·80	91·20
58	37·60	45·85	91·75	109·03		58·99	68·23	90·76	109·31	41·15	92·56	106·96
59	29·46	36·32	93·14	110·94		50·70	110·99	27·04	33·04	94·00	108·70	
60	21·37	26·66	94·71	112·88		41·90	48·00	93·90	112·92	20·56	25·01	95·55
61	12·63	16·58	96·05	115·c3		33·06	37·78	95·28	114·56	13·57	16·43	97·14
62	04·25	06·34	97·91	116·71		24·26	27·34	96·92	116·20	06·64	07·96	98·68
63	37995·14	37895·92	99·22	118·58		14·89	16·86	98·03	118·35	34499·66	34399·44	100·22
64	86·60	85·67	100·93	119·91		05·57	05·91	99·66	120·18	92·71	90·72	101·99
65	77·89	75·23	102·66	121·86		38596·12	38494·71	101·41	122·06	85·29	82·01	103·28
66	68·78	64·74	104·04	124·08		86·63	83·51	103·12	123·69	78·01	73·06	104·95
67	59·12	53·81	105·31	125·70		76·69	72·43	104·26	125·79	70·45	64·02	106·43
68	50·07	43·08	106·99	127·29		66·49	60·84	105·65	127·36	62·46	54·59	107·87
69	40·22	31·83	108·39	129·48		49·33	49·33	129·35	54·71	45·20	109·51	126·63
70	31·11	20·59	110·52	131·27		45·97	37·14	108·83	133·10	46·97	35·83	111·14
71	20·52	08·95	111·57	133·33		35·72	25·30	110·42	135·04	38·79	26·18	112·61
72	10·75	37797·78	112·97			24·88	12·87	112·01	135·46	30·80	16·62	114·18
73	00·38					14·14	00·68	113·46	136·80	22·09	06·59	115·50
74	37890·38					02·82	38388·08	114·74	138·41	13·55	34296·62	116·93
75	79·50					38491·52	75·73	115·79	140·30	04·57	86·00	118·57
76	68·81					80·01	62·52	117·49	142·14	34395·81	75·80	120·01
77	57·94					68·79	49·38	119·41	143·97	86·96	65·26	121·70
78	47·02					57·21	36·04	121·17	145·65	77·85	54·62	123·23
79	35·99					45·46	23·14	122·32	147·21	68·86	44·14	124·72
80	24·20					33·68	10·00	123·68	149·65	59·34	33·05	126·29
81	12·98					20·02	38205·81	125·11	151·46	50·14	22·31	127·83
82	01·33					08·67	82·22	126·45	153·26	40·33	11·12	129·21
83						38306·00	67·66	128·34	154·78	30·32	34199·80	130·52
84						83·60	53·89	129·71		20·57	88·37	132·20
85						71·96				10·64	76·74	133·90
86						58·70				00·84	65·40	135·44
87						45·46				34290·24		
88						31·71				79·60		
89						18·21				68·81		
90						04·82				58·07		
91						38291·29				48·40		
92						76·67				37·64		
93						62·10				26·48		
94						48·17				14·87		
95										03·51		
96										34192·33		
97										81·68		
98										68·97		
99										58·71		



and

$$D_v = D_e + \beta(v + \frac{1}{2}) \\ = D_0 + \beta v.$$

Here  $B_e$  and  $D_e$  are the extrapolated values of  $B_v$  and  $D_v$  corresponding to a non-vibrating and non-rotating molecule.

The mean value of the combination differences have been taken in cases where there was more than one datum available for a particular pair of rotational levels. For each vibrational level, the first approximate value of  $B_v$  was determined by a graphical method. This was used to calculate also the approximate value of  $D_v$  from several data of  $\Delta_2 T(K)$ . Then by successive approximation and repeated trials  $B_v$  and  $D_v$  were assigned their final values. When  $(\Delta_2 T(K) - 8D_v(K + \frac{1}{2})^3)$  is plotted against  $K$ , the points lie very closely on a straight line; this shows that there is no need for considering higher-power terms to represent  $\Delta_2 T(K)$ .

The variation of  $D_e$  with  $v$  was found to be of negligible magnitude. From the variation of  $B_v$  the values of  $z$  and  $B_e$  were determined.  $I_e$  and  $r_e$  were then evaluated from the following relations:

$$I_e = \frac{27.66 \pm 0.04}{B_e} \times 10^{-40} \text{ g./cm}^2$$

and

$$r_e^2 = \frac{I_e(A_1 + A_2)}{1.649 A_1 A_2} \times 10^{24} \text{ cm}^2,$$

where  $A_1$  and  $A_2$  are the atomic weights of the constituent atoms of the diatomic molecule. In table 2 the values of the several constants thus evaluated are given.

Table 2. Rotational constants of GeO

Upper ${}^1\Sigma$ state	Lower ${}^1\Sigma$ state
$B_e' = 0.4018 \text{ cm}^{-1}$	$B_e'' = 0.4704 \text{ cm}^{-1}$
$B_0' = 0.4000 \text{ cm}^{-1}$	$B_0'' = 0.4689 \text{ cm}^{-1}$
$B_1' = 0.3960 \text{ cm}^{-1}$	$B_3'' = 0.4601 \text{ cm}^{-1}$
$B_2' = 0.3926 \text{ cm}^{-1}$	$\alpha'' = 0.0029 \text{ cm}^{-1}$
$\alpha' = 0.0037 \text{ cm}^{-1}$	$D_e'' = -4.30 \times 10^{-7} \text{ cm}^{-1}$
$D_e' = -6.07 \times 10^{-7} \text{ cm}^{-1}$	$r_e'' = 1.647 \times 10^{-8} \text{ cm.}$
$r_e' = 1.782 \times 10^{-8} \text{ cm.}$	$I_e'' = 58.89 \times 10^{-40} \text{ g.cm}^2$
$I_e' = 68.94 \times 10^{-40} \text{ g.cm}^2$	

To ensure the correct evaluation of  $B_v$  and  $D_v$  for each vibrational state, values of  $\Delta_2 T(K)$  were calculated from the theoretical equation and compared with the observed data. In general the agreement between them was satisfactory. A check on the correctness of the values of  $B$  and  $D$  is afforded by the theoretical relation, viz.,

$$\omega_e^2 = -\frac{4B_e^3}{D_e}.$$

On substitution of the proper values of  $B_e$  and  $D_e$  it is found that  $\omega_e' = 653.8 \text{ cm}^{-1}$  and  $\omega_e'' = 984.1 \text{ cm}^{-1}$ . These values are in sufficiently close agreement with those obtained from the vibrational structure analysis of the bands on the basis of the data of their band heads.

A further check on the correctness of the analysis is obtained from the approximate relation between  $r_e$  and  $\omega_e$  as given by Morse<sup>(5)</sup>, viz.,  $\omega_e r_e^3 = \text{a constant}$ , which

has a value equal to  $3000 \times 10^{-24} \text{ cm}^2$  for diatomic molecules composed of atoms of nearly equal mass. But if the masses of the atoms are unequal, as in the present case, the value of this constant should be greater. This condition is satisfied, since we have

$$\omega_e' r_e'^3 = 3689 \times 10^{-24} \text{ cm}^2 \quad \text{and} \quad \omega_e'' r_e''^3 = 4384 \times 10^{-24} \text{ cm}^2$$

An additional check is afforded by a rule due to Birge<sup>(6)</sup> which states that the quantity  $2x_e B_e / \alpha$  is approximately equal to  $1.4 \pm 0.2$ . In the present case one finds

$$\frac{2x_e' B_e'}{\alpha'} = 1.39 \quad \text{and} \quad \frac{2x_e'' B_e''}{\alpha''} = 1.20.$$

The value of the internuclear distance in the ground state of GeO, obtained from the present analysis, is also of the right order of magnitude as is evident from a comparison of values of  $r_e''$  for the other monoxides of group IVb included in table 3.

Table 3. Internuclear distances of the ground states of group IVb monoxides

Molecule	$r_e''$	Source
CO	1.127	Read <sup>(7)</sup>
SiO	1.505	Saper <sup>(8)</sup>
GeO	1.647	Present work
SnO	1.832	Mahanti and Sen Gupta <sup>(9)</sup>
PbO	1.918	Christy and Bloomenthal <sup>(10)</sup>

### § 5. ROTATIONAL ISOTOPE EFFECT

Aston<sup>(11)</sup> has reported that germanium has five isotopes as follows:

Mass number	70	72	73	74	76
Abundance	21.2	27.3	7.9	37.1	6.5

The spectroscopic evidence of the existence of all these isotopes has been secured by Shapiro and his co-workers<sup>(1)</sup> from observations of isotopic heads in the less refrangible band system of GeS. Very recently the author<sup>(3)</sup> as well as Jevons and his co-workers<sup>(4)</sup> have also identified band-heads due to the less abundant molecules, <sup>70</sup>GeO and <sup>72</sup>GeO, accompanying, in favourable cases, those of the main molecule <sup>74</sup>GeO in the band system in question. One may, therefore, expect to observe the isotope effect in the rotational structure of the bands under investigation.

From the theory of the isotope effect in the band spectra of diatomic molecules it is evident that the total isotopic shift (which is the algebraic sum of the constant vibrational shift and the varying rotational shift) in the (2, 0) and (1, 0) bands will gradually diminish at first from its maximum value at the head to zero, and then increase with opposite sign. Thus in each of these two bands we should have a region in which the lines would appear fairly sharp, while on either side of this region they would appear broad or diffuse if the dispersion is not sufficient to resolve their isotopic components. Such features have actually been observed in these two bands. The structure of the (2, 0) band near the head looks very complex, owing

*Rotational analysis of the ultra-violet bands of germanium monoxide* 67

Table 4. Rotational isotope effect of germanium in the (0, 3) band of GeO

K	<sup>72</sup> GeO			<sup>70</sup> GeO		
	$R^i(K)$	$\Delta\nu$ (obs.)	$\Delta\nu$ (calc.)	$R^i(K)$	$\Delta\nu$ (obs.)	$\Delta\nu$ (calc.)
67	34461·39	8·78	8·66	34452·45	17·72	17·77
68	53·24	8·92	8·70	44·75	17·41	17·86
69	†45·83	8·68	8·73	36·55	17·96	17·93
70	37·90	8·79	8·77	28·77	17·92	18·01
71	29·62	9·07	8·81	20·78	17·91	18·09
72	*21·88	8·58	8·85	12·19	18·27	18·18
73	*13·37	8·51	8·90	03·82	18·06	18·27
74	*04·51	8·86	8·94	*395·58	17·79	18·35
75	*395·58	8·93	8·98	†86·43	18·08	18·44
76	†86·43	9·15	9·03	77·42	18·16	18·53
77	*77·85	9·11	9·07	*68·56	18·40	18·62
78	*68·56	9·29	9·11	58·94	18·91	18·71
79	59·52	9·04	9·16	49·50	19·06	18·81
80	34350·14	8·90	9·21	†34340·43	18·61	18·90
81	†40·43	9·11	9·25	†30·69	18·85	19·00
82	†30·69	9·23	9·30	21·11	18·81	19·10
83	*20·46	9·37	9·35	†10·73	19·10	19·20
84	†10·73	9·73	9·40	01·33	19·13	19·30
85	*00·84	9·34	9·45	290·84	19·34	19·40
86	291·43	9·41	9·50	81·22	19·62	19·50
87	80·79	9·45	9·55	70·79	19·45	19·60
88	70·23	9·37	9·60	59·93	19·67	19·71

\* Superposed on a main branch line. † Superposed on an isotopic branch line.

Table 5

K	<sup>72</sup> GeO			<sup>70</sup> GeO		
	$P^i(K)$	$\Delta\nu$ (obs.)	$\Delta\nu$ (calc.)	$P^i(K)$	$\Delta\nu$ (obs.)	$\Delta\nu$ (calc.)
54	34462·97	8·47	8·65	34453·62	17·82	17·76
55	55·10	9·00	8·69	†45·83	18·27	17·84
56	47·76	8·86	8·72	*38·69	17·93	17·91
57	40·57	8·53	8·76	31·00	18·10	17·99
58	32·08	9·07	8·80	22·77	18·38	18·07
59	23·98	9·06	8·84	14·54	18·50	18·15
60	†16·43	8·58	8·88	06·89	18·12	18·23
61	*34407·96	8·47	8·92	34398·34	18·09	18·32
62	*34399·44	8·52	8·96	89·69	18·27	18·41
63	*90·72	8·72	9·01	81·32	18·12	18·49
64	*82·01	8·71	9·05	71·99	18·73	18·58
65	*73·06	8·95	9·09	—	—	18·67
66	*64·02	9·04	9·14	*54·59	18·47	18·76
67	*54·59	9·43	9·18	*45·30	18·72	18·85
68	*45·30	9·29	9·23	*35·83	18·76	18·95
69	*35·83	9·47	9·27	*26·29	19·01	19·04
70	*26·29	9·54	9·32	*16·62	19·21	19·14
71	*16·62	9·67	9·37	†07·49	18·80	19·24
72	†07·49	9·13	9·42	†34297·46	19·16	19·34
73	†34297·46	9·13	9·47	†87·51	19·08	19·44
74	†87·51	9·21	9·52	†77·11	19·61	19·54
75	†77·11	9·38	9·57	66·94	19·55	19·64
76	66·32	9·64	9·62	56·34	19·62	19·75

\* Superposed by a main line. † Superposed by an isotopic line.

probably to the overlapping of the resolved isotopic components of the lines of the two branches.

On the other hand, the vibrational and rotational isotopic shifts are of the same sign on the low-frequency side of the origin of the (0, 3) band and thus add together to give the total isotopic shift. For this band, the magnitude of the vibrational isotopic displacement alone is also fairly large, being  $7.6 \text{ cm}^{-1}$  for  $^{72}\text{GeO}$  and  $15.5 \text{ cm}^{-1}$ , for  $^{70}\text{GeO}$ . One may, therefore, expect the isotopic components of the lines to be resolved under the dispersion used. In fact, their presence has been definitely ascertained. In several cases, however, they are found to be superposed upon the lines of the main molecule. It is only for high values of  $K$  that the superposition is less prominent and the agreement between observed and calculated isotopic shifts is fairly satisfactory. For illustration a few of these lines are included in tables 4 and 5.

#### § 6. ACKNOWLEDGEMENTS

The author desires to offer his best thanks to Prof. Dr P. N. Ghosh for continual interest and encouragement in the course of the investigation and to Dr P. C. Mahanti for many helpful discussions.

#### REFERENCES

- (1) SHAPIRO, C. V., GIBBS, R. C. and LAUBENGAYER, A. W. *Phys. Rev.* **40**, 354 (1933).
- (2) SHAW, R. W. *Phys. Rev.* **51**, 12 (1937).
- (3) SEN GUPTA, A. K. *Z. Phys.* **105**, 487 (1937).
- (4) JEVONS, W., BASHFORD, L. A. and BRISCOE, H. V. A. *Proc. Phys. Soc.* **49**, 543 (1937).
- (5) MORSE, P. M. *Phys. Rev.* **34**, 57 (1929).
- (6) BIRGE, R. T. *Phys. Rev.* **31**, 919 (1927).
- (7) READ, D. N. *Phys. Rev.* **46**, 571 (1934).
- (8) SAPER, P. G. *Phys. Rev.* **42**, 498 (1932).
- (9) MAHANTI, P. C. and SEN GUPTA, A. K. *Z. Phys.* (in the Press).
- (10) CHRISTY, A. and BLOOMENTHAL, S. *Phys. Rev.* **35**, 46 (1930).
- (11) ASTON, F. W. *Mass Spectra and Isotopes* (1933).

# THE CHARACTERISTIC TEMPERATURE OF MAGNESIUM OXIDE

By G. W. BRINDLEY, M.Sc., Ph.D.,  
Mackinnon Student of the Royal Society

AND

P. RIDLEY, Ph.D., Physics Laboratories, University of Leeds

*Received 3 August 1938. Read in title 11 November 1938*

**ABSTRACT.** The characteristic temperature of magnesium oxide is derived from measurements of the intensity of x-ray reflections at  $86^\circ$  and  $293^\circ$  K. The result obtained,  $\Theta = 715 \pm 44$ , agrees favourably with a recent determination by Ribner and Wollan who give  $\Theta = 743^\circ$  K., a value which, they state, carries "a rather large probable error".

In a recent paper Wollan and Harvey<sup>(6)</sup> have suggested that magnesium oxide is a particularly suitable substance to use as a standard in making comparative measurements of the intensities of x-ray reflections from powders at different temperatures, since "it has the advantage that it is readily obtainable in the form of a fine powder and also, due to its very high characteristic temperature, the effect of temperature on the intensity of reflection is very small". We thought it desirable to determine the characteristic temperature of magnesium oxide by the x-ray method before utilizing this suggestion. In the meantime Ribner and Wollan<sup>(5)</sup> have published the results of an entirely independent x-ray determination of this quantity which agrees approximately with the value we have obtained, but in view of the great difficulty of making an accurate determination by means of x rays, it seems worth while to give a brief account of our own experiments.

The experiment consists in measuring the intensities of reflections at two temperatures, actually  $86^\circ$  and  $293^\circ$  K. Then assuming that the exponent  $M$  in the expression for the dependence of the reflected intensity on temperature is given by the Debye-Waller expression,\*

$$M = (6h^2T/mk\Theta^2) [\Phi(x) + x/4] (\sin^2 \theta)/\lambda^2, \quad \dots\dots (1)$$

where  $\Theta$  is the characteristic temperature,  $x = \Theta/T$ , and  $\Phi(x)$  is the Debye function, we can calculate  $\Theta$  from the experimental results. If  $I_{293}$  and  $I_{86}$  are the intensities

\* This applies strictly to cubic lattices containing atoms of one kind only; for lattices containing more than one kind of atom,  $M$  will be different for the different atoms. Ribner and Wollan show that for magnesium oxide a mean value of  $M$  is obtained by assuming a single value of  $M$  for the even order reflections and taking  $m$  in the Debye-Waller expression to be the mean atomic mass.

of a reflection  $hkl$  at the two temperatures, then

$$(I_{86}/I_{293}) = \exp \{2(M_{293} - M_{86})_{hkl}\} = \exp (2\Delta M_{hkl}),$$

or

$$\log_e (I_{86}/I_{293}) = 2\Delta M_{hkl}. \quad \dots\dots(2)$$

For two reflections  $hkl$  and  $h'k'l'$ , we have

$$\begin{aligned} 2(\Delta M_{hkl} - \Delta M_{h'k'l'}) &= \log_e \left\{ \left( \frac{I_{86}}{I_{293}} \right)_{hkl} / \left( \frac{I_{86}}{I_{293}} \right)_{h'k'l'} \right\} \\ &= \log_e \left\{ \left( \frac{I_{hkl}}{I_{h'k'l'}} \right)_{86} / \left( \frac{I_{hkl}}{I_{h'k'l'}} \right)_{293} \right\}. \end{aligned} \quad \dots\dots(3)$$

From a consideration of these equations it is seen that we could obtain  $\Theta$  by combining equations (1) and (2) provided we could measure directly the ratio  $(I_{86}/I_{293})_{hkl}$ . Since the intensities  $I_{86}$  and  $I_{293}$  must be measured on separate occasions, their ratio cannot be obtained unless there is some means of measuring or controlling very exactly the intensity of the radiation incident on the powder at the two temperatures. This difficulty might be overcome by utilizing Brentano's suggestion<sup>(1)</sup> for inserting a thin reflecting powder or crystal in the primary beam before it reaches the powder under investigation, a reflection from which would give a measure of the intensity in the primary beam. It will be seen, however, that in the present connexion the difficulty is eliminated by using equations (1) and (3), for then we have to measure only the ratios of the intensities of two reflections separately at the two temperatures. Since four intensity measurements are required to evaluate the quantity  $\{(I_{hkl}/I_{h'k'l'})_{86}/(I_{hkl}/I_{h'k'l'})_{293}\}$  in equation (3), it might appear that the use of equations (1) and (2) has an advantage in that only *two* intensity-measurements are required, but as two intensity-measurements would also be required for the substance inserted in the primary beam, there would still be four intensity-measurements necessary for each determination of  $\Theta$ . The use of equations (1) and (3) is therefore not attended by any disadvantage which would not also be present in the use of equations (1) and (2). It is easily seen that in order to use equations (1) and (3) successfully to evaluate  $\Theta$  the two reflections  $hkl$  and  $h'k'l'$  must be separated as widely as possible, for otherwise the quantity in the curly brackets will be of the order of unity and the probable error in the natural logarithm will be comparatively large. Since for cubic crystals,

$$(\sin \theta)/\lambda = \sqrt{(h^2 + k^2 + l^2)/2a},$$

equation (1) may be written in the form

$$M = b(h^2 + k^2 + l^2) = b\Sigma h^2,$$

where

$$b = (3h^2 T / 2a^2 m k \Theta^2) [\Phi(x) + x/4],$$

and equation (3) can be written in the form

$$2\Delta b [\Sigma h^2 - \Sigma h'^2] = \log_e \left\{ \left( \frac{I_{hkl}}{I_{h'k'l'}} \right)_{86} / \left( \frac{I_{hkl}}{I_{h'k'l'}} \right)_{293} \right\},$$

whence

$$\Delta b = \log_e \left\{ \left( \frac{I_{hkl}}{I_{h'k'l'}} \right)_{86} / \left( \frac{I_{hkl}}{I_{h'k'l'}} \right)_{293} \right\} / 2[\Sigma h^2 - \Sigma h'^2]. \quad \dots\dots(4)$$

The experimental method consisted in reflecting radiation from a flat plate of powder in the manner previously described<sup>(2, 3)</sup>. The widest range of reflections which could be obtained with a single setting of the powder, CuK $\alpha$  radiation being used, was from the 220 to the 422. Since magnesium oxide has the rocksalt type of structure, the structure factor for the even order reflections is of the form 4(Mg+O) and, as Ribner and Wollan<sup>(5)</sup> have shown in detail, we are able from measurements of these reflections to obtain a mean characteristic temperature for the lattice. We have therefore confined our attention to making careful measurements of the 220, 420 and 422 reflections; their relative intensities at the two temperatures together with the probable errors calculated by the usual Gaussian formula are given in table 1. In table 2 are shown the essential stages in the calculation of  $\Delta b$ . Since the quantity  $\{(I_{hkl}/I_{h'k'l'})_{86}/(I_{hkl}/I_{h'k'l'})_{293}\}$  has values which do

Table 1. Relative intensities at 86° and 293° K.

$hkl$	$I_{86}$	$I_{293}$
220	104.7 ± 0.7 <sub>5</sub>	99.4 ± 0.6 <sub>6</sub>
420	108.7 ± 0.6 <sub>2</sub>	97.5 ± 0.6 <sub>6</sub>
422	116.7 ± 0.8 <sub>4</sub>	103.1 ± 0.5 <sub>7</sub>

Table 2. Calculation of  $\Delta b$ 

$hkl$	$h'k'l'$	$\Sigma h^2$	$\Sigma h'^2$	$\Sigma h^2 - \Sigma h'^2$	$\left\{ \left( \frac{I_{hkl}}{I_{h'k'l'}} \right)_{86} / \left( \frac{I_{hkl}}{I_{h'k'l'}} \right)_{293} \right\}$	$\Delta b = \frac{\log_e \{ \dots \}}{2 [\Sigma h^2 - \Sigma h'^2]}$
420	220	20	8	12	1.058 ± 0.013 <sub>7</sub>	0.0023 <sub>5</sub> ± 0.0005 <sub>5</sub>
422	220	24	8	16	1.075 ± 0.014 <sub>0</sub>	0.0022 <sub>5</sub> ± 0.0004 <sub>0</sub>

$$\text{Mean } \Delta b = 0.0023_0 \pm 0.0003_4$$

not differ greatly from unity the question of the probable error in the final results must be carefully considered. We have taken the probable percentage error in  $\{(I_{hkl}/I_{h'k'l'})_{86}/(I_{hkl}/I_{h'k'l'})_{293}\}$  to be the square root of the sum of the squares of the probable percentage errors in the four separate intensities. The probable error in  $\Delta b$  has been found by taking the logarithms of the upper and lower limits of the quantity in curly brackets. The probable error in the final mean value of  $\Delta b$  is taken as the mean of the errors in the separate values of  $\Delta b$ , divided by  $\sqrt{2}$ ; this error is of the order of 15 per cent. Fortunately  $\Theta$  is approximately proportional to  $\sqrt{\Delta b}$ , so that the probable error in  $\Theta$  will be of the order of 7 per cent.

From the expression for  $b$  given above we easily calculate values of  $\Delta b$  for a range of values of  $\Theta$ , and hence by interpolation we obtain the value of  $\Theta$  corresponding to the experimentally determined  $\Delta b$ . The result obtained is

$$\Theta = 715^\circ \pm 44^\circ \text{ K.}$$

This result agrees within the limits of experimental error with the value found by Ribner and Wollan<sup>(5)</sup>, namely 743° K.; they state that the value carries "a rather large probable error" but they give no estimate of its magnitude. Assuming their

error to be of the same order of magnitude as in the present work, we may take the average of the two investigations as being the most probable value of  $\Theta$  obtained by x-ray methods, namely

$$\Theta = 729^\circ \pm 30^\circ \text{ K.}$$

From specific-heat measurements, Günther<sup>(4)</sup> has obtained a value for  $\Theta$  equal to  $768^\circ$ ; Ribner and Wollan<sup>(5)</sup> have also estimated a value of  $\Theta$  from available specific-heat data and they give a value of  $744^\circ$ . The limits of probable error are not specified in either case but they are stated to be large by Ribner and Wollan; from the data given by the latter authors, it appears that the probable error is of the order of  $\pm 20^\circ$ . There is, then, a general agreement between the x-ray and the specific-heat values of  $\Theta$ , though the former appears to be somewhat smaller than the latter.

The experiments described above were assisted by a grant for apparatus from the Government Grant Committee, and by a maintenance grant from the Department of Scientific and Industrial Research to one of us (P. R.).

#### REFERENCES

- (1) BRENTANO, J. *Z. Phys.* **99**, 65 (1936).
- (2) BRINDLEY, G. W. and SPIERS, F. W. *Proc. Phys. Soc.* **46**, 841 (1934); **50**, 17 (1938).
- (3) BRINDLEY, G. W. and RIDLEY, P. *Proc. Phys. Soc.* **50**, 757 (1938).
- (4) GÜNTHER, P. *Ann. Phys., Lpz.*, **51**, 828 (1916).
- (5) RIBNER, H. S. and WOLLAN, E. O. *Phys. Rev.* **53**, 972 (1938).
- (6) WOLLAN, E. O. and HARVEY, G. G. *Phys. Rev.* **51**, 1054 (1937).

# AN X-RAY INVESTIGATION OF ATOMIC VIBRATIONS IN CADMIUM

By G. W. BRINDLEY, M.Sc., Ph.D.,

Mackinnon Student of the Royal Society

AND

P. RIDLEY, Ph.D., Physics Laboratories, University of Leeds

*Received 3 August 1938. Read in title 11 November 1938*

**ABSTRACT.** Measurements are made of the intensities of x-ray reflections from cadmium powder at  $86^\circ$  and  $293^\circ$  K. Absolute values of the ratio  $I_{86}/I_{293}$  are obtained from comparative measurements on a composite specimen of cadmium and aluminium powders. The results are discussed in relation to recent theoretical work regarding the effect of lattice vibrations in hexagonal metals on the intensities of x-ray reflections. It is shown that the lattice vibrations in cadmium are considerably greater parallel to the *c* axis than in the basal plane. Values are calculated for the mean atomic displacements in different directions in the metal at  $86^\circ$  and  $293^\circ$  K. (see figure 2), and the results are also expressed in terms of characteristic temperatures:  $\Theta_0$  (parallel to the *c* axis) =  $107^\circ$  and  $\Theta_{90}$  (normal to the *c* axis) =  $164.5^\circ$  K. These results are compared briefly with similar results for zinc and magnesium, and with values obtained from specific-heat measurements.

## § 1. INTRODUCTION

A N investigation of the asymmetry of the atomic vibrations in cadmium has been carried out by the method recently used for a similar investigation of magnesium<sup>(2)</sup> in which the intensities of x-ray reflections from the powdered metal are measured at two temperatures, room temperature  $293^\circ$  K., and liquid-air temperature,  $86^\circ$  K. Previous measurements on cadmium at room temperature made by one of us<sup>(1)</sup> some years ago indicated a marked asymmetry of the atomic vibrations but gave no absolute values for the atomic displacements. It therefore seemed worth while to apply the technique described in the paper on magnesium to a detailed study of cadmium.

## § 2. EXPERIMENTAL DETAILS

The cadmium powder was prepared by precipitation from cadmium sulphate solution by the addition of finely powdered zinc. The best conditions for obtaining a powder free from appreciable impurities were carefully determined. In the method finally adopted zinc powder, freshly filed from a pure zinc rod and sieved through a gauze with 350 meshes to the inch, was added to a cold solution of cadmium sulphate; the solution was vigorously shaken and the precipitate washed by decantation and quickly dried on filter paper at room temperature.

The measured values of the intensities reflected from the cadmium powder at the two temperatures were standardized by comparing suitable cadmium reflections with reflections from aluminium, a specimen of mixed cadmium and aluminium powders being used. The same experimental arrangements were employed as have been described in the recent paper on magnesium<sup>(2)</sup>.

### § 3. RESULTS

The experimental results are set out in table I, the first four columns of which give respectively the indices of the reflections, the relative intensities\*  $I_{86}$  and  $I_{293}$  corresponding to the two temperatures at which measurements were made, and the

Table I. Intensities of x-ray reflections from cadmium at 86° and 293° K.

1	2	3	4	5	6	7
Reflections	$I_{86}$	$I_{293}$	$I_{86}/I_{293}$	$\left( \frac{\phi_{293} A_{293}}{\phi_{86} A_{86}} \right)$	$(f_{86}/f_{293})^2$	
	Relative values			Relative	Absolute	
1122	111.5	108.6	1.026	0.982	1.008	1.334
2020	19.2	21.3	0.901	0.991	0.893	1.181
2021	88.5	91.4	0.968	0.998	0.966	1.278
1014	29.3	23.2	1.261	0.989	1.247	1.650
2022	29.8	28.6	1.040	0.996	1.036	1.370
2023	77.6	60.8	1.276	0.995	1.270	1.680
2130	30.1	26.2	1.149	0.994	1.141	1.509
2131	157.9	137.3	1.150	0.979	1.125	1.488
2132	60.9	44.9	1.356	0.987	1.338	1.769
2025	89.8	42.3	2.121	0.945	2.004	2.651
3032	175.1	122.9	1.425	0.964	1.374	1.816

ratio  $I_{86}/I_{293}$ . The change in the lattice dimensions of cadmium when cooled to 86° K. is sufficiently large to produce an appreciable change in the angles at which reflections occur; since the intensity of reflection depends, among other things, on the Bragg angle  $\theta_>$ , allowance must be made for the change of  $\theta$  when the crystal is cooled. The intensity reflected by a flat layer of powder is given by the relation

$$I \propto p S^2 f_T^2 \phi(\theta) A, \quad \dots \dots (1)$$

where

$$\phi(\theta) = (1 + \cos^2 2\theta) / (\sin \theta \sin 2\theta),$$

$$A = [\sin(2\theta - \alpha)] / [\sin(2\theta - \alpha) + \sin \alpha],$$

$\alpha$  is the angle of incidence of the radiation on the surface of the powder,  $f_T$  is the scattering factor at temperature  $T$ ,  $p$  is the multiplicity factor, and  $S$  is the structure factor. We can therefore make allowance for the change of intensity of a reflection due to a change in the lattice dimensions between two temperatures, by means of the following relation:

$$\left( \frac{f_{86}}{f_{293}} \right)^2 = \left( \frac{I_{86}}{I_{293}} \right) \left\{ \frac{\phi(\theta)_{293} A_{293}}{\phi(\theta)_{86} A_{86}} \right\}. \quad \dots \dots (2)$$

\* Whereas previously in measuring relative intensities we have set one reflection (usually a strong reflection which is well focused) equal to 100.0, in the present case we have preferred to set the sum of the two reflections, 1122 and 2021, equal to 200.0 since under the conditions of the experiment they are equally well focused and are of comparable intensities.

For the majority of the reflections investigated  $\phi(\theta)$  and  $A$  change in opposite directions when the powder is cooled and consequently the factor in the curly brackets differs from unity by less than 1 per cent, but for the higher-order reflections it amounts to several per cent and cannot, therefore, be neglected. In calculating this factor we have taken the mean coefficients of thermal expansion between  $293^\circ$  and  $86^\circ$  K. to be  $55 \times 10^{-6}$  parallel to the  $c$  axis and  $15 \times 10^{-6}$  normal to the  $c$  axis; these values are based on the results obtained by Owen and Roberts<sup>(7)</sup>. The following values have been published for the lattice constants of cadmium:

$$a = 2.97235 \quad c = 5.60388 \text{ (Owen and Roberts<sup>(7)</sup>, at } 18^\circ \text{ C.)}$$

$$a = 2.97311 \quad c = 5.60694 \text{ (Jette and Foote<sup>(6)</sup>)}$$

$$a = 2.9736 \quad c = 5.6095 \text{ (Fuller<sup>(3)</sup>.)}$$

We have used the values obtained by Jette and Foote<sup>(6)</sup>, since these lie intermediate between those of Owen and Roberts<sup>(7)</sup> and of Fuller<sup>(3)</sup>.

The values of  $(\phi_{293} A_{293}/\phi_{86} A_{86})$  calculated from these data are given in the fifth column of table 1, and hence we obtain the values of  $(f_{86}/f_{293})^2$  given in the sixth column of the table.

The second part of the investigation consists in placing these values of  $(f_{86}/f_{293})^2$ , which are essentially relative values, on an absolute scale by a comparison of suitably placed reflections from a mixture of cadmium and aluminium. The most favourable reflections for such a comparison are the  $11\bar{2}2$  and  $20\bar{2}1$  from cadmium and the  $220$  and  $311$  from aluminium. The results are set out in table 2. The intensities of

Table 2. Comparison of intensities from cadmium and aluminium

1	2	3	4	5	6			8
					$(f_{86}/f_{293})^2$			
Reflections	$I_{293}$	$I_{86}$	$I_{86} I_{293}$	$\left( \frac{\phi_{293} A_{293}}{\phi_{86} A_{86}} \right)$	Relative	Absolute	Mean absolute values	
Al 220	100.0	100.0	1.000	1.001	1.001	1.118		
Cd 1122	135.7	160.9	1.185	0.998	1.183	1.322		
Cd 2021	104.1	117.6	1.130	1.004	1.134	1.266		
Al 311	100.0	100.0	1.000	1.003	1.003	1.166		
Cd 1122	103.9	120.3	1.158	0.998	1.156	1.345	Cd 1122: 1.334	
Cd 2021	79.2	87.5	1.105	1.004	1.109	1.291	Cd 2021: 1.278	

the cadmium reflections are given relative to the aluminium reflections at the two temperatures and hence knowing the values of  $(f_{86}/f_{293})^2$  for the aluminium reflections we can calculate the corresponding values for the cadmium reflections. The essential stages of the calculation are indicated in the table, and it will be seen that we have again made allowance for the effect on the reflected intensities of the small changes in  $\phi(\theta)$  and  $A$ . The values assumed for  $(f_{86}/f_{293})$  for the aluminium reflections have been calculated from the experimental results obtained by James, Brindley and Wood<sup>(5)</sup> who investigated the intensities reflected by single crystals of aluminium between room temperature and that of liquid air. Their results are

expressed in the following form: the scattering factor  $f_T$  at temperature  $T$  is related to the scattering factor  $f$ , for the atom at rest, by the equation

$$f_T = fe^{-M},$$

where, for the  $(h, k, l)$  reflection,

$$M = (h^2 + k^2 + l^2) [3.87 \times 10^{-5} T + 0.177/T - 277/T^3]. \quad \dots(3)$$

Hence

$$(f_{86}/f_{293})^2 = e^{2(M_{293} - M_{86})}.$$

It will be seen from the seventh column of table 2 that for each of the two cadmium reflections there is good agreement between the two values of  $(f_{86}/f_{293})^2$  obtained by comparison with the aluminium reflections, the mean values of which are given in the final column of the table.

We now use the absolute values of  $(f_{86}/f_{293})^2$  for the  $11\bar{2}2$  and  $20\bar{2}1$  reflections to place the relative values in the sixth column of table 1 on an absolute basis. The necessary data are collected together in table 3 and the final absolute values of  $(f_{86}/f_{293})^2$  are given in the seventh column of table 1.

Table 3

Reflections	$(f_{86}/f_{293})$		Ratio of absolute values relative values
	Absolute values from table 2, column 8	Relative values from table 1, column 6	
11 $\bar{2}$ 2	1.334	1.008	1.323
20 $\bar{2}$ 1	1.278	0.966	1.323

Mean ratio, 1.323

#### § 4. DISCUSSION OF RESULTS

It has been shown in previous papers<sup>(2, 9, 10)</sup> that for hexagonal crystals the exponent  $M$  in the equation  $f_T = fe^{-M}$  can be expressed in the form

$$M_\psi = \frac{6h^2T}{mk} \left[ \left( \frac{Q}{\Theta^2} \right)_0 \cos^2 \psi + \left( \frac{Q}{\Theta^2} \right)_{90} \sin^2 \psi \right] (\sin \theta/\lambda)^2, \quad \dots(4)$$

where  $\psi$  is the angle between the  $c$  axis and the normal to the reflecting plane,  $Q$ , the so-called "quantization factor", is  $[\phi(x) + x/4]$ ,  $\phi(x)$  being the Debye function while  $x = \Theta/T$ ,  $\Theta$  is the characteristic temperature which is to be regarded as a function of  $\psi$ ,  $m$  is the mass of the atom and the other symbols have their usual significance. The suffixes 0 and 90 attached to the quantity  $(Q/\Theta^2)$  indicate values corresponding to directions parallel and perpendicular to the  $c$  axis. This equation can be compared with the experimental results as follows. We have

$$\log_e (f_{86}/f_{293})^2 = 2(M_{293} - M_{86}) = 2\Delta M, \quad \dots(5)$$

whence

$$\frac{\log_e (f_{86}/f_{293})^2}{(\sin \theta/\lambda)^2} = \frac{12h^2}{mk} \left[ \left\{ \Delta \left( \frac{TQ}{\Theta^2} \right)_0 - \Delta \left( \frac{TQ}{\Theta^2} \right)_{90} \right\} \cos^2 \psi + \Delta \left( \frac{TQ}{\Theta^2} \right)_{90} \right], \quad \dots(6)$$

where the symbol  $\Delta(TQ\Theta^2)$  denotes the change in  $(TQ/\Theta^2)$  between  $86^\circ$  and  $293^\circ$  K. In table 4 are given the values of  $\psi$  and  $\cos^2 \psi$  calculated from the equation

$$\cos \psi = \left(\frac{l}{R}\right) \{4(h^2 - kh + k^2)/3 + (l/R)^2\}^{-\frac{1}{2}}, \quad \dots\dots(7)$$

where  $h$ ,  $k$  and  $l$  are the indices of the reflection and  $R$  is the axial ratio; this table also gives the values of  $[\log_e(f_{86}/f_{293})^2] (\sin \theta/\lambda)^{-2}$ .

According to equation (6) we should expect to obtain a linear relation between  $[\log_e(f_{86}/f_{293})^2] (\sin \theta/\lambda)^{-2}$  and  $\cos^2 \psi$ . These quantities are plotted in figure 1, where the vertical line attached to each observation indicates the probable experimental error; the error has been calculated from the probable errors in the measured

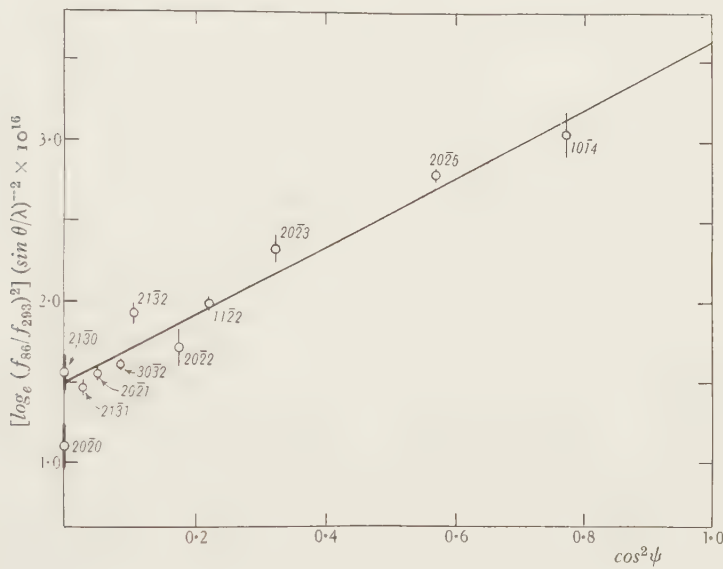


Figure 1.

Table 4

Reflection	$10^{-16}(\sin \theta/\lambda)$ at $293^\circ$	$\psi$ (degrees)	$\cos^2 \psi$	$(f_{86}/f_{293})^2$	Probable percentage error	$\log_e(f_{86}/f_{293})^2 / (\sin^2 \theta/\lambda^2) \times 10^{16}$
1122	0.381	62.1	0.220	1.334	0.6	$1.99 \pm 0.04$
2020	0.388	90.0	0.000	1.181	2.0	$1.10 \pm 0.13$
2021	0.397	77.1	0.050	1.278	0.7	$1.55 \pm 0.04$
1014	0.406	28.6	0.771	1.650	2.4	$3.04 \pm 0.14$
2022	0.428	65.3	0.174	1.370	1.9	$1.72 \pm 0.12$
2023	0.472	55.4	0.322	1.680	2.0	$2.33 \pm 0.09$
2130	0.514	90.0	0.000	1.509	3.0	$1.56 \pm 0.11$
2131	0.522	80.1	0.029	1.488	1.4	$1.46 \pm 0.05$
2132	0.544	70.9	0.107	1.769	2.2	$1.93 \pm 0.07$
2025	0.591	41.0	0.569	2.651	1.6	$2.79 \pm 0.05$
3032	0.610	73.0	0.086	1.816	1.2	$1.61 \pm 0.03$

intensities obtained by means of the usual Gaussian formula. The best straight line calculated by the method of least squares is shown; the point corresponding to the  $2\bar{0}\bar{2}0$  reflection lies well off this line and was therefore neglected in making the calculation. From the gradient and intercept of the line we obtain the following:

$$\frac{12h^2}{mk} \left[ \Delta \left( \frac{TQ}{\Theta^2} \right)_0 - \Delta \left( \frac{TQ}{\Theta^2} \right)_{90} \right] = 2.12_6 \times 10^{-16}$$

and

$$\frac{12h^2}{mk} \Delta \left( \frac{TQ}{\Theta^2} \right)_{90} = 1.50_2 \times 10^{-16},$$

whence

$$\frac{12h^2}{mk} \Delta \left( \frac{TQ}{\Theta^2} \right)_0 = 3.62_8 \times 10^{-16}.$$

Taking  $h = 6.554 \times 10^{-27}$ ,  $k = 1.372 \times 10^{-16}$  and  $m = 112.4 \times 1.649 \times 10^{-24}$ ,

we obtain

$$\Delta(TQ/\Theta^2)_{90} = 0.741 \times 10^{-2}$$

and

$$\Delta(TQ/\Theta^2)_0 = 1.789 \times 10^{-2}.$$

The corresponding values of  $\Theta$  derived by a graphical method are

$$\Theta_0 = 107^\circ \text{ K.},$$

$$\Theta_{90} = 164.5^\circ \text{ K.}$$

Using these values of  $\Theta$  we now calculate the root-mean-square atomic displacements as a function of  $\psi$  and of the temperature. For the particular cases  $0^\circ$  and  $90^\circ$ , we have for the mean-square displacements

$$\overline{u_0^2} = \frac{3h^2T}{4\pi^2 mk} \left( \frac{Q}{\Theta^2} \right)_0 \quad \text{and} \quad \overline{u_{90}^2} = \frac{3h^2T}{4\pi^2 mk} \left( \frac{Q}{\Theta^2} \right)_{90},$$

and for the mean-square displacement in any direction

$$\overline{u^2}_\psi = \overline{u_0^2} \cos^2 \psi + \overline{u_{90}^2} \sin^2 \psi.$$

The following numerical results, expressed in Angstrom units, are obtained:

$$T = 86^\circ \text{ K.}: \overline{u_0^2} = 0.0101, \overline{u_{90}^2} = 0.00447; \sqrt{\overline{u_0^2}} = 0.100, \sqrt{\overline{u_{90}^2}} = 0.066_8,$$

$$\text{when } T = 293^\circ \text{ K.}: \overline{u_0^2} = 0.0330, \overline{u_{90}^2} = 0.0140; \sqrt{\overline{u_0^2}} = 0.182, \sqrt{\overline{u_{90}^2}} = 0.118.$$

Figure 2 shows the root-mean-square displacements at  $86^\circ$  and  $293^\circ$  K. as functions of the angle  $\psi$ .

Finally it is of interest to compare the present results for cadmium with those obtained by Wollan and Harvey<sup>(8)</sup> for zinc using a similar x-ray method. The characteristic temperatures obtained by Grüneisen and Goens<sup>(4)</sup> from experiments on the thermal expansion of single crystals of cadmium and zinc may also be considered. These data are set out in table 5. For both metals the  $\Theta$ 's from the x-ray data are less than those given by Grüneisen and Goens, while the ratio  $\Theta_{90}/\Theta_0$  has larger values from the x-ray measurements than from the thermal-expansion data. When the values of  $\Theta$  for zinc are compared with the corresponding values for cadmium obtained by the two methods, we see that there is a somewhat greater difference between the  $\Theta$ 's derived from the x-ray data than between those obtained from the thermal expansion data.

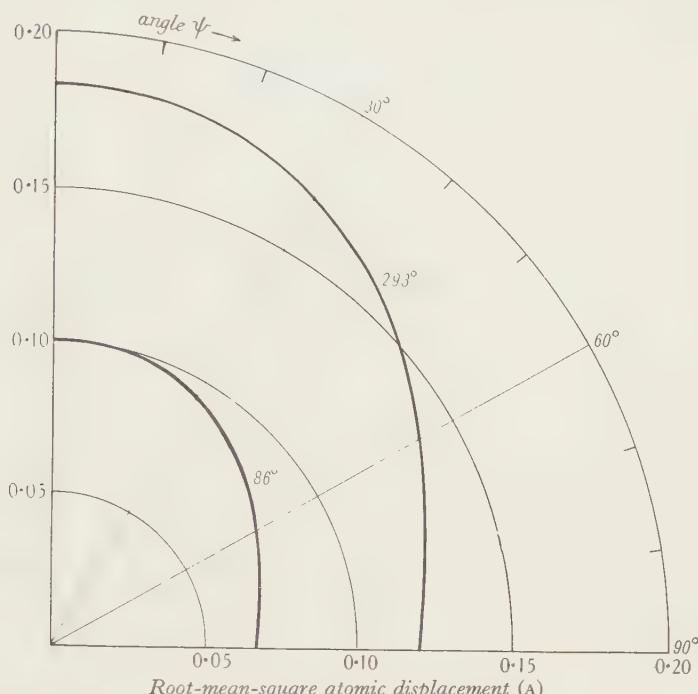


Figure 2. Polar diagram of root-mean-square atomic displacements in cadmium at  $86^\circ$  and  $293^\circ$  K. The vertical axis of the diagram corresponds to the  $c$  axis of the crystal and the horizontal axis to the basal plane.

Table 5. Comparison of the characteristic temperatures of cadmium and zinc

		Cadmium	Zinc	Zinc/ cadmium
x-ray determinations	$\left\{ \begin{array}{l} \Theta_0 \\ \Theta_{90} \\ \Theta_{90}/\Theta_0 \end{array} \right.$	107 164.5 1.54	170 285 1.68	1.59 1.73 —
Given by Grüneisen and Goens from thermal expansion data	$\left\{ \begin{array}{l} \Theta_0 \\ \Theta_{90} \\ \Theta_{90}/\Theta_0 \end{array} \right.$	160 214 1.34	200 320 1.60	1.25 1.49 —

## § 5. COMPARISON OF X-RAY MEASUREMENTS WITH SPECIFIC-HEAT MEASUREMENTS.

*Added in proof, 5 December 1938*

It is also of interest to compare the  $\Theta$ s from the x-ray data with the values obtained from specific-heat measurements. Since the latter are values averaged over all directions in the crystal lattice, we must first calculate average values from

the x-ray results. The mean square displacement in a hexagonal crystal is given by the equation

$$\overline{u_{av.}^2} = \frac{1}{3} (\overline{u_0^2} + 2\overline{u_{90}^2}). \quad \dots\dots(8)$$

Correspondingly we have

$$\overline{\Theta_{av.}^2} = \frac{1}{3} \left( \frac{\overline{\Theta_0^2}}{\Theta_0^2} + \frac{2}{\Theta_{90}^2} \right). \quad \dots\dots(9)$$

The results are collected together in table 6 for the three hexagonal metals magnesium, zinc and cadmium. In our previous paper on magnesium<sup>(2)</sup> we pointed out that there was an appreciable difference between the mean x-ray value, 331°, and the specific-heat value, 290°. In the meantime, Dr Blackman has kindly drawn our attention to a more recent determination of the specific heat of magnesium by Clusius and Vaughan<sup>(11)</sup>, who state that "above 30°K. a Θ value of 322° reproduces a fairly satisfactory atomic heat value". This improves very considerably the agreement between the Θs from the x-ray data and from specific-heat data. For zinc there is also a reasonably good agreement between the Θ values obtained in the two ways, but for cadmium the agreement is not so close.

Table 6. Comparison of Θ from x-ray data and Θ from specific-heat data

Metal	Axial ratio	From x-ray data			From specific-heat data
		$\overline{\Theta_0}$	$\overline{\Theta_{90}}$	$\overline{\Theta_{av.}}$	
Magnesium	1.624	339	327	331	322
Zinc	1.856	170	285	225	235
Cadmium	1.886	107	164.5	136.5	172

#### § 6. ACKNOWLEDGEMENTS

Finally we wish to thank Prof. Whiddington, F.R.S., for his interest in this work, the Department of Scientific and Industrial Research for a maintenance grant to one of us (P. R.), and the Government Grant Committee for a grant with which part of the apparatus was purchased.

#### REFERENCES

- (1) BRINDLEY G. W. *Proc. Leeds Phil. Lit. Soc.* **3**, 200 (1936).
- (2) BRINDLEY, G. W. and RIDLEY, P. *Proc. Phys. Soc.* **50**, 757 (1938).
- (3) FULLER, M. L. See *A Study of Crystal Structure and its Applications*, p. 399, by W. P. Davey.
- (4) GRÜNEISEN, E. and GOENS, E. *Z. Phys.* **29**, 141 (1924).
- (5) JAMES, R. W., BRINDLEY, G. W. and WOOD, R. G. *Proc. Roy. Soc. A*, **125**, 401 (1929).
- (6) JETTE, E. R. and FOOTE, F. *J. Chem. Phys.* **3**, 616 (1935).
- (7) OWEN, E. A. and ROBERTS, E. W. *Phil. Mag.* **22**, 290 (1936).
- (8) WOLLAN, E. O. and HARVEY, G. G. *Phys. Rev.* **51**, 1054 (1937).
- (9) ZENER, C. *Phys. Rev.* **49**, 122 (1936).
- (10) ZENER, C. and BILINSKY, S. *Phys. Rev.* **50**, 101 (1936).
- JAUNCEY, G. E. M. and BRUCE, W. A. *Phys. Rev.* **51**, 1067 (1937).
- (11) CLUSIUS, K. and VAUGHAN, J. V. *J. Amer. Chem. Soc.* **52**, 4686 (1930).

# THE CRITICAL-FREQUENCY METHOD OF MEASURING UPPER-ATMOSPHERIC IONIZATION

BY E. V. APPLETON, F.R.S., Cavendish Laboratory, Cambridge  
 R. NAISMITH AND L. J. INGRAM  
 Radio Department, National Physical Laboratory

*Received 27 July 1938*

*ABSTRACT.* The formulae normally employed in the application of the critical-frequency method of measuring upper-atmospheric ionization are examined and are shown to be appropriate in the case of ionospheric regions which are thick when measured in terms of a wave-length. The complications arising from the occurrence of ionized clouds or strata embedded in the normal regions are described and interpreted.

## § 1. INTRODUCTION

THE critical-frequency method of measuring upper-atmospheric ionization, using vertical radio-wave sounding<sup>(1, 2)</sup>, has now been adopted by many stations in different parts of the world and a fairly extensive long-term investigation of the ionosphere by means of it is now in progress. The essential procedure is as follows. The equivalent height  $h'$  is found as a function of the radio-wave frequency  $f$ , and, from the  $\{h', f\}$  curve, the critical frequencies are noted. From the magnitude of the critical frequency for either the ordinary or the extraordinary wave components, the maximum ionization-density in any region can be calculated.

## § 2. THE RELATION BETWEEN CRITICAL FREQUENCY AND MAXIMUM IONIZATION-DENSITY

The various critical phenomena which attend the propagation of waves in the ionosphere are usually interpreted in terms of the magneto-ionic theory. In the general formulation of this theory, Appleton<sup>(3)</sup> has shown that the refractive index  $\mu$  of the ionized medium becomes equal to zero when

$$\alpha = -1, \quad \dots\dots(1)$$

or when

$$\alpha = -1 \pm \gamma_H, \quad \dots\dots(2)$$

while  $\mu$  attains an infinite value when

$$\alpha^2 = \left( \frac{\alpha}{1 + \alpha} \right) \gamma_T^2 + \gamma_L^2. \quad \dots\dots(3)$$

The nomenclature here adopted is somewhat similar to that used by Lorentz, and may be conveniently written as follows:

$$\alpha = -\frac{\pi m f^2}{N e^2} - l,$$

$$\gamma_H = \frac{\pi m f f_H}{N e^2},$$

$$\gamma_T = \frac{\pi m f f_T}{N e^2},$$

and

$$\gamma_L = \frac{\pi m f f_L}{N e^2}.$$

Here  $N$  represents the number of electrons, of charge  $e$  and mass  $m$ , per cm.<sup>3</sup>,  $f$  is the frequency of the exploring radio waves, and  $f_H$ ,  $f_T$  and  $f_L$  are the electron gyro-frequencies corresponding respectively to the earth's total, transverse and longitudinal magnetic components. The so-called Lorentz polarization term is denoted by  $l$ .

By virtue of the fortunate fact that the normal conditions for the reflection of either the ordinary or the extraordinary wave at normal incidence (i.e.  $\mu^2=0$ ) are independent of the angle between the wave track and the direction of the earth's magnetic field—see equations (1) and (2)—the same formulae relating the maximum ionization-density in a given region to the critical penetration frequency  $f$  can be used in any part of the world. The numerical magnitude of  $N$  depends, however, on whether the Lorentz polarization term  $l$  is included or not in the fundamental formulae of the magneto-ionic theory. If the polarization term is neglected, so that  $l=0$ , equations (1) and (2) become, in practical form,

$$N = \frac{\pi m}{e^2} f_0^2 = 1.24 \times 10^{-8} f_0^2 \text{ (ordinary wave)}, \quad \dots\dots(4)$$

$$\text{and } N = \frac{\pi m}{e^2} (f_x^2 \pm f_x f_H) = 1.24 \times 10^{-8} (f_x^2 \pm f_x f_H) \text{ (extraordinary wave)}, \quad \dots\dots(5)$$

where  $f_0$  and  $f_x$  are the critical frequencies for the ordinary and extraordinary waves respectively. The first of these two formulae is applicable as the expression of the condition for zero refractive index ( $\mu=0$ ) for all values of  $f_0$ . The second formula (upper sign) is valid when  $f_x < f_H$ . When  $f_x > f_H$  the same formula with the lower sign is relevant.

For the conditions expressed above the group velocity of the waves falls to zero with the refractive index. The group velocity is zero also when the refractive index becomes infinite. The practical relation between  $N$  and  $f$  for such conditions ( $l=0$ ) may then be obtained from equation (3) as follows:

$$N = 1.24 \times 10^{-8} f^2 \left( \frac{f_H^2 - f^2}{f_L^2 - f^2} \right). \quad \dots\dots(6)$$

Equation (6) applies for the extraordinary wave when  $f > f_H$ , and for the ordinary wave when  $f < f_L$ . When  $f_L < f < f_H$  the condition  $\mu = \infty$  cannot be fulfilled. When

$f > f_H$ , equation (4) applies alone for the ordinary wave. For the extraordinary wave, condition (5) is reached before condition (6), so that the wave is reflected at the level at which the refractive index is zero. Some experimenters<sup>(4)</sup>, however, claim that they have observed simultaneous reflections from ionization levels given by conditions (4), (5) and (6).

When  $f < f_L$ , condition (4) is reached before condition (6) for the ordinary wave, so that the former relation should still be used as the criterion of reflection. Martyn and Munro have, it is true, claimed that they have detected critical effects expressed by both equations, but it is possible that they were confusing ordinary waves and extraordinary waves<sup>(5)</sup>.

When the Lorentz polarization term is included,\* so that  $l = \frac{1}{3}$ , equations (1) and (2) become, respectively,

$$N = \frac{3}{2} \frac{\pi m f_0^2}{e^2} = 1.86 \times 10^{-8} f_0^2 \quad \dots\dots(7)$$

and  $N = \frac{3}{2} \frac{\pi m}{e^2} (f_x^2 \pm f_x f_H) = 1.86 \times 10^{-8} (f_x^2 \pm f_x f_H). \quad \dots\dots(8)$

The corresponding equation (3) for  $\mu = \infty$  becomes, for the quasi-transverse conditions we are considering, rather complicated and is best illustrated by the  $\{\mu^2, N\}$  curves given by Miss M. Taylor<sup>(6)</sup>. One special point of practical interest which arises in this case may, however, be mentioned here. Although at low frequencies the condition  $\mu^2 = 0$  determines the levels of reflection for both the ordinary and extraordinary waves—see equations (7) and (8)—there is a certain range  $f_\lambda < f < f_H$  of frequencies in which the condition  $\mu^2 = \infty$  is reached for the extraordinary wave before the condition  $\mu^2 = 0$ . In an  $\{h', f\}$  curve the value of  $h'$  would then be expected to increase rapidly as  $f$  increases towards  $f_\lambda$ . Since the value of  $f_\lambda$  is not related to the maximum ionization of the layer in question, it must not be confused with a true critical penetration frequency. It represents, in fact, the lowest frequency for which the condition  $\mu^2 = \infty$  is reached, with increasing  $N$ , before the condition  $\mu^2 = 0$ . In the corresponding case in which the Lorentz polarization term is not included ( $l = 0$ ) a similar, though not physically analogous,  $\{h', f\}$  curve is to be expected as  $f$  approaches  $f_H$ . This particular matter has been lucidly explained by Goubau<sup>(7)</sup> in his exposition of the fundamental magneto-ionic equations.

Two important problems arise in connexion with the selection of critical frequencies from  $\{h', f\}$  data. The first arises from the fact that, for the conditions in which the refractive index  $\mu$  of the medium vanishes (this being the criterion chosen to represent the condition of reflection) the ray treatment breaks down and a wave treatment has to be substituted. This particular matter is of interest in the determination of both region-*E* and region-*F* critical frequencies. The second matter arises in connexion with what we have called the abnormal region-*E* phenomenon<sup>(8)</sup>.

\* Evidence in favour of its inclusion has recently been published by Booker and Berkner<sup>(20)</sup>.

### § 3. THE INFLUENCE OF LAYER-THICKNESS ON THE RELATIONS BETWEEN GROUP HEIGHT, ECHO-INTENSITY, AND FREQUENCY

In order to discuss this matter it is necessary to consider first the relation between electron-content  $N$  and the height  $h$  in the atmosphere. Following Chapman we shall assume that the relation between  $N$  and  $h$  is

$$N = N_0 e^{\frac{1}{2}(1-z-e^{-z} \sec \chi)}, \quad \dots\dots(9)$$

where

$$z = \frac{h-h_0}{H} \quad \dots\dots(10)$$

and  $N_0$  is the maximum ionization formed at height  $h_0$  when the angle of incidence  $\chi$  of the sun's rays is zero. Thus  $z$  is the height measured in terms of  $H$  as the unit reckoned from the level  $h_0$ . From equation (9) we can show that  $N$  is a maximum when  $\cos \chi = e^{-z_m}$ . Let the value of this maximum be  $N_{\max}$  and its height  $h_m$ . It is then easy to show that

$$N = N_{\max} e^{\frac{1}{2}(1-(z-z_m)-e^{-(z-z_m)})}, \quad \dots\dots(11)$$

or

$$N = N_{\max} e^{\frac{1}{2}(1-y/H-e^{-y/H})}, \quad \dots\dots(12)$$

where  $y$  is the height, relative to the level of maximum ionization, measured now in ordinary, not scale-height, units.

Since we are especially interested, so far as penetration phenomena are concerned, in conditions near the top of the layer in question we can expand equation (12) for small values of  $y$ . It then becomes

$$N = N_{\max} \left( 1 - \frac{y^2}{4H^2} \right). \quad \dots\dots(13)$$

In other words we may assume as a first approximation that the distribution of ionization is parabolic. We shall consider critical-frequency phenomena for such a region first in terms of a ray treatment and secondly in terms of a wave treatment. To simplify the discussion we neglect the influence of the earth's magnetic field.

It has previously been shown<sup>(9)</sup> for a parabolic distribution of ionization, in which

$$N = \frac{\pi m}{e^2} f_c^2 \left( 2 \frac{y}{y_m} - \frac{y^2}{y_m^2} \right), \quad \dots\dots(14)$$

that the relation between group path  $P'$  and frequency  $f$  for the ordinary wave is

$$P' = 2h' = y_m \frac{f}{f_c} \log \left( \frac{f_c + f}{f_c - f} \right). \quad \dots\dots(15)$$

Here  $f_c$  is the critical frequency and  $y_m$  is the semi-thickness of the layer. Thus, in terms of a ray treatment, the equivalent height  $h'$  should tend to infinity as  $f$  approaches the critical value  $f_c$ . Also it is obvious from the ray treatment that the intensity of reflection should drop sharply to zero as soon as the frequency exceeds the critical value.

We now turn to consider similar matters in terms of a wave treatment. The

case of a layer having a triangular distribution has already been considered by Hartree<sup>(10)</sup>, so far as variation of reflection coefficient with frequency is concerned, and from his investigation it is possible to show that, for a layer which is thick in relation to the vacuum wave-length  $\lambda_c$  corresponding to the critical frequency, there is a very rapid fall of reflection coefficient with frequency increase near the critical value, and that the reflection coefficient  $\rho$  is always 0·5 at the critical frequency.

The corresponding matter for a parabolic layer has been investigated by Dr H. G. Booker, to whom we are greatly indebted for permission to quote here his results. Dr Booker finds for such a region, where  $f(=)f_c$ , and  $y_m \gg \frac{\lambda_c}{2\pi}$ , that

$$\frac{\rho^2}{1-\rho^2} = \exp \left\{ \frac{4\pi^2}{c} y_m (f_c - f) \right\}. \quad \dots \dots (16)$$

In this case the value of  $\rho$  is 0·707 when  $f=f_c$ . Now reasons have been given<sup>(9)</sup> recently for concluding that a rough approximation for region  $E$  is obtained by assuming a parabolic distribution with  $y_m$  equal to 20 km., the corresponding value for region  $F$  being 100 km. On substitution of either of these values for  $y_m$  in Booker's formula, it is easily shown that there should be a very sharp change from reflection to penetration at the normal values of critical frequency.

It should, of course, be added that we have so far considered only the question of electron-limitation, having neglected the influence of collisional-friction absorption. Now the work of Eckersley<sup>(11)</sup>, Farmer and Ratcliffe<sup>(12)</sup>, and White and Brown<sup>(13)</sup> has shown that such absorption becomes very marked when the frequency approaches the critical value, causing the value of  $\rho$  to fall rapidly as  $f$  approaches  $f_c$ . For a thick layer we now see that it must be the important factor, and the above considerations confirm the correctness of the assumption made by the above-mentioned authors, that electron-limitation is not appreciably effective when  $f$  is less than  $f_c$ .

From his wave treatment of the parabolic layer Dr Booker has further shown that the equivalent height at the critical frequency is not infinite, as indicated by the ray treatment, but is given by

$$h'_c = h_0 + \frac{y_m}{2} \left[ \frac{9}{7} + \log_e \frac{8\pi y_m}{\lambda_c} \right], \quad \dots \dots (17)$$

where  $h_0$  is the height of the lower boundary.

If, as before, we assume that  $y_m = 20$  km. for region  $E$ , and also take  $h_0$  as 90 km., we find that at the critical frequency  $h'_c = 286$  km. In the corresponding case of region  $F$ , where we take  $y_m = 100$  km. and  $h_0 = 200$  km., we find that when  $f=f_c$ ,  $h'_c = 1462$  km. In both cases, therefore, we should expect very great group-retardation effects as shown by great effective heights. With senders of great power it might be possible to measure this maximum equivalent height though, with the powers normally used, absorption limitation phenomena usually cause the echoes to fail before  $h'$  reaches the value  $h'_c$  given by equation (17).

§ 4. THE SELECTION OF CRITICAL FREQUENCIES  
FROM  $\{h', f\}$  DATA

From the above discussion we may say that if electron-limitation alone were operative the critical frequency of either region  $E$  or region  $F$  (both regions being thick as measured in terms of a vacuum wave-length) could be selected as the frequency at which the reflection coefficient falls sharply. With a very high-powered sender it is probable that this criterion might be useful, but with the lower-powered senders mainly used the exact frequency at which echoes from any region cease to be detected is usually determined by the absorption associated with group retardation. It is therefore more reliable, in the present state of our technique, to select the frequency at which the increase of  $h'$  with  $f$  is very rapid. We have already seen that in the case of both regions  $E$  and  $F$  the increase of equivalent height due to group retardation for frequencies just less than the critical value should be very considerable. This is the criterion which is used by us in connexion with the published measurements of critical frequency made at the Radio Research Station, Slough. It should, however, be added that in practice the differences obtained by means of the two criteria are extremely small. Days of severe absorption can be detected because the part of the  $\{h', f\}$  curve where  $h'$  increases rapidly with  $f$  is then blotted out. This fact is important in the determination of  $f_{F_2}$ , where we are concerned chiefly with the border between reflection and no reflection. On the other hand, for regions  $E$  and  $F_1$  we are concerned, in the absence of intense abnormal region- $E$  ionization, with the sudden discontinuity of the height of reflection. Except in the case of very severe absorption  $f_E^\circ$  is then clearly evident. It is, in fact, remarkable how sharp the discontinuity in the  $\{h', f\}$  curve is, there being practically no frequency overlap of simultaneous reflection from regions  $E$  and  $F$ . In the case of the determination of  $f_{F_1}$ , which can be made in the day time only, no ambiguity exists because we are concerned with the determination of the frequency at which a maximum of  $h'$  occurs for conditions under which the reflected wave (the ordinary wave especially) is of quite appreciable intensity.

§ 5. CRITICAL-FREQUENCY PHENOMENA FOR REGION  $E$

As was pointed out in the last section, the determination of  $f_E^\circ$  is quite straightforward except when it is complicated by the presence of what we have called the abnormal region- $E$  phenomenon. There is then no very marked increase of  $h'$  with  $f$ . Moreover, the frequency at which the change-over from reflection from region  $E$  to reflection from region  $F$  occurs often varies in an irregular manner. A fairly complete account of the incidence of this abnormal region- $E$  phenomenon in both high and medium latitudes has been given by us recently<sup>(8)</sup>. In the present paper the discussion will be continued.

We can best approach the matter by considering conditions in which the abnormal region- $E$  phenomenon is absent. Such conditions are often found at the equinoxes. In figure 1 is shown an  $\{\text{equivalent-height}, \text{frequency}\}$  curve for the magneto-ionic

ordinary component on 9 October 1937 at 1430. It will be seen that the marked group-retardation effects which are experienced in studying region-*F* critical-frequency phenomena are here present, so that the selection of the region-*E* critical frequency is now a simple matter. There are, however, many occasions, particularly during the day time in summer, when the  $\{h', f\}$  curve is as shown in

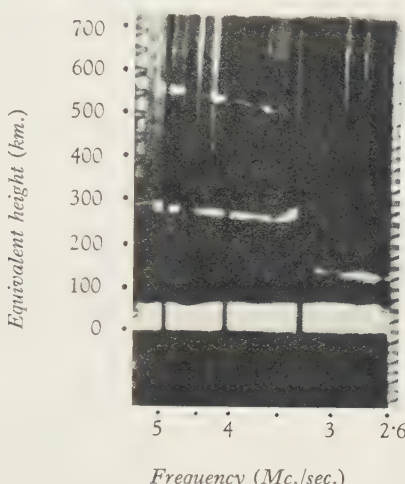


Figure 1. Simple  $\{\text{equivalent-height}, \text{frequency}\}$  curve at 1430 G.m.t. at Slough on 9 October 1937

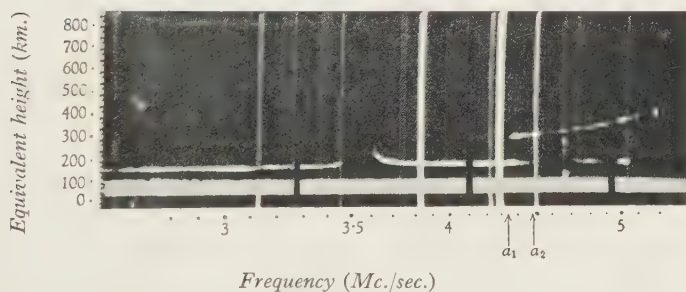


Figure 2.  $\{\text{equivalent-height}, \text{frequency}\}$  curve for Slough at noon on 4 May 1937, showing abnormal region-*E* phenomenon.

figure 2, which represents conditions at noon on 4 May 1937. It will be seen that where  $f < f_E^\circ$  (note  $f_E^\circ$  is shown at 3.55 Mc./sec. in figure 2) the  $\{h', f\}$  curve is normal except that very marked group-retardation phenomena, which occur when  $f$  approaches  $f_E^\circ$ , are not shown. Instead, the value of  $h'$  after reaching a certain value falls rapidly to a height which is maintained constant. There is to be noted also at a higher frequency, marked  $a_1$  in figure 2, a change-over from reflection at region-*E* levels to region-*F* levels with little or no group retardation. Moreover, there is a certain amount of frequency overlap  $a_1 a_2$  in the process. At a higher

frequency the same phenomena are discernible for the extraordinary wave. For the time being, however, we concern ourselves only with the phenomena of the ordinary wave.

It is very important that observers should state what criterion has been selected to denote the critical frequency for the normal region  $E$  caused by ultraviolet light when conditions are such as are illustrated by the  $\{h', f\}$  curve in figure 2, since some take what we have called above  $f_E^\circ$  while others take the frequency  $f_{AE}$ , at which region- $F$  echoes are first seen.\* As will be seen later, we believe that the value shown as  $f_E^\circ$  is very close to the true critical frequency for the normal region  $E$ , and that the frequency  $f_{AE}$  has no significance at all in this connexion.

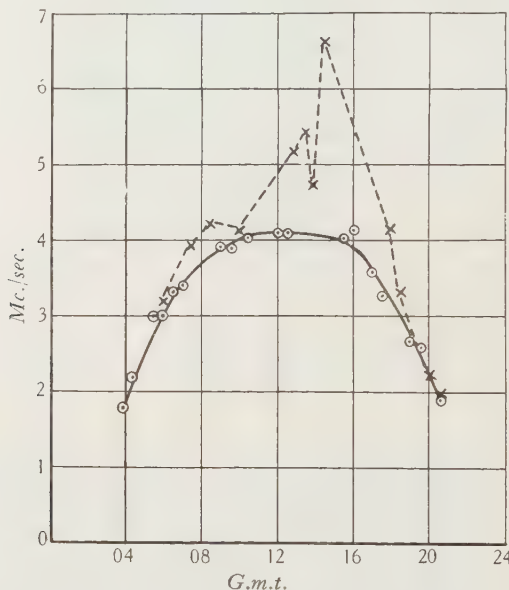


Figure 3. Typical variation of  $f_E^\circ$  and  $f_{AE}$  on a summer day.  
 $f_E^\circ$ , —○—;  $f_{AE}$ , ---×---.

In figure 3 is shown a plot of values of  $f_E^\circ$  and  $f_{AE}$  during a summer day. It will be seen that  $f_E^\circ$  varies regularly over the day-time period while the frequency  $f_{AE}$  varies irregularly. We now turn to a more detailed consideration of the significance of the latter.

It might, at first sight, be thought that the persistence of reflection beyond the normal critical frequency of region  $E$  is to be explained on the basis of the region being a thin one. We have, however, argued against such an explanation by pointing out that on a day on which the phenomenon is absent the  $\{h', f\}$  curve shows that region  $E$  must be many wave-lengths thick, and that there is no reason for assuming that the value of the scale height  $H$  of the atmosphere, which determines this thickness, should vary from day to day. Instead we have suggested that there are,

\* Judson<sup>(14)</sup>, for example, takes the critical frequency to be "the lowest radio frequency which penetrates the region at normal incidence".

embedded in the normal region  $E$ , scattering centres or reflecting strata of greater ionization-density which produce the persistence of reflection for frequencies higher than  $f_E$ . This suggestion at once explains the group-retardation phenomena associated with  $f_E$  in figure 2, for region  $E$  is sufficiently thick to cause them. If the patches or strata of abnormal region  $E$  are assumed to be thin as compared with the normal region  $E$ , the absence of marked group retardation in the frequency range  $a_1 a_2$ , and in the case of  $M$ -reflections (which we have previously shown to be caused by the agency of the abnormal region  $E$ ) is also explained.

Best, Farmer and Ratcliffe<sup>(15)</sup> have pointed out that, under very slightly disturbed conditions, abnormal effects may be due to clouds of more intense ionization immersed in a simple region. Very often we have found that, when the extension of reflection beyond  $f_E$  is not large, the echoes returned are irregular in character such as might be caused by scattering from patches. But when abnormal region- $E$  echoes are returned for frequencies extending over 1 Mc./sec. beyond  $f_E$ , the heterogeneous character disappears and reflection persists from a fairly constant level. It is probable that, on such occasions, a thin sheet is formed by the coagulation of a large number of ionized clouds. On rarer occasions this thin sheet may be so dense as to constitute what we have called "intense- $E$ " conditions. On such occasions reflection persists up to frequencies beyond the region- $F$  critical value.

We have made a number of experiments to see if abnormal region- $E$  conditions are simultaneously observed at the two stations of Slough and Cambridge, which are 60 miles apart. No marked agreement was found between the results obtained at the two stations, a fact which illustrates the local character of the phenomenon. Under intense- $E$  conditions in summer, however, the densely ionized stratum must be of much greater extent since, as was found some years ago<sup>(16)</sup>, they are frequently associated with conditions extremely favourable to long-distance transmission.

*The influence of abnormal region- $E$  height on normal region- $E$  critical frequency.* If we suppose, as an extreme case, that the abnormal region  $E$  has a sharp boundary, it is easy to see that the measurement of  $f_E$  will be strictly accurate only when this boundary is at or above the level of maximum ionization in normal region  $E$ . If the abnormal region  $E$  is slightly lower than the maximum in region  $E$ , the measured value of  $f_E$  as shown in figure 2 will be too low. The evidence we have been able to gather from a study of events on successive days with varying values of  $f_{AE}$  supports this view. When the equivalent height of the abnormal region  $E$  is low,  $f_E$  is correspondingly reduced.

We have very frequently noticed that, when the height of abnormal region  $E$  ( $h'_{AE}$ ) is abnormally low, the group retardation effect round  $f_E$  is less marked and  $f_{AE}$  is high. In other words, the further the agency causing abnormal region  $E$  penetrates downwards in normal region  $E$  the more intense is the ionization caused by it. We thus see how the abnormal region  $E$  can develop into what we have called "intense region  $E$ ". On such occasions the phenomena indicating  $f_E$  are entirely absent and reflections from a constant level occur over the whole frequency range.

*The seasonal variation of abnormal region- $E$  height.* In figure 4 are shown plots of the monthly means of  $h'_E$  and  $h'_{AE}$  at noon. In the same graph are exhibited

the monthly means of the heights of abnormal region  $E$  at night. Interesting differences are noted in the seasonal trend of these three quantities. In the first place the variation of  $h'_E$  is such as we should expect. Owing to the more nearly vertical solar incidence in summer we should expect  $h'_E$  to be less in summer than in winter. It is, however, possible that this difference is exaggerated, since with our present experimental arrangements, in which region- $E$  echoes cannot be determined for very low frequencies, it is possible that group retardation has added somewhat to the equivalent height  $h'_E$  in winter, since measurements have to be made at frequencies nearer to the critical value. The fact that  $h'_{AE}$  in the day time varies to a much greater extent, even though the measurements are unlikely to be influenced by group-retardation phenomena, is very surprising. That it varies in this way confirms our view that abnormal region  $E$  is due not merely to local irregularities

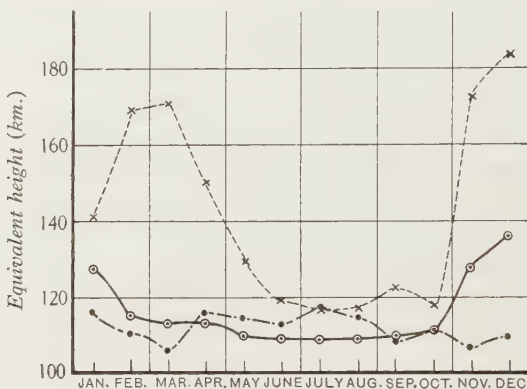


Figure 4. Monthly means of  $h'_E$ , —○—;  $h'_{AE}$  (day), ---×---; and  $h'_{AE}$  (night), -●---.

in normal region  $E$  but to an additional agency which forms additional patches or strata of ionization.

*Temporal sequences in the formation of abnormal region  $E$ .* It quite frequently happens in the day time that, on frequencies exceeding  $f_E^{\circ}$ , echoes are returned from several regions of different heights which are all less than that of region  $F_1$ . If the history of these regions is traced on a succession of half-hourly  $\{h', f\}$  records it is found that they are first noticeable as ledges on region  $F_1$  and that their penetration frequencies are then only slightly greater than that of the normal region  $E$ . At this stage they cause the usual group-retardation effects for frequencies nearly critical. They can next be detected as separate regions at an equivalent height of 150 to 180 km. Later, they still produce a small amount of group retardation on waves just penetrating them, but they are evidently becoming thinner and more densely ionized. They continue to fall in height and increase in density until they lose their separate identity and form the abnormal region- $E$  stratum described above. The number of intermediate regions, as the ionization levels between regions  $E$  and  $F_1$  may be called, existing at one time is never large. It is unusual to observe more than two or three. Generally it may be said that this phenomenon

of ionization falling in height and building up the abnormal region *E* begins just after sunrise and continues until about noon; the reverse process of regions of ionization increasing in height has never been observed. There is a tendency, though less marked, for the process to be repeated in the afternoon just before sunset. During the dark hours abnormal region-*E* reflections are returned from a fairly constant level, though often there is a slight fall in height immediately after the onset of reflection and a slight rise in height just before reflection ceases.

*The trailing-echo phenomenon.* On many occasions we have noted echoes of weak intensity from a level of about 90 to 100 km. persisting throughout the whole of the frequency range, which may otherwise reveal normal conditions. Such echoes are returned from levels well below the abnormal region-*E* centres or strata, and very rarely obstruct completely the passage of the waves to higher levels.

#### § 6. FURTHER DISCUSSION OF THE ABNORMAL REGION-*E* PHENOMENON

We have previously<sup>(17)</sup> noted a transient type of reflection, lasting only a few seconds and caused by scattering from temporary ionic cloudlets, which is found by day and night round about the 100 km. level. We stated that these short-lived echoes were not registered by the usual method of recording. Using greater sender power and faster photographing equipment Watt, Wilkins and Bowen<sup>(18)</sup>, and later Eckersley<sup>(19)</sup>, have succeeded in obtaining registration of these transient effects. They also confirm our observation that the effects occur during the night as well as during the day.

It may be that the abnormal region *E* is formed as the aggregate of such ionic cloudlets, but in many cases they must be sufficiently closely situated to form a definite stratum which is impenetrable for a certain frequency range. When an abnormal region-*E* echo is noted simultaneously with a region-*F* echo of normal amplitude, it is clear that the abnormal region-*E* echo is scattered from a cloud which may not necessarily be, and probably is not, overhead. On the other hand, when region *F* is cut off altogether one must assume an abnormal region-*E* sheet which is immediately overhead. This need not be very large, and indeed it is probable that the phenomenon is, to some extent, dependent on the relation between the size of the obstacle and the relevant Fresnel half-wave zones.

A word should be said concerning the phenomena attending the penetration of abnormal region *E* when reflection is gradually transferred from region *E* to region *F* with a certain amount of frequency overlap, as shown for instance at  $a_1 a_2$  in figure 2. Since we have pictured abnormal region *E* as resulting from the coagulation of a number of electronic cloudlets we may consider the stratum as being irregular in its maximum ionization in horizontal extent. Penetration of the more weakly ionized parts may therefore be considered as starting at  $a_1$  while that of the more densely ionized parts is complete at  $a_2$ .

### § 7. SCATTERING IN REGION F

We have examined our region-*F* records to see if there is any evidence of a phenomenon comparable to that experienced in the case of region *E*. In summer, both by night and by day, the  $\{h', f\}$  curves are quite simple and show few traces of reflection for frequencies beyond the critical value. During the winter nights, however, it is most usual to find persisting reflection of an irregular character when the critical frequency is exceeded. From the beginning of October the number of hours during which the phenomenon is encountered gradually increases, night after night, reaching a maximum in December, when it occurs for more than 12 hr. around midnight, and afterwards gradually becoming less prominent until the end of March. The phenomenon is rarely encountered during the months from April to September.

There is, however, a marked difference between region-*F* scattering and the abnormal region-*E* phenomenon. The echoes in the former case are always broadened and complicated in character; moreover, the equivalent height of the lower delay edge of the echo gradually increases with increase of frequency. When the critical frequency is exceeded there is no rapid fall of equivalent height followed by reflection from a constant level, such as is experienced in the fully developed region-*E* phenomenon.

The region-*F* scattering is evidently due to local irregularities which appear to form within the region when the sun is down, whereas the abnormal region-*E* reflections are due to reflection from a preferred height, from strata which may, on occasion, coagulate to form an intensely-ionized sheet.

### § 8. ACKNOWLEDGEMENT

This work has been carried out as part of the programme of the Radio Research Board of the Department of Scientific and Industrial Research.

### REFERENCES

- (1) APPLETON. *Nature, Lond.* (7 Feb. 1931).
- (2) APPLETON and NAISMITH. *Proc. Roy. Soc. A*, **137**, 36 (1932).
- (3) APPLETON. *Proc. Union Rad. Sci. Int. Washington* (October 1927).
- (4) PANT and BAJPAI. *Sci. and Cult.* **2**, 409 (1937).
- (5) APPLETON, FARMER and RATCLIFFE. *Nature, Lond.*, **141**, 409 (5 March 1938).
- (6) TAYLOR, M. *Proc. Phys. Soc.* **45**, 245 (1933).
- (7) GOUBAU. *Hochfrequenztech. u. Elektroakust.* **44**, 138 (1934).
- (8) APPLETON, NAISMITH and INGRAM. *Philos. Trans. A*, **236**, 191–259 (1937).
- (9) APPLETON. *Proc. Roy. Soc. A*, **162**, 451 (1937).
- (10) HARTREE. *Proc. Camb. Phil. Soc.* **25**, 97 (1929).
- (11) ECKERSLEY. *Nature, Lond.*, **135**, 435 (1935).
- (12) FARMER and RATCLIFFE. *Nature, Lond.*, **135**, 485 (1935).
- (13) WHITE and BROWN. *Proc. Roy. Soc. A*, **153**, 639 (1936).
- (14) JUDSON. *Proc. Inst. Radio Engrs, N.Y.*, **25**, 38 (1937).
- (15) BEST, FARMER and RATCLIFFE. *Proc. Roy. Soc. A*, **164**, 96 (1938).
- (16) APPLETON and NAISMITH. *Proc. Roy. Soc. A*, **150**, 691 (1935).
- (17) APPLETON, NAISMITH and INGRAM. *Philos. Trans. A*, **236**, 254 (1937).
- (18) WATT, WILKINS and BOWEN. *Proc. Roy. Soc. A*, **161**, 181 (1937).
- (19) ECKERSLEY. *Nature, Lond.*, **140**, 846 (1937).
- (20) BOOKER and BERKNER. *Nature, Lond.*, **141**, 562 (1938).

# THE ATMOSPHERIC HEIGHT DISTRIBUTION OF BAND-ABSORBED SOLAR RADIATION

By S. CHAPMAN, M.A., D.Sc., F.R.S.

*Received 5 May 1938. Read 14 October 1938*

*ABSTRACT.* The band absorption of radiation incident on the atmosphere at any zenith angle  $\chi$  is considered, when the relation between the absorption coefficient  $\alpha$  and the wave-length  $\lambda$  has the form of the error function, so that

$$\alpha_\lambda = \alpha_0 e^{-(\lambda - \lambda_0)^2 / \lambda_w^2} \equiv \alpha_0 e^{-l^2},$$

where  $l = (\lambda - \lambda_0) / \lambda_w$ , and the intensity of the incident radiation is either constant across the absorption band or varies linearly across it.

The height distribution of absorbed-energy density, the height of maximum volume absorption, the spectral composition of the energy absorbed at any level, and the proportionate daily variation of absorption density, are first discussed without any special assumption as to the height distribution of the absorbing constituent in the atmosphere.

The height distribution of absorbed energy per unit mass of air is shown to depend only on a single function of a single parameter  $\mu$ , which itself depends on the level, the angle of incidence  $\chi$ , and the total absorption coefficient  $A_0$  of the atmosphere in the centre of the absorption band.

The general results are afterwards discussed in relation to the special case of an exponential height distribution of the absorbing constituent, with scale-height  $H$ . It is shown that in this case, whatever the angle  $\chi$ , (i) the height of maximum absorption per unit volume is at a distance  $0.616H$  below the level of maximum monochromatic absorption at the centre  $\lambda_0$  of the band; (ii) the maximum volume density of absorbed energy at angle  $\chi$  is  $\cos \chi$  times that for vertical incidence, as in the case of monochromatic absorption; (iii) above the level of maximum band absorption the height distribution of absorption differs only slightly from that in the case of monochromatic absorption, but below the maximum level the band-absorption layer extends further down than the monochromatic-absorption layer. If the absorption in the band-fringes where  $|l| \geq 2$  be neglected, the band-absorption layer is thicker than the monochromatic-absorption layer by approximately  $2H$ , the excess thickness being in the part of the layer below the level of maximum absorption.

---

## § 1. INTRODUCTION

In two previous papers<sup>(1, 2)</sup> I have considered the absorption of monochromatic radiation in an atmosphere which was either plane-stratified<sup>(1)</sup> or on a spherical earth<sup>(2)</sup>. It proved possible to express the results in a simple and general form by the use of suitable units and parameters. In particular, it was shown that the graph giving the height distribution of the volume density of absorbed energy was of a simple definite form for any atmosphere in which the density varies exponentially with the height;\* individual cases differ only in respect of the scales of

\* Such an atmosphere will be called an *exponential atmosphere*.

height and energy density. The volume density of absorbed energy was referred to in <sup>(1)</sup> and <sup>(2)</sup> as the rate of ion-production, it being supposed that each absorbed quantum of the monochromatic light ionized one atom or molecule, or at least that the number of ions produced was proportional to the amount of light absorbed.

The principal radiations absorbed in the earth's atmosphere are not monochromatic, nor are all the absorbing constituents distributed exponentially. In the case of absorption by ozone, in particular, neither condition is satisfied. The absorption in the terrestrial atmosphere is in large part effected by molecules, not by atoms, and is of band character, not line absorption. The former results are valid for each monochromatic component in an absorption band, but the height distribution of the total absorbed energy for any band involves an integration of overlapping monochromatic distributions.

So far as I know, this subject has not hitherto been treated mathematically, and our ideas are rather vague as to how the resultant height-absorption curves will differ from those for line absorption. In the latter case the distribution may fairly be called layer-like, since most of the absorption of a monochromatic beam occurs within a height-interval of about  $4H$ , where  $H$  is the local scale-height of the atmosphere\* ( $\S\ 3$ ). When the absorption occurs over a spectral range in which the coefficient of absorption  $\alpha_\lambda$  at the wave-length  $\lambda$  varies from a maximum  $\alpha_0$  to zero, the energy distribution may be expected to be less layer-like; but it is desirable to gain proper quantitative information on the subject.

This is here attempted, by considering a specially simple and mathematically convenient form of absorption band ( $\S\ 2$ ). In §§ 2–11 general formulae are developed for an atmosphere in which absorption is effected by a single constituent gas distributed in height in any manner. In §§ 12–16 the special form of these results is considered for an atmosphere in which the density of the absorbing constituent is an exponential function of the height.

## PART I

### § 2. THE ASSUMED FORM OF ABSORPTION BAND

In actual absorption bands the curve giving  $\alpha_\lambda$  as a function of the wavelength  $\lambda$  is often complex and serrated; it is hardly necessary to take account of the details of such bands, and in this paper I consider the simple relation

$$\alpha_\lambda = \alpha_0 \exp \{ -(\lambda - \lambda_0)^2 / \lambda_w^2 \} = \alpha_0 e^{-l^2}, \quad \dots\dots(1)$$

where

$$l = (\lambda - \lambda_0) / \lambda_w. \quad \dots\dots(2)$$

This represents a band symmetrical about its mean wave-length  $\lambda_0$ , at which  $\alpha$  attains its maximum value  $\alpha_0$ . The distribution corresponds to the well-known error law, and the constant  $\lambda_w$  determines the spread or width of the band.

Half the area under the  $\{\alpha, \lambda\}$  curve is contained within a  $\lambda$ -interval of width  $0.954\lambda_w$  and centred at  $\lambda_0$ , that is within the range  $\lambda_0 - 0.477\lambda_w \leq \lambda \leq \lambda_0 + 0.477\lambda_w$ .

\* The term "scale-height" was introduced in my article in *Reports on Progress in Physics*, 3, 42 (1936).

Within the range fourfold as large, namely between  $\lambda_0 \pm 2\lambda_w$ , 99·5 per cent of the area under the  $\{\alpha, \lambda\}$  curve is included; further, at  $\lambda \pm 2\lambda_w$ , or  $l = \pm 2$ ,  $\alpha = \alpha_0 e^{-4}$  or  $0.0183\alpha_0$ . The band within this range will be called the *limited band*, and the parts outside will be called the *band fringes*.

### § 3. THE DISTRIBUTION OF THE ABSORBING GAS

Suppose that the absorption expressed by equation (1) is due solely to one atmospheric constituent gas. Let  $M$  denote the total mass of this constituent in a complete vertical column of unit cross-section. Let  $mM$  denote the amount in this column above a height  $h$ , so that  $m$  denotes the fraction of the gas that lies above this height. The height distribution of the gas depends on the relation between  $m$  and  $h$  so that, say,

$$m = f(h). \quad \dots\dots(3)$$

The density  $\rho$  of the gas at the height  $h$  is given by

$$\rho dh = -M dm,$$

or

$$\rho = -M \frac{dm}{dh}; \quad \dots\dots(4)$$

the minus sign corresponds to the obvious fact that  $m$  decreases upwards. Clearly

$$m = 0 \text{ at } h = \infty, \quad m = 1 \text{ at } h = 0. \quad \dots\dots(5)$$

It is convenient to say that the height  $h$  corresponds to "the level  $m$ ," where  $m$  is given in terms of  $h$  by equation (3).

In the previous papers<sup>(1, 2)</sup> it was supposed that the absorbing gas was distributed exponentially, i.e., that

$$\rho = \rho_0 e^{-h/H}, \quad \dots\dots(6)$$

where  $H$  is a constant called the "local scale-height" of the atmosphere. In this case it is readily seen that

$$M = \rho_0 H, \quad m = e^{-h/H}. \quad \dots\dots(7)$$

In the present paper  $m$  will often be used instead of the height  $h$  as the independent variable specifying level. This makes it possible to deal with the absorption in a general way, whatever the height distribution of the absorbing gas, and to defer consideration of particular height distributions to a later stage.

It is convenient to write

$$A_0 \equiv \alpha_0 M, \quad \dots\dots(8)$$

and to call  $A_0$  the *total central absorption factor* for the band.

### § 4. THE GENERAL EQUATIONS OF ABSORPTION

Consider a beam of monochromatic radiation within the small range of wavelength  $\lambda$  to  $\lambda + d\lambda$ , incident at an inclination  $\chi$  to the vertical on a plane-stratified atmosphere.

Let  $S(m, \chi, \lambda) d\lambda$  or, more briefly,  $S_\lambda d\lambda$ , denote the intensity of this beam at the level  $m$ . The intensity outside the atmosphere will be denoted by  $S_\infty(\lambda) d\lambda$ , independent of  $\chi$ . Thus

$$S_\infty(\lambda) = S(0, \chi, \lambda). \quad \dots\dots(9)$$

In traversing the interval of level from  $m$  to  $m+dm$  the beam-intensity changes by the amount  $dS_\lambda$ , where  $dS_\lambda = -\alpha_\lambda M S_\infty(\lambda) \sec \chi dm$ ,

$\alpha_\lambda$  being the absorption coefficient for radiation of this wave-length. Hence

$$S_\lambda = S_\infty(\lambda) \exp(-\alpha_\lambda Mm \sec \chi). \quad \dots \dots (10)$$

The *mass density* of absorbed energy of this wave-length, that is, the energy absorbed per unit mass at the level  $m$ , will be denoted by  $E(m, \chi, \lambda) d\lambda$  or, more briefly, by  $E_\lambda d\lambda$ ; thus the energy absorbed per unit area in the thin layer between  $m$  and  $m+dm$  is  $ME_\lambda d\lambda dm$ . Since the normal cross-section of the inclined beam passing through unit area of this layer is  $\cos \chi$ , we have

$$E_\lambda = -\frac{1}{M} \frac{dS_\lambda}{dm} \cos \chi = \alpha_\lambda S_\infty(\lambda) \exp(-\alpha_\lambda Mm \sec \chi). \quad \dots \dots (11)$$

The *volume density* of energy absorbed at this level  $m$  or height  $h$  will be denoted by  $I(h, \chi, \lambda) d\lambda$  or, more briefly, by  $I_\lambda d\lambda$ ; clearly  $I_\lambda dh = -ME_\lambda dm$ , so that

$$I_\lambda = -ME_\lambda \frac{dm}{dh}. \quad \dots \dots (12)$$

The above formulae apply to each spectral element within an absorption band. We wish to consider the total mass density  $F(m, \chi)$  and volume density  $J(h, \chi)$  of absorbed energy, these being the integrals of  $E_\lambda$  and  $I_\lambda$  over the whole band. Clearly

$$F(m, \chi) = \int_{-\infty}^{\infty} E(m, \chi, \lambda) d\lambda = \int_{-\infty}^{\infty} E_\lambda d\lambda, \quad \dots \dots (13)$$

$$J(h, \chi) = \int_{-\infty}^{\infty} I(h, \chi, \lambda) d\lambda = \int_{-\infty}^{\infty} I_\lambda d\lambda, \quad \dots \dots (14)$$

$$J = -MF \frac{dm}{dh}. \quad \dots \dots (15)$$

The corresponding integrals over the range of  $\lambda$  corresponding to  $-L \leq l \leq L$  will be denoted by adding the suffix  $L$  to  $F$  or  $J$ .

## § 5. THE TOTAL-ABSORPTION MASS AND VOLUME DENSITIES $F, J$ FOR THE SPECIAL BAND-FORM

We now introduce into equation (11) and thence into equation (13) the special band-form (1), obtaining

$$F = \alpha_0 \int_{-\infty}^{\infty} S_\infty(\lambda) \exp(-l^2 - \alpha_0 Mm e^{-l^2} \sec \chi) d\lambda, \quad \dots \dots (16)$$

whence, writing  $\mu = \alpha_0 Mm \sec \chi = A_0 m \sec \chi$   $\dots \dots (17)$

(cf. (8)), we get  $F = \alpha_0 \lambda_w \int_{-\infty}^{\infty} S_\infty(\lambda) \exp(-l^2 - \mu e^{-l^2}) dl. \quad \dots \dots (18)$

This value, inserted into (15), gives  $J$  for the special band-form considered.

### § 6. THE INITIAL SPECTRAL DISTRIBUTION OF THE ABSORBED RADIATION

Further discussion of equation (18) depends on the form of the function  $S_\infty(\lambda)$ , which represents the spectral intensity distribution of the radiation before the latter enters the atmosphere. Two simple cases alone, which on account of the symmetry of the band-form are equivalent as regards  $F$ , will be considered here. The first is

$$S_\infty(\lambda) = S_\infty, \quad \dots\dots(19)$$

where  $S_\infty$  is a constant; the second is

$$S_\infty(\lambda) = S_\infty + lS'_\infty \quad (l = (\lambda - \lambda_0)/(\lambda_w)), \quad \dots\dots(20)$$

where  $S'_\infty$  is another constant, representing the slope of the spectral-energy graph; equation (20) corresponds to a uniform increase or decrease of  $S_\infty(\lambda)$  with respect to  $l$  or  $\lambda$ , and equation (19) is merely the particular case of vanishing slope  $S'_\infty$ . In the case of the solar radiation absorbed in the earth's atmosphere, equation (20) is a rough first approximation to the form of the spectral-energy curve, over the main part of each principal absorption band; a closer approximation could of course be obtained by expressing  $S_\infty(\lambda)$  in the form of a power series in  $l$ , the next approximation being the addition of a term  $\frac{1}{2}l^2S''_\infty$  to equation (20).

### § 7. THE ABSORBED-ENERGY MASS DENSITY AT ANY LEVEL

On substituting in equation (18) the expression for  $S_\infty(\lambda)$  given in equations (19) or (20), we get, in either case,

$$F = F_0 \Phi(\mu), \quad \dots\dots(21)$$

where

$$F_0 = \frac{1}{2}\pi^{\frac{1}{2}}\alpha_0 S_\infty \lambda_w, \quad \dots\dots(22)$$

and

$$\Phi(\mu) = 2\pi^{-\frac{1}{2}} \int_0^\infty \exp(-l^2 - \mu e^{-l^2}) dl, \quad \dots\dots(23)$$

in which the initial factor is taken so that

$$\Phi(0) = 1, \quad \dots\dots(24)$$

and

$$F_{\mu=0} = F_0. \quad \dots\dots(25)$$

The simplicity of the relation (21) is notable: for it shows that  $F(m, \chi)/F_0$  is expressible as a function of the single variable  $\mu$  given by equation (17)—which depends on  $A_0$  (defined as  $\alpha_0 M$ ),  $\chi$ , and the level  $m$ , but not on the half-width  $\lambda_w$  of the band, nor on the position  $\lambda_0$  of the band in the spectrum.

The corresponding results for line absorption or monochromatic radiation may be put in the form

$$E_\lambda(m) = E_{\lambda_0} \Phi_\lambda(\mu_\lambda) = E_{\lambda_0} e^{-\mu_\lambda}, \quad \dots\dots(26)$$

where

$$E_{\lambda_0} = \alpha_\lambda S_\infty(\lambda), \quad \dots\dots(27)$$

and

$$\mu_\lambda = \alpha_\lambda M m \sec \chi. \quad \dots\dots(28)$$

In both cases, at the top of the atmosphere where  $m=0$  and therefore  $\mu=0$  and  $\mu_\lambda=0$ , the function  $\Phi$  or  $\Phi_\lambda$  is unity, so that  $F_0$  and  $E_{\lambda 0} d\lambda$  represent the initial density of the absorbed energy per unit mass. As we descend in the atmosphere  $m$  and  $\mu$  or  $\mu_\lambda$  increase and  $\Phi$  or  $\Phi_\lambda$  steadily decrease; that is, the mass density of the absorbed energy decreases steadily downwards, owing of course to the increasing attenuation of the beam.

If we consider the energy ( $F_L$ , say, or  $F_0 \Phi_L$ ) absorbed within the range  $-L \leq l \leq L$  of the band, ignoring the energy of shorter and long wave-lengths, equation (21) must be replaced by

$$F_L = F_0 \Phi_L(\mu) \equiv F_0 2\pi^{-\frac{1}{2}} \int_0^L \exp(-l^2 - \mu e^{-l^2}) dl. \quad \dots \dots (29)$$

When  $L=2$  this gives the mass density of absorption excluding the band fringes (§ 2).

### § 8. THE FUNCTIONS $\Phi$ AND $\Phi_L$

Since 
$$\exp(-l^2 - \mu e^{-l^2}) = \sum_0^\infty (-\mu)^n \frac{e^{-(n+1)l^2}}{n!}, \quad \dots \dots (30)$$

and 
$$2\pi^{-\frac{1}{2}} \int_0^\infty e^{-(n+1)l^2} dl = \frac{1}{\sqrt{(n+1)}}, \quad \dots \dots (31)$$

it is clear that 
$$\Phi(\mu) = \sum_0^\infty \frac{(-\mu)^n}{n! \sqrt{(n+1)}}. \quad \dots \dots (32)$$

This series enables  $\Phi$  to be conveniently calculated, directly up to about  $\mu=5$ , and thereafter up to about  $\mu=10$  by using Euler's transformation.\* From about  $\mu=10$ , however, even when this transformation is used, the calculation of  $\Phi$  from this alternating series becomes increasingly laborious, and another form of expression for  $\Phi$  must be used.

Column (3) of table 1 gives values of  $\Phi$  calculated from equation (32) for values of  $\mu$  from 0 to 10. Column (2) gives values of  $\Phi_\lambda(\mu)$ , which by equation (26) is  $e^{-\mu}$ , for comparison. The fourth column gives values of

$$\frac{1 - e^{-\mu}}{\mu \sqrt{(\pi \log_e \mu)}}, \quad \dots \dots (33)$$

when  $\mu \geq 1$  (this expression is not real when  $\mu < 1$ ); this is an asymptotic approximation to  $\Phi(\mu)$ , as is shown below; the fifth column of the table shows the percentage error of the approximation.

To obtain the approximation (33) for  $\Phi$ , the integral in equation (23) is divided into two parts over the ranges 0 to  $l_0$  and  $l_0$  to  $\infty$ , where

$$l_0 = \sqrt{\log_e \mu};$$

\* Cf. Bromwich<sup>(3)</sup>. A check on the calculations is obtained by applying the transformation from two different values of  $n$ .

*The atmospheric height distribution of band-absorbed solar radiation* 99

at  $l_0$ , if  $\mu > 1$ , the integrand has its maximum value, which is  $1/\mu e$ ; this is small when  $\mu$  is large. Changing the variable from  $l$  to  $u$ , where

$$l^2 = l_0^2 + u, \text{ so that } 2ldl = du,$$

and

$$e^{-l^2} = e^{-u}/\mu, \exp(-l^2 - \mu e^{-l^2}) = (1/\mu) \exp(-u - e^{-u}),$$

equation (23) becomes

$$\Phi(\mu) = \frac{I}{\mu \sqrt{\pi}} (i_1 + i_2), \quad \dots\dots(34)$$

where

$$i_1 = \int_{-l_0^2}^0 \frac{\exp(-u - e^{-u})}{\sqrt{(l_0^2 + u)}} du = \int_0^{l_0^2} \frac{\exp(v - e^v)}{\sqrt{(l_0^2 - v)}} dv,$$

$$i_2 = \int_0^\infty \frac{\exp(-u - e^{-u})}{\sqrt{(l_0^2 + u)}} du.$$

Table 1.  $\Phi_\lambda(\mu)$ ,  $\Phi(\mu)$ , and  $\Phi_2(\mu)$

$\mu$	$\Phi_\lambda(\mu)$ or $e^{-\mu}$ ( $\times 10^5$ )	$\Phi(\mu)$ ( $\times 10^5$ )	$\frac{1 - e^{-\mu}}{\mu \sqrt{(\pi \log_e \mu)}}$ ( $\times 10^5$ )	Error (per cent)	$\Phi(\mu) - \Phi_2(\mu)$ ( $\times 10^5$ )
0.0	100,000	100,000	—	—	468
0.2	81,873	86,949	—	—	467
0.4	67,032	75,846	—	—	466
0.6	54,881	66,383	—	—	466
0.8	44,933	58,304	—	—	465
1.0	36,788	51,393	$\infty$	+ $\infty$	464
1.5	22,313	38,107	45,889	+ 20.4	462
2.0	13,534	28,946	29,297	+ 1.2	460
2.5	8,208	22,531	21,641	- 4.0	457
3.0	4,979	17,964	17,049	- 5.1	455
4.0	1,832	12,212	11,760	- 3.7	451
5.0	674	8,742	8,834	- 1.3	448
6.0	248	6,967	7,007	+ 0.6	444
8.0	34	4,793	4,889	+ 2.7	436
10.0	5	3,589	3,718	+ 3.6	426
20.0	—	—	1,630	—	389
25.0	—	—	1,258	—	370
50.0	—	—	570	—	300

In  $i_1$  the exponential factor is very small except when  $v$  is quite small; clearly

$$i_1 > \frac{I}{l_0} \int_0^{l_0^2} \exp(v - e^v) dv = \frac{I}{l_0} \int_1^\mu e^{-e^v} de^v = \frac{I}{l_0} (e^{-1} - e^{-\mu}),$$

and the difference between  $i_1$  and  $(e^{-1} - e^{-\mu}) l_0$  is very small when  $l_0$  is large. Similarly

$$i_2 < \frac{I}{l_0} \int_0^\infty \exp(-u - e^{-u}) du = \frac{I}{l_0} \int_0^1 e^{-e^{-u}} de^{-u} = \frac{I}{l_0} (1 - e^{-1}),$$

but  $(1 - e^{-1}) l_0$  is very nearly equal to  $i_2$  when  $l_0$  is large. Hence an approximation to equation (34), when  $l_0$  is large, is

$$\Phi(\mu) \sim \frac{I}{\mu l_0 \sqrt{\pi}} (e^{-1} - e^{-\mu} + 1 - e^{-1}) = \frac{1 - e^{-\mu}}{\mu \sqrt{(\pi \log_e \mu)}}, \quad \dots\dots(35)$$

namely equation (33). It is not difficult to see that when  $l_0$  is large, the error in the above approximation to  $i_2$  exceeds that in the approximation to  $i_1$ , and that there-

fore equation (33) will tend to  $\Phi(\mu)$  from above. This is in accordance with table 1; when  $\mu$  is 1 or nearly 1, the percentage error of equation (33) is large and positive, but near  $\mu=2$  it falls to zero and, changing sign, rises to a negative numerical maximum of about 5 per cent at  $\mu=3$ , whence it decreases to zero again at about  $\mu=5.7$ ; when  $\mu > 5.7$  the percentage error would appear to be positive; at  $\mu=10$  it seems to be still on the up grade, but it must ultimately decrease to zero.

In June 1936 I referred to the function  $\Phi(\mu)$  in a letter to Prof. N. S. Koshliakov of Leningrad, mentioning that I had obtained the first term  $1/\mu\sqrt{(\pi \log_e \mu)}$  in its asymptotic expansion and saying that I had been unable to obtain further terms. A few days after the receipt of my letter he sent me the following asymptotic expansion, which had been obtained and proved in different ways independently by himself and by his colleagues Drs A. Svetlov and Stroganov; they kindly allow me to quote it here:

$$\Phi(\mu) = \frac{1}{\mu\sqrt{(\pi \log_e \mu)}} \left\{ 1 + \sum_{k=1}^{n-1} \frac{1 \cdot 3 \cdot 5 \dots (2k-1)}{2^k \cdot k! (\log_e \mu)^k} \int_0^\infty e^{-t} (\log_e t)^k dt + O\left(\frac{1}{(\log_e \mu)^n}\right) \right\}.$$

Owing to the lack of tables of the integrals appearing as coefficients in this formula I have not been able to use the expansion for numerical calculation.

With a view to the evaluation of  $\Phi_L$ , we may also consider  $\Phi - \Phi_L$ , which is given by

$$\Phi - \Phi_L = \frac{2}{\sqrt{\pi}} \int_L^\infty \exp(-l^2 - \mu e^{-l^2}) dl \equiv f(L, \mu).$$

Clearly

$$f(L, 0) = \text{erf}(L) \equiv \frac{2}{\sqrt{\pi}} \int_L^\infty e^{-l^2} dl,$$

$$\frac{\partial^n f(L, \mu)}{\partial \mu^n} = \frac{2(-1)^n}{\sqrt{\pi}} \int_L^\infty \exp\{- (n+1)l^2 - \mu e^{-l^2}\} dl,$$

$$\left\{ \frac{\partial^n f(L, \mu)}{\partial \mu^n} \right\}_{\mu=0} = \frac{2(-1)^n}{\sqrt{\pi}} \int_L^\infty e^{-(n+1)l^2} dl = \frac{(-1)^n}{\sqrt{(n+1)}} \text{erf}\{\sqrt{(n+1)}L\},$$

so that by Maclaurin's theorem

$$\begin{aligned} \Phi(\mu) - \Phi_L(\mu) &= \text{erf}(L) + \sum_{n=1}^{\infty} \frac{(-1)^n \mu^n}{n! \sqrt{(n+1)}} \text{erf}\{\sqrt{(n+1)}L\} \\ &= \text{erf} L - \frac{1}{\mu L \sqrt{\pi}} \sum_{n=2}^{\infty} \frac{(-\mu e^{-L^2})^n}{n!} L(L\sqrt{n}), \quad \dots \dots (36) \end{aligned}$$

where  $L(x)$  denotes Laplace's continued fraction, which is a slowly varying function.\*

From this formula ( $L$  being taken as 2) the values of  $\Phi - \Phi_L$  in the last column of table 1 have been calculated.

\* J. Burgess<sup>(4)</sup> has given the values of  $L(x)$ , to 15 decimal places, for values of  $x$  at intervals of 0.1 from  $x=3.0$  to 6.0, in which range  $L(x)$  increases from 0.9518 to 0.9866. Burgess also gives values of  $(1 - \text{erf } x)$  for values of  $x$  from 0 to 3 at intervals of 0.001 or 0.002.

§ 9. THE HEIGHT OF MAXIMUM VOLUME ABSORPTION

The volume density  $J$  of absorbed energy is given by equations (15) and (21), as follows:

$$J = -MF dm/dh = -MF_0(dm/dh)\Phi(\mu). \quad \dots\dots(37)$$

The corresponding result for line absorption is

$$I_\lambda = -ME_\lambda(dm/dh) = -ME_{\lambda_0}(dm/dh)e^{-\mu_\lambda}. \quad \dots\dots(38)$$

It is of interest to find the maximum values of these expressions (which will be denoted by  $J_\chi$  and  $I_{\lambda\chi}$ , since they naturally depend on the inclination  $\chi$  of the beam of radiation) and the heights  $h_\chi$  or  $h_{\lambda\chi}$  at which they occur; the corresponding values of  $m$  and  $\mu$  (or  $\mu_\lambda$ ) will be distinguished by the same suffixes.

The condition for the maximum may be expressed in the form

$$\frac{d \log_e \Phi(\mu)}{d\mu} \frac{d\mu}{dm} \frac{dm}{dh} + \frac{d \log_e (dm/dh)}{dh} = 0,$$

or, since  $d\mu/dm = \mu/m$ , by equation (17),

$$\mu \frac{\Phi'(\mu)}{\Phi(\mu)} = -m \frac{d^2 m}{dh^2} / \left( \frac{dm}{dh} \right)^2 \equiv -\psi(m), \quad \dots\dots(39)$$

where ' denotes differentiation. Clearly  $\psi$ , being a function of  $h$ , is also a function of  $m$ .

Since, by equation (23),

$$\Phi'(\mu) = 2\pi^{-\frac{1}{2}} \int_0^\infty \exp(-2l^2 - \mu e^{-l^2}) dl,$$

it follows that

$$\Phi'(\mu) < \Phi(\mu)$$

for all values of  $\mu$  greater than 0.

Using the expression (32) for  $\Phi(\mu)$ , the condition (39) may be put in the form

$$\psi(m) = \mu \frac{\sum_0^\infty (-\mu)^n n! \sqrt{(n+2)}}{\sum_0^\infty (-\mu)^n n! \sqrt{(n+1)}}. \quad \dots\dots(40)$$

The corresponding equation in the case of line absorption is

$$\psi_\lambda(m_\lambda) = -\mu_\lambda \frac{\Phi'_\lambda(\mu_\lambda)}{\Phi_\lambda(\mu_\lambda)} = \mu_\lambda, \quad \dots\dots(41)$$

by equation (26).

These equations cannot be solved until the height distribution of mass in the atmosphere is assigned, since  $\psi(m)$ , as equation (39) shows, depends essentially on this distribution.

§ 10. THE SPECTRAL COMPOSITION OF THE ENERGY ABSORBED  
AT ANY LEVEL

The spectral composition of the energy absorbed at any level is represented by  $E_\lambda F$ , the integral of which over all wave-lengths is unity by equation (13). When the band-form is given by equation (1), and the spectral intensity of the radiation outside the atmosphere is uniform as in equation (19),

$$\frac{E_\lambda}{F} = \frac{2}{\sqrt{\pi}} \frac{\exp(-l^2 - \mu e^{-l^2})}{\Phi(\mu)}, \quad \dots\dots (42)$$

which, when expressed, as here, in terms of the variable  $l$  instead of  $\lambda$ , depends only upon the one parameter  $\mu$ . It is illustrated in figure 1 for values of  $\mu$  from

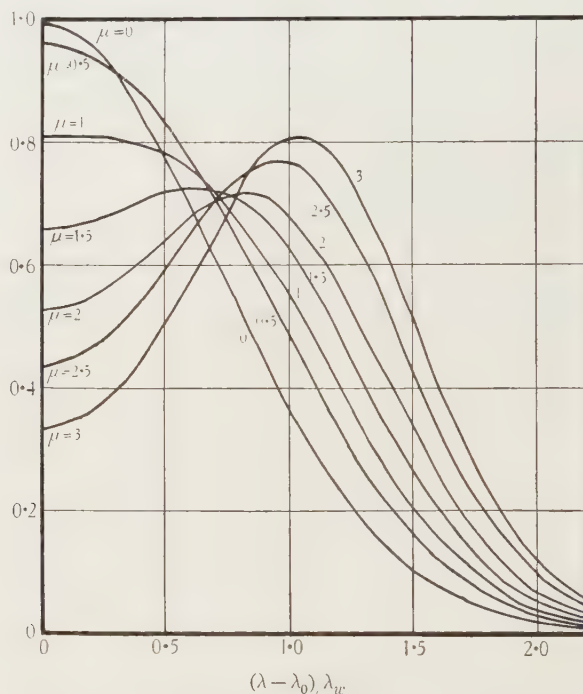


Figure 1. Spectral composition of the band-absorbed energy at different levels.

$\circ$  to  $3$ ;  $\mu=0$  corresponds to vanishingly small absorption, in which case (for light of uniform spectral intensity) the spectral distribution of the absorbed energy is simply proportional to the band-form (1). When  $0 < \mu < 1$  the function  $E_\lambda F$  has a single maximum,  $2e^{-\mu}/\sqrt{\pi}$ , at  $l=0$ ; when  $\mu > 1$  it has two maxima, of amount  $2/e\mu\Phi(\mu)\sqrt{\pi}$ , at  $l=\pm\sqrt{\log_e \mu}$ , and at  $l=0$  it has a minimum value  $2e^{-\mu}/\sqrt{\pi}$ .

In general  $S_\infty(\lambda)$  will not be uniform over the band; if it has a uniform variation across the band, as in equation (20),  $F$  is unaltered, but a term  $(lS_\infty'/S_\infty)E_\lambda$  is added to  $E_\lambda$ . This will modify the curves of figure 1, raising the ordinates on one side of  $l=0$  or  $\lambda=\lambda_0$  and lowering them on the other.

§ 11. THE PROPORTIONATE DAILY VARIATION OF ABSORPTION DENSITY

At a station at an angular distance  $\theta$  (the co-latitude) from the north pole, the zenith distance  $\chi$  of the sun, the source of the absorbed radiation, varies throughout the day according to the equation

$$\cos \chi = \sin \delta \cos \theta + \cos \delta \sin \theta \cos \phi, \quad \dots\dots(43)$$

where  $\phi$  denotes the local time reckoned from noon in angular measure at the rate  $2\pi$  per day, and  $\delta$  denotes the sun's north declination at the season considered.

At noon, when  $\phi=0$ ,

$$\chi \equiv \chi_0 = \frac{1}{2}\pi - (\theta + \delta). \quad \dots\dots(44)$$

At the equinoxes  $\delta=0$  and  $\phi$  ranges between  $+\frac{1}{2}\pi$  and  $-\frac{1}{2}\pi$ ; at other seasons the limiting values of  $\phi$  are given by

$$\cos \phi = -\tan \delta \cos \theta, \quad \dots\dots(45)$$

the range being greater or less than  $\pi$  according as  $\delta > 0$  or  $\delta < 0$ . In all cases  $\chi$  ranges from  $\chi_0$  to  $90^\circ$ .

The mass density of absorbed energy  $F$  bears the same ratio to the volume density  $J$  at all heights  $h$  or levels  $m$ , by equation (15), assuming that the composition of the atmosphere itself is uniform; this may not be true at high levels, though it is probably substantially true, except as regards ozone and atomic oxygen, up to 100 km. Hence their proportionate variation throughout the day is the same, thus

$$\frac{J(h, \chi)}{J(h, \chi_0)} = \frac{F(m, \chi)}{F(m, \chi_0)} = \frac{\Phi(\alpha_0 Mm \sec \chi)}{\Phi(\alpha_0 Mm \sec \chi_0)}. \quad \dots\dots(46)$$

The corresponding formula for monochromatic radiation of wave-length  $\lambda_0$  is

$$\frac{E(m, \chi, \lambda_0)}{E(m, \chi_0, \lambda_0)} = \exp^{-\alpha_0 Mm (\sec \chi - \sec \chi_0)}. \quad \dots\dots(47)$$

In reference (1) curves were given (figures 2-5) showing the variation of the ratio (47) as a function of the solar time. Similar curves for equation (46) could easily be constructed for any value of  $\alpha_0 Mm$ , but will not be given here; since  $\Phi(\mu)$  decreases less rapidly than  $e^{-\mu}$  as  $\mu$  increases, it is clear that the ratio (46) will exceed the corresponding ratio (47) for the same values of  $\alpha_0 Mm$ ,  $\chi$  and  $\chi_0$ .

## PART II

§ 12. THE HEIGHT OF MAXIMUM VOLUME ABSORPTION

The results of § 9 will now be completed for an exponential atmosphere (§ 3), for which, as in equation (7),

$$m = e^{-h/H}, \quad \dots\dots(48)$$

so that, by equation (39),

$$\psi(m) = 1. \quad \dots\dots(49)$$

In this case the level  $m_{\lambda_X}$  or  $h_{\lambda_X}$  of maximum volume density of absorption of monochromatic radiation of wave-length  $\lambda$  is given by equation (41) as

$$\mu_{\lambda_X} = 1, \quad \dots\dots(50)$$

or

$$m_{\lambda_X} = 1/\alpha_\lambda M \sec \chi, \quad \dots\dots(51)$$

$$\begin{aligned} h_{\lambda_X} &= H \log_e (\alpha_\lambda M \sec \chi) \\ &= h_\lambda + H \log_e \sec \chi, \end{aligned} \quad \dots\dots(52)$$

where  $h_\lambda$  is the value of  $h_{\lambda_X}$  corresponding to vertical incidence, for which  $\chi=0$ ; that is,

$$h_\lambda = H \log_e (\alpha_\lambda M). \quad \dots\dots(53)$$

In the case of band absorption the level of maximum absorption for an exponential atmosphere is given by equations (40) and (49), thus

$$\mu \frac{\sum_0^{\infty} (-1)^n \mu^n / n! \sqrt{(n+2)}}{\sum_0^{\infty} (-1)^n \mu^n / n! \sqrt{(n+1)}} = 1; \quad \dots\dots(54)$$

the solution is

$$\mu_0 = 1.8517, \quad \dots\dots(55)$$

or

$$m_\chi = \mu_0 / \alpha_0 M \sec \chi,$$

or

$$\begin{aligned} h_\chi &= H \log_e (1/m_\chi) \\ &= H \log_e (\alpha_0 M \sec \chi / \mu_0) \\ &= h_0 + H \log_e \sec \chi, \end{aligned} \quad \dots\dots(56)$$

where

$$\begin{aligned} h_0 &\equiv H \log_e (\alpha_0 M / \mu_0) \\ &= h_{\lambda_0} - H \log_e \mu_0 = h_{\lambda_0} - 0.61626H. \end{aligned} \quad \dots\dots(57)$$

Consequently the level of maximum volume absorption of the band absorption is at a distance  $0.616H$  below the corresponding level for the monochromatic radiation in the centre  $\lambda_0$  of the absorption band. It is of course natural that the level of maximum volume absorption should be lower, in the case of an absorption band, than the level for monochromatic absorption in the centre of the band, because this is the least penetrating component of the band. It is remarkable that *the difference of level is the same for all values of  $\chi$* .

We may note also that at the level of maximum volume density of band absorption, where  $\mu = \mu_0 = 1.8517$ ,

$$\Phi(\mu_0) = 0.31326, \quad \Phi_2(\mu_0) = 0.30866, \quad \dots\dots(58)$$

whereas at the level of maximum monochromatic absorption ( $\mu = \mu_{\lambda_X} = 1$ ),

$$\Phi_\lambda(\mu_{\lambda_X}) = \Phi_\lambda(1) = e^{-1} = 0.36788. \quad \dots\dots(59)$$

### § 13. THE MAXIMUM VOLUME ABSORPTION

The maximum volume density of absorbed energy, at any angle of incidence  $\chi$ , is denoted by  $I_{\lambda_X} d\lambda$  for monochromatic radiation of line width  $d\lambda$ , and by  $J_\chi$  for the band absorption. The former is given by equations (12), (26) and (28), after the substitutions  $dm/dh = -m/H$ , and  $\mu_\lambda = 1$ ; this gives

$$I_{\lambda_X} = \frac{m M E_{\lambda_0} \exp(-\mu_\lambda)}{H} = \frac{(\mu_\lambda S_\infty(\lambda) \cos \chi)}{H \exp 1} = I_{\lambda_0} \cos \chi, \quad \dots\dots(60)$$

where

$$I_{\lambda_0} \equiv S_{\infty}(\lambda)/H \exp \chi; \quad \dots\dots(61)$$

$I_{\lambda_0} d\lambda$  is clearly the maximum volume density of absorbed energy for vertical incidence.

For band radiation we have, from equations (15), (21), (17) and (22), putting  $\mu = \mu_0$ ,

$$\begin{aligned} J_{\chi} &= \frac{m M F_0}{H} \Phi(\mu_0) = \frac{\sqrt{\pi}}{2} \frac{S_{\infty} \lambda_w}{H} \mu_0 \Phi(\mu_0) \cos \chi \\ &\equiv J_0 \cos \chi, \end{aligned} \quad \dots\dots(62)$$

where

$$\begin{aligned} J_0 &\equiv \frac{\sqrt{\pi}}{2} \frac{S_x \lambda_w}{H} \mu_0 \Phi(\mu_0) = 0.514 \frac{S_x \lambda_w}{H} \\ &= 1.397 I_{\lambda_0} \lambda_w. \end{aligned} \quad \dots\dots(63)$$

This radiation of course extends over all wave-lengths. The last form given for  $J_0$  implies that the maximum volume density of absorbed energy for the actual band is the same as that which would correspond to a uniform absorption band of width  $1.397 \lambda_w$ , in which  $\alpha_{\lambda}$  and  $S_{\infty}(\lambda)$  had the constant values  $\alpha_0$  and  $S_{\infty}$  (cf. the last paragraph of § 2).

#### § 14. THE HEIGHT DISTRIBUTION OF VOLUME ABSORPTION

The height distribution of the volume density of absorbed monochromatic energy of wave-length  $\lambda$  is given by equations (37, 38), which for an exponential atmosphere may be expressed in the form

$$I_{\lambda}(h, \chi) = I_{\lambda_0} \exp(1 - z_{\lambda} - e^{-z_{\lambda}} \sec \chi)^*, \quad \dots\dots(64)$$

where  $z_{\lambda}$  is a new measure of the level, reckoned from the height  $h_{\lambda}$ , equation (53), as datum, the unit of height being now taken as  $H$ ; that is

$$z_{\lambda} = (h - h_{\lambda})/H. \quad \dots\dots(65)$$

The factor  $I_{\lambda_0}$  is the maximum volume density of absorbed monochromatic energy at vertical incidence.

The corresponding result for the absorption band is

$$\begin{aligned} J(h, \chi) &= J_0 e^{-z} \Phi(\mu)/\Phi(\mu_0) = J_0 e^{-z} \Phi(\alpha_0 M e^{-h/H} \sec \chi)/\Phi(\mu_0) \\ &= J_0 e^{-z} \Phi(\mu_0 e^{-z} \sec \chi)/\Phi(\mu_0) \\ &= 3.192 J_0 e^{-z} \Phi(\mu_0 e^{-z} \sec \chi), \end{aligned} \quad \dots\dots(66)$$

where

$$z = (h - h_0)/H = z_{\lambda_0} + \log_e \mu_0 = z_{\lambda_0} + 0.616. \quad \dots\dots(67)$$

The difference between  $z$  and  $z_{\lambda_0}$  corresponds to the difference between the levels  $h_0$  and  $h_{\lambda_0}$  already referred to in § 12. At  $z=0$ , when  $\chi=0$ ,  $J(h, \chi)=J_0$ . The maximum value of  $J$ , for any given value of  $\chi$ , occurs at the level  $z_{\chi}$ , where, by equation (56),

$$z_{\chi} = (h_{\chi} - h_0)/H = \log_e \sec \chi.$$

\* Compare equation (17) of reference (1).

In figure 1 of reference (1) graphs of  $I_{\lambda_0}(h, \chi)/I_{\lambda_0}$  are given for various values of  $\chi$ , for monochromatic radiation of wave-length  $\lambda_0$ ; they give the height distribution of monochromatic absorption in the centre of the band, at the angle of incidence  $\chi$ , as a fraction of the maximum absorption (at  $z_{\lambda_0}=0$ ) at vertical incidence ( $\chi=0$ ). Two of these curves, for  $\chi=0$  and  $\chi=45^\circ$ , are reproduced as broken lines in figure 2, for comparison with the corresponding curves  $J(h, \chi)/J_0$  for band absorption for various values of  $\chi$ . The  $I/I_0$  curve is on a height scale  $z_{\lambda_0}$ ; the height scale for the  $J/J_0$  curves refers to  $z$ , so that, as is convenient for comparison, the  $I/I_0$  and  $J/J_0$  curves for any value of  $\chi$  have at their maximum the same level and the same abscissa. If the  $J/J_0$  curves were drawn on the same height scale as the  $I/I_0$  curve they should all be lowered through a distance 0.616.

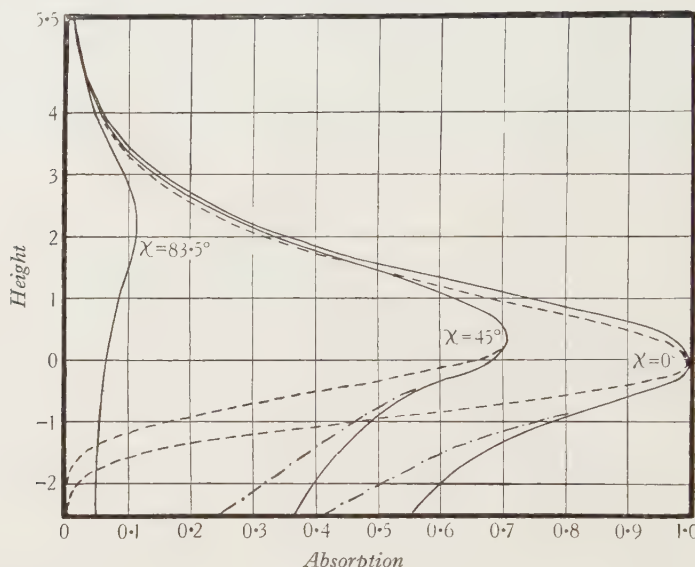


Figure 2. Relative height distribution of absorbed energy: ——  $J/J_0$  for total band; - - -  $J_2/J_0$  for limited band; - · -  $I/I_0$  for monochromatic absorption in the centre of the band. The unit of height is  $H$ , and the level of maximum band absorption is 0.616 $H$  below the level of maximum monochromatic absorption in the centre of the band. The curves  $I/I_0$  are drawn so as to make their maximum coincide with that of the curves  $J/J_0$  for the same zenith angle; actually they should all be raised through a height 0.616 $H$ .

The ratio of  $J/J_0$  to  $I/I_0$ , that is, the ratio of the abscissae of corresponding points on the  $J/J_0$  and  $I/I_0$  curves in a figure such as figure 2, is given by

$$\frac{J(h, \chi)/J_0}{I(h', \chi)/I_0} = \frac{3.1922 e^{-z} \Phi(\mu_0 e^{-z} \sec \chi)}{e^{1-z-e^{-z} \sec \chi}}, \quad \dots\dots(68)$$

where  $h'=h+0.616H$ . This ratio (68) is a function of the single parameter  $y$  given by

$$y \equiv e^{-z} \sec \chi, \quad \mu = \mu_0 y, \quad \dots\dots(69)$$

so that

$$\frac{J/J_0}{I/I_0} = \frac{3.192 \Phi(\mu_0 y)}{2.718 e^{-y}} = 1.174 e^y \Phi(\mu_0 y). \quad \dots\dots(70)$$

Table 2 gives the values of this ratio for various values of  $y$ ; the corresponding values of  $z$  when  $\chi=0$  and when  $\chi=45^\circ$  are indicated also. Since

$$z = \log_e \sec \chi - \log_e y,$$

the values of  $z$  corresponding to two different values of  $\chi$ , say  $\chi_1$  and  $\chi_2$ , but to the same value of  $y$ , differ by  $\log_e (\sec \chi_1 \sec \chi_2)$ , which is independent of  $y$ . (It may be noted that, for any value of  $\chi_1$ ,  $y=1$  at the level of maximum  $J/J_0$  or  $I/I_0$ , that is, at the level  $z_\chi$ , since  $z_\chi = \log_e \sec \chi$ , in which case  $\log_e y=0$ , and  $y=1$ .)

Table 2

$y$	$(J/J_0)/(I/I_0)$	$z$ when $\chi=0$	$z$ when $\chi=45^\circ$
0	1.174	$\infty$	$\infty$
$\frac{1}{5\mu_0} = 0.1080$	1.129	2.226	2.572
$\frac{1}{\mu_0} = 0.5400$	1.035	0.616	0.962
1	1	0	0.346
$\frac{5}{\mu_0} = 2.7025$	1.531	-0.994	-0.658
$\frac{10}{\mu_0} = 5.4005$	9.33	-1.686	-1.340

Table 2 shows that when  $y < 1$ , corresponding to heights above the level of maximum  $J/J_0$  or  $I/I_0$  for any given value of  $\chi$ ,  $J/J_0$  somewhat exceeds  $I/I_0$ , though their ratio is not greatly different from 1; the ratio increases from the minimum value of 1, for the pair of corresponding levels where  $J/J_0$  and  $I/I_0$ , for any value of  $\chi$ , are at their maximum, to 1.17 at infinite height.

When  $y > 1$ , corresponding to levels below that of maximum  $J/J_0$  or  $I/I_0$ , the above ratio rapidly increases, so that  $J/J_0$  comes to exceed  $I/I_0$  very considerably at quite small distances below the level of their maximum. This is because  $J/J_0$  decreases much more slowly than  $I/I_0$ . This may be seen from the following approximate expression for  $J/J_0$ , derived by adopting the approximation (33) for  $\Phi$  and putting  $\mu=\mu_0y$ :

$$J/J_0 = 3.192 y \cos \chi \Phi(\mu_0 y) = \frac{0.972 \cos \chi (1 - e^{-\mu_0 y})}{\sqrt{(0.616 + \log_e y)}}. \quad \dots \dots (71)$$

The approximation (33) is correct within a few per cent when  $\mu > 2$ , so that equation (71) is valid if  $\mu_0 y \geq 2$ , or if  $y \geq 2/\mu_0$ , or  $z \leq \log_e(\mu_0/2) - \log_e \cos \chi$ , which equals  $-0.077 - \log_e \cos \chi$ . In this range, equation (71) indicates that  $J/J_0$  decreases very slowly as  $z \rightarrow -\infty$ ; even when  $z = -100$ ,  $J/J_0 \cos \chi$  is still only slightly less than 0.1.

Consequently, for any value of  $\chi$ , the band nature of the absorption only slightly affects the height distribution of the volume absorption, in relation to the level and the value of the maximum volume absorption, above this level of maximum; but below it, the absorption extends downwards much farther than in the monochromatic case, that is, the absorption layer is much less sharply limited on its under than on its upper side.

§ 15. ABSORPTION IN THE LIMITED BAND, AND IN  
THE BAND FRINGES

It is not difficult to see, however, that the slow decrease of  $J/J_0$  below the level of maximum for any value of  $\chi$ , that is, below  $z=z_\chi=\log_e \sec \chi$ , is largely due to the slight but very deeply extending absorption of the radiation in the band fringes.

The ratio of the absorption in the fringes to the total absorption, for any value of  $\mu$ , is the ratio of the sixth to the third column in table 1. When  $\mu < \mu_0$  or  $1.8517$  this ratio is less than  $461/31326$  or  $0.0147$ ; hence if  $\mu = \mu_0 y$ , this ratio ( $0.0147$  or less) corresponds to  $y \leq 1$ , or to heights above the level of maximum  $J/J_0$ . Consequently in the upper part of the band-absorption layer, for any value of  $\chi$ , the fringe absorption at any level is less than  $1\frac{1}{2}$  per cent of the total absorption at the same level.

When much greater values of  $\mu$  are considered, however, the ratio increases rapidly; thus, for the fraction of the total absorption corresponding respectively to the band fringes, and to the limited band  $|l| \leq 2$ , we have the values given in table 3, for five values of  $\mu$  or  $y$ .

Table 3

$\mu$	5	10	25	50	
$y$	$5/\mu_0$ , i.e. $2.702$	$10/\mu_0$ , i.e. $5.405$	$25/\mu_0$ , i.e. $13.51$	$50/\mu_0$ , i.e. $27.02$	
Fringe (per cent of total)	5.1	11.5	29.4	52.7	
Limited band (per cent of total)	94.9	88.5	71.6	47.3	
$\chi=0$	$z$ $J/J_0$ $J_2/J_0$	-0.99 0.754 0.708	-1.69 0.619 0.549	-2.60 0.542 0.383	-3.30 0.491 0.232
$\chi=45^\circ$	$z$ $J/J_0$ $J_2/J_0$	-0.66 0.533 0.501	-1.34 0.438 0.388	-2.35 0.383 0.270	-2.95 0.347 0.164

The height  $z$  corresponding to  $\mu$  is  $\log_e \sec \chi + \log_e \mu_0 - \log_e \mu$ , values of which, in the cases  $\chi=0$  and  $\chi=45^\circ$ , are also given in table 3. In the next rows are given the corresponding values of  $J/J_0$  and  $J_2/J_0$ , where  $J_2$  denotes the value of  $J$  for the limited band, between  $l=+2$  and  $l=-2$ . The value  $0.23$  of  $J_2/J_0$ , which may be taken as roughly marking the lower limit of the absorption layer, is attained (if  $\chi=0$ ) when  $z=-3.3$ , whereas  $I/I_0$ , for radiation of wave-length  $\lambda$  equal to  $\lambda_0$ , attains this value, if  $\chi=0$ , when  $z$  equals about  $-1.3$ . Thus the absorption layer due to the limited band has a thickness, below its maximum level, exceeding that for a monochromatic absorption band by about  $2H$ .

Below the level  $z=-3.3$  the major part of the radiation absorbed is radiation in the band fringes. It is not unlikely that though the absorption formula (1) is satisfactory for the purpose of discussing the absorption of radiation within a

moderate wave-length interval from the wave-length of maximum absorption coefficient, it is unsuitable for the radiation farther away, where the value of  $\alpha$ , in actual absorption bands, may decrease with  $|l|$  more rapidly than  $e^{-l^2}$ .

In figure 2, the absorption curves for the limited band, in the cases  $\chi=0$ ,  $\chi=45^\circ$  for levels below the level of maximum  $J/J_0$ , are indicated by dot-and-dash lines; at and above the level of maximum  $J/J_0$ , the  $J_2/J$  curves are scarcely distinguishable, on the scale of the figure, from the  $J/J_0$  curves.

#### § 16. CONCLUDING REMARKS

If the absorbed radiation here considered were effective in dissociating or ionizing the absorbing molecules, the rate of dissociation or ion-production per unit volume by absorption of radiation of wave-length  $\lambda$  would be proportional to  $I_\lambda(h, \chi)$ ; the factor of proportionality would in general be a function of  $\lambda$ , perhaps varying inversely as the quantum energy  $h\nu$  (where  $\nu$  is the frequency, equal to  $c\lambda$ ) and therefore as  $\lambda$ , if the efficiency per quantum is the same for all wave-lengths within, say, the limited band. If the variation of  $\lambda$  over the width of the limited band can be neglected, then the rate of dissociation or ion-production will be proportional to  $J(h, \chi)$ ; in that case the preceding theory enables curves giving the rate of ion-production to be drawn, as a function of time (at any height) or of height (at any hour angle  $\phi$ ), as was done in reference (1) for monochromatic radiation.

Further, if the dissociated constituents recombine at the rate  $\rho nn'$ , where  $n$  and  $n'$  are their numbers (supposed equal) per unit volume, and  $\rho$  is a recombination coefficient, either varying with or independent of the height, it is possible, at least by graphical methods, to calculate the value of  $n$  at any height and time<sup>(1)</sup>. This will not be done here, however; nor will we here consider the height distribution of the band absorption and the dissociated molecules, atoms or ions, when the absorbing constituent is not distributed with a density varying exponentially with the height (although the earth's atmosphere presents such a case, in the absorption of light in more than one band, by ozone or by water vapour). It is hoped, however, that the present theory will be of value as a first step towards such more complicated problems, should they need to be considered in detail in the future.

#### § 17. ACKNOWLEDGEMENTS

The computations and diagrams of this paper were made under the supervision of Mrs P. M. Truscott in the computing bureau of the Department of Mathematics at the Imperial College; this bureau is maintained by a research grant from the Clothworkers' Company.

#### REFERENCES

- (1) CHAPMAN, S. *Proc. Phys. Soc.* **43**, 26 (1931).
- (2) CHAPMAN, S. *Proc. Phys. Soc.* **43**, 483 (1931).
- (3) BROMWICH. *Infinite Series*, p. 55 (1908).
- (4) BURGESS, J. *Trans. Roy. Soc. Edinb.* **39**, 321 (1898).

# THE LIMITING POLARIZATION OF MEDIUM WAVES REFLECTED FROM THE IONOSPHERE

BY T. L. ECKERSLEY, F.R.S. AND G. MILLINGTON, M.A.

Marconi's Wireless Telegraph Co., Ltd., Research and Development  
Department

*Received 7 July 1938. Read 14 October 1938*

**ABSTRACT.** A method is described of measuring the polarization of a downcoming wireless wave which has been reflected obliquely from the ionosphere. Two rotatable crossed loops are adjusted to be in quadrature by dephasing one forwards and the other backwards  $45^\circ$  from resonance. With the usual goniometer technique the search coil gives zero pick-up when the tangent of the angle at which it is set is equal to the ratio of the axes of the projected polarization ellipse, and the frames are turned so that their planes are along the axes of this ellipse. Results obtained on medium-wave broadcasting stations are compared with ellipses calculated on the magnetoionic theory for an assumed angle of emergence and direction of the earth's magnetic field. The comparison shows that, within the present accuracy of the apparatus, the absorption due to electronic collisions does not appreciably affect the limiting polarization of the emergent wave, and sets an upper limit of  $10^6$  per sec. to the collisional frequency in the region where the polarization assumes its limiting value. The experiments also suggest that the ratio of the number of ions to the number of electrons in this region is not greater than 10,000, and further work with increased accuracy should give valuable information relevant to the inclusion of the Lorentz term in the magnetoionic theory for the *E* layer.

---

## § 1. INTRODUCTION

**I**T is well known that according to the simple ray treatment of the magnetoionic theory, as given by Appleton<sup>(1)</sup>, the limiting polarization of a wireless wave emerging from the ionosphere depends only on the characteristics at the lower edge, and not on the unknown distribution of ionic density above. The more complete analysis of Booker<sup>(2)</sup> shows that this conclusion is in general justified when the initial gradient of ionic density, with respect to height measured in terms of wave-lengths, is small.

As the ray comes down through the ionosphere, it travels into regions where the ionic density is decreasing, but the collisional frequency is increasing. Thus although the state of polarization becomes less affected by the density, it may be modified by the increasing absorption. In the lower regions of the ionosphere the absorption may therefore influence the polarization, if the coefficient of absorption is large where the density is still appreciable.

For short waves, since the absorption term  $\alpha$  is inversely proportional to the wave frequency,\* the limiting polarization depends only on the angle between the

\*  $\alpha$  is the ratio of the collisional frequency to the wave frequency, except for a constant.

emerging ray and the direction of the earth's field, and on the ratio of the gyro-magnetic frequency to the wave frequency. On long waves, however, the absorption may be the controlling factor, and cause the limiting polarization to become circular under all conditions, except when the ray is nearly perpendicular to the magnetic field; this point is further discussed in appendix I.

It follows, therefore, that in the measurement of the polarization of the down-coming ray, we have a method of determining whether the absorption is producing any appreciable modification, since we can with reasonable accuracy predict the polarization in the absence of absorption. In the event of the experimental results confirming the calculated values, we can interpret them as setting an upper limit to the collisional frequency at the lower edge of the ionosphere. We can also confirm, in this case, that it is the free electrons in the ionosphere which play the predominant part in the process of ionic refraction.

## § 2. GENERAL EXPERIMENTAL METHOD

The technique of polarization measurements has been developed by Appleton and Ratcliffe<sup>(3)</sup> in England, and by Green<sup>(4)</sup> in Australia, and they have shown that waves in the medium broadcast band reflected from the ionosphere have a left-handed polarization in the northern hemisphere, and a right-handed polarization in the southern hemisphere. These observations are in accordance with the magneto-ionic theory, which predicts that in general the extraordinary ray is more heavily absorbed than the ordinary ray, especially when the wave frequency is in the region of the gyromagnetic frequency. These experiments have been mainly concerned with conditions in which the polarization is nearly circular.

The experiments to be described were carried out in 1933, and in them an attempt was made to work at more oblique incidence, and to check the observed shape and position of the polarization ellipse with the computed values. As the fundamental principle of the experiments consists in receiving the downcoming ray on a pair of crossed vertical loops, the characteristics actually measured are those of the ellipse obtained by projecting the magnetic vectors in the wave-front on to the ground. For the wave-lengths with which we are concerned, we can assume that the earth is a perfect conductor, so that the wave reflected from the ground merely adds to the downcoming wave, without altering the characteristics of the projected ellipse. The dimensions of the loops and their height above the ground are small in comparison with the wave-length.

In appendix II the analysis is outlined by which we have related the ellipse on the wave-front to the ellipse on the ground. The experimentally observed ellipses are compared with these computed ellipses, which are obtained by assuming that the ray has not suffered any lateral deviation, and that the angle of elevation on arrival is known in terms of the distance between the transmitter and receiver and of a given equivalent height of the ionosphere.

The crossed loops are mounted on a common vertical support, so that they can be revolved together, and are connected by means of slip rings to the field coils of

a goniometer. They thus form a small rotatable Bellini-Tosi system, but each loop contains a series condenser so that it can be tuned to resonance. If the loops are both accurately tuned to the incoming frequency, a vertically incident circularly polarized ray will induce equal currents in the goniometer field coils, which will be in quadrature, whatever the position of the loops. If, however, we detune one loop  $45^\circ$  forwards and the other loop  $45^\circ$  backwards, so that their impedances are both increased by a factor of  $\sqrt{2}$  but are now in quadrature, the currents in the field coils, though still equal in amplitude, will be in phase or antiphase. The search coil, instead of picking up equally in all directions, will now give a zero at one of the  $45^\circ$  positions and a maximum at the other, and these positions will be interchanged if the sense of rotation of the circularly polarized ray is reversed.

The application of this system to the determination of the sense of polarization of wireless echoes reflected at vertical incidence has already been described<sup>(5)</sup>. As the earth's field in England makes an angle of about  $20^\circ$  with the vertical, the downcoming rays at vertical incidence will be very nearly circularly polarized. The presence of a split pair of echoes is therefore strikingly shown by the see-saw effect, as one echo is suppressed and the other appears, when the search coil is rapidly turned from one  $45^\circ$  position to the other.

A signal arriving at oblique incidence will produce the same effect on the loops as a signal at vertical incidence possessing the polarization characteristics of the ellipse obtained by projection on the ground, as described above. If the loops are both in tune, the currents in the field coils will now only be in quadrature when the loops are rotated so that they lie along the axes of this ellipse. Then when the loops are detuned  $45^\circ$  backwards and forwards respectively, the search coil will again give a zero. But this zero will no longer be at one of the  $45^\circ$  positions, but at an angle whose tangent is the ratio of the axes of the ellipse. To obtain a zero we must therefore have two conditions fulfilled simultaneously: (1) the loops must lie along the axes of the ellipse, and (2) the search coil must be set at an angle whose tangent is equal to the ratio of the axes of the ellipse.

Conversely, if a zero is obtained, the positions of the loops and the search coil define the orientation and the shape of the ellipse; moreover, the sense of rotation can be deduced from the quadrant in which the zero on the search coil is obtained. The loops thus form a polarimeter with which the ellipse can be completely defined. It is obvious that when the ratio of the axes is nearly unity, i.e. the polarization is nearly circular, this ratio can be measured with good accuracy, but the position of the axes will be indefinite. Similarly when the ellipse is very narrow, the position of the axes can be determined with considerable accuracy, but the ratio can only be measured very approximately. In comparing the observed results with the computed values it is therefore best to choose the conditions so that the ratio of the axes is between, say, 0.3 and 0.6.

In practice, of course, a good and steady zero can only be obtained if the incoming signal consists of a single reflected ray. If more than one ray is present (for instance, if there is a second-order reflection, or if both left-hand and right-hand components are present) the resultant polarization may have any

characteristics, depending upon the accidental amplitude and phase relations of the individual rays. By using the pulse technique it may be possible to separate the echoes and examine the polarization of each in turn. But in the medium broadcast band it may not be allowable to transmit pulses, and it is in any case difficult on the longer waves to obtain the necessary resolution.

The experiments described in this paper were actually made on the carrier waves of several broadcasting stations. To obtain accurate polarizations we have to rely on the fact that the extraordinary ray is generally suppressed by absorption, and that the first-order reflection from the *E* region is sometimes predominant. The observations indicate quite clearly whether this is the case or not, and only those which give definite evidence of a single reflected ray are selected for comparison with theory. Before proceeding to the experimental results we will give a brief description of the apparatus and the technique involved.

### § 3. DESCRIPTION OF APPARATUS

The successful use of the polarimeter depends upon the accurate phasing of the loops. The necessary adjustments are made by using a local signal from a screened oscillator and attenuator. The output from the attenuator is fed into the loops by two similar variable mutual inductances. These mutuals are screened from one another, and are mounted in the box containing the goniometer and the socket in

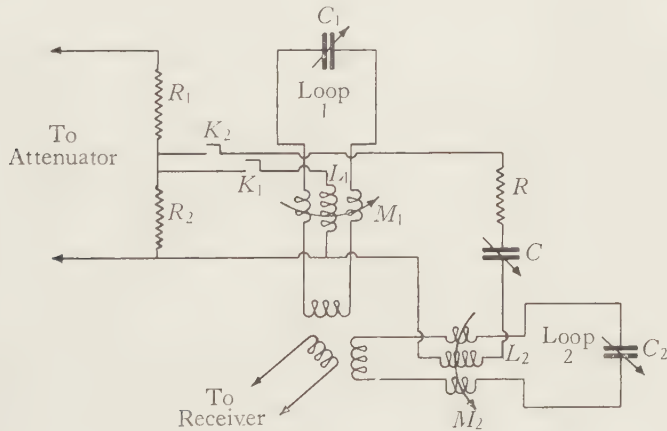


Figure 1.

which the support of the loops rotates. The secondaries of the mutuals are connected symmetrically, by means of split windings, into their respective loop circuits, and the primaries can be connected, either singly or together, by means of low capacity switches to the output potentiometer of the attenuator, see figure 1.

The mutuals and the attenuator are calibrated so that, if required, the loops can be used to measure the absolute field-strength of an incoming signal by comparison with a standard signal from the oscillator, as in a field-measuring set working on this principle. The loops shown, consisting of a single turn in the form of a

square on a diagonal of 5 ft., were made for work on 60 m., for which the apparatus was designed. For the medium-wave tests, similar loops with five turns were used, and it was found that the short-wave mutuals and goniometer were still satisfactory and gave ample sensitivity.

The output from the goniometer search coil is fed into a superheterodyne receiver, in which the second detector is followed by a d.c. amplifying valve. The anode of this valve is connected to the work plate of a cathode-ray tube, which will therefore register the presence of an incoming carrier wave, even in the absence of modulation. The local signal is first accurately adjusted to the required frequency by causing it to beat with the carrier wave of the broadcasting station to be observed. The adjustments are then made in the daytime, either by using a local signal very strong compared with the ground wave from the station, or by choosing a time when the station is not transmitting; this was more feasible at the time when the experiments were made in 1933 than at the present time with the greatly increased service hours.

During the adjustment of one loop the other is open-circuited, and the primary of its mutual is disconnected from the attenuator. The loop is first tuned accurately to resonance, the cathode-ray tube being used as a visual indicator, and then the strength of the signal is adjusted to bring the displacement on the screen to a predetermined mark. From the known calibration of the mutual the coupling is then altered until the injected e.m.f. is increased by a factor of  $\sqrt{2}$ . The loop is now detuned, by increasing the capacity, until the displacement on the screen is brought back to the standard mark, when its impedance will have a phase angle of  $+45^\circ$ . In this way the adjustment is made entirely independent of the calibration and linearity of the receiver. The process is then repeated for the other loop, except that, in detuning, the capacity is decreased to produce a phase angle of  $-45^\circ$ .

The loops have now to be tested for possible coupling between them. A signal is injected into one of the loops, with the other disconnected, and the output of the search coil is cut down to zero by rotating the coil until it has zero coupling with the field coil in the loop circuit. The other loop is then connected, the primary of its mutual being left in the open-circuited condition. As the search coil will be making maximum coupling with the field coil of this loop, any e.m.f. induced from the first loop will be registered to the fullest extent. An adjustment is provided on the framework supporting the loops for altering the angle between their planes until the induced e.m.f. is reduced to zero. When this adjustment has been made the loops should be ready for use.

If now two equal equiphasic signals are induced in the loops, the currents will be equal but in quadrature, and the output of the search coil will be independent of its position. This condition may be used as a criterion of the correct adjustment of the loops, but a much more accurate test is to inject e.m.fs. in quadrature so that the currents are in phase or antiphase, when the search coil will give a zero at one of the  $45^\circ$  positions, as with a vertically incident circularly polarized ray. This result can be achieved by making the primary circuit of one of the mutuals purely inductive and the other purely resistive.

In figure 1 the two loops with their tuning condensers  $C_1$  and  $C_2$ , the split secondaries of the mutuals, and the goniometer field coils are shown diagrammatically. The two mutual primaries  $L_1$  and  $L_2$  can be joined in parallel, through the low capacity keys  $K_1$  and  $K_2$ , across the resistance  $R_2$  of the potentiometer  $R_1 + R_2$ . The part  $R_1$  is made large compared with  $R_2$  and with the output impedance of the attenuator, so that there will be no appreciable throw-back from the loops on to the attenuator. The circuit of  $L_2$  also contains a series resistance  $R$  and a condenser  $C$ . When the key  $K_2$  is closed at the beginning of the adjustments to loop 2, the condenser  $C$  is used to tune the primary circuit to resonance. Assuming that the resistances of the primary windings  $L_1$  and  $L_2$  are small compared with the inductive impedances, the impedance across  $R_2$  due to the circuit of  $L_2$  is simply the resistance  $R$ , while that due to the circuit of  $L_1$  is the inductive impedance  $i\rho L_1$ .

If  $e$  is the e.m.f. across  $R_2$  when both circuits are connected across it, and if the two mutuals are adjusted to  $M_1$  and  $M_2$  respectively, the ratio of the two induced e.m.fs. will be

$$\frac{e}{i\rho L_1} i\rho M_1 / \frac{e}{R} i\rho M_2 = \frac{M_1}{M_2} \frac{R}{i\rho L_1}.$$

The e.m.fs. are thus in quadrature.  $R$  is a fixed resistance for any given range of frequencies, so that it will only be equal to  $\rho L_1$  on one particular frequency. The ratio of the e.m.fs. can, however, be made equal to unity by adjusting the values of the mutuals  $M_1$  and  $M_2$ . This is not, however, really necessary, as a zero can be obtained with the search coil at some angle other than  $45^\circ$ , as with a vertically incident elliptically polarized ray when the loops are along the axes of the ellipse. The proper adjustment by this method is not determined by the position where the zero on the search coil occurs, but by the goodness of the zero so obtained.

It remains to show how the sense of polarization can be determined with the polarimeter. Depending upon which of the loops is tuned forwards and which backwards, the sense of rotation is related to the quadrant in which the zero on the search coil lies; obviously to each zero there will be another one in the opposite quadrant. If we adopt the convention that a particular loop is always detuned forwards and the other one backwards, it is a comparatively simple matter to determine the sense of polarization always to be associated with any given quadrant. A ground wave from a local transmitter is received with both loops connected and tuned to resonance. The direction in which the signal is coming relative to the loops, and the quadrant in which the search coil gives a zero, are noted. Knowing for which of the loops, considered separately, the  $0^\circ$  and  $90^\circ$  positions of the search coil respectively correspond to maximum coupling, we can then work out the required relation.

When the loops had been set up in this way, they were used to determine the sense of polarization of echoes at vertical incidence, and the results agreed with the observations of other workers in confirming the predictions of the magnetoionic theory.

## § 4. EXPERIMENTAL RESULTS

Of a number of stations observed, only two gave results which could definitely be interpreted in terms of a single reflected ray, Radio Normandie and Poste Parisien. Particulars of these two stations are given in table 1; the wave-lengths have, of course, been altered since the time the observations were made in 1933.

Table 1

Station	Wave-length (m.)	Frequency (Mc./sec.)	True bearing E. of N. (deg.)	Distance from Chelmsford (km.)
Radio Normandie	225·9	1·33	183·5	220
Poste Parisien	328·2	0·914	156	350

At Chelmsford, Essex, where the observations were made, these stations in the daytime gave a good ground wave, but in the evening the sky wave was predominant. The presence of the ground wave prevented the obtaining of a perfect zero when the polarimeter was adjusted to suppress the sky wave, and the criterion of a good balance was the steadiness of the residual signal. Actually, however, as the unbalanced sky wave was so much stronger than the ground wave, the residual signal due to the ground wave did not seriously blur the sharpness of the minimum in the balanced position.

Some preliminary experiments were carried out on Hilversum, with a wavelength 298·2 m. and at a distance of 320 km., before the technique described above was perfected. Settings were not carefully observed, but the results served to show that a position could be found where the received signal was nearly constant at its day value. These tests showed that the polarimeter could be used as an anti-fading device for a station near enough to give a workable ground ray at the receiver. During periods when the signal reflected from the ionosphere was predominantly a single left-hand polarized ray, this ray could be suppressed by correctly setting the polarimeter, even though it was many times stronger than the residual ground ray, so that in effect the steady ground ray alone was received.

This effect was even more strikingly observed on Radio Normandie. On the evening of 1 April 1933, the signals from this station were remarkable for the extent and rapidity of the fading. This varied over an extreme range of the order of 50 to 1 in the course of 4 or 5 sec. In spite of this, an adjustment of the polarimeter could be obtained for which the signals maintained their uniform residual day value. Although variations could be seen on the screen of the cathode-ray tube, they could not be detected by ear over a period of about an hour and a half.

On other occasions, however, conditions were much more variable, implying that the reflected ray was complex. On a wave whose frequency 1·33 Mc./sec. was so near to the gyromagnetic frequency 1·32 Mc./sec., it is unlikely that there was any measurable right-handed (extraordinary) component, so that the complexity

was attributable to multiple reflections, or to partial penetration through the *E* region with reflection from the *F* region above. Even when conditions were variable, it was found that there were short periods during which the signals remained steady, and the polarization ellipse took up a limiting position.

It was thus possible to tell when the simple conditions prevailed for which the results could be selected for comparison with the theory. When the conditions were variable, the changes were often too quick to be followed on the polarimeter. In order to help in detecting the steady periods among the prevailing variable conditions, it was found useful to set the loops along the axes of the calculated ellipse. During the steady periods the position of the goniometer search coil was then quite sharply defined, although the correct orientation of the loops was not. It was obvious, however, that the minor axis of the ellipse lay nearly along the great-circle direction of the transmitter.

On 1 April 1933, when the conditions were unusually steady, the setting of the search coil was  $31^\circ$ , implying a ratio of axes equal to  $\tan 31^\circ$  or 0.601. The setting of the loops gave the minor axis at  $20.5^\circ$  west of north, although, as has been explained, this was indefinite. Observations were also made on 28 September and on 8 and 9 October, when conditions were much more variable. On 28 September, however, after sunset, good conditions became more prevalent, and minima were obtained on the search coil at values between  $30^\circ$  and  $33^\circ$ , giving ratios between 0.58 and 0.65, while the setting of the loops gave the minor axis at  $9.5^\circ$  east of north.

Now if it is assumed that the limiting polarization is unaffected by absorption, the ratio of the axes of the ellipse on the wave-front is 0.88. The polarization is nearly circular, so that we should expect the minor axis of the ellipse on the ground to lie near to the great-circle direction. If the equivalent height for the ray-path is taken to be 100 km., the angle of elevation of the ray at the ground is  $42^\circ 18'$ , and computation shows that the ratio of the axes on the ground for the ordinary ray is 0.595, with the minor axis at  $5.5^\circ$  east of north. The observed values, which were for a left-handed polarization, show reasonable agreement with these computed values.

If we suppose, however, that absorption is affecting the limiting polarization, and take the extreme case when the polarization on the wave-front is circular, the projected ellipse will have its minor axis along the great-circle direction,  $3.5^\circ$  east of north in the present case, and the ratio of the axes will simply be  $\sin 42^\circ 18'$  or 0.673. In deciding between the two extreme cases, we can compare the observed ellipse with the computed ellipses, as regards both the ratio and the position of the axes. In our present case the computed position of the minor axis for no absorption is too near to the great-circle direction, and the experimental values too indefinite, for this criterion to be of any use. The experimental values for the ratio of the axes favour the no-absorption condition, but we obviously need a case in which the difference between the two ellipses is more marked.

Fortunately the other station, Poste Parisien, which also gave good experimental conditions, provides a much more definite distinction between the two cases. For no absorption the ratio of the axes on the wave-front is 0.665, and the projected

ellipse has a ratio of 0.348, with a minor axis at  $26^{\circ}3'$  west of north. Assuming again an equivalent height of 100 km., the angle of elevation is  $29^{\circ}44'$ , and in the extreme case of absorption the ratio of the axes is 0.495 with the minor axis along the great-circle direction of  $24^{\circ}$  west of north. Thus although the directions of the minor axis in the two cases are again too close to be of any use as a criterion, there is a considerable difference between the two computed ratios.

A test was made on the evening of 27 September, when good balances were obtained with the loops giving a position for the minor axis at  $28^{\circ}5'$  west of north, with a variation of  $5^{\circ}$  on either side. The most consistent reading for the search coil was  $18^{\circ}$ , but all the readings, though not numerous, were contained between  $15^{\circ}$  and  $19^{\circ}$ . The ratio given by  $\tan 18^{\circ}$  or 0.325 is thus close to the computed value for no absorption, while the ratio of 0.495, corresponding to the other extreme, would imply a search-coil setting of  $26^{\circ}20'$ . While it must be admitted that the number of observations was not large, some half-dozen in all, this setting of  $26^{\circ}20'$  lies well outside the range  $15^{\circ}$  to  $19^{\circ}$  in which the readings for the minimum on the search coil all actually occurred. Thus these results show that the absorption does not play a controlling part, and that, on the other hand, within the limits of accuracy of the apparatus, it does not produce an appreciable effect on the limiting polarization.

The experimental and computed data are summarized in table 2 for reference and comparison.

Table 2

Station	Calculated ellipse no absorption			Calculated ellipse limiting absorption			Observed ellipse		
	Gonio- meter set- ting (deg.)	Ratio of axes	Bearing of minor axis	Gonio- meter set- ting (deg.)	Ratio of axes	Bearing of minor axis	Gonio- meter set- ting (deg.)	Ratio of axes	Bearing of minor axis
Radio Normandie	30.7	0.595	5.5° E. of N.	34.0	0.673	3.5° E. of N.	30 to 33 31	0.58 to 0.65 0.601	9.5° E. of N. 20.5° W. of N.
Poste Parisien	19.2	0.348	26.3° W. of N.	26.3	0.495	24° W. of N.	15 to 19	0.268 to 0.344	28.5° ± 5° W. of N.

## § 5. DISCUSSION OF RESULTS

In seeking to interpret these results as giving an upper limit to the collisional frequency at the lower edge of the ionosphere, we need to know how large the absorption term  $\alpha$  can be before an appreciable change occurs in the polarization ellipse. The analysis in appendix I, in which the ratio of the magnetic vectors in the wave-front, in and perpendicular to the plane containing the direction of the ray and the direction of the earth's field, is given as a function of  $1 - i\alpha$ , shows that this ratio, when  $\alpha$  is small, is altered in magnitude by a factor between 1 and  $\sqrt{1 + \alpha^2}$  by the inclusion of  $\alpha$ . The vectors are no longer in quadrature, but the phase is only changed by an angle which is less than  $\tan^{-1} \alpha$ .

When  $\alpha = 0.1$ , it follows that the change in the shape and position of the polarization ellipse on the wave-front, and hence of the projected ellipse, is very small, and would not be measurable with the polarimeter. But in the particular case we are considering of Poste Parisien, a value of  $\alpha$  equal to 1 changes the ratio of the axes of the projected ellipse from 0.348 to 0.38, and the position of the minor axis from  $26.3^\circ$  to  $20.5^\circ$  west of north. Now a ratio of 0.38 would imply a search-coil setting of about  $21^\circ$ , and we can therefore construct table 3.

Table 3

Search-coil setting	Condition
$19^\circ$	Computed for $\alpha = 0$
$21^\circ$	Computed for $\alpha = 1$
$26^\circ 20'$	Computed for $\alpha$ very large
$18^\circ$	Observed with polarimeter (Limits $15^\circ$ to $19^\circ$ )

While it must be admitted that there is some uncertainty as to the limits of accuracy to be assigned to the setting of the search coil, the general results obtained both on Radio Normandie and on Poste Parisien suggest that in the latter case the true setting would not exceed  $21^\circ$  as an outside limit, the value of  $26^\circ 20'$  being well outside the probable value, as has been stated above. We feel therefore that the observed results may be interpreted as setting an upper limit of 1 to the value of  $\alpha$  at that part of the ionosphere which controls the limiting polarization.

Now since, in terms of the collisional frequency  $\nu_c$ , the absorption term  $\alpha$  is given by

$$\alpha = \nu_c / \beta \pi \nu,$$

where  $\nu$  is the wave frequency (equal to  $0.914$  Mc./sec.) and  $\beta$  is a constant equal to  $\frac{3}{2}$  according to Burnett<sup>(6)</sup>, the condition  $\alpha < 1$  gives  $\nu_c < \beta \pi \nu$ , i.e.  $< 4.3 \times 10^6$  collisions per sec. From the table given by Chapman<sup>(7)</sup>, the value of  $\nu_c$  for electrons is  $3.3 \times 10^6$  at a height of 80 km. and is  $3.5 \times 10^5$  at 100 km. We thus conclude from our results that, as far as its effect on the propagation of medium wireless waves is concerned, the ionic density is inappreciable at a height of about 80 km.

In interpreting these results, we have assumed that the gyromagnetic frequency is determined in terms of electronic charge and mass. If the refraction of the waves were controlled by ionic charges, the effective value of  $\tau$ , the ratio of the gyro-magnetic frequency to the wave frequency, would be controlled by the mass of the ion. On the medium waves we are concerned with, this would imply that the limiting polarization in the wave-front should be circular. Our contention that the limiting polarization is only modified slightly, if at all, by the absorption, is therefore also equivalent to showing that the free electrons must play the predominant part in ionospheric refraction.

If we assume that the ions present are singly charged oxygen atoms, their effect would only be comparable with that of the electrons if the ratio of the number of ions to the number of electrons were of the order of 15,000. But we

should expect a ratio of, say, 10,000 to produce an appreciable effect on the limiting polarization. This figure is interesting, for it is given by Booker and Berkner<sup>(8)</sup> as the probable value deduced from their  $P'f$  results, which they quote in support of the suggestion that the Lorentz theory holds in the  $E$  region. It therefore appears desirable to make further observations before the difficult problem of deciding whether the Lorentz term should be included can be settled.

It would be useful to carry out further medium-wave tests with pulse transmissions. If, for instance, conditions could be found in which the downcoming ray was at right-angles to the earth's field (as, for example, for vertical incidence on the magnetic equator where the earth's field is horizontal), the effect of the absorption term would be to leave the ray plane-polarized but to twist the plane of polarization through an angle  $\tan^{-1} \alpha$ . This suggests that we could lower the limit set to  $\alpha$  by choosing conditions in which the field is nearly transverse to the emergent ray, since  $\alpha$  has then a big effect on the orientation of the polarization ellipse.

Some preliminary work has been done on short waves with the pulse technique, which shows that extremely well-defined minima can be found for which the settings of the search coil and of the loops are quite critical. The readings show a systematic variation with changing ionospheric conditions (for instance, in the region of the critical frequency), and imply, for an oblique transmission, that the angle of arrival is altering. The polarimeter, in effect, gives an indirect method of measuring the angle of incidence of downcoming rays, and should supplement the spaced-frame technique. Alternatively if the angle of incidence is determined with a pair of spaced frames, the polarimeter can be used to check the magnetoionic theory without having to assume an equivalent height of the ionosphere.

These short-wave tests were largely vitiated by local distortion. The site on which the original medium-wave experiments were made has since become unsuitable for such measurements, partly owing to the unavoidable accumulation of other apparatus near the loops in a small hut. The polarimeter is soon to be moved to a large hut on a new site, and it will be set up in a relatively isolated position, where the incoming signal should be free from local distortion. By taking special care to avoid stray pick-up, and by careful calibration of the goniometer, it is hoped to narrow down the limits of accuracy on the medium waves so that the upper limit of  $\alpha$  may be more closely defined.

#### § 6. CONCLUSION

We have seen that a pair of crossed loops can form a polarimeter enabling us to measure completely the polarization characteristics of a downcoming wireless wave. Medium waves at oblique incidence can be used to test the correctness of the magnetoionic theory, and to decide whether the polarization is appreciably affected by the absorption caused by collisions. Although the results so far obtained are of a rather preliminary nature, they indicate that the effect is small, and they allow us to set an upper limit to the collisional frequency at the lower edge of the ionosphere.

The polarimeter has proved to be a useful instrument of research. It suffers from the disadvantage that, unlike the comparator, it is not direct-reading and cannot be used to follow rapidly changing conditions. But, on the other hand, when its use is combined with the pulse technique, it is capable of a higher resolution and accuracy in the examination of the structure of a complex echo pattern, where the individual echoes maintain their characteristics long enough for a balance position to be found. The polarimeter has the additional advantage that, since the information is obtained from the setting of the aerial system itself, the results are independent of the adjustment of the receiver, whereas accurate alignment of the two receivers is necessary in the comparator method. Further, the cathode-ray tube merely becomes an indicator of a zero adjustment in conjunction with an ordinary linear time base, the measurements being unaffected by any distortion or defocusing that may be present in the tube.

The use of the polarimeter is therefore a helpful supplement to direct observation with the comparator. A cross check on the two methods is thus provided, and their respective advantages are combined.

#### REFERENCES

- (1) APPLETON, E. V. *J. Instn. Elect. Engrs*, **71**, No. 430, 642-50 (Oct. 1932).
- (2) BOOKER, H. G. *Proc. Roy. Soc. A*, **155**, 235-57.
- (3) APPLETON, E. V. and RATCLIFFE, J. A. *Proc. Roy. Soc. A*, **117**, 576 (1928).
- (4) GREEN, A. L. Radio Research Board, Commonwealth of Australia, *Bulletin* No. 59 (1932).
- (5) ECKERSLEY, T. L. *Nature, Lond.*, **130**, 398 (10 Sept. 1932).
- (6) BURNETT, D. *Proc. Camb. Phil. Soc.* **27**, 578 (1931).
- (7) CHAPMAN, S. *Proc. Roy. Soc. A*, **122**, 369 (1929).
- (8) BOOKER, H. G. and BERKNER, L. V. *Nature, Lond.*, **141**, 562 (26 March 1938).

#### APPENDIX I

In presenting the analysis relating to the limiting polarization and the projection of the ellipse on to the ground, in a form applicable to all cases, care has to be taken in defining the conventions to be used.

We take a set of rectangular axes  $Ox$ ,  $Oy$  and  $Oz$  such that  $Oz$  is vertically upwards, and in the horizontal plane  $Oy$  is  $90^\circ$  measured anticlockwise from  $Ox$ .  $Oy$  is chosen as the great-circle direction from the transmitter to the receiver.

A point  $T$  is taken on  $Oz$ , figure 2, and through it a line  $TR$  is drawn parallel to the downcoming ray and cutting  $Oy$  in  $R$ . Another line  $TH$  is drawn parallel to the direction of the earth's field and cutting the horizontal plane  $xOy$  in  $H$ .

The elevation of the ray at  $R$  is  $\angle TRO$ , equal to  $\phi$ , say, and the elevation of  $TH$  at  $H$  is  $\angle THO$ , equal to  $D$ , so that, by definition,  $\phi$  and  $D$  are both essentially positive and between  $0$  and  $90^\circ$ . If  $\angle ROH = \theta$ ,  $\theta$  will be defined as positive when  $OH$  is measured anticlockwise from  $Oy$ , and to include all possible positions it can be taken as positive from  $0$  to  $180^\circ$ , and negative from  $0$  to  $-180^\circ$ .

Now through  $T$  draw  $U'TU$  parallel to  $Ox$ , so that  $U'TU$  will be the horizontal line in the wave-front through  $T$ , and  $V'TV$  in the vertical plane  $zOy$  and perpendicular to  $TR$ .  $V'TV$  is chosen so that  $TV$  makes an acute angle with  $Oz$ .

In figure 3 the plane of the paper represents the wave-front through  $T$ , with the ray going down through the paper at  $T$ .  $TV$  is therefore  $90^\circ$  measured anticlockwise from  $TU$ . On this plane two lines at right angles,  $TP$  and  $TQ$ , can be drawn which are respectively perpendicular to and in the plane  $RTH$ . The ratio of the magnetic vectors along  $TP$  and  $TQ$  is given by the magnetoionic theory in terms of the angle  $\epsilon$  between  $TR$ , the direction of the ray, and the direction of the earth's field, the ratio  $\tau$  of the gyromagnetic frequency to the wave frequency, and the absorption term  $\alpha$ . At the lower edge of the ionosphere the limiting polarization is independent of the Lorentz term.

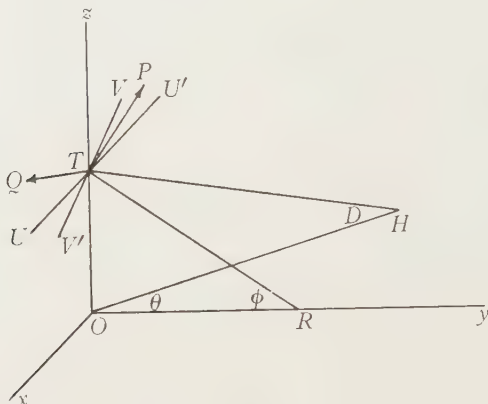


Figure 2.

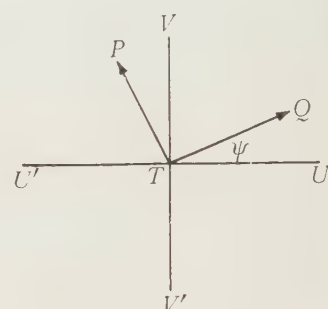


Figure 3.

As the direction cosines of  $TR$  are  $0, \cos \phi, -\sin \phi$ , and those of  $TH$  are  $-\sin \theta \cos D, \cos \theta \cos D, -\sin D$ , the value of  $\epsilon$  is given by

$$\cos \epsilon = \pm [\cos \theta \cos D \cos \phi + \sin D \sin \phi]$$

according as the field acts towards or away from the earth.

The general equation for the ratio of the magnetic vectors on the wave-front is

$$R = \iota \left[ -\frac{\tau \sin \epsilon \tan \epsilon}{2(1-\iota\alpha)} \pm \sqrt{\left\{ 1 + \left( \frac{\tau \sin \epsilon \tan \epsilon}{2(1-\iota\alpha)} \right)^2 \right\}} \right],$$

and the rays become plane-polarized when  $\epsilon = 90^\circ$ , i.e. when  $\tan \phi = -\cos \theta \cot D$ . When  $\epsilon = 0$  the rays become circularly polarized.

When the field is transverse and the rays are plane-polarized, the ordinary ray is unaffected by the earth's field. The magnetic vector is therefore perpendicular to the earth's field, i.e. the magnetic vector is along  $TP$ . Similarly for the extraordinary ray the magnetic vector is along  $TQ$ . Since for the two rays the reciprocal relation

$$\left( \frac{TQ}{TP} \right)_{\text{ord}} = \left( \frac{TP}{TQ} \right)_{\text{ext}}$$

always holds, then as  $\epsilon$  goes from 0 through  $90^\circ$  to  $180^\circ$ ,  $(TQ/TP)_{\text{ord}}$  and  $(TP/TQ)_{\text{ext}}$  go from 1 to 0 and back to 1 again.

It is therefore only necessary to evaluate  $R$  for values of  $|R|$  between 0 and 1. If  $\frac{1}{2}|\tau \sin \epsilon \tan \epsilon| = x$ , then when  $\alpha=0$ ,  $|R| = -x + \sqrt{(1+x^2)}$ . By writing  $x = \cot \omega$ , where  $\omega$  is in the range 0 to  $\pi/2$ ,  $|R|$  is obtained, thus

$$|R| = -\cot \omega + \operatorname{cosec} \omega = \tan \frac{1}{2}\omega.$$

If  $\epsilon_0$  is the angle in the range 0 to  $\pi/2$  for which  $\sin \epsilon_0 = |\sin \epsilon|$  it is a simple matter, by means of the parameter  $\omega$ , to plot  $|R|$  as a function of  $\epsilon_0$  for various values of  $\tau$ , as in figure 4. From these curves, for  $\alpha=0$ , the ratio of the axes of the polarization ellipse in the wave-front can be obtained, and the sense of rotation is determined by the rule that the ordinary ray is left-handedly polarized, and the extraordinary

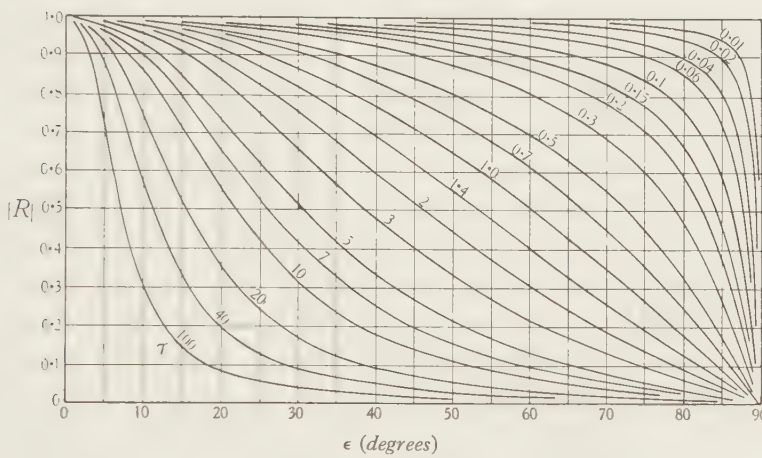


Figure 4.

ray is right-handedly polarized, when  $\epsilon$  is less than  $90^\circ$ , and vice versa when  $\epsilon$  is greater than  $90^\circ$ .

If  $\alpha$  is not zero but is very small, then for the extraordinary ray

$$R = \pm i |R_0| [1 - i\alpha \cos \omega],$$

according as  $\epsilon <$  or  $> 90^\circ$ , where  $|R_0|$  is the value of  $|R|$  when  $\alpha=0$ . The initial effect of introducing  $\alpha$  is therefore to produce a very small change of amplitude, and a phase-shift of  $-\tan^{-1}(\alpha \cos \omega)$ . When, however,  $\alpha$  is not small, the changes in  $R$  must be worked out from the complete expression.

When  $\alpha$  is very large,  $R$  approaches  $\pm i$ , i.e. the limiting polarization becomes circular, except when  $\epsilon$  is nearly  $90^\circ$ . In this latter case the effect of  $\alpha$  is to change  $R$  from  $\pm i/2x$  to  $\pm i(1-i\alpha)/2x$ , i.e. the amplitude ratio is increased by a factor  $\sqrt{(1+\alpha^2)}$  and the phase is altered by  $-\tan^{-1} \alpha$ .

## APPENDIX II

In considering the projection of the ellipse on to the ground it is first necessary to know the angle between the axes  $TP$  and  $TQ$ , and the axes  $TU$  and  $TV$  in the wave-front. The direction cosines of  $TP$  can be expressed in terms of  $\theta$ ,  $D$ , and  $\phi$  from the fact that it is perpendicular both to  $TR$  and to  $TH$ . The direction cosines of  $TQ$  can then be determined from the fact that it is perpendicular to  $TR$  and  $TP$ .

If in figure 3 the angle between  $TQ$  and  $TU$  is  $\psi$ , considered positive when  $TQ$  is anticlockwise from  $TU$ , then from the direction cosines of  $TQ$  it follows that

$$\tan \psi = \tan D \operatorname{cosec} \theta \cos \phi - \cot \theta \sin \phi.$$

As a check that the sign of  $\tan \psi$  is correct,  $\theta$  may be taken as  $+90^\circ$  and  $\phi$  as  $0^\circ$ , so that the ray is horizontal; with our conventions it is then obvious geometrically that  $\psi = D$ , which agrees with the form  $\tan \psi = \tan D$  assumed by the equation.

For a given pair of values for  $D$  and  $\theta$ , as  $\phi$  is increased from  $0$  to  $90^\circ$ , the axes  $TP$  and  $TQ$  revolve in the wave-front relative to the axes  $TU$  and  $TV$ . By differentiation we get

$$\sec^2 \psi d\psi = -[\tan D \operatorname{cosec} \theta \sin \phi + \cot \theta \cos \phi] d\phi.$$

Since  $D$  and  $\phi$  are essentially positive and between  $0$  and  $\frac{1}{2}\pi$ , when  $\theta$  is between  $0$  and  $\frac{1}{2}\pi$  the rotation is clockwise. When  $\theta$  is between  $0$  and  $-\frac{1}{2}\pi$  the rotation is anticlockwise. But when  $\theta$  is between  $\frac{1}{2}\pi$  and  $\pi$ , or  $-\frac{1}{2}\pi$  and  $-\pi$ , the rotation changes its sense when  $\tan \phi = -\cos \theta \cot D$ . As we should expect, this is also the condition that the polarization shall become plane, when  $\epsilon = 90^\circ$  and the field is transverse to the ray, as was seen in appendix I.

The angle  $\psi$  having been determined, the magnetic vectors along  $TP$  and  $TQ$  can be resolved along  $TU$  and  $TV$ . The resultant vectors along  $TU$  and  $TV$ , which are not in general in quadrature, project on to the ground without change of phase,  $TU$  projecting along  $Ox$  and being unaltered in amplitude, while  $TV$  projects along  $Oy$  with reduction in amplitude by a factor  $\sin \phi$ .

If we call these vectors  $(Ox)_I$  and  $(Oy)_I$ , in the case of an imperfectly conducting earth we must add the effects of the reflected waves  $(Ox)_R$  and  $(Oy)_R$ , so that for the total vectors we have

$$(Ox) = (Ox)_I + (Ox)_R$$

and

$$(Oy) = (Oy)_I - (Oy)_R.$$

Now

$$(Ox)_R = (Ox)_I \rho_x,$$

where the reflection coefficient  $\rho_x = |\rho_x| e^{i\chi_x}$  and is given by

$$\rho_x = \frac{(\epsilon - 2i\sigma\lambda c) \sin \phi - \sqrt{(\epsilon - 2i\sigma\lambda c - \cos^2 \phi)}}{(\epsilon - 2i\sigma\lambda c) \sin \phi + \sqrt{(\epsilon - 2i\sigma\lambda c - \cos^2 \phi)}},$$

and similarly  $(Oy)_R = (Oy)_I \rho_y$ , where

$$\rho_y = |\rho_y| e^{i\chi_y} = \frac{\sin \phi - \sqrt{(\epsilon - 2i\sigma\lambda c - \cos^2 \phi)}}{\sin \phi + \sqrt{(\epsilon - 2i\sigma\lambda c - \cos^2 \phi)}},$$

in which  $\epsilon - 2\sigma\lambda c$  is the equivalent specific inductive capacity of the earth when the conductivity  $\sigma$  is measured in e.m.u.

Thus the effect of the reflected ray may be included by modifying  $(Ox)_I$  by an amplitude factor

$$\sqrt{(1 + 2 |\rho_x| \cos \chi_x + |\rho_x|^2)}$$

and a phase angle of

$$\tan^{-1} \frac{|\rho_x| \sin \chi_x}{1 + |\rho_x| \cos \chi_x},$$

and modifying  $(Oy)_I$  by an amplitude factor

$$\sqrt{(1 - 2 |\rho_y| \cos \chi_y + |\rho_y|^2)}$$

and a phase angle of

$$\tan^{-1} \frac{|\rho_y| \sin \chi_y}{1 - |\rho_y| \cos \chi_y}.$$

From the ratio of the amplitudes and the relative phases of the vectors  $(Ox)$  and  $(Oy)$  the orientation and shape of the final ellipse can be obtained. This process

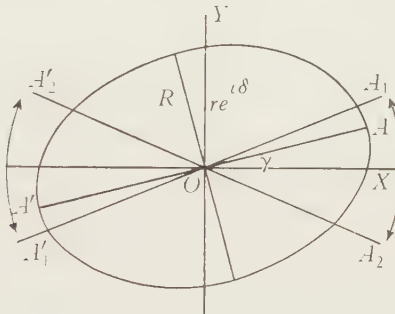


Figure 5.

can be reduced to a simple graphical one by the construction of two charts relating the ratio of the axes of the ellipse, and the angle the major axis makes with  $Ox$  or  $Oy$ , to the ratio and phase of the vectors along  $Ox$  and  $Oy$ .

Consider in figure 5 two vectors at right angles along  $OX$  and  $OY$ .  $Ox$  is chosen to be the vector of greater magnitude and  $OY$  is defined to be  $90^\circ$  anticlockwise from  $OX$ . We can then write

$$OY/OX = re^{i\delta},$$

where  $r \ll 1$  and  $\delta$  is the phase angle of  $OY$  relative to  $OX$ . Now as  $\delta$  alters, the major axis oscillates between two limiting positions  $A_1'OA_1$ , and  $A_2'OA_2$  at an angle of  $\tan^{-1} r$  on either side of  $OX$ , i.e. it always makes an angle which  $< 45^\circ$  with the direction of the larger vector. If the angle  $XOA$  be called  $\gamma$  for phase angle  $\delta$ , and if  $\gamma$  be taken as positive when  $OA$  is measured anticlockwise from  $OX$ , we have the following rules: (1) When  $\sin \delta$  is positive, the sense of rotation is right-handed or clockwise, and when  $\sin \delta$  is negative, the sense of rotation is left-handed or anticlockwise. (2) When  $\delta$  is in the range  $-\frac{1}{2}\pi, 0, \frac{1}{2}\pi, \gamma$  is positive, and when  $\delta$  is in the range  $\frac{1}{2}\pi, \pi, \frac{3}{2}\pi, \gamma$  is negative.

If  $R$  is the ratio of the minor to the major axis of the ellipse, so that  $R=0$  when  $\delta=0$  or  $\pi$ , and  $R=r$  when  $\delta=\frac{1}{2}\pi$  or  $-\frac{1}{2}\pi$ , then we require relations for  $|\gamma|$  and  $R$  in terms of  $r$  and  $\delta$ . These relations are

$$\tan 2|\gamma| = \frac{2r |\cos \delta|}{1 - r^2}$$

and

$$R = \tan \frac{1}{2}\Omega,$$

where

$$\sin \Omega = \frac{2r |\sin \delta|}{1 + r^2},$$

$\Omega$  being between 0 and  $\frac{1}{2}\pi$ .

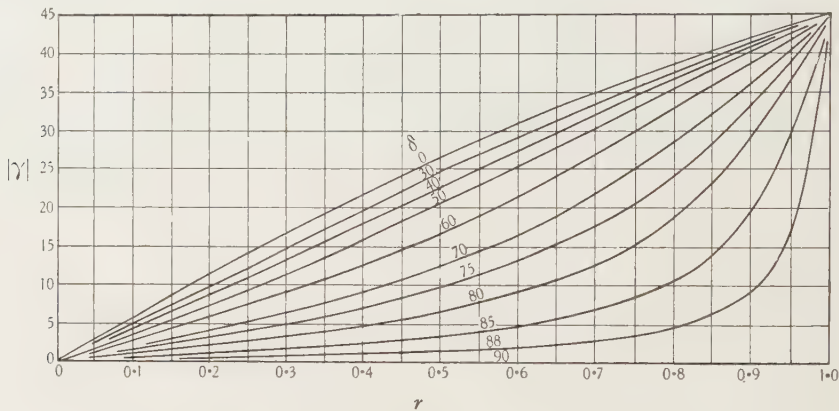


Figure 6.

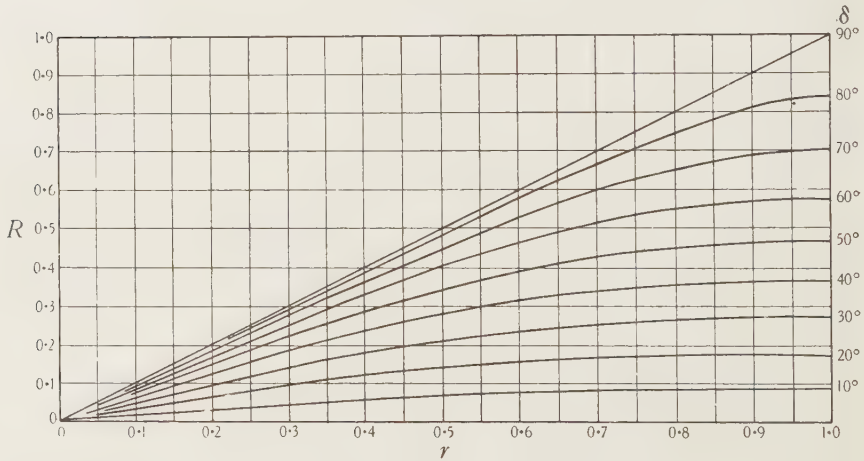


Figure 7.

In figures 6 and 7, curves for  $|\gamma|$  and  $R$ , derived from these expressions, are plotted as a function of  $r$  for various values of  $\delta_0$ , where  $\delta_0$  is the angle between 0 and  $\frac{1}{2}\pi$  for which  $\sin \delta_0 = |\sin \delta|$ . When  $r$  and  $\delta$  are thus given,  $|\gamma|$  and  $R$  can be read immediately from these curves, and from the rules given above we can decide the sign of  $\gamma$  and the sense of rotation.

In the wave-front, for the case in which  $\alpha$  can be neglected, we have exactly the converse process. The magnetic vectors along  $TP$  and  $TQ$  define the axes of the ellipse, and we have to find the resolved vectors along  $TU$  and  $TV$ .  $|\gamma|$  is given by  $|\psi|$  or  $90^\circ - |\psi|$  according to which ray we are considering, and  $R$  is obtained by the method described in appendix I from the values of  $\tau$  and  $\epsilon$ , from which we

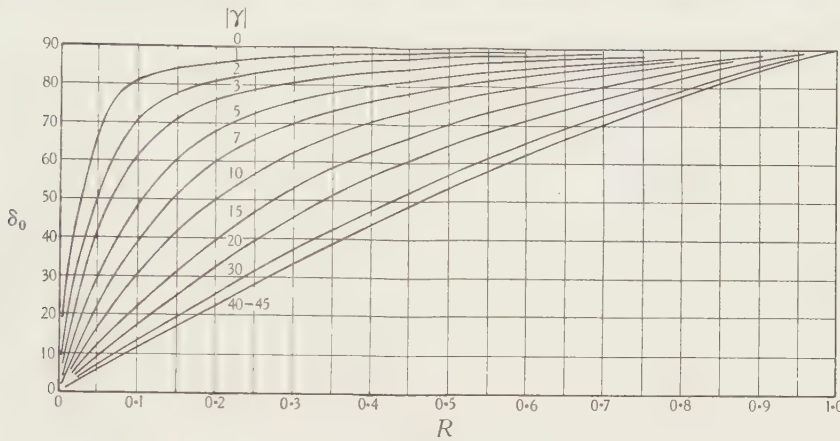


Figure 8.

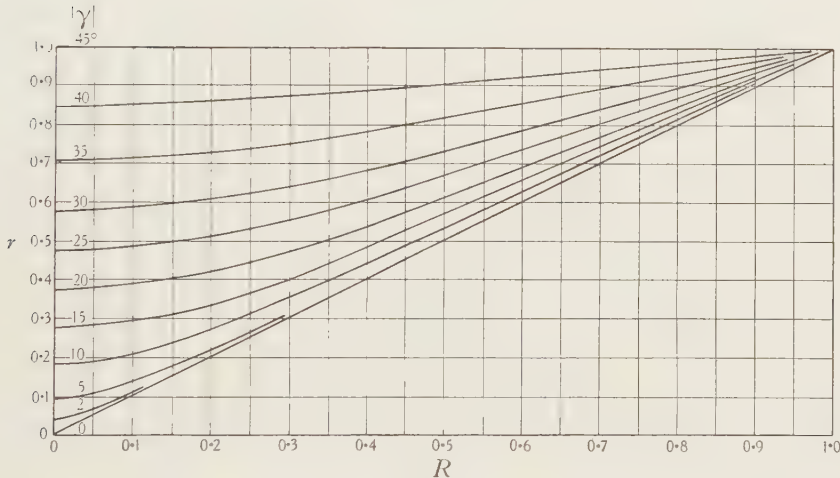


Figure 9.

have to find  $r$  and  $\delta$ . Now from the curves of figures 6 and 7, or by computing from the relations

$$\tan \delta_0 = \frac{2R \operatorname{cosec} 2|\gamma|}{1 - R^2}$$

$$r = \sqrt{\frac{R^2 + \tan^2 |\gamma|}{1 + R^2 \tan^2 |\gamma|}}$$

and we can construct a converse set of curves as in figures 8 and 9 for determining  $r$  and  $\delta$  when  $R$  and  $\gamma$  are given. The value of  $\delta$  is determined from  $\delta_0$  by a converse

application of the rules given above. If, for instance, with our definitions  $\gamma$  is positive,  $\delta$  must be in the range  $-\frac{1}{2}\pi$ ,  $0$ ,  $\frac{1}{2}\pi$ , and if in addition the ellipse is assumed to the right-handed so that  $\sin \delta$  is positive,  $\delta$  must lie in the range  $0$  to  $\frac{1}{2}\pi$ .

In the general case in which  $\alpha$  modifies the polarization ellipse, so that the vectors along  $TP$  and  $TQ$  are not in quadrature, we can obtain the resolved vectors along  $TU$  and  $TV$  by first finding the position and shape of the ellipse relative to  $TP$  and  $TQ$  from figures 6 and 7; this ellipse is then resolved into the vectors along  $TU$  and  $TV$  by means of figures 8 and 9. In this way the most general case can be treated by means of these curves, so long as care is taken to observe the conditions attached to  $R$ ,  $r$ ,  $\delta$ , and  $\gamma$ , namely that (1)  $R$  and  $r < 1$ ; (2)  $\delta$  is the phase of the smaller vector  $OY$  relative to the larger  $OX$ , where the former is measured  $90^\circ$  anticlockwise from the latter; and (3)  $\gamma$  is measured positive when the major axis  $OA$  is measured anticlockwise from  $OX$ .

In applying this analysis to the computation of the cases quoted in the paper, the value of  $D$  was taken as  $70^\circ$ , and the magnetic north was assumed to be  $11^\circ$  west of true north. The gyrofrequency was taken as  $1.32$  Mc./sec., corresponding to a wave-length of  $227.1$  m.

# THE ORIGIN OF RADIO-WAVE REFLECTIONS IN THE TROPOSPHERE

By J. H. PIDDINGTON, M.Sc., B.E., Ph.D.,  
Walter and Eliza Hall Fellow of the University of Sydney  
Cavendish Laboratory, Cambridge

*Communicated by Prof. E. V. Appleton, F.R.S., 21 June 1938*

**ABSTRACT.** The evidence relating to the reflection of radio waves in the lower atmosphere is critically examined. It is shown that reflection is most probably due, not to ionized layers as was previously supposed, but to discontinuities in the concentration and state of the water content. It is considered probable that all reflections causing echoes of semi-path less than about 25 km. (B-region echoes) take place within the troposphere.

## § I. INTRODUCTION

IN a number of papers published within the last few years, experiments demonstrating that radio waves are reflected from atmospheric levels within, or very near, the troposphere<sup>(1, 2, 3)</sup> have been described. Of such experimental investigations, the most convincing is that adopted by Watson Watt, Wilkins and Bowen<sup>(4)</sup>, who have obtained definite photographic evidence of the radio echoes in question. By using the well-known Breit and Tuve technique of radio-pulse-production they succeeded in detecting echoes with group-time delays corresponding to a semi-path as short as 10 km. The results were interpreted by them as demonstrating the semi-permanent existence of four or more highly reflecting ionized strata in the lower atmosphere, about 10 km. above ground level, each with a reflection coefficient of the order of 0·7.

The same phenomena have more recently been examined by Appleton and Piddington<sup>(5)</sup> who, as a result of experiments in which accurate measurement of effective reflection coefficients were included, conclude that the echoes under consideration are not reflected from layers at all, but are signals of very low intensity indeed reflected from scattering centres in the lower atmosphere. If the equivalent reflection coefficient  $\rho$  is defined as the ratio of the electric field produced by the scattering agency at the receiver to that due to an infinite, plane, perfectly reflecting layer situated at the same distance, Appleton and Piddington find that  $\rho$  is of the order of 0·00003 instead of the value 0·7 stated above. They therefore suggested that if their conclusions concerning the magnitude of the reflection coefficients were correct the echoes were not necessarily due to ionization, but might possibly be caused by other types of atmospheric discontinuities, constituting what they term the B region.

In the present paper the nature of the possible reflecting agencies is considered in greater detail. The value of  $\rho$  assumed for purposes of calculation is 0.00002 at a signal frequency of 9 Mc./sec.; this is in accordance with the experimental results referred to above<sup>(5)</sup>. It should, however, be mentioned that such a low value of  $\rho$  is not in agreement with the conclusions of Colwell and Friend<sup>(1)</sup>, who interpret their results as indicating the presence of well-defined layers of some permanence and capable of effecting noticeable absorption of wireless waves which have been reflected from higher atmospheric levels.

## § 2. THE LOCALIZATION OF THE SCATTERING CENTRES

If the transmitter and receiver used in observing echoes from scattering centres are situated a short distance apart, as is usually the case, then the intensity at the receiver of a wave reflected from a small scattering centre is inversely proportional to the square of its distance  $r$  from the point of observation. If, however, there are a number of such centres, say  $n$  per unit volume, distributed uniformly, then the number at distances between  $r$  and  $r + \delta r$  from the receiver is proportional to  $r^2$ , and as the echoes from these arrive at random phases the total intensity is proportional to the square root of the number of centres in the given zone. Combining the two factors thus operative it is seen that the echo-intensity should be inversely proportional to  $r$ . It is unlikely, of course, that  $n$  would be independent of height above ground level, so that the above relation may be expected to hold only approximately.

The authors of reference (4) have pointed out that in a typical snap photo of B-region echoes, the amplitude of what they term the fifth-order reflection is about 0.2 times that of the first-order reflection. But if we cease to regard the gradually decaying echo system as comprising multiple reflections from a small number of discrete layers, the obvious interpretation to be placed upon this fact is that the reflection coefficient of the scattering centres is everywhere the same, the gradual decay being caused by spacial attenuation and complying with the simple distance law enunciated above. The agency causing reflection might, therefore, be in the form of clouds, and since these would be effective as reflectors when situated above a point some distance from the transmitter, an echo which has a delay corresponding to a semi-path of 20 km. might really be reflected from a region of a height much below 20 km.

The experimental technique of Watson Watt, Wilkins and Bowen<sup>(4)</sup> did not permit of the detection of echoes of semi-path much below 10 km. There is every indication from their records, however, and from those of other workers<sup>(1, 3)</sup> that reflection takes place from centres situated well within the troposphere.

Other experiments, the details of which need not be given here, have given support to the view that the echoes may arrive at the receiver from directions making considerable angles with the vertical, and in the light of the subsequent theoretical investigation of the nature of the reflecting agency it is regarded as highly probable that all B-region echoes might well originate within the troposphere.

### §3. THE POSSIBILITY OF REFLECTION BY LAYERS OR CENTRES OF IONIZATION

Let us first examine the possibility of reflection due to ions or electrons. Four cases may be considered: layers of electrons, layers of heavy ions, clouds of electrons and clouds of heavy ions. The ions would most probably be singly charged oxygen molecules, and if there are  $N$  of these present per  $\text{cm}^3$  and the conductivity is  $\sigma$  e.s.u. and the dielectric constant  $K$  e.s.u., then the reflection coefficient of a layer with a sharp boundary is given by

$$\rho^2 = \frac{(n-1)^2 + \kappa^2}{(n+1)^2 + \kappa^2}, \quad \dots\dots(1)$$

where  $n$  and  $\kappa$  are the refractive index and absorption coefficient respectively of the ionized medium. Further,

$$2n^2 = \sqrt{(K^2 + 4\sigma^2\tau^2) + K}, \quad \dots\dots(2)$$

$$2\kappa^2 = \sqrt{(K^2 + 4\sigma^2\tau^2) - K}, \quad \dots\dots(3)$$

if  $\tau$  is the period of the reflected wave.

If we follow Appleton and Chapman in putting the retarding force on an ion in the medium as  $m\nu u$ , where  $m$  and  $u$  are the mass and the velocity of the ion and  $\nu$  its frequency of collision with neutral molecules, then the usual Lorentz theory gives

$$K = 1 - \frac{4\pi Ne^2}{m(p^2 + \nu^2)}, \quad \dots\dots(4)$$

$$\sigma = \frac{Ne^2\nu}{m(p^2 + \nu^2)}, \quad \dots\dots(5)$$

where  $e$  is the electronic charge and  $p$  the wave angular frequency. From equations (4) and (5)

$$1 - K = \frac{4\pi\sigma}{\nu} = 2\sigma\tau(p/\nu).$$

Since we are interested at the moment in frequencies of the order of 9 Mc./sec. we have  $p = 5 \times 10^7$ . At a height of 10 km. above ground level the pressure<sup>(9)</sup> is about 190 mm. and the temperature is 220° K.; the collisional frequency of electrons with molecules is, therefore, about  $1.3 \times 10^{11}$  per second and of heavy ions  $6 \times 10^9$ . The condition  $\nu \gg p$  is therefore seen to hold in both cases, so that  $(1 - K)$  is small compared to  $2\sigma\tau$  and the case is one of conductivity reflection. Equations (2) and (3) become

$$2n^2 = \sqrt{(1 + 4\sigma^2\tau^2) + 1},$$

$$2\kappa^2 = \sqrt{(1 + 4\sigma^2\tau^2) - 1}.$$

If  $\sigma\tau$  is small, as is the case, we may write, approximately,

$$n = 1 + \frac{\sigma^2\tau^2}{2},$$

$$\kappa = \sigma\tau,$$

so that equation (1) becomes

$$\rho = \frac{\sigma\tau}{2}. \quad \dots\dots(6)$$

If we now put  $\rho = 2 \times 10^{-5}$  and  $\tau = 10^{-7}$  sec., then

$$\sigma = 400 \text{ e.s.u.},$$

the corresponding ion-density being given by

$$N = \frac{m\nu\sigma}{e^2} = 6 \times 10^8 \text{ ions per cm}^3$$

If, on the other hand, the reflecting body is a cloud of ions small compared to a wave-length, the reflection coefficients may be shown to be given by

$$\rho = \frac{2Q}{r} \left( \frac{e^2}{mc^2} \right) \frac{p}{\nu} \quad \text{when } p \ll \nu,$$

where  $c$  is the velocity of light in vacuo,  $r$  the distance of the cloud from the observer, and  $Q$  the total number of ions in the cloud. Substituting the original values of  $p$ ,  $\nu$  and  $\rho$  we have, approximately,

$$Q = 2 \times 10^{20} \text{ ions}$$

necessitating a density of about  $4 \times 10^{11}$  ions/cm<sup>3</sup> if the cloud is a sphere of diameter 10 m.

If the reflecting agency is an electron cloud or layer we find equally high values of conductivity to be necessary, and as the collision frequency is  $1.3 \times 10^{11}$  per second and the probability of attachment to oxygen molecules is about  $10^{-5}$  per collision, the rate of production of free electrons must be enormous, about  $5 \times 10^{10}$  per cm<sup>3</sup>/sec. in the case of a layer of electrons.

The greatest difficulty encountered in trying to account for B-region echoes in terms of free electricity is to account for the high conductivity required. In this connexion it is important to note that the highest value of conductivity found in the troposphere when continuous recording was used on the Explorer II balloon flight<sup>(6)</sup> was  $2.5 \times 10^{-3}$  e.s.u., which is in agreement with the earlier works of Wigand<sup>(7)</sup>. The least value necessary to account for the echoes has been shown to be 400 e.s.u., which is greater by a factor of about 160,000. It seems unnecessary to dwell on the difficulty of explaining the processes of production and maintenance of sharply bounded volumes of ionization in the troposphere, since if they had existed their presence would almost certainly have been detected during the frequent measurements of conductivity carried out during balloon ascents.

#### § 4. THE PROBABLE PROCESS OF REFLECTION

We have seen above that it is highly improbable that B-region echoes could be due to a process of reflection by free electrons or ions. We therefore now proceed to consider the possibility that these echoes may result from reflections from dis-

continuities of the atmospheric dielectric constant, due to changes in composition. It is at once apparent that water-vapour molecules, which have a large permanent dipole moment, make a very considerable contribution to the total dielectric constant of a moist atmosphere. If we write  $(K - 1)$  as the contribution to the dielectric constant due to any particular gas present in the atmosphere, then  $(K - 1)$  for air at normal temperature and pressure is  $5.9 \times 10^{-4}$  and for water vapour at its saturation vapour pressure at  $0^\circ\text{C}.$ ,  $(K - 1)$  is  $3.9 \times 10^{-4}$ . The distribution of water vapour in the atmosphere is much more irregular than that of the other common components and, in addition, the three states in which water exists have widely different dielectric constants at the frequencies under consideration. Water is, therefore, the most probable agency to account for the observed reflections.

A radio wave incident on a surface at which the dielectric constant changes will be partially reflected, and if the transition is sudden the reflection coefficient may be written

$$\rho = \frac{n - 1}{n + 1},$$

where  $n$  is the refractive index on one side of the boundary and unity that on the other. In the atmosphere  $n = \sqrt{K}$ , and to a sufficient degree of accuracy we may write

$$\rho = \frac{K - 1}{4}.$$

In the case of water in its three states,  $K$  will vary irregularly throughout the atmosphere because of variations in the amount present per  $\text{cm}^3$  and also because of variations in its state.

The value of the dielectric constant of water vapour at radio frequencies has been determined experimentally by several workers. Stranathan<sup>(8)</sup> appears to have eliminated the usual errors due to adsorption at the plates of the test condenser, and his results will be used. We may write for the dielectric constant

$$K - 1 = A + B/T,$$

where  $A$  and  $B$  are constants for given water-vapour density and  $T$  is the absolute temperature. Stranathan's results only extend down to about  $20^\circ\text{C}.$ , but if we extrapolate we find

$$K - 1 = 12.7q \text{ e.s.u. at } 273^\circ\text{K.}$$

where  $q \text{ g./cm}^3$  is the water-vapour density. This value is in agreement with the calculated value if we take the permanent dipole moment of a molecule to be  $1.8 \times 10^{-18} \text{ e.s.u.}$  We then find

$$K - 1 = 12.1q \text{ e.s.u. at } 273^\circ\text{K.}$$

The small discrepancy is due to neglecting the term  $A$ , which allows for the mean polarisability of the molecules in the field of force. The dielectric constant of water in the liquid state maintains a value of about 80 e.s.u. up to the frequencies with which we are dealing<sup>(9)</sup>, so that for the liquid state we have

$$K - 1 = 80q \text{ e.s.u.}$$

Ice, however, shows a rapid fall in dielectric constant at frequencies of a few kc./sec., and at 6 Mc./sec. it has a value of about 3 e.s.u. according to the *International Critical Tables*, so that

$$K - 1 = 3q \text{ e.s.u.}$$

It is clear, therefore, that any change of state of water which occurs in the troposphere so as to form a boundary which is sharp compared to a wave-length may result in partial reflection of electromagnetic waves.

In the table are shown the mean temperatures for the year at various levels in the troposphere, as measured with sounding-balloons sent up from Kew Observatory in 1935<sup>(10)</sup>. During the balloon flights measurements were also made of the relative humidity of the atmosphere by means of a hair hydrograph. Although this instrument is not very reliable, and the measurements of the relative humidity at very low temperatures are probably far from accurate, the results are suggestive, and in view of the scarcity of other similar data we quote them.

The hydrograph is calibrated by immersion in water, the reading being taken as corresponding to a relative humidity of 95 to 100 per cent. It is suggested that when the reading exceeds this value supersaturation may exist. Of 47 balloon flights during which the humidity was measured, 17 suggest supersaturation at one height at least, while in 30 cases the relative humidity at one or more heights was over 90 per cent. Since successive readings were taken at points  $\frac{1}{2}$  or 1 km. apart in height, the rate of change of humidity cannot be traced.

We include, therefore, in the table the values of the density of water vapour corresponding to the saturation vapour pressure at the various temperatures. In the next column are shown the values of the contribution to the dielectric constant of this water if it is in the liquid state. In the final column are listed the reflection coefficients which would result from a sudden discontinuity in the presence of water. It is not suggested that any such complete discontinuity occurs, the tabulation being made as a basis for further reasoning.

Height (km.)	Mean temperature (° K.)	Saturation density of water (g./cm. <sup>3</sup> × 10 <sup>6</sup> )	Dielectric constant (e.s.u. × 10 <sup>5</sup> )	Reflection coefficient × 10 <sup>5</sup>
2	273	4.85	39	10
4	262	1.98	16	4.0
6	249	0.62	5	1.2
8	235	0.15	1.2	0.3
10	223	0.04	0.3	0.07

Two processes now appear to be the most likely to form a sharp reflecting boundary. Saturated or supersaturated water vapour, by cooling and condensing, will raise the dielectric constant very considerably, even though the total amount of water is the same on either side of the boundary. Such a process might cause noticeable reflection without the formation of clearly marked clouds, since reflecting strata need only be very thin. Drops of water solidifying to ice would give a similar result. If the drops were supercooled, in the manner that has often been indicated

by ice-formation on aircraft<sup>(11)</sup>, a sharp boundary might result. The former process might be expected in the alto-cumulus and cirro-stratus levels, and lower, and would be particularly marked in thunderstorm areas where large quantities of warm moist air are moving upwards. Watson Watt, Wilkins and Bowen<sup>(4)</sup> find a marked correlation between the strength of B-region echoes and thunderstorms, which they attribute to the ionizing effect of the latter.

In considering reflections from small clouds it is of interest to note that a comparison may be made between the reflection coefficients of a cloud and those of an infinite plane layer of the same dielectric constant by an application of Huyghens' principle. The secondary waves originating at the various parts of the reflecting surface combine at the receiver to give a signal strength depending on their amplitudes and relative phases. If the problem is simplified by assuming that the cloud presents a flat circular face to the receiver, then the method of Fresnel zones is easily applicable and it may be shown that the equivalent reflection coefficient of such a cloud, of diameter 775 m., at a distance of 5 km. for 30-metre waves, is double that of an infinite plane layer of the same refractive index. Thus, small clouds may be quite effective reflectors of radio waves, and if the reflecting surface is at all concave towards the transmitter the equivalent reflection coefficient may be many times greater than that of an infinite plane sheet. Such effects are often noticed in reflections from ionospheric regions E and F.

We conclude that the observed value of  $\rho$ , namely  $2 \times 10^{-5}$ , can be accounted for on a theory of reflection by water molecules. If this explanation is correct, a new method of investigating the distribution of water in the troposphere is available and further work with very high-powered pulse transmitters sending signals of duration less than  $20 \mu\text{sec}$ . may be expected to add greatly to our knowledge in this field.

#### §5. ACKNOWLEDGEMENTS

I wish to thank Professor E. V. Appleton for his help and advice and Dr T. W. Wormell and Dr J. L. Pawsey for very helpful discussions

#### REFERENCES

- (1) COLWELL, R. C. and FRIEND, A. W. *Nature, Lond.*, **137**, 782 (1936); *Phys. Rev.* **50**, 632 (1936).
- (2) WATT, R. A. W., BAINBRIDGE-BELL, L. H., WILKINS, A. F. and BOWEN, E. G. *Nature, Lond.*, **137**, 866 (1936).
- (3) RAKSHIT, H. and BHAR, J. N. *Nature, Lond.*, **138**, 283 (1936).
- (4) WATT, R. A. W., WILKINS, A. F. and BOWEN, E. G. *Proc. Roy. Soc. A*, **161**, 181 (1937).
- (5) APPLETON, E. V. and PIDDINGTON, J. H. *Proc. Roy. Soc. A*, **164**, 467 (1938).
- (6) GISH, O. H. and SHERMAN, K. L. *Sixième Assemblée Générale de l'Union Géodésique et Géophysique Internationale*, Édimbourg, 1936. Camelot Press Ltd. (London and Southampton, 1937).
- (7) WIGAND, A. *Phys. Z.* **26**, 81 (1925).
- (8) STRANATHAN, J. D. *Phys. Rev.* **48**, 538 (1935).
- (9) DRAKE, F. H., PIERCE, G. W. and DOW, M. T. *Phys. Rev.* **35**, 613 (1930).
- (10) *The Observatories Year Book*. Air Ministry, Meteorological Office (1935).
- (11) Meteorological Office. *Professional Notes*, Nos. 6, 81 and 82.

## DISCUSSION

**Dr F. J. W. WHIPPLE.** The author has apparently found that ordinary clouds can reflect wireless waves. When it is recalled that clouds are very efficient reflectors of the very short aetherial waves which constitute light this is not very surprising. Perhaps it would be more remarkable if clouds did not interfere at all with the propagation of wireless waves.

**Dr R. L. SMITH-ROSE.** I gather that the object of the paper is to suggest that under certain conditions radio waves may be reflected in the troposphere at a surface of discontinuity between air and a cloud containing water in the liquid or solid form as well as vapour. If this interpretation is correct, the sentence immediately above the table on p. 134 is rather strange.

I should like to enquire what justification the author finds for assuming that the relations giving the dielectric constant of gaseous mixtures may be applied with equal validity to a non-molecular mixture of air and water in the liquid or solid form. This assumption is the basis of the equations at the foot of p. 133 and top of p. 134. In a cloud in which some 50 per cent of the water present may exist in liquid form, the actual volume of such liquid amounts to only 2 or 3 parts in a million of the total volume of the cloud, and the water will be in the form of discrete drops. Is it certain that in such a case the dielectric constant of the mixture of air and water can be derived in the same way as in the case of a mixture of gases by taking into account the partial pressures?

The figure for the value of ( $K - 1$ ) for water vapour on p. 133, line 7, appears to be incorrect. It should be  $0.62 \times 10^{-4}$  (i.e.  $12.7 \times 4.85 \times 10^{-6}$ ). Also the heading of the 4th column of the table on p. 134 is incorrect in that the figures tabulated refer to the value  $K - 1$  and not  $K$ . It would be as well to emphasize throughout the paper that since the values of reflection coefficient sought are very small, the corresponding values of  $K$  do not depart very much from unity, and this is the basis for assuming the equation  $\rho = (K - 1)/4$  to hold (see p. 133).

**Dr E. H. RAYNER.** The short-time variability of radiotransmission which has been mentioned may be associated with another type of variability which has been disclosed as a result of international radio research. On behalf of the Union Radio Scientifique Internationale I have organized special transmissions for the international comparison of standards of frequency and for physical research. One method has been to generate a frequency at Teddington which is constant to the order of 1 part in 100 million. By means of a multivibrator a wide selection of frequencies is available from any basic frequency and 1000 c./sec. is convenient to choose, as it is audible and suitable for telephonic transmission. This frequency is sent by wire to the British Broadcasting Corporation and used to modulate one or more transmitters simultaneously. On reception it is compared with the local standard by measurements of the beat frequency between them. In general the direct

measurement of two standard frequencies of 1000 c. sec. is not satisfactory since, if they are correct to about 1 in a million, which is common, the beat will be only once in a quarter of an hour; and transmission conditions may render its determination uncertain. A method of increasing the accuracy of comparison is to multiply the incoming frequency automatically by, say, 1000, raising it to the level of a million, and to obtain a frequency of a nominal value of a million from the local standard. A difference in the fundamental frequencies of 1 in a million will now produce 1 beat a second instead of one about every quarter of an hour and, if the beat frequency is steady, a comparison to a few parts in 100 million can be made in a few seconds.

It is found, however, that the beat frequency is generally unsteady under these conditions. Records of it have been made at the Laboratory of the Union Internationale de Radiodiffusion in Brussels with a siphon recorder registering the transmission from Droitwich. The effect is more marked at greater distances and with higher carrier frequencies. The beat frequency is irregularly fast and slow compared with the correct mean value, generally changing appreciably every second, and it has been found in Berlin, using the medium wave band (250 to 350 metres), that the wobble of the modulation frequency in about three seconds may have the same effect as a change of path of the order of 60 km.

These experiments, for traffic reasons, have had to be made in the early hours of the morning, and in order to determine whether the effect might be due to equipment, etc. it was repeated in daylight, when reception at Brussels showed that it had practically disappeared. There seems, therefore, to be a kind of fluttering of the transmission conditions at night, even over comparatively short distances and with long carrier waves.

At the Congress of the Union Radio Scientifique Internationale held in September, 1938, in Venice, a special Committee was set up at my suggestion to follow up the possibilities of research in this direction.

Mr R. NAISMITH. Several years ago it was shown\* that, near the Orfordness site, there were marked coastal deviation effects amounting to an error in bearing of as much as  $2.5^\circ$  on a wave-length of 1000 m. Now that the reflection coefficient is as low as 0.00003 it would seem quite possible to obtain energy corresponding to this value from various points along such a coast even when the antenna system is not favourable for this direction of transmission.

This suggestion would also explain the semi-permanent nature of the reflecting strata which has been observed.

AUTHOR'S REPLY. The author's reply will be published in a later part of the *Proceedings*.

\* R. L. Smith-Rose, *Radio Research Special Report No. 10* (H.M. Stationery Office).

# THEORETICAL IONIZATION CURVES FOR THE E REGION

BY M. V. WILKES, M.A.

The Mathematical Laboratory, Cambridge

*Communicated by Prof. E. V. Appleton, F.R.S., 10 August 1938.  
Read in title 11 November 1938*

*ABSTRACT.* This paper contains some ionization curves for the *E* region based on Chapman's theory of the solar ionization of a rotating atmosphere, and calculated mechanically by means of a Bush differential analyser. An attempt is made to reproduce the experimental results obtained by Best, Farmer and Ratcliffe in Cambridge, and it is found necessary to assume a greater rate of recombination during the day than during the night. This assumption is confirmed by some curves calculated for observations made at Washington on 31 August 1932, when an eclipse of the sun took place. The observational data have been published by Kirby, Gilliland and Judson.

## § 1. INTRODUCTION

In two well-known papers Chapman<sup>(1)</sup> has shown how to calculate the ionization in the ionosphere on the following assumptions: (1) that the atmosphere is spherical, (2) that the molecular density decreases exponentially with height (so as to be an isothermal homogeneous atmosphere), (3) that the incident radiation is absorbed according to a mass absorption law, (4) that electrons are lost by recombination, the recombination coefficient being constant. He has shown that the ionization-density at any instant and at any height is given by a certain differential equation containing an adjustable parameter  $\sigma_0$  depending on the recombination coefficient and on the intensity of the ionizing radiation.

Chapman has obtained some numerical solutions of this equation showing the variation of ionization-density at different levels in the atmosphere throughout the day at certain specified places and at various times of the year. In connexion with the interpretation of radio experiments it is usually more important to know how the maximum value of the ionization-density varies with time than to know the actual distribution with height. Millington<sup>(2)</sup> has given a method of obtaining the maximum value approximately without calculating the density at all levels, and has made a series of calculations by using this method. The numerical work involves a great deal of labour.

In connexion with the interpretation of the results of radio investigations of the ionosphere it is of importance to be able to calculate the ionization-distribution and the maximum ionization-density as a function of time, for various assumed values of the parameter  $\sigma_0$  in Chapman's equation. If several different values are

to be taken for comparison with experiments it is important to be able to perform the calculations rapidly.

This paper is an account of some calculations of this kind carried out mechanically by means of a Bush differential analyser. The curves shown here were calculated for conditions corresponding to some experiments which had been performed in Cambridge by Best, Farmer and Ratcliffe<sup>(4)</sup>, and in America by Kirby, Gilliland and Judson<sup>(5)</sup>. Different values of  $\sigma_0$  were taken in order to see which fitted best.

In addition to the curves necessary to determine the maximum value of the ionization, special attention has been paid to the ionization at low levels in the ionosphere, in view of the fact that this is important in connexion with the absorption of short waves and the reflection of very long ones.

## § 2. METHOD OF CALCULATION

The notation used is taken from Chapman's paper.  $H$  is the scale height of the atmosphere,  $h$  the height under consideration,  $I$  rate of production of electrons at height  $h$ , and  $N$  number of electrons per c.c. at height  $h$ ;  $I$  and  $N$  are functions of the height and the zenith angle of the sun. Further,  $h_0$  is the height at which  $I$  is maximum when the sun is overhead,  $I_0$  is the value of  $I$  at  $h_0$  when the sun is

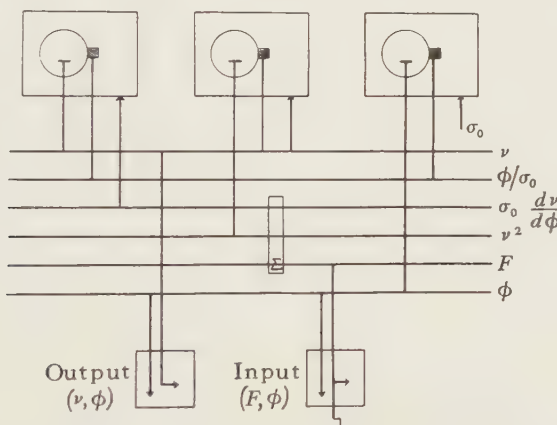


Figure 1. Set-up of the differential analyser for the equation

$$\sigma_0 \frac{dv}{d\phi} + v^2 = F(\phi, z).$$

overhead;  $N_0$  the equilibrium value of  $N$  at height  $h$  when the sun is overhead, and  $\alpha$  the recombination coefficient in seconds units.

Write

$$z = (h - h_0)/H,$$

$$v = N/N_0,$$

$$F = I/I_0,$$

$$\sigma_0 = 7.27 \times 10^{-5}/\alpha N_0,$$

and let  $\phi$  be the time in radians.

The differential equation for the number of electrons per cm<sup>3</sup> at a fixed point as a function of time, when recombination is allowed for, is then

$$\sigma_0 \frac{d\nu}{d\phi} + \nu^2 = F(\phi, z). \quad \dots\dots(1)$$

Chapman shows how to calculate the function  $F$  for an exponential atmosphere illuminated by homogeneous radiation; it is given by

$$F = \exp(1 - z - e^{-z}f),$$

where  $f$  is a function of the zenith angle,  $\chi$ , of the sun, and of  $H$ , and is tabulated by Chapman. Unless  $\chi$  is large it is very nearly equal to  $\sec \chi$ .

During the night  $F=0$ , and equation (1) has the solution

$$\frac{1}{\nu} = \frac{\phi}{\sigma_0} + \text{constant}.$$

The set-up of the differential analyser is shown in Bush's notation in figure 1. It will be seen that the function  $F$  is introduced from an input table, and that  $\nu^2$  is obtained by integrating  $\nu$  with respect to itself. The condition imposed on the solution of the equation is that the initial value of  $\nu$  shall be reproduced after 24 hr. The correct value is easily determined by trial and error.

In all of the present work a value of 10 km. has been taken for the height  $H$  of the homogeneous atmosphere in the  $E$  region. The actual height in kilometres above the datum level to which each of the following curves refers is therefore ten times the value of  $z$  corresponding to it. A curve for a given value of  $z$  would not be much altered if  $H$  were subjected to a small change, but it would then refer to a different height.

Two different values of  $\sigma_0$  have been taken, namely 0.098 and 0.032. If  $N_0$  is taken as  $1.9 \times 10^5$ , these imply that  $\alpha = 4 \times 10^{-9}$  and  $1.2 \times 10^{-8}$  respectively, in seconds units.

### § 3. DISCUSSION OF THE CURVES

Figures 2 and 3 give the detailed curves for Cambridge on 31 July and 21 December respectively; the value of  $\sigma_0$  is 0.098. Figures 4 and 5 are the corresponding curves for  $\sigma_0 = 0.032$ . Some supplementary curves for very low levels are given in figure 6.

As would be expected, the curves for the larger value of  $\sigma_0$  (smaller  $\alpha$ ) show more lag between the changes of ionization and the movement of the sun than do those for the smaller value. In each case, however, the lag is small where the layer is densest, but increases as we come down from this level. It will also be noticed from figure 6 that at very low levels the maximum ionization attained is less for the larger value of  $\sigma_0$  (smaller  $\alpha$ ) than for the smaller one. This means that a layer in which there is much lag has a sharper lower boundary than one in which there is less lag.

The data in figures 1 to 4 have already been discussed by Best, Farmer and Ratcliffe. In figures 8 and 11 of their paper they plot their experimental values for the maximum density of ionization present in the *E* region at various times of day,

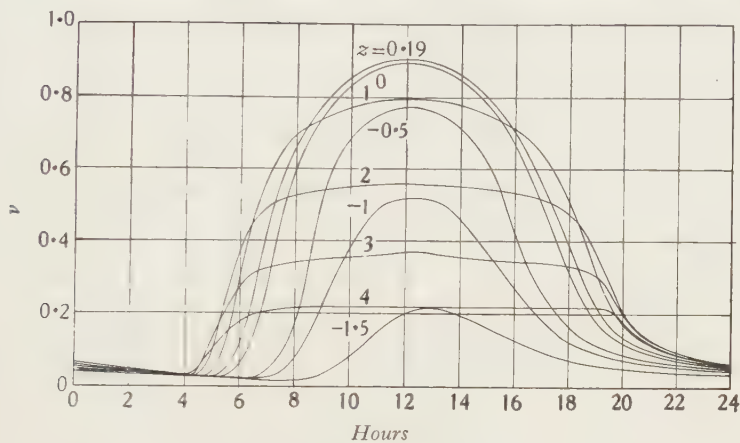


Figure 2. Cambridge, July 31;  $\sigma_0 = 0.098$ .

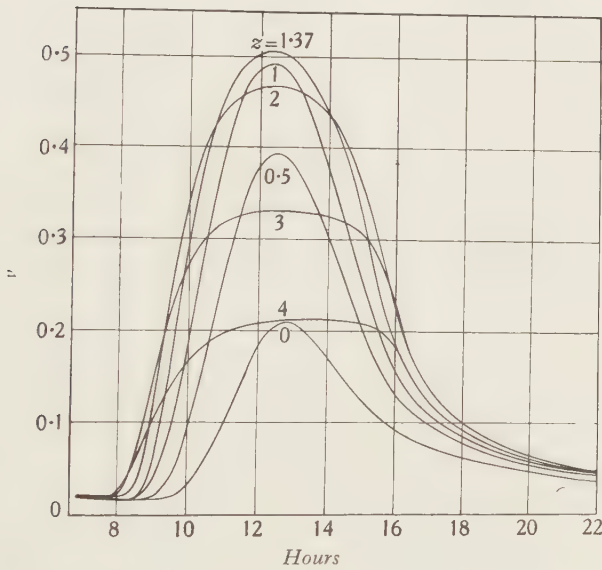
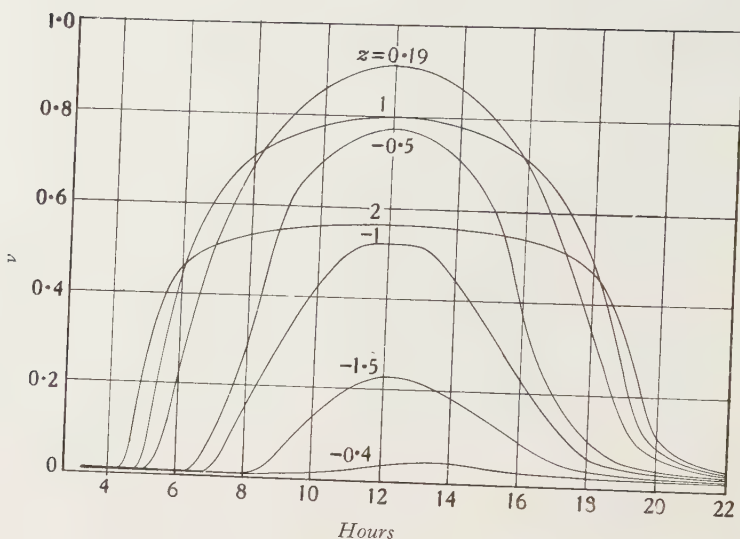
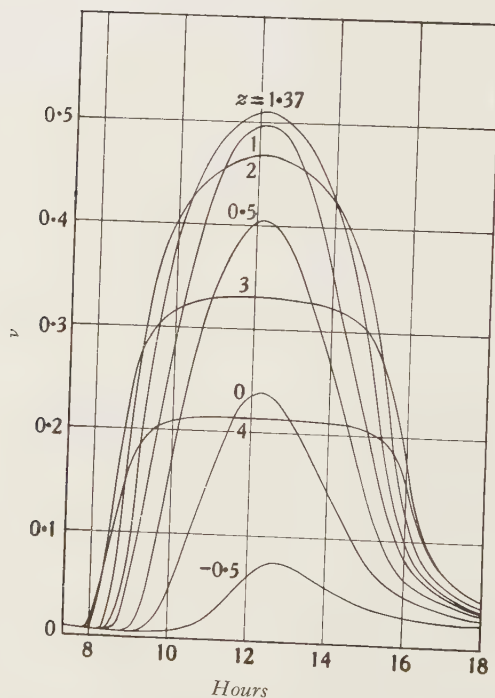


Figure 3. Cambridge, December 21;  $\sigma_0 = 0.098$ .

and also the theoretical curves for  $\sigma_0 = 0.098$  and for  $\sigma_0 = 0.032$ , obtained by taking the envelope of the curves in this paper. They point out that whereas the value  $\sigma_0 = 0.098$  is in agreement with the rate of decay of ionization during the night, both in summer and in winter, it gives too much lag in the daytime. The curves for  $\sigma_0 = 0.032$  are in better agreement with the daytime experimental results, but if anything still show too much lag.

Figure 4. Cambridge, July 31;  $\sigma_0 = 0.032$ .Figure 5. Cambridge, December 21;  $\sigma_0 = 0.032$ .

In support of this observation they refer to some measurements made by Kirby, Gilliland and Judson<sup>(5)</sup> in Washington during eclipses of the sun. To check the conclusion further some theoretical curves have been worked out for the latitude of Washington and the time of the year, 31 August (1932), at which one of the eclipses took place. Figures 7 and 8 give the curves for a day on which no eclipse takes place, and figures 9 and 10 for the eclipse day. Only the afternoon portion of the latter curve is shown, as the morning part is the same whether there is an eclipse or not. These curves were obtained by multiplying Chapman's rate of

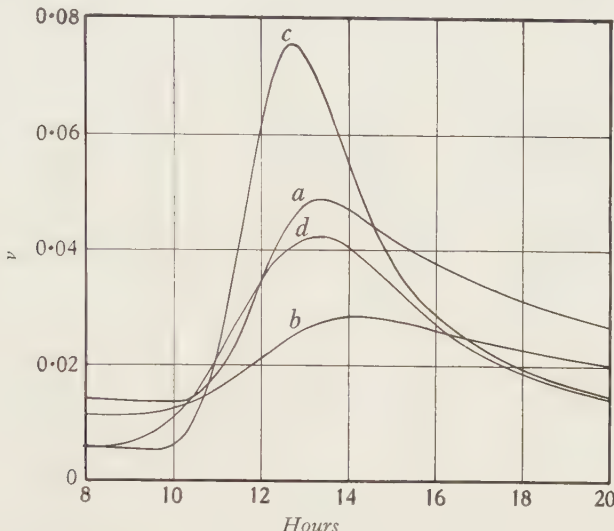


Figure 6. Cambridge; curves for very low levels. *a*, July 31,  $z = -2$ ,  $\sigma_0 = 0.098$ ; *b*, December 21,  $z = -1$ ,  $\sigma_0 = 0.098$ ; *c*, July 31,  $z = -2$ ,  $\sigma_0 = 0.032$ ; *d*, December 21,  $z = -1$ ,  $\sigma_0 = 0.032$ .

ionization  $F$  by a factor representing the fraction of the sun's disc exposed (given by Kirby, Gilliland and Judson in their paper) and solving the differential equation (1) with this as the input function.

By comparing the curves with and without the eclipse the ratio of the ionization during the eclipse to its value at the same time on a normal day can be found. This is plotted in figure 11 for the two values of  $\sigma_0$  concerned, and also for quasi-equilibrium conditions ( $\sigma_0 = 0$ ,  $\alpha$  very large). The experimental results also are included in the figure.

Here again the agreement of the experimental values is with the quasi-equilibrium curve, or with the curve for  $\sigma_0 = 0.032$ , rather than with the one for  $\sigma_0 = 0.098$ .

#### § 4. APPROXIMATING TO THE ENVELOPE

Mention has been made of Millington's method of approximating to the envelope of the  $\{\nu, \phi\}$  curves without drawing the individual curves. It consists in solving the differential equation

$$\sigma_0 \frac{d\nu}{d\phi} + \nu^2 = G(\phi),$$

where  $G(\phi)$  is the envelope of the set of  $F(\phi, z)$  curves. This method has been applied to all the cases given above, including the eclipse, the machine being used

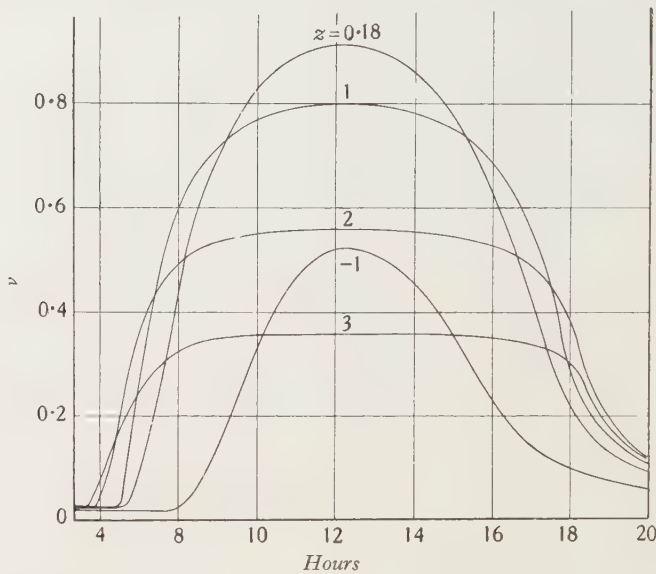


Figure 7. Washington, August 31;  $\sigma_0 = 0.098$ . The time is local time = E.S.T. + 8 min.

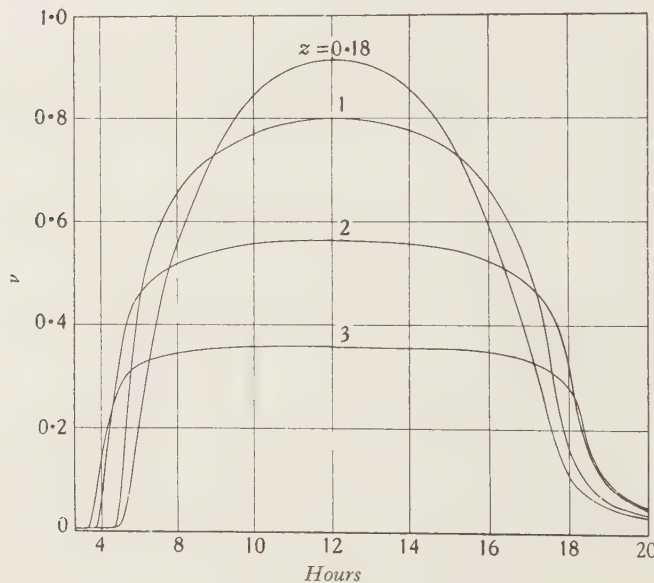


Figure 8. Washington, August 31;  $\sigma_0 = 0.032$ .

to solve the equation. On the straightforward diurnal curves for Cambridge or Washington it gives results agreeing very closely over the mid-day period, and showing a discrepancy amounting to not more than 2 per cent of the maximum

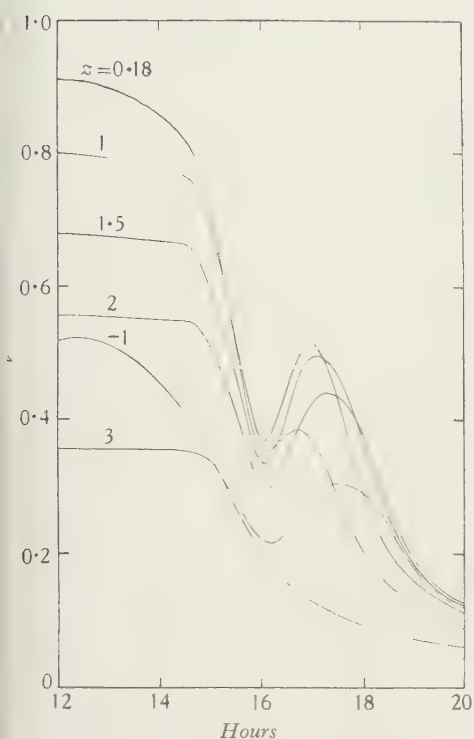


Figure 9. Washington, August 31, with eclipse.  
 $\sigma_0 = 0.098$ .

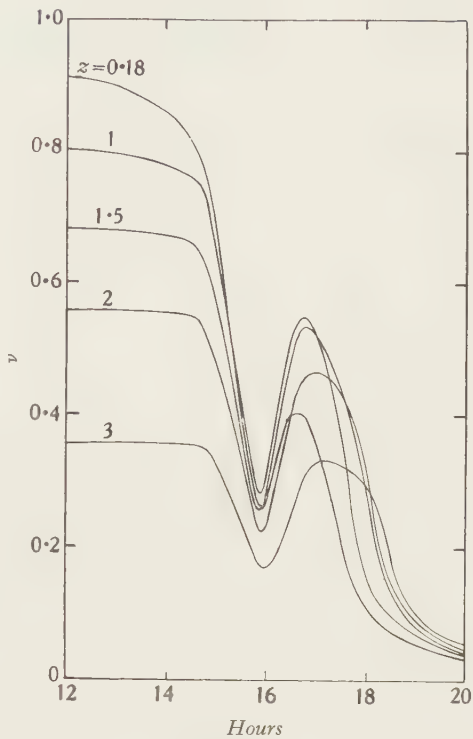


Figure 10. Washington, August 31, with  
 $\sigma_0 = 0.032$ .

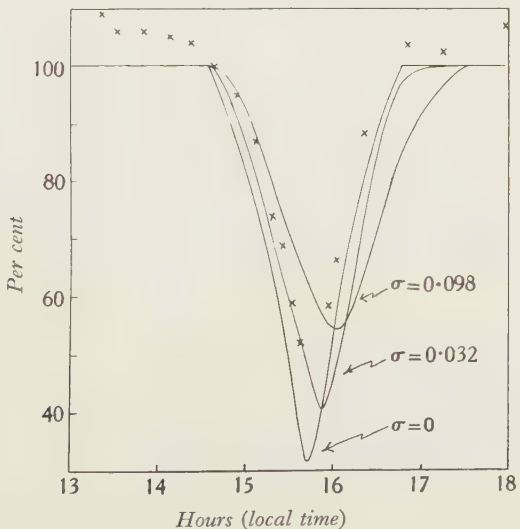


Figure 11. Percentage of ionization during the eclipse compared with its value on a normal day. The crosses are experimental points.

ionization at other times. The same accuracy is shown in the case of the eclipse curves. It would therefore appear that the method is quite reliable for these values of  $\sigma_0$ .

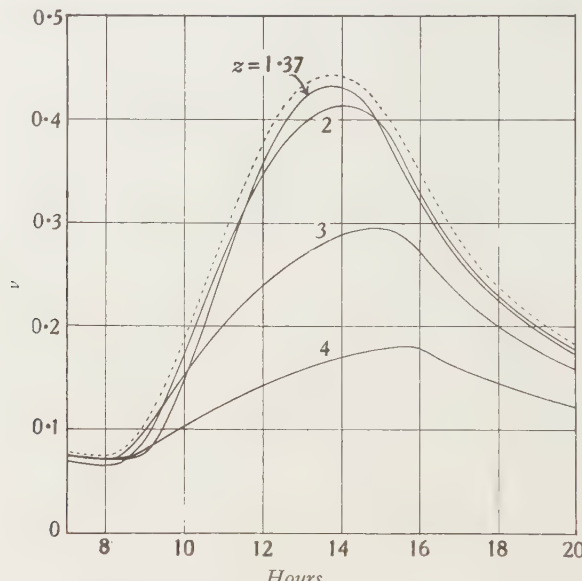


Figure 12. Cambridge, December 21;  $\sigma_0=0.4$ . The dotted curve is the approximate envelope obtained by Millington's method.

As a matter of interest, and to test the method in a more severe case, some curves have been worked out for  $\sigma_0=0.4$ . These are shown in figure 12, together with the approximate envelope. The error here is greater than before. It amounts to  $4\frac{1}{2}$  per cent in places, and affects also the mid-day period.

#### § 5. ACKNOWLEDGEMENTS

I would like to thank Mr J. A. Ratcliffe for suggesting the problem to me, and for his help given in many ways, and also Prof. J. E. Lennard-Jones, F.R.S., Director of the Mathematical Laboratory, Cambridge, in connexion with the use of the model differential analyser.

#### REFERENCES

- (1) CHAPMAN. *Proc. Phys. Soc.* **43**, 26, 483 (1931).
- (2) MILLINGTON. *Proc. Phys. Soc.* **44**, 580 (1932); **47**, 263 (1933).
- (3) BUSH. *J. Franklin Inst.* **212**, 447 (1931).
- (4) BEST, FARMER and RATCLIFFE. *Proc. Roy. Soc. A*, **164**, 96 (1938).
- (5) KIRBY, GILLILAND and JUDSON. *Proc. Inst. Radio Engrs, N. Y.*, **24**, 1027 (1936).

# THE VARIATION WITH TEMPERATURE OF THE ELECTRICAL RESISTANCE OF CARBON AND GRAPHITE BETWEEN $0^{\circ}$ C. AND $900^{\circ}$ C.

By L. J. COLLIER, D.F.C., M.A., W. S. STILES, PH.D.  
AND W. G. A. TAYLOR

Photometry Division of the National Physical Laboratory, Teddington, Middlesex

*Received 22 August 1938. Read in title 25 November 1938*

**ABSTRACT.** The variation with temperature of the electrical resistance of specimens of amorphous carbon and of Acheson graphite has been determined for temperatures between  $0^{\circ}$  c. and  $900^{\circ}$  c. The results obtained are compared with those recorded by other investigators. The work is to some extent complementary to that of Powell and Schofield, who determined the thermal and electrical conductivities of the same materials between  $750^{\circ}$  c. and  $2500^{\circ}$  c. Two samples of Acheson graphite showed minima of resistance at about  $390^{\circ}$  c. and  $430^{\circ}$  c. respectively.

## § 1. INTRODUCTION

THE work described in this paper formed part of a joint investigation carried out some years ago by the Physics and Electricity Departments of the National Physical Laboratory. The materials dealt with were the same as those examined by Powell and Schofield<sup>(1)</sup>, namely a particular kind of amorphous carbon (containing 80 per cent of petroleum coke and 20 per cent of lamp-black) and Acheson graphite. The investigation made by Powell and Schofield was directed mainly to the determination of the electrical and thermal conductivities of these materials at temperatures between about  $750^{\circ}$  c. and  $2500^{\circ}$  c. The work described here was concerned with the measurement of the electrical resistance of the same materials between  $0^{\circ}$  c. and about  $900^{\circ}$  c. and was thus complementary to their work.

## § 2. EXPERIMENTAL ARRANGEMENTS AND PROCEDURE

The materials, in the form of rods 57 cm. long and 1·6 cm. in diameter, were heated *in vacuo* in a nichrome-wound resistor-furnace sufficiently long to enclose the whole rod (figure 1). For the resistance-measurements a fixed current from a battery was passed through the rod and through a standard resistance of 0·0107  $\Omega$ . in series with the rod, and the potential-difference across the working section of the rod was compared with that across the standard resistance. The rod itself was

fitted into a cradle consisting of four steatite rings, large enough to slip over the rod and mounted symmetrically on two lengths of steel studding provided with nuts to secure the rings in position. Graphite end caps, screwed on to the ends of the rod, prevented any appreciable movement of the latter in the cradle and provided good electrical contact for the measuring-current leads. The measuring-current leads were attached to copper terminals screwed into the graphite caps. The whole framework afforded a secure support for the specimen, the thermocouples, and the potential leads. The steatite rings also served as radiation shields and helped to maintain a uniform temperature over the working section of the rod.

The temperature of the working section was determined with two chromel-alumel thermocouples, situated about 6 in. apart between the two inner steatite rings and previously calibrated in the Heat Division of the National Physical Laboratory. The thermocouples and potential leads, enclosed in silica tubing for insulation, were carried through holes in the rings. Owing to their tendency to break away during heating, the thermocouples could not be fixed into the rods;

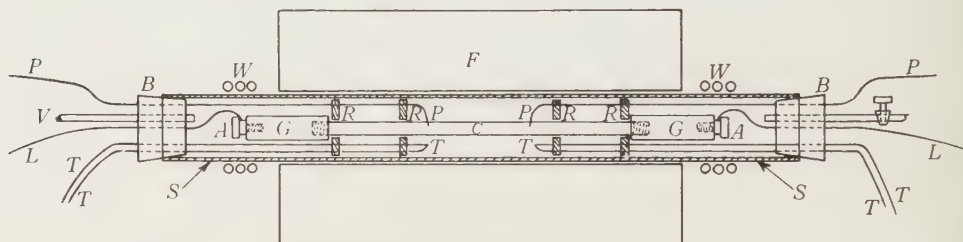


Figure 1. *A*, copper terminals; *B*, rubber bungs; *C*, carbon; *F*, furnace; *G*, graphite end caps; *L*, measuring-current leads; *P*, potential leads; *R*, steatite rings; *S*, silica tube; *T*, thermocouples; *V*, connexion to vacuum pump; *W*, water cooling.

they were therefore mounted just above the surface of the specimens. The potential leads were of nichrome wire tamped firmly with lamp black into holes, usually 6 in. apart (in one case 5 in.), drilled radially in the rod. The whole assemblage was enclosed in a silica tube, 1 metre long, which could be evacuated, the ends of the tube being closed with rubber bungs carefully sealed into it. The necessary leads were passed through the bungs, which were then coated with sealing-wax solution to prevent air leakage at the points of emergence of the leads. The silica tube was inserted in the furnace and, with the heating current switched on, was adjusted in position until the temperatures registered by the two thermocouples were practically the same. In this position the ends of the tube projected from the furnace, and were water-cooled to prevent melting of the seals. The pressure in the silica tube was measured with a McLeod gauge reading down to a pressure of 0.005 mm. of mercury.

After the rod had been adjusted in the cradle, its resistance was determined at room-temperature. The furnace current was then switched on and measurements were made at intervals corresponding to temperature increases of about 50°. In making an individual resistance measurement, the thermocouple readings were

first determined. Next the measuring current was adjusted to a fixed value, and the potential difference across the working section was measured. The measuring current was then reversed and the potential difference redetermined. By taking the mean, any thermal or stray electromotive forces were eliminated; generally the potential-differences before and after reversal agreed within one part in one thousand. The thermocouple readings were again taken and finally the potential-difference across the standard resistance was determined. The temperatures registered by the two thermocouples seldom differed by more than 1 per cent. In general the specimen was taken steadily up to as high a temperature as possible and then allowed to cool, measurements being made both during the heating and cooling processes. A complete run usually occupied about 24 hr. Except during the preliminary heating, when gas occluded in the carbon was given off, the pressure inside the silica tube rarely exceeded 0.1 mm. of mercury at temperatures up to about 750° C. Between this temperature and 900° C. it rose sharply in all runs to about 1.0 mm. It is possible that air diffused more readily through the silica at temperatures above 750° C. than at lower temperatures, and this may have accounted for the increase in pressure between 750° C. and 900° C.

### § 3. RESULTS

Five carbon rods were examined. With one exception two complete sets of observations were made on each rod; a complete set of observations involved resistance-measurements during both the heating and the cooling of the specimen. The {resistance, temperature} curves were practically identical in character for all

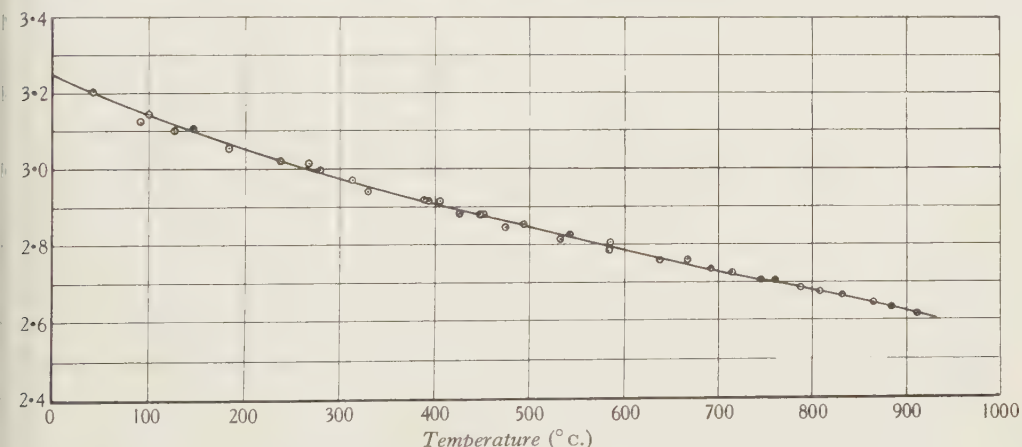


Figure 2. Variation with temperature of the resistance of a 5-inch section of a carbon rod.  
(Specimen 5.) ◎ experimental points.

the specimens; a typical example is shown in figure 2. In all cases the resistance at room-temperature (about 18° C.) was unaltered by heating up to 900° C.

The values of  $R_t/R_0$ , where  $R_t$  is the resistance at  $t^\circ$  C., were determined by interpolation from the individual {resistance, temperature} curves and are tabulated

in table 1; the value of  $R_0$ , the resistance at  $0^\circ\text{C}$ ., was easily determined by extrapolation. The maximum variation in the value of  $R_t/R_0$  at any given temperature was less than 1 per cent.

Table 1. Values of  $R_t/R_0$  for five carbon rods

Temp. ( $^\circ\text{C}$ )	Rod 1	Rod 2	Rod 3	Rod 4	Rod 5	Mean
0	1.000	1.000	1.000	1.000	1.000	1.000
60	0.982	0.980	0.982	0.980	0.980	0.981
120	0.964	0.963	0.966	0.964	0.962	0.964
180	0.949	0.948	0.950	0.949	0.944	0.948
240	0.934	0.932	0.934	0.934	0.930	0.933
300	0.919	0.919	0.918	0.918	0.916	0.918
360	0.905	0.906	0.904	0.909	0.904	0.906
420	0.889	0.891	0.890	0.897	0.892	0.892
480	0.881	0.882	0.878	0.886	0.880	0.881
540	0.870	0.871	0.868	0.874	0.868	0.870
600	0.860	0.860	0.857	0.864	0.858	0.860
660	0.850	0.851	0.848	0.854	0.847	0.850
720	0.842	0.840	0.838	0.844	0.838	0.840
780	0.832	0.831	0.827	0.834	0.830	0.831
840	0.820	0.821	0.818	0.824	0.820	0.821
900	0.806	0.810	0.807	0.814	0.808	0.809

A relation of the form

$$R_t = R_0 (1 - 3.17 \times 10^{-4} t + 1.73 \times 10^{-7} t^2 - 6.3 \times 10^{-11} t^3)$$

was found to represent the experimental results with considerable accuracy. The same relation also gave values of resistance in satisfactory agreement with those determined by Powell and Schofield<sup>(1)</sup> for similar carbons at temperatures between  $750^\circ\text{C}$ . and  $1300^\circ\text{C}$ . Powell and Schofield found that when the carbons were heated much above the latter temperature permanent changes occurred, affecting the shape of the {resistance, temperature} relation, the magnitude of the effect being dependent on the temperature to which the specimen was raised. For example, a carbon fired to  $1100^\circ\text{C}$ . had at  $1000^\circ\text{C}$ . a resistance 78 per cent of that at  $0^\circ\text{C}$ .; for a carbon fired to  $2430^\circ\text{C}$ . the corresponding value was 46 per cent. Hansen<sup>(2)</sup>, working with carbon electrodes made by the American National Carbon Company, observed that when the carbon was heated to temperatures above that at which it was fired during manufacture, the {resistance, temperature} relation altered. Decrease in the cold resistance and in the weight of the specimen also occurred, the amount of decrease in both cases being dependent on the temperature to which the carbon was heated.

The resistivities at  $0^\circ\text{C}$ . of the five carbons referred to in table 1 were 0.0051, 0.0050, 0.0055, 0.0051 and 0.0052  $\Omega\text{-cm}$ . respectively with a mean of 0.0052. These values were about 12 per cent lower than those found by Powell and Schofield for similar carbon in the form of tubes.

The variation of the resistance of carbon with temperature has also been studied by Somerville<sup>(3)</sup>, Noyes<sup>(4)</sup> and Hansen<sup>(2)</sup>. Somerville does not specify the nature of his carbon, but it would seem that it was of the extruded variety.

For comparison his values of  $R_t$ ,  $R_0$  at different temperatures are shown in figure 3. Up to about  $800^\circ\text{C}$ . they are practically identical with those obtained in the present investigation. The specimens examined by Noyes consisted of untreated carbon filament made from braided silk. Their resistances were measured over a temperature range of  $2200^\circ\text{K}$ . A direct comparison with his results can be made less readily, since Noyes recorded relatively few results between  $0^\circ\text{C}$ . and  $900^\circ\text{C}$ . and none at all between  $100^\circ\text{C}$ . and  $700^\circ\text{C}$ . The broken line shown in figure 3 was derived from the linear relation which he considered to represent his values

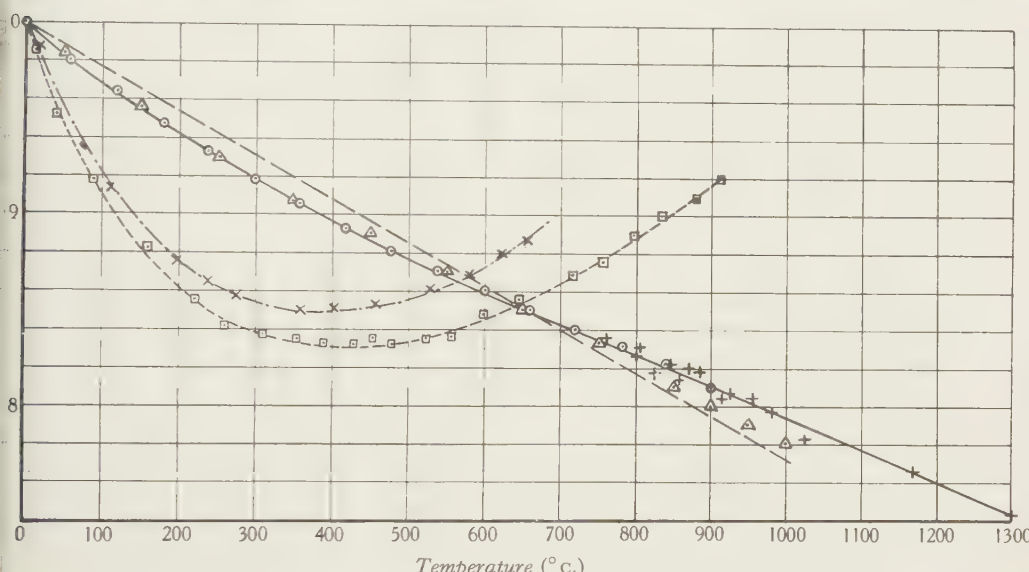


Figure 3. —, curve calculated from the relation

$$R_t = R_0 (1 - 3.17 \times 10^{-4}t + 1.73 \times 10^{-7}t^2 - 6.3 \times 10^{-11}t^3);$$

○, experimental values for carbon (see table 1); +, experimental values obtained by Powell and Schofield for similar carbon; △, values obtained by Somerville for carbon; ---, relation obtained by Noyes for carbon; □, Acheson graphite specimen 1 (*in vacuo*); ×, Acheson graphite specimen 2 (*in nitrogen*).

adequately over the whole experimental range. Between  $0^\circ\text{C}$ . and  $900^\circ\text{C}$ . this relation does not differ by more than 2 per cent from the values given in table 1; this is perhaps rather surprising in view of the fact that the carbons examined were not of the same type. Hansen, on the other hand, found that the resistance of the carbon electrodes examined by him decreased more rapidly with temperature. For example, at  $400^\circ\text{C}$ . the resistance was about 83 per cent of the value at  $0^\circ\text{C}$ ., while at  $900^\circ\text{C}$ . it had fallen to 63 per cent. The corresponding values for the carbons referred to in table 1 were 89.5 per cent and 81 per cent respectively. The resistivity of the latter was about one and a half times that of Hansen's carbon, whose resistivity was  $0.00348 \Omega\text{-cm}$ .

For purposes of comparison the effect of temperature on the resistance of Acheson graphite also was investigated. The results of measurements made on a

rod of this material *in vacuo* are shown in figure 3. Values obtained for another specimen heated in an atmosphere of nitrogen are also shown in that figure. Although for the first 200° the resistance of the graphite decreased with increase in temperature more rapidly than that of the carbon, it ultimately reached a minimum and then increased with further increase in temperature. The two specimens had resistivities at 0° C. of 0.00079 and 0.00088 Ω.-cm. respectively, approximately one-sixth of that of the carbon; and the minima occurred at about 390° C. and 430° C. At these temperatures their resistances had fallen to 84.6 per cent and 83.1 per cent respectively of the corresponding values at 0° C. Samples of Acheson graphite examined by Powell and Schofield<sup>(1)</sup>, with resistivities at 0° C. of 0.00082 and 0.001054 Ω.-cm. respectively, showed minima at 450° C. and 520° C.; at these temperatures their resistances decreased to 80.4 per cent and 74.6 per cent of the corresponding resistances at 0° C. Noyes<sup>(4)</sup> and Hansen<sup>(2)</sup> have also studied the behaviour of heated Acheson graphite. Noyes did not state the resistivity of his specimen, but found that the resistance was a minimum at 550° C., when its value was 77.5 per cent of that at 0° C. Hansen's graphite had a resistivity of about 0.001 Ω.-cm. at 25° C. The resistance appeared to be a minimum at about 1500° C., a much higher temperature than in the cases already mentioned; the minimum resistance was, however, only about 65 per cent of the value at 25° C.

The results suggest that the minimum resistance occurs at a lower temperature and is larger relative to the resistance at 0° C. in the case of the better-conducting varieties. Nishiyama<sup>(5)</sup>, who subjected carbon to very high temperatures, found that the temperatures at which the resistance became a minimum depended on the temperature to which the sample had been previously heated and on the duration of the heating process. His work suggested that the more complete the graphitization of the sample, the lower became its resistivity at 0° C. and the temperature at which the minimum occurred. The variation in the resistivities of the different samples of Acheson graphite mentioned above, and in the temperatures at which the minimum occurred, may be due to differences in the degree of graphitization.

#### REFERENCES

- (1) POWELL, R. W. and SCHOFIELD, F. H. P. 153 of this volume.
- (2) HANSEN, C. A. *Trans. Amer. Electrochem. Soc.* **16**, 335 (1909).
- (3) SOMERVILLE, A. A. *Phys. Rev.* **31**, 270 (1910).
- (4) NOYES, B. *Phys. Rev.* **24**, 195 (1924).
- (5) NISHIYAMA, Z. *Sci. Rep. Tōhoku Univ.* **21**, 171-92 (1932).

# THE THERMAL AND ELECTRICAL CONDUCTIVITIES OF CARBON AND GRAPHITE TO HIGH TEMPERATURES

By R. W. POWELL, B.Sc., Ph.D.

AND

F. H. SCHOFIELD, B.A., D.Sc.

Physics Department, National Physical Laboratory, Teddington, Middlesex

*Received 22 August 1938. Read in title 25 November 1938*

**ABSTRACT.** The thermal conductivity  $K$  is derived in terms of the difference in temperature which, in the steady state, is set up between the axis and the surface of a rod or tube of the material when the latter is electrically heated in an evacuated enclosure. The electrical conductivity  $\sigma$  is derived in the course of the same experiment from measurements of the current flowing in, and the potential-difference across, a length of the rod located near the centre. Solutions of the heat-flow equations are obtained for the case in which  $K$  and the electrical resistivity  $\rho$  are not constant but vary with temperature in a linear manner.

Experimental results are given for a variety of carbon consisting of 80 per cent of petroleum coke combined with 20 per cent of lampblack at temperatures up to about  $2000^{\circ}\text{C}$ . and for Acheson graphite up to about  $2700^{\circ}\text{C}$ . Evidence for the graphitization of carbon is obtained in that the results for this material at the highest temperatures tend to conform with those for graphite.

At normal temperatures the Lorenz functions,  $K\rho/T$  of carbon and graphite are respectively about 17 and 200 times as great as the value normally obtained for metals. The values, however, decrease rapidly with increase in temperature, and at  $1700^{\circ}\text{C}$ . the Lorenz functions of both materials are only about 4 times as great as those of metals.

---

## § 1. INTRODUCTION

THE main purpose of the present paper is to describe a method which has been employed at the National Physical Laboratory for the determination of the thermal conductivities of a number of varieties of carbon up to very high temperatures.

The only materials of general interest dealt with were graphite and a particular make of amorphous carbon, and these alone are discussed below. The investigation was primarily designed for very high temperatures (a limit of  $2700^{\circ}\text{C}$ . was reached) and the method of measuring thermal conductivity tended to decrease in accuracy towards the lower limit of temperature, namely  $750^{\circ}\text{C}$ . This latter consideration applied particularly to graphite, owing to its high conducting power, and as some theoretical interest attaches to this material it was thought worth while to continue the investigation of it, by a different method, down to atmospheric temperature.

The work just mentioned has now been completed by one of us (R. W. P.) and described in detail elsewhere<sup>(1)</sup>. The relevant data are incorporated in the present paper.

### § 2. THE THEORY OF THE METHOD

Of the methods available for the measurement of thermal conductivity, that suggested by Mendenhall for materials which are conductors of electricity, and applied by Angell<sup>(2)</sup> to aluminium and nickel, appeared to be the most promising for the present investigation. In this method a steady current of electricity is passed through a long cylindrical bar of the material. For an appreciable distance on each side of the centre section of such a bar, the temperature of the surface and of each of the underlying cylindrical shells will be sensibly uniform, so that the electrical energy dissipated in this portion will flow radially to the surface. The thermal conductivity can then be obtained from a measurement of the rate of energy-dissipation in the chosen portion of the bar and the difference in temperature between the axis and the surface. It will be observed that, provided the theoretical condition of cylindrical isothermals is fulfilled, the stray leakage of heat is eliminated, the only sink being that constituted by radiation from the surface. This freedom from leakage of stray heat, and independence of auxiliary heating systems, gives the present method considerable advantages for measurements at extremely high temperatures.

Consider a section of a bar of radius  $r$  and length  $x$ , in which, as was postulated above, the isothermal surfaces are cylindrical, and let its thermal conductivity and electrical resistivity be denoted by  $K$  and  $\rho$  respectively. Suppose further that a steady current of electricity is flowing through the bar and that the fall of potential is  $E$  volts per cm. of length. Then the equation which expresses the fact that the heat flowing radially out of a cylindrical surface within the bar is equal to the electrical energy dissipated inside this surface is as follows:

$$-2\pi rxK \frac{dT}{dr} = \int_0^r \frac{E^2 x 2\pi r dr}{\rho}, \quad \dots\dots(1)$$

where  $T$  is the temperature at any point within the bar. If  $K$  and  $\rho$  are constants this leads, as Angell shows, to

$$T_2 - T_1 = \frac{E^2 r_1^2}{4K\rho}, \quad \dots\dots(2)$$

where  $r_1$  is the radius of the bar and  $T_1$  and  $T_2$  the temperatures at the surface and axis of the bar respectively. In most practical cases  $K$  and  $\rho$  vary with temperature, and this disturbs the radial temperature-distribution given by equation (2). Using this equation, however, Angell obtained a second approximation and was able to show that in the cases with which he was concerned, namely bars of nickel and aluminium 1.2 cm. in diameter, the disturbance was negligible. The maximum temperature-difference between the surface and the axis of the bar in the cases dealt with by Angell appears to have been only of the order of 1° c. Since, however, in the experiments on carbons now to be described, temperature-differences as great as 300° c. are encountered, it is necessary to consider the matter in greater

detail. This can conveniently be done by assuming that both the thermal conductivity and the electrical resistivity vary with temperature in a linear way for the range of temperature between the surface and axis of the bar in any particular experiment. Thus

$$K = K_2 \{1 + \alpha(T - T_2)\} \quad \text{and} \quad \rho = \rho_2 \{1 + \beta(T - T_2)\}.$$

Substituting in equation (1) and solving in series\* form we obtain

$$T_2 - T_1 = Ar_1^2 \left\{ 1 + \left( \frac{2\alpha + \beta}{4} \right) Ar_1^2 + \left( \frac{18\alpha^2 + 11\alpha\beta + 5\beta^2}{36} \right) (Ar_1^2)^2 \right. \\ \left. + \left( \frac{360\alpha^3 + 266\alpha^2\beta + 145\alpha\beta^2 + 59\beta^3}{576} \right) (Ar_1^2)^3 + \dots \right\}, \dots \dots (3)$$

where

$$A = E^2 / 4K_2\rho_2.$$

This expression gives the temperature-distribution inside the rod in terms of  $K_2$  and  $\rho_2$ , which are the axial values of the thermal conductivity and electrical resistivity, and the temperature variation of these quantities.

For the purpose of an actual measurement of thermal conductivity it is convenient to express the temperature-difference between the axis and the surface in terms of the mean conductivity and resistivity. Thus if  $K_{am}$  and  $\rho_{am}$  are the arithmetic means of  $K$  and  $\rho$  for the axis and surface, it can be shown that the formula transforms to

$$T_2 - T_1 = Cr_1^2 \left[ 1 - \frac{\beta}{4} Cr_1^2 - \frac{\beta(5\alpha - \beta)}{72} (Cr_1^2)^2 - \frac{\beta(14\alpha^2 - 29\alpha\beta - 7\beta^2)}{576} (Cr_1^2)^3 \dots \right], \dots \dots (4)$$

where

$$C = E^2 / 4K_{am}\rho_{am}.$$

Since, as will be shown later,  $\rho_{am}$  is very nearly equal to the true mean resistivity, the formula can be expressed in terms of  $W$ , the watts-dissipation per unit length, by substituting  $W/4\pi K_{am}$  for  $Cr_1^2$ . It will be noted that the series on the right-hand side of equation (4) depends mainly on the value of  $\beta$ , the temperature variation of electrical resistivity, all the terms after the first vanishing when  $\beta$  is equal to zero.

The data set out in table 1 give an indication of the energy necessary to heat carbon rods of different diameters in vacuo to various external temperatures, and enables an idea to be obtained of the magnitude of the temperature-difference between the axis and the surface, and of the relative importance of the various terms of equation (4).

These calculations were originally made from the very meagre information available at the time as to the various constants, but in table 1 the data have been recalculated in the light of our own determinations. The values employed were  $K = 0.03$  w./cm.-°C.,  $\rho = 0.004$  Ω.-cm.,  $\alpha = 0.0008$ , and  $\beta = -0.0002$ . Since only the general order of the effects are now in question it suffices to treat  $\rho$  and  $K$  as constants (see columns 4 and 7), except when the convergence of the series is under examination (see the last 3 columns of table).

\* We are indebted to Dr W. S. Stiles of the National Physical Laboratory for advice in the solution of this equation.

Table I. Calculated data for carbon rods of various diameters

Diameter of rod (cm.)	Surface tem- perature (°K.)	Energy radiated (w./cm.)	Resistance (Ω./cm.) (ρ constant)	Current (amp.)	Potential- gradient (v./cm.)	Tempera- ture-differ- ence between axis and surface (°C.) (k constant)	Relative values of terms of equation (4) (per cent of first term)		
							2nd term	3rd term	4th term
0.5	1000	9	0.021	21	0.44	25	0.1	0.0	0.0
	1300	26		35	0.74	70	0.4	0.0	0.0
	1600	59		54	1.12	160	0.8	0.0	0.0
	2000	144		84	1.76	380	1.9	0.0	0.0
1.0	1000	18	0.0052	60	0.31	50	0.3	0.0	0.0
	1300	52		100	0.52	140	0.7	0.0	0.0
	1600	118		150	0.80	320	1.6	0.1	0.0
	2000	288		240	1.20	760	3.8	0.6	0.0
2.5	1000	45	0.0008	230	0.19	120	0.6	0.0	0.0
	1300	130		400	0.32	350	1.7	0.1	0.0
	1600	295		600	0.50	800	4.0	0.7	0.2
4.0	1000	72	0.0003	470	0.15	200	1.0	0.0	0.0
	1300	210		790	0.26	550	2.7	0.3	0.0
	1600	470		1200	0.37	1250	6.2	1.7	0.9

From consideration of these data and a knowledge of the energy-supplies available it was decided that for experiments up to about 1200° C. rods about 2.5 cm. in diameter should be used, and that proportionately smaller rods should be employed for higher temperatures. It is seen that for the 2.5-cm. rod the second term of equation (4) only amounts to 1.7 per cent of the first for the external temperature of 1027° C., and in all cases it appears that the subsequent terms can be neglected.

In practice it was thought desirable to use a specimen in the form of a thick-walled tube, as this enabled the inner temperature to be observed by sighting into the small axial hole.

The full solution corresponding to equations (3) and (4), that is, taking into account the temperature variation of both  $K$  and  $\rho$ , has not been found for this case. Apparently a series cannot be obtained in terms of  $r$ , nor a convergent expansion in terms of  $(r_1 - r_2)/r_2$  unless the internal radius  $r_2$  is greater than half of the external radius  $r_1$ . However, assuming a temperature variation of thermal conductivity but a constant electrical resistivity, the following expressions are found.

For the overall temperature-difference in terms of  $K_{am}$

$$T_2 - T_1 = \frac{E^2}{4K_{am}\rho} \left\{ r_1^2 - r_2^2 \left( 1 + 2 \log \frac{r_1}{r_2} \right) \right\}, \quad \dots \dots (5)$$

and for the temperature-distribution over the cross-section in terms of  $K_2$

$$T_2 - T = B \left\{ 1 + \frac{\alpha}{2} B + \frac{\alpha^2}{2} B^2 + \frac{5\alpha^3}{8} B^3 + \dots \right\}, \quad \dots \dots (6)$$

where

$$B = \frac{E_2}{4K_2\rho} \left\{ r^2 - r_2^2 \left( 1 + 2 \log \frac{r}{r_2} \right) \right\}.$$

The effect on the value of  $(T_2 - T_1)$  of the temperature-variation of resistivity in the case of a solid rod has been shown to be equivalent to a correction of 1·7 per cent for the case mentioned above. It is obvious that the effect would be of similar magnitude for the case of the thick-walled tube actually used. Subject to this small correction, formula (5) has been adopted for evaluating  $K_{am}$  for specimens in tubular form.

In the preceding account, attention has been devoted mainly to a method for the determination of thermal conductivity. In all investigations of thermal conductivity it is of interest to make simultaneous measurements of the electrical conductivity. For many good conducting metals the ratio of the two conductivities has been found to be so closely proportional to the absolute temperature as to enable the thermal conductivity to be predicted from a measurement of the electrical resistivity. Although it was not anticipated that a simple relation of this kind would be found for the class of materials to be included in the present investigation, it was at the outset considered that the inclusion of measurements of the electrical resistivity would probably yield results of theoretical interest, which would subsequently become of practical importance should they eventually enable approximate values of the thermal conductivity of carbon materials to be deduced from the simpler measurement of electrical resistivity.

A further advantage of the present method is that the electrical resistance of the working portion of the specimen is measured incidentally to the determination of the energy-dissipation. It should be borne in mind, however, when a comparison is attempted, that whereas the thermal conductivity is measured radially the electrical conductivity is measured longitudinally, and that the two conductivities would not be equally affected if local variations, such as transverse cracks, should occur in the material.

Since the measurement is of the total resistance of a section of a specimen in which a heavy radial gradient exists, it becomes necessary to determine to what temperature this resistivity is to be assigned. If  $\rho_m$  is the mean resistivity as found in any experiment, then in the case of a solid rod we have

$$\frac{\pi r^2}{\rho_m} = \int_0^{r_1} \frac{2\pi r}{\rho_2 \{1 + \beta(T - T_2)\}} dr. \quad \dots\dots(7)$$

If the temperature-distribution is assumed to be given by equation (3), this can be shown to reduce to

$$\rho_m = \rho_2 \left\{ 1 + \beta \frac{Ar_1^2}{2} \left[ 1 + \frac{\alpha + \beta}{3} (Ar_1^2) + \frac{18\alpha^2 + 23\alpha\beta + 17\beta^2}{72} (Ar_1^2)^2 + \dots \right] \right\}. \quad \dots\dots(8)$$

Now the temperature  $T_m$  to which  $\rho_m$  is to be assigned is given by

$$\rho_m = \rho_2 \{1 + \beta(T_m - T_2)\}. \quad \dots\dots(9)$$

Hence

$$(T_m - T_2) = - \frac{Ar_1^2}{2} \left\{ 1 + \frac{\alpha + \beta}{3} (Ar_1^2) + \frac{18\alpha^2 + 23\alpha\beta + 17\beta^2}{72} (Ar_1^2)^2 + \dots \right\}. \quad \dots\dots(10)$$

The temperature  $T_m$  does not differ greatly from the mean of the axial and surface temperatures  $(T_1 + T_2)/2$ , which is given by

$$\frac{T_1 + T_2}{2} - T_2 = -\frac{Ar_1^2}{2} \left\{ 1 + \frac{2\alpha + \beta}{4} (Ar_1^2) + \frac{18\alpha^2 + 11\alpha\beta + 5\beta^2}{36} (Ar_1^2)^2 + \dots \right\}. \dots\dots\dots (11)$$

Therefore

$$\begin{aligned} T_m - \frac{T_1 + T_2}{2} &= \frac{Ar_1^2}{2} \left\{ \frac{2\alpha - \beta}{12} (Ar_1^2) + \frac{18\alpha^2 - \alpha\beta - 7\beta^2}{72} (Ar_1^2)^2 + \dots \right\} \\ &= (T_2 - T_1)^2 \left\{ \frac{2\alpha - \beta}{24} + \frac{6\alpha^2 - \alpha\beta - 4\beta^2}{144} (T_2 - T_1) \right\} \\ &= \frac{2\alpha - \beta}{24} (T_2 - T_1)^2 \text{ approx.} \end{aligned} \dots\dots\dots (12)$$

Hence  $T_m$ , the resistance temperature, is obtained from the mean of the axial and surface temperatures by applying a correction proportional to the square of the difference between these temperatures. For a temperature-difference of  $300^\circ \text{C}$ . and on the basis of the values of  $\alpha$  and  $\beta$  given earlier the correction amounts to  $7^\circ \text{C}$ .

The equation (12) applies only to the case of a solid rod and the corresponding formula has not been obtained for the case of the thick-walled tube used in some of our experiments. However, equation (6) gives the temperature-distribution in this latter case as affected by the  $\alpha$  coefficient, which is the more important in determining the magnitude of the correction, and using this equation for a step by step integration, it would appear that the corrections for carbon range from about  $3^\circ \text{C}$ . for a temperature-difference of  $100^\circ \text{C}$ . to  $18^\circ \text{C}$ . for a temperature-difference of  $300^\circ \text{C}$ .

### § 3. APPARATUS AND EXPERIMENTAL PROCEDURE

Preliminary observations had shown that for a rod  $2.54 \text{ cm}$ . in diameter a length of  $75 \text{ cm}$ . gave a central portion well over  $20 \text{ cm}$ . in length which was uniform in temperature. For the initial experiments a tube of this size having an axial hole about  $0.3 \text{ cm}$ . in diameter was chosen.

In figure 1 the tube is shown supported along the axis of a cylindrical water-cooled enclosure capable of being evacuated. The water flows through the space formed by two concentric tubes of brass, soldered to brass end pieces, and fitted with brass frames to hold two glass windows  $20 \text{ cm}$ . long and  $1.8 \text{ cm}$ . wide. These were situated on opposite sides of the enclosure and allowed a full view of both sides of the specimen to be obtained and enabled the surface temperature of the central section of the rod to be measured by means of an optical pyrometer sighted normally through the window. The left-hand end of the apparatus was closed by means of a brass plate fitted at the centre with a water-cooled glass window. Through this window it was possible to sight along the axis of the specimen, and to observe the internal temperature by means of an optical pyrometer focused on to a small piece of refractory material located at the centre of the specimen.

The brass plate which fitted the other end of the apparatus carried the two electrodes. This arrangement permitted the assembly of the specimen, and any auxiliary gear, to be completed before insertion into the cylindrical container. The details of this part of the apparatus are shown in figure 2. Each electrode consisted of an unbroken run of copper pipe, with a go and return passing through the end plate to allow a water circulation. The copper pipe was bent to the shape indicated, with a vertical loop, at the extremity farthest removed from the end plate. To the top of this loop was sweated a brass plate, while lower down on each

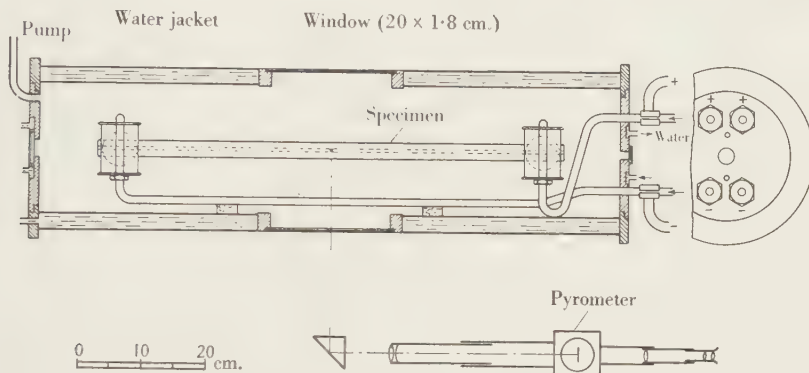


Figure 1. General lay-out of apparatus.

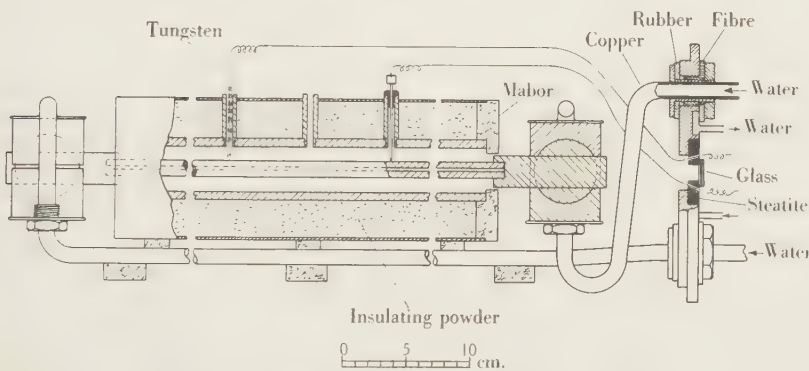


Figure 2. Details of apparatus attached to end plate.

branch of the loop a thread was soldered carrying a nut so as to give a vertical adjustment for a second brass plate sliding on the loop. Between these brass plates were held two blocks of graphite internally capped so as to grip a true sphere, also of graphite. The sphere was drilled with a hole 2·54 cm. in diameter, for the insertion of the full-sized specimen, or of an adapter of the same diameter for use, as described later, with a smaller specimen. The sphere was split into three portions, to give an adjustable grip on the specimen. This use of a cup-and-ball construction gave two self-aligning bearings for the specimen, and on tightening up the bottom nuts the electrode assembly could be rigidly clamped without strain on the specimen, at the same time giving an excellent contact for the heavy current required, which

ranged up to some 800 amperes. Each copper pipe was insulated from the end plate by fibre bushes, the joints being made vacuum-tight by pulling down on to rubber washers as shown. The adapters referred to above consisted of graphite rods 2·54 cm. in diameter, drilled at one end to allow the insertion of smaller specimens, figure 2. Thus the size of the specimen, both as to diameter and length, could be chosen so as to fit in with the temperatures it was desired to reach and the particular pressures of electric power available. The limit of power, namely 12 kva., was not sufficient to allow of the attainment of high temperatures with the larger-sized specimens when these were allowed to radiate freely to the water-cooled enclosure, and with a view to extending the temperature range for such specimens a radiation shield could be interposed between the specimen and enclosure. This shield, a section of which is shown in figure 2, consisted of a tube of carbon let into end pieces of mabor and thermally insulated with soot, the whole being contained in an outer brass cylinder. The shield was pierced with holes which could be used

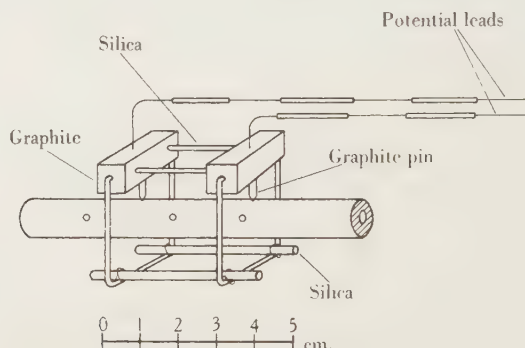


Figure 3. Device for measuring potential-drop on specimen.

for sighting on to the specimen or for carrying potential leads required for the energy measurements.

Several forms of potential contact were used, two of which are shown in figure 2. That on the right of the figure consists of a graphite rod passing through a closely fitting bush in the radiation shield and resting with its sharply pointed end on the surface of the specimen. On the left is shown a tungsten wire 0·015 cm. in diameter, insulated with fireclay or thoria tubing and inserted into a small hole in the specimen so as to serve as a potential contact. For the lower temperatures the wire was usually cemented into the hole with a mixture of pitch and carbon, while for higher temperatures contact was made in various ways, for example, by tying the wire after passing it through a small hole skimming the surface, or by hanging the wire over the specimen. When graphite rods were used as potential leads without the radiation shields, they were held in the rider arrangement shown separately in figure 3. This method was found to be the most satisfactory and with it readings were obtained up to 2700° C.

For the energy-supply alternating current was used, the skin-effect being negligible for the frequency of 50 cycles employed. Several methods were used for the

measurement of the energy supplied to the working section. For example, the watts could be read directly from a Drysdale-Tinsley astatic wattmeter, in which the main current was passed through the heavy stationary coil, and the suspended pressure coil was connected to the potential leads from the specimen. The total resistance of the leads, including contact resistance at the surface of the specimen, was about  $10\ \Omega$ . The resistance of the pressure-coil circuit of the wattmeter was varied from 100 to  $300\ \Omega$ , and a small proportionate correction for the lead resistance applied to the readings.

The energy was also determined by an independent measurement of the current through and resistance of the working portion of the specimen. For the former measurement a Weston precision ammeter of the dynamometer type was used. The resistance was measured immediately after the a.-c. supply had been switched off by comparing the potential-drop across the working section with that across a standard resistance when the same direct current passed through each. The e.m.fs. were measured on a potentiometer and by using a Moll galvanometer of very short period and by switching the direct current over from a steady circuit of similar resistance, it was found that the voltage drop on the working section could, after several trials, be obtained within about 2 sec. after switching off. The process was repeated with the current reversed so as to enable stray e.m.fs. to be eliminated.

To provide a further check on the energy-measurements the voltage drop on the working section was determined by a low-range Weston a.-c. voltmeter. As the resistance of the potential leads was of the same order as that of the instrument, a somewhat large correction had to be applied which, however, could be checked by a comparison of the values obtained on the two scales of the instrument.

The energy-measurements given by the three methods outlined above seldom differed by more than 1 per cent and pointed to a power factor for the circuit of nearly unity.

In addition to the measurement of energy, the dimensions of the specimen and also the difference in temperature between its axis and surface had to be determined. The former presented no special difficulties, but in the case of the latter, precautions had to be observed. Both surface and axial temperatures were measured by means of a disappearing-filament optical pyrometer, which had been calibrated by sighting through a specimen of the window glass on to a black-body furnace. Calibrations were also obtained with a totally reflecting prism included in the system, as this was frequently used to avoid overmuch shifting of the pyrometer itself.

It was necessary to verify that the optical pyrometer focused on to the plug at the centre of the axial hole in the specimen gave the true value for the internal temperature. Satisfactory agreement was obtained when a thermocouple was also used to measure this temperature, a result which was to be expected, as the internal conditions approximated closely to those of a black body. In the case of the external temperature it was not practicable to use thermocouples, and with the optical pyrometer allowance had to be made for the emission coefficient of the specimen.

The conditions of the experiment allowed an estimate of the emission coefficient to be formed, owing to the fact that the apparent black-body temperature of a surface, of emissivity less than 1, differs according as the temperature is estimated on the basis of monochromatic or of total radiation. The difference in the value of the apparent temperature obtained by the two methods is illustrated in table 2, which gives the figures for emissivities from 0.8 to 1.0.

Table 2

Tem- pera- ture (°c.)	Method of obtaining tem- perature, $M$ , monochromatic radiation for $0.65\mu$ ; $R$ , total radiation	Difference between apparent black-body and true temperatures for emis- sivities of			
		1.0	0.90	0.85	0.80
700	$R$	0	25	36	49
	$M$	0	5	7	10
	$R - M$	0	20	29	39
1000	$R$	0	31	48	63
	$M$	0	8	12	17
	$R - M$	0	23	36	46

In the case of our experiments the apparent temperature of the outer surface of the specimen for monochromatic radiation was given by the optical pyrometer, which worked on an effective wave-length of  $0.65\mu$ , while the apparent temperature for total radiation was calculated from a knowledge of the area of the working section and the energy radiated from it. The last-mentioned quantity was obtained by deducting from the total energy dissipated, as given by the electrical measurements, the small loss due to convection in the rarefied gases in the enclosure, which can be shown to be about 1 per cent of the total. The mean of a large number of experiments on carbon between temperatures of  $700^\circ$  and  $1000^\circ$  c. gave a difference between the monochromatic and total radiation temperatures of  $30^\circ$  c. It will be observed from table 2 that the mean difference over this range is  $33^\circ$  c. for an emissivity of 0.85 and  $22^\circ$  c. for an emissivity of 0.90, so that apparently the emissivity of the carbon tube falls within these limits.

It is of course recognized that this conclusion is based on the assumption of a constant emissivity for carbon throughout its spectrum. However, the estimate is not inconsistent with the value obtained by Mendenhall and Forsythe<sup>(3)</sup>, who by a different method found an emissivity of 0.86 for carbon at  $1000^\circ$  c.

The corrections to the pyrometer readings required for an emissivity of 0.86 are  $+7^\circ$  c. at  $700^\circ$  c. and  $+11^\circ$  c. at  $1000^\circ$  c. For carbon these corrections amount to about 6 per cent of the difference between the internal and external temperatures, and hence affect the values of the thermal conductivity to a like amount.

#### § 4. RESULTS

The experimental results which it is proposed to consider are those obtained for a typical variety of carbon and for some specimens of Acheson graphite. The carbon specimens were stated to consist of 80 per cent of petroleum coke combined

with 20 per cent of lampblack, a baking temperature of the order of  $1100^{\circ}\text{C}$ . having been employed in their manufacture.

*Thermal conductivity of carbon.* Figure 4 contains the results for a number of determinations of the thermal conductivity which were carried out by means of the method previously described at mean temperatures ranging from  $750^{\circ}$  to  $1200^{\circ}\text{C}$ ., on three specimens of carbon having external and internal diameters of approximately 2.6 and 0.5 cm. respectively. A straight line has been drawn through these points which indicates that the thermal conductivity of the carbon increases from 0.00575 cal./cm.-sec. $^{\circ}\text{C}$ ., at  $750^{\circ}\text{C}$ . to a value of 0.0080 at  $1200^{\circ}\text{C}$ . This line has been reproduced in figure 5, where results covering a much wider temperature range are given, and in which data obtained for carbon by other investigators are included.

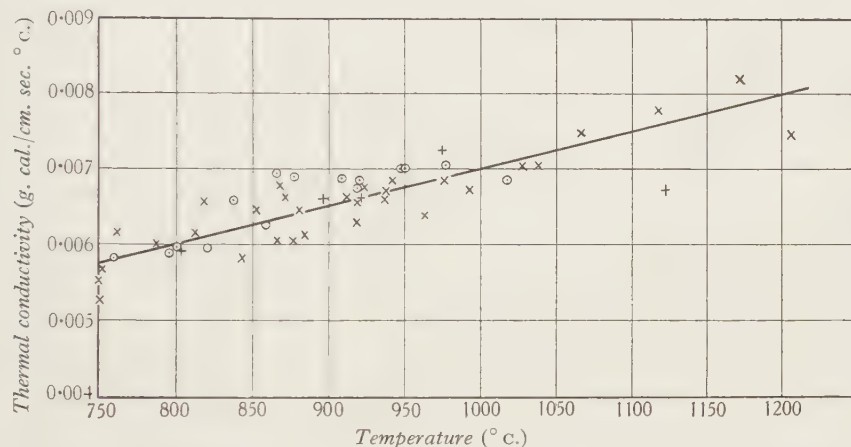


Figure 4. Variation of thermal conductivity of carbon with temperature over range  $750$  to  $1200^{\circ}\text{C}$ .  
x Specimen no. 1. o Specimen no. 2. + Specimen no. 3.

The experimental results at higher temperatures were obtained for two tubes having an external diameter of only 0.985 cm. and an axial hole 0.46 cm. in diameter. These smaller tubes were composed of the same type of carbon as the larger ones previously used. It will be seen from the data given later in table 3 that the room-temperature electrical resistivities of these carbons did not differ greatly from that of the larger specimens. In figure 5 the results for the smaller tubes have been numbered to show the sequence in which they were observed. The {thermal-conductivity, temperature} curve from  $1200^{\circ}\text{C}$ . upwards appears to be a reasonably good extension of the line found for the lower temperature range, but shows a marked curvature in the direction of increasing conductivity at the higher temperatures. After heating to temperatures above about  $1500^{\circ}\text{C}$ ., points obtained on cooling lie above the initial curve. The amount by which the thermal conductivity has been increased is seen to be greater the higher the temperature to which the carbon has been heated.

It should be remarked that the measurement of thermal conductivity at the highest temperatures was accompanied by experimental difficulties. For an

accurate determination it is necessary to ensure that the steady state of temperature has been reached, and then to measure the difference between the internal and external temperatures. The point numbered 9, for instance, was obtained under conditions which were considerably removed from this. Apart from the changes occurring in the material as a result of its being heated to the high temperature, the pressure in the enclosure no longer appeared to be sufficient to prevent a certain amount of burning, and the appearance of the surface was continually changing. This rendered the actual measurement of the surface temperature difficult, and made the magnitude of the emissivity correction uncertain. However, the temperature-difference amounted in this instance to some  $140^{\circ}\text{C}$ ., so even for these poor conditions the probable error is not likely to exceed 20 per cent. The thermal-conductivity curve obtained after heating the carbon to about  $2000^{\circ}\text{C}$ . is seen to be in

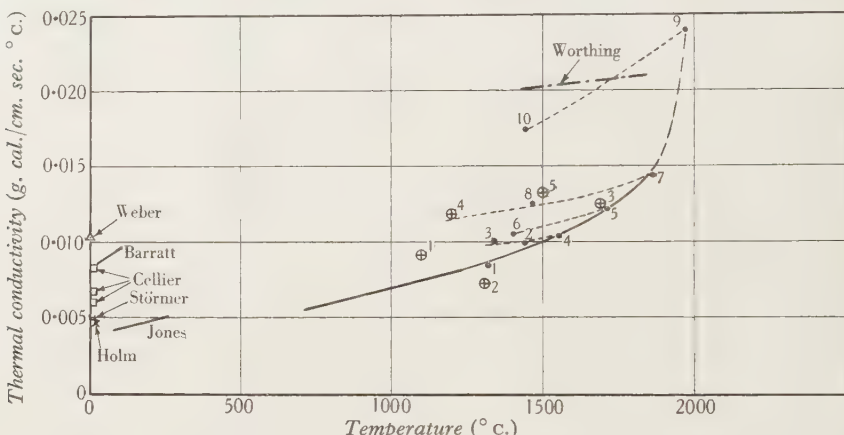


Figure 5. Variation of thermal conductivity of carbon with temperature over range 0 to  $2000^{\circ}\text{C}$ .  
 ⊕ Specimen no. 4. ● Specimen no. 5.

approximate agreement with that obtained by Worthing<sup>(4)</sup> for a carbon filament. Several low-temperature determinations which have been made for carbon are also given in figure 5. These include determinations by Weber<sup>(5)</sup>, Barratt<sup>(6)</sup>, Störmer<sup>(7)</sup> and Holm<sup>(8)</sup> for various gas carbons and by Cellier<sup>(9)</sup> for arc carbons, and the results of some measurements carried out at the National Physical Laboratory by D. E. A. Jones on a specimen taken from another batch of 80/20 carbon, which at  $20^{\circ}\text{C}$ . had a specific resistance of 0.0066  $\Omega\text{-cm}$ . The results of the present investigation have shown that the firing temperature has a large effect on the conductivity, and this, as well as other factors, such as possible differences in the raw materials and methods of manufacture, probably accounts for the variations. It is noteworthy that a positive coefficient of conductivity with rising temperature is shown in all cases.

*Electrical resistivity of carbon.* The results of some of the electrical resistance measurements, which were made in the course of the same experiments, are plotted in figure 6. Data for five different specimens are reproduced, and in order that the general character of the effect of temperature on the resistance may be more clearly seen, the results for the different specimens have in each case been

adjusted to correspond to an initial resistivity of  $0.0056 \Omega\text{-cm}$ . The actual initial and final resistivities obtained for the various specimens are set out in table 3, and the initial resistivities are seen to be sufficiently alike to justify this procedure.

Table 3. Specific resistances of carbon specimens before and after heating

Details of the specimens			Maximum temperatures reached ( $^{\circ}\text{C}$ .)		Specific resistance at $0^{\circ}\text{C}$ . ( $\Omega\text{-cm}$ .)	
No.	Diameters (cm.)		Internal	External	Before heating	After heating
	Internal	External				
1	0.52	2.62	1356	1059	0.00572	0.00630
2	0.50	2.61	1124	912	0.00560	0.00638
3	0.52	2.61 <sub>6</sub>	1251	995	0.00556	0.00552
4	0.46	0.98 <sub>5</sub>	1780	1603	0.00564	0.00580
5	0.46	0.98 <sub>4</sub>	—	2000	0.00566	0.00598
6	0.44 <sub>5</sub>	0.98 <sub>4</sub>	2240	2000	0.00591	0.00641
7	0.24 <sub>1</sub>	0.50 <sub>5</sub>	2500*	2360	0.00624	0.00591

\* By approximative calculation.

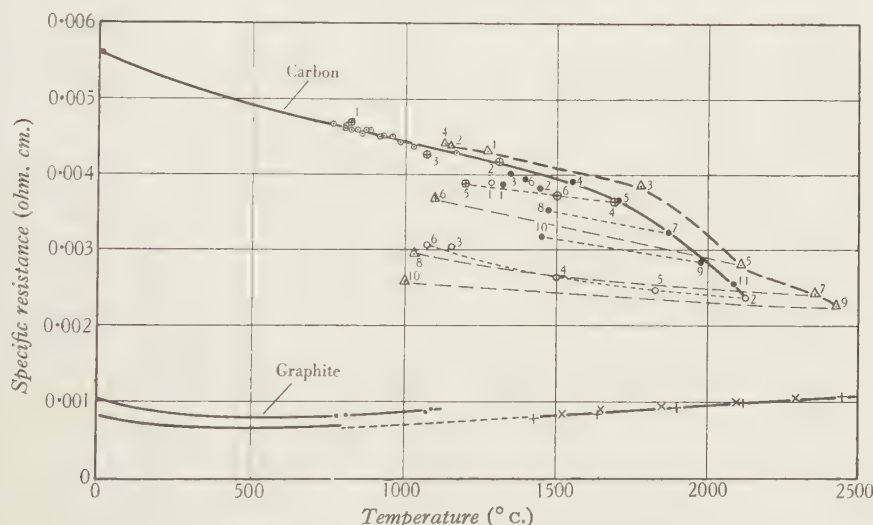


Figure 6. Variation of electrical resistivity of carbon to  $2100^{\circ}\text{C}$ . and of graphite to  $2450^{\circ}\text{C}$ . Carbons:  $\odot$  Specimen no. 2.  $\oplus$  Specimen no. 4.  $\bullet$  Specimen no. 5.  $\circ$  Specimen no. 6.  $\triangle$  Specimen no. 7. Graphites:  $\cdot$  Specimen no. 2.  $+$  Specimen no. 3.  $\times$  Specimen no. 4.

Over the temperature range  $750$ - $1200^{\circ}\text{C}$ . experimental points have been plotted in figure 6 for one of the larger-sized tubes. The general agreement is such that the inclusion of all the data would lead to confusion in the diagram. The mean curve gives values of  $0.83$  and  $0.78$  for  $\rho_T/\rho_0$  at  $800^{\circ}$  and  $1000^{\circ}\text{C}$ . respectively, which are in close agreement with values obtained by Somerville<sup>(10)</sup>, and also those obtained by Collier, Stiles and Taylor at this Laboratory. The curve drawn in figure 6 over the lower temperature range is based on results obtained by the last-mentioned workers, being taken from figure 3 of the accompanying paper<sup>(11)</sup>.

It will be observed from the data given in table 3 that specimens no. 1 and no. 2 showed increases in resistivity of 10 and 14 per cent respectively as a result of the heat treatment, whereas that of no. 3 showed a slight decrease. These changes, which only occurred after points at the highest temperatures had been obtained, probably result from a combination of diverse effects. The decrease may result from changes, such as the volatilization or alteration of constituents, which take place when the baking temperature is exceeded. The increase may be due to oxidation, or to a longitudinal separation of the particles as a result of the strains caused by the inner surface of the tube being at a considerably higher temperature than the exterior. Such cracks were at times observed to have developed in planes at right angles to the axis, and specimen no. 2 actually broke into three portions during cooling after the maximum temperature had been reached.

In dealing with the determinations in the high-temperature range the experimental points obtained for each specimen have again been numbered in the order in which the observations were made. When a close examination of these results is attempted one again finds evidences for the presence of opposing influences, tending on the one hand to decrease the resistivity, and on the other to cause an increase. Thus the points in the neighbourhood of  $1300^{\circ}$  c. which were first obtained for both specimens no. 5 and no. 6 lie below the extrapolation of the line originally drawn to  $1200^{\circ}$  c.; but after the specimens have been taken to higher temperatures, the increase in resistance occurs and the points for these specimens and for no. 4 lie on a common curve.

As regards the general character of the results, it is quite evident that on heating beyond  $1500^{\circ}$  c. the resistivity follows a curve that bends downwards from the direction of the original line. The heavy line which has been drawn from  $1200^{\circ}$  to  $2130^{\circ}$  c. passes through points obtained on first heating specimens nos. 4, 5 and 6. The results for specimen no. 7, whose initial resistivity was somewhat greater than that of the other specimens, fall on a curve very similar in shape, but displaced to give rather higher values. Electrical-resistivity results for this specimen were obtained up to a measured external temperature of  $2360^{\circ}$  c. In this experiment the specimen was surrounded by the radiation shield, and no observations of the internal temperature were made. Approximate values for this were derived by assuming a knowledge of the thermal conductivity and calculating the temperature-drop through the walls of the tube. The results obtained indicate that the rate of fall of resistivity with increase in temperature becomes smaller beyond  $2100^{\circ}$  c. Successively lower curves are again followed on cooling to lower temperatures, and the greatest reduction observed for this type of material is obtained after heating to the mean temperature of  $2430^{\circ}$  c. Whereas the resistivity of the carbon after being fired at  $1100^{\circ}$  c. decreases on heating to  $1000^{\circ}$  c. to 78 per cent of its value at  $0^{\circ}$  c., the resistivity of a carbon which has been fired at  $2430^{\circ}$  c. decreases to 46 per cent of its value at  $0^{\circ}$  c. on being heated to  $1000^{\circ}$  c. It seems reasonable to conclude that still greater decreases would be obtained by heating to yet higher temperatures.

When figures 5 and 6 are compared, it is seen that each increase in thermal

conductivity which has resulted from the specimen being fired at a higher temperature has been accompanied by a corresponding decrease in electrical resistivity, that is, by a corresponding increase in electrical conductivity.

Reverting to the resistivity data given in table 3, it is seen that the heat treatment does not appear to have produced a correspondingly large decrease in the resistivity at normal temperatures; in fact, for five of the specimens the resistivity is greater after heating than before. It is again difficult to assess to what extent a decrease due to one effect is masked by the opposing effects already mentioned, and the fact that for two of the specimens a small decrease is observed indicates that some change of the kind noted at high temperatures is apparent at normal temperatures, although its magnitude appears to be considerably smaller.

In order to obtain further information on this point an experiment was subsequently carried out in which a small carbon tube was placed inside a larger carbon tube. The outer tube was heated by the passage of an electric current, and maintained at an external temperature of  $2000^{\circ}\text{C}$ . for 3 min. It was hoped that when heated in this way the inner carbon rod would be less affected by strain and oxidation. Table 4 shows the results of measurements made before (*I*) and after (*F*) heating.

Table 4. Changes of carbon produced by heating to  $2000^{\circ}\text{C}$ . for 3 min.  
*I* denotes initial and *F* the final value

		1st test	2nd test
External diameter (cm.)	<i>I</i>	0.585	0.586
	<i>F</i>	0.575	0.576
Internal diameter (cm.)	<i>I</i>	0.28	0.28
	<i>F</i>	0.28	0.28
Length between potential points (cm.)	<i>I</i>	3.44	3.52
	<i>F</i>	3.40	3.48
Mass (g.)	<i>I</i>	—	1.88
	<i>F</i>	—	1.835
Resistance per unit length ( $\Omega/\text{cm.}$ )	<i>I</i>	0.0273	0.0274
	<i>F</i>	0.0277	0.0279
Percentage change		+ 1.5	+ 1.8
Resistivity ( $\Omega\text{-cm.}$ )	<i>I</i>	0.00568	0.00570
(allowing for shrinkage) <i>F</i>		0.00549	0.00555
Percentage change		- 3.3	- 2.7

It will be observed that shrinkage of the specimen has occurred in each of the tests. This is an effect which had not been considered in the earlier experiments. Had the potential leads been pegged into the rod and had the contraction of the latter been ignored, the final resistance per unit length would have agreed to within 1 per cent with the initial value. When allowance is made for shrinkage of the specimen a decrease in the true specific resistance of the order of 3 per cent is obtained. This additional evidence supports the earlier conclusion that the heat treatment has a much smaller effect on the resistance at room-temperature than it has on the subsequent {resistance, temperature} curve at higher temperatures.

It should be mentioned that Hansen<sup>(12)</sup> has quoted very different results from the foregoing for carbon electrodes manufactured by the National Carbon Company. Carbons having an original cold resistivity of  $0.0035 \Omega\text{-cm}$ . were fired to temperatures of  $1200^\circ$ ,  $1600^\circ$ ,  $2000^\circ$ ,  $2400^\circ$ ,  $2800^\circ$  and  $3500^\circ$  c., after which the cold resistances were  $0.0032$ ,  $0.0030$ ,  $0.0027$ ,  $0.0023$ ,  $0.0018$  and  $0.00078 \Omega\text{-cm}$ . respectively. His results also differed in giving a much more rapid decrease in resistance with increase in temperature; thus the resistance at  $1200^\circ$  c. was about 60 per cent of the cold resistance compared with the value of 76 per cent obtained in the present work. Shrinkage and loss of weight were observed by Hansen also.

*Thermal conductivity of Acheson graphite.* Acheson graphite was found to have a thermal conductivity at  $800^\circ$  c. of the order of twenty times that of carbon. This

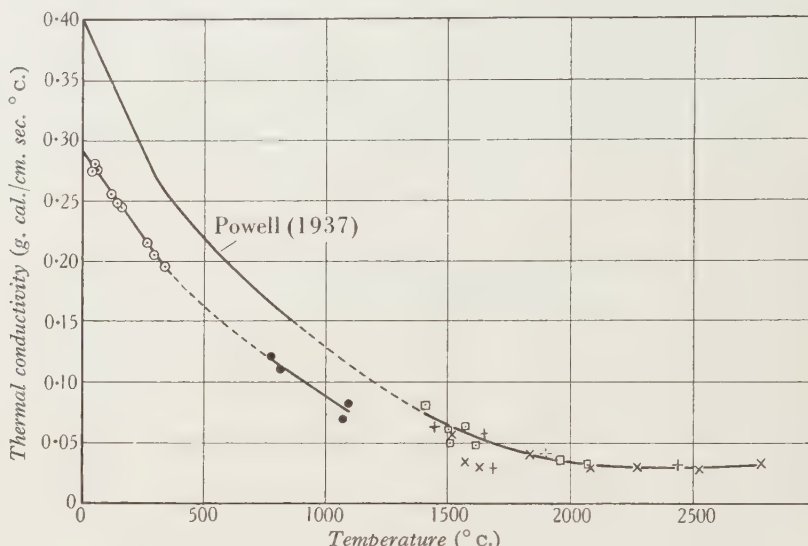


Figure 7. Thermal conductivity of Acheson graphite to  $2700^\circ$  c.  $\odot$  Specimen no. 1.  
 $\bullet$  Specimen no. 2.  $+$  Specimen no. 3.  $\times$  Specimen no. 4.  $\square$  Specimen no. 5.

high conductivity made it very difficult to carry out the tests on specimens of the normal size over the lower part of the visible temperature range. Indeed, the temperature-drop through the walls of the material was so small compared with the correction to be applied to the surface temperature that at times the corrected surface temperature exceeded the measured axial temperature. Values of the thermal conductivity for specimen no. 2, derived from four sets of data for which reasonable temperature-differences ranging from  $8^\circ$  to  $27^\circ$  c. were obtained, are plotted in figure 7, but for specimens limited to an outer diameter of 2.6 cm. the method was not really considered suitable for tests on graphite at these temperatures. On the other hand, the high thermal conductivity of the material made it practicable to employ the normal longitudinal heat-flow method for tests at lower temperatures. Determinations were made in this way over the temperature range  $30$ – $270^\circ$  c. for another specimen of the standard size, specimen no. 1, for which

$\rho_{0^\circ\text{C.}} = 0.00110 \Omega\text{-cm.}$  A heating coil was wound on one end of the tube, and a water-flow calorimeter was fitted to the other end. Heat-losses from the specimen were prevented by an outer guard tube, and the heat flowing in the rod was determined from the rate of flow of water in the calorimeter and its rise in temperature. Measurement of the temperature-gradient established in the specimen was made by means of a series of thermocouples pegged into its surface. This gave sufficient data for the thermal conductivity to be evaluated, and the results are plotted in figure 7. They indicate a conductivity of 0.29 at  $0^\circ\text{C.}$  The curve through this series of points has been extrapolated to pass through those obtained in the range  $800^\circ$  to  $1100^\circ\text{C.}$  for specimen no. 2 which had a similar resistivity ( $\rho_{0^\circ\text{C.}} = 0.00105 \Omega\text{-cm.}$ ).

The other specimens for which experimental points are plotted in this figure were in the form of solid rods, 0.965 and 0.62 cm. in diameter. Specimens no. 3 and no. 4 had the same initial resistivity,  $\rho_{0^\circ\text{C.}} = 0.00077 \Omega\text{-cm.}$ , whereas that of specimen no. 5 was 0.00067  $\Omega\text{-cm.}$  Thermal conductivity values have been obtained for these specimens over the temperature range  $1400^\circ$  to  $2700^\circ\text{C.}$  by the present radial heat-flow method. To enable the axial temperature of the rod to be measured, small radial holes about 1 mm. in diameter were drilled to the centre of the rod, and the pyrometer was sighted into the bottom of these holes. An objection to this procedure is that the presence of such a hole interferes with the current-distribution at the point where the temperature-difference is measured. In the case of the smaller rod, for which this disturbance would be the greater, the hole will cause the resistance at its mid-plane to be about 10 per cent greater than in the rest of the rod. Some of this extra energy would no doubt be conducted laterally by the graphite, so the error due to the presence of the hole will be less than 10 per cent. A more serious practical difficulty was again the measurement of the surface temperature, for frequently at these high temperatures the rod no longer appeared uniform; its surface became pitted and assumed a very mottled appearance. However, at temperatures above  $2000^\circ\text{C.}$ , where this trouble became most noticeable, the temperature-difference between the axis and the surface of the rod ranged from  $150^\circ$  to  $340^\circ\text{C.}$ , so the errors in the ultimate values of the thermal conductivity should not be unduly great.

Independently of the present investigation, one of the authors has since published<sup>(1)</sup> results of the thermal and electrical conductivities of a sample of Acheson graphite from  $0^\circ$  to  $800^\circ\text{C.}$  This material had a specific resistivity at  $0^\circ\text{C.}$  of 0.00082  $\Omega\text{-cm.}$ , so does not differ greatly from that of specimens nos. 3 and 4. The effect of temperature on the thermal conductivity of this sample of graphite is shown by the heavy line drawn in figure 7; and it will be seen that a reasonable extrapolation of this curve passes through the points obtained at much higher temperatures in the present investigation. The thermal conductivity of graphite appears to reach a minimum value of 0.026 at about  $2400^\circ\text{C.}$  The points in the region of  $1600^\circ\text{C.}$  which lie well below the curve were mostly obtained after the rod had been heated to much higher temperatures.

*Electrical resistivity of Acheson graphite.* Curves showing the temperature-variation of the specific resistance of the various graphites have been included in

figure 6. The upper curve was obtained for specimen no. 2 over the complete range from room-temperature to  $1100^{\circ}\text{C}$ . at a time when the temperature could be measured by means of a thermocouple inserted into the axial hole. The curve has a minimum at about  $520^{\circ}\text{C}$ ., at which the resistivity is 74·6 per cent of the value at  $0^{\circ}\text{C}$ . ( $0\cdot001054\Omega\text{-cm}$ ). The curve below this is that obtained in the independent investigation to which reference has been made. It also indicates a minimum value, but for this specimen, which had specific resistance at  $0^{\circ}\text{C}$ . of  $0\cdot00082\Omega\text{-cm}$ ., the minimum value occurs at  $450^{\circ}\text{C}$ . and is only 80·4 per cent of the  $0^{\circ}\text{C}$ . value. Curves for two other specimens of graphite are also given by Collier, Stiles and Taylor<sup>(11)</sup>, and it will be seen that these are similar in character and show a similar variation as regards the position and magnitude of the minimum.

At higher temperatures the experimental values for the rods with  $\rho_0$  equal to  $0\cdot00077$  lie on a linear extrapolation of a curve situated about 5 per cent below that for the specimen with  $\rho_0$  equal to  $0\cdot00082\Omega\text{-cm}$ .

#### § 5. DISCUSSION OF RESULTS

*Evidence for graphitization of carbon.* In considering the causes of the changes which occur in the conductivities of carbon heated to sufficiently high temperatures, the well-known fact that graphite is formed by such heating of amorphous carbon appears to give a likely explanation. It is evident from the results plotted in figures 5 and 6 that a change which can be attributed to partial graphitization of the carbon occurs when the material is heated above about  $1700^{\circ}\text{C}$ . For not only are the absolute values of the thermal and electrical conductivities of carbon tending towards those obtained for graphite, but after carbon has been heated to  $2400^{\circ}\text{C}$ . the form of the {resistance, temperature} curve appears to be intermediate between that of the original carbon and graphite. Our observations on two specimens of graphite show each of these curves to have a minimum which is more pronounced and occurs at a higher temperature for the poorer conducting graphite, whilst the carbon, which has only been heated to  $2400^{\circ}\text{C}$ ., and is a very much poorer graphite, shows signs of approaching a minimum resistance of just under 40 per cent of the room-temperature value. Since the foregoing work was completed, Nishiyama<sup>(13)</sup> has studied carbon filaments which have been heated to successively higher temperatures, and has obtained further evidence for changes of this type. After  $1\frac{1}{2}$  hr. heating at  $3000^{\circ}\text{C}$ . the minimum was brought to so low a temperature that a graphite was obtained which had a positive coefficient from room-temperature upwards. X-ray analysis showed the graphitization to be accompanied by the growth of larger crystals within the carbon, which, prior to heat treatment, had given the diffuse photograph of an amorphous material.

#### § 6. RELATION OF THERMAL AND ELECTRICAL CONDUCTIVITIES

For most metallic conductors the value of the Lorenz function, that is, the thermal conductivity multiplied by the electrical resistivity and divided by the absolute temperature, is about  $0\cdot58 \times 10^{-8}$  and remains nearly constant over wide

ranges of temperature. The values of this function for the two carbon materials studied in the present investigation are set out in table 5 and have been plotted in figure 8. Data for the two graphites which had resistivities at  $0^{\circ}\text{C}$ . of  $0.0001054\Omega\cdot\text{cm}$ . respectively are included. The value given at  $0^{\circ}\text{C}$ . for carbon is derived from the experimental data obtained by Jones. It will be seen that at  $0^{\circ}\text{C}$ . carbon and graphite have Lorenz functions which are respectively 17 and 200 times as great as that possessed by good metallic conductors.

Table 5. The Lorenz function  $L$  of carbon and graphite

Temp. ( $^{\circ}\text{C}$ )	Carbon			Graphite I			Graphite II		
	Resistivity	$K$	$L \times 10^8$	Resistivity	$K$	$L \times 10^8$	Resistivity	$K$	$L \times 10^8$
0	0.00663	0.0039	9.5	0.001054	0.29	112	0.00082	0.402	120.8
250	—	—	—	0.00084	0.218	35	0.00068	0.29	37.8
500	—	—	—	0.00078 <sub>5</sub>	0.16	16.2	0.000659	0.21 <sub>2</sub>	18.5
700	0.00474	0.0055	2.7	0.00080 <sub>1</sub>	0.128	10.5	0.00068	0.178	12.4
1000	0.00444	0.0070	2.44	0.00086	0.088	6.0	0.00072	0.128	7.28
1200	0.00426	0.0080	2.31	—	—	—	0.00076	0.100	5.15
1500	0.00395	0.010	2.23	—	—	—	0.00082	0.064	2.96
2000	0.00284	0.025	3.12	—	—	—	0.00096	0.036	1.52
2500	—	—	—	—	—	—	0.00109	0.029	1.14
3000*	0.00315	0.018	3.03	—	—	—	—	—	—

\* After being heated to  $2000^{\circ}\text{C}$ .

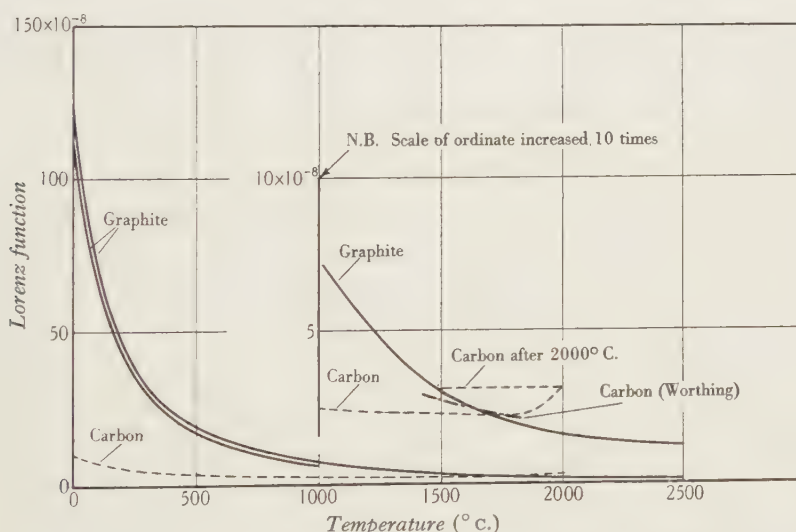


Figure 8. Variation of Lorenz function of carbon and graphite with temperature.

It is well known that metals of low thermal conductivity have Lorenz functions which at room-temperature are about twice as great as those of good conducting metals, and that these high values decrease with increase in temperature. The departure is of a quite different order for the materials now under consideration, and in this instance it is the better-conducting material which shows the greater departure. Indeed, at normal temperatures, the thermal conductivity of graphite

is higher than that of many metals which show no departure from the Wiedemann-Franz-Lorenz law.

With increase in temperature the Lorenz functions of carbon and graphite also are seen to decrease rapidly. The two curves meet at about  $1700^{\circ}\text{C}$ . where the value is only about 4 times the normal metallic value. In this temperature region the present value is seen from the figure to be in fairly good agreement with the curve representing Worthing's values<sup>(4)</sup> for a carbon filament.

The curve for graphite continues to decrease with increase in temperature, and by  $2500^{\circ}\text{C}$ . the Lorenz function is only  $1.14 \times 10^{-8}$ . The equation suggested for the Lorenz function of graphite in the earlier paper<sup>(1)</sup>, viz.  $L = 0.0294 T^{-1.8}$ , only holds for the present results to a temperature of about  $1200^{\circ}\text{C}$ . Beyond this temperature the equation gives higher values than those obtained experimentally, the predicted value at  $2500^{\circ}\text{C}$ . being  $1.87 \times 10^{-8}$ .

With regard to this divergence, and also to the increase in the Lorenz function which is observed to take place for carbon as  $2000^{\circ}\text{C}$ . is approached, it should be remembered that the present values are derived on the assumption that the thermal conductivity, measured in a radial direction, and the electrical conductivity, measured in a longitudinal direction, are comparable quantities. This assumption is no longer true if local changes which have more effect on conduction in one of these directions than the other occur in the specimens on heating. It will therefore be realized that the foregoing results for the Lorenz function, whilst they can be accepted as showing the general nature of the change which occurs in this quantity over the range of temperature covered by the experiments, cannot be regarded as having an accuracy as great as that of the determination of either the thermal or the electrical conductivity.

#### § 7. ACKNOWLEDGEMENTS

The authors are pleased to record their indebtedness to Mr F. J. Filby, who constructed the vacuum enclosure used in this investigation; and they also desire to thank him and his successor Mr E. E. Smith for assistance in connexion with the observational work.

#### REFERENCES

- (1) POWELL, R. W. *Proc. Phys. Soc.* **49**, 419 (1937).
- (2) ANGELL, M. F. *Phys. Rev.* **33**, 421 (1911).
- (3) MENDENHALL, C. E. and FORSYTHE, W. E. *Astrophys. J.* **37**, 380 (1913).
- (4) WORTHING, A. G. *Phys. Rev.* **4**, 535 (1914).
- (5) WEBER. *Arch. Sci. Phys. Nat.* **33**, 590 (1895).
- (6) BARRATT, T. *Proc. Phys. Soc.* **27**, 81 (1915).
- (7) STÖRMER, R. *Siemens K. Wiss. Verh.* **13**, 1, 30 (1934).
- (8) HOLM, R. *Z. Phys.* **43**, 466 (1927).
- (9) CELLIER, L. *Ann. Phys. Chem.* **61**, 511 (1897).
- (10) SOMERVILLE, A. A. *Phys. Rev.* **31**, 270 (1910).
- (11) COLLIER, L. J., STILES, W. S. and TAYLOR, W. G. A., p. 147 of this volume.
- (12) HANSEN, C. A. *Trans. Amer. Electrochem. Soc.* **16**, 335 (1909).
- (13) NISHIYAMA, Z. *Sci. Rep. Tōhoku Univ.* **21**, 171 (1932).

# MEASUREMENT OF THE SPECIFIC INDUCTIVE CAPACITY OF DIAMONDS BY THE METHOD OF MIXTURES\*

By S. WHITEHEAD, M.A., PH.D. AND W. HACKETT, B.Sc., PH.D.

*Received 20 July 1938. Read 28 October 1938*

**ABSTRACT.** The specific inductive capacity of diamonds in bulk has been measured by the method of mixtures, the most accurate single determination being 5.66 at 27.8° C. and 800 c./sec. A general mean value of 5.7 applies within a standard error of 1.5 per cent over the range of temperature from -65° C. to +85° C. and from 300 to 3000 c./sec. and within a standard error of 3.2 per cent for a frequency range from 50 to 5000 c./sec. while no change within a standard error of 2 per cent was observed up to 1.6 Mc./sec. Reasons are given for supposing the present value more accurate than those hitherto obtained, and it is also shown that the value deduced agrees satisfactorily with the refractive index on the basis of Maxwell's law and shows consistency with the relationships of specific inductive capacity to atomic number and the periodic table which hold for other elements. Some observations are made on other physical properties of the diamond and on the theory of the specific inductive capacity of mixtures.

## § I. INTRODUCTION

*Origin of the investigation.* In two communications Addenbrooke<sup>(1)</sup> has drawn attention to a number of relations which hold between the dielectric constant or specific inductive capacity of the non-metallic elements and their other physical properties. In particular, Maxwell's law relating to the refractive index appears to be fairly accurately obeyed, a fact which does not receive the attention which it deserves in text books. Data on the specific inductive capacity of carbon as diamond were uncertain and at Mr Addenbrooke's suggestion, and with his good offices and assistance, the Electrical Research Association undertook its measurement. The diamonds employed were only available on short loan on account of their value, so that great refinements in technique were not possible, but data to a known reliability were obtained over as wide a range as time permitted.

An early determination by Pirani<sup>(2)</sup> at audio frequencies gave a specific inductive capacity of 16.5 but his experimental methods were open to serious objection. Schmidt<sup>(3)</sup> used very short waves, probably of the order of  $10^8$  to  $10^9$  c./sec. (30 cm. to 3 m.) and a method of mixtures. The test condenser formed part of an oscillating circuit coupled to a Lecher-wire circuit with a movable bridge and adjusted to resonance. A calibration was obtained with liquids of known specific

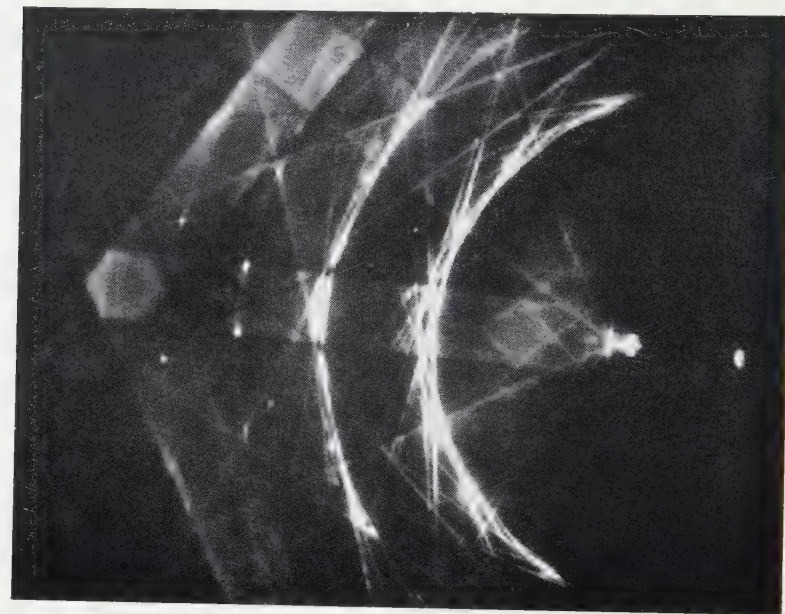
\* Based on Ref. L/T87 of the British Electrical and Allied Industries Research Association.

inductive capacity. A second calibration was obtained with the diamond immersed in the liquids. Where the two curves intersected the specific inductive capacities of diamond and liquid were equal and the value for the former could thus be deduced. By this means a value of 5·50 was obtained with an estimated accuracy of 5 per cent. More recently Sir Robert Robertson, Fox and Martin<sup>(4)</sup> found the specific inductive capacities of the two types of diamonds discovered by them. They used a high frequency of the order of 50 Mc./sec., determining, by substitution in an oscillating circuit, the change in capacity of an air condenser due to the insertion of a diamond; the irregular shape was allowed for by comparison tests on glass models of known specific inductive capacity. They quoted values of 5·01 and 4·88 for the two types, but considered this difference to be within the limits of experimental error. Mention should also be made of the work of Rosenholtz and Smith<sup>(5)</sup> who immersed mineral powders in a mixture of methyl alcohol and carbon tetrachloride in the presence of a divergent electric field produced between two needle points. The alcohol was added until the powder was no longer attracted to the needles, when it was assumed that the specific inductive capacity of powder and liquid were the same. The specific inductive capacity of the liquid was then deduced from the composition. A value of 4·58 is given as the result for diamond powder by this method, but it must be regarded as a lower approximation of low accuracy since it is admitted by the authors that different results are obtained if the specific inductive capacity of the liquid is decreased from a higher value than if increased from a lower value.

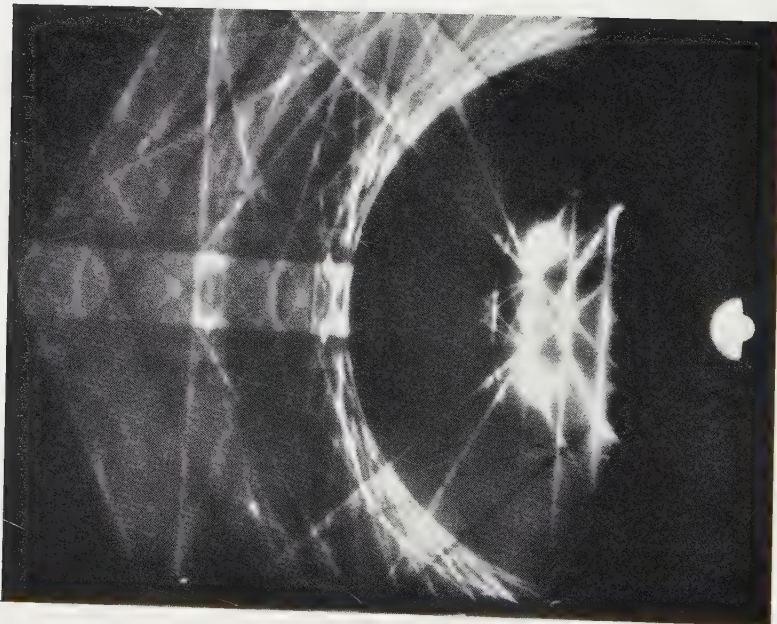
The measurements made on single diamonds require, in effect, the value of, or ratio between, very small capacities, and encounter the difficulties inherent in such tests. In addition, large crystals of a certain shape must be used, and are likely to give anomalous results. Accordingly, it was desired to make a measurement of the average value for a large number of small crystals, as perfect as possible, over as wide a range of frequency as possible. By this means a larger capacity can be employed with correspondingly increased accuracy and range of frequency. One obtains, however, a mean value for the various orientations of the crystal, but Schmidt showed with other crystals that the change of specific inductive capacity with orientation is usually small and he was unable, apparently, to observe any differences in the diamond.

*Type of diamonds used.* The Diamond Corporation, when approached by Mr Addenbrooke, agreed to assist and referred the question to their adviser, Prof. W. T. Gordon. After the latter, with Mr Addenbrooke, had inspected a large collection of diamonds of all types, a collection of fine blue-white melee stones was considered the most suitable. These stones were small natural crystals of octahedral form selected to be as perfect and as regular as possible by the experts of the Diamond Corporation and afterwards passed by Prof. Gordon. Since the crystals were selected to be of this regular characteristic diamond form, no further account of the morphology is required except to indicate that, although the collection included a certain number of split, broken and imperfect crystals, the number of twin or multicrystals, conchoidal fractures and fragments, was very small. The crystals





(a) Cube face



(b) Cleavage face

Figure 1. Representative electron diffraction patterns for diamond (Professor Finch).

were all of about the same size, the average diameter being 1.85 mm. and the average weight 10.5 mg., so that an unusually homogeneous collection of good, natural crystals was employed. About 6000 stones were originally loaned, of which about 4000 were employed in the tests.

Two main determinations of the density were made on portions of the collection giving values of 3.514 and 3.518 at 20° C. Cohen and Olie<sup>(6)</sup> give 3.514 at 18° C., Wigand<sup>(7)</sup> gives 3.518 at room-temperature, while Robertson, Fox and Martin<sup>(4)</sup> give a number of values for different diamonds ranging from 3.508 to 3.517 at 15° C. for their type I, which is the common type.

Some specimen electron-diffraction patterns were obtained by the courtesy of Prof. Finch, who selected a small set of specimen stones. Two patterns at different orientations, obtained by reflection, are shown in figure 1. Prof. Finch reported that all the diamonds examined gave normal characteristic patterns, while the definition and simplicity of the patterns indicated that the surface planes were parallel to the true crystal faces, that is, the stones were true natural crystals. It was considered, therefore, that the diamonds employed might be taken as typical of this form of crystalline carbon. No attempt was made to separate the two types of diamonds, since the second type is so rare as to be unlikely to affect the results in tests of the nature envisaged.

*Electrical resistance of diamonds.* Some experiments were made on the electrical resistivity of typical diamonds selected by Prof. Gordon as representative, the diamonds used in the capacity tests being too small for this purpose. The method employed was the electrostatic induction-balance method of Townsend for the measurement of small currents. About 100 v. was employed and the electrodes were of thin metal foil backed by soft metal pads. No consistent differences were observed where it was possible to test in more than one direction, but owing to the irregular shape of the specimens the accuracy was probably only about 10 or 20 per cent.

Table 1. Resistivity

Specimen no.	Description	Resistivity at 25° C. (Ω.-cm <sup>3</sup> )
D.2	Octahedron, blue white, Angola	9.6 × 10 <sup>12</sup>
D.3	Octahedron, blue-white, Congo	5.5 × 10 <sup>12</sup>
D.5	Cube-Octa-Dodecahedron, B.C.K.	10 × 10 <sup>12</sup>
D.6	Cube-Dodecahedron, B.C.K.	4.8 × 10 <sup>10</sup>
D.8	Spinel Twin, B.C.K.	5.7 × 10 <sup>12</sup>
D.9	Cube, B.C.K.	11 × 10 <sup>12</sup>
D.10	Cube-Octa-Dodecahedron, black, B.C.K.	14 × 10 <sup>12</sup>
D.11	Cube, yellow	5.5 × 10 <sup>12</sup>
D.13	Carbonado, Brazil	About 10 <sup>8</sup>
D.14	Carbonado, Brazil	About 10 <sup>7</sup>
D.15	Cube-Octa-Dodecahedron, B.C.K.	1.1 × 10 <sup>12</sup>

It is seen that the values for all the diamonds proper are of the same order and indicate highly insulating properties. The low-resistance carbonados or borts are black, but are valued on account of their greater hardness.

## § 2. EXPERIMENTAL METHODS

The method used consists essentially in the determination of the specific inductance capacity of a mixture of the solid with a liquid or gaseous medium of which the specific inductive capacity either has been predetermined or is measured simultaneously. By the use of several immersion media of which the specific inductive capacities lie on either side of that of the solid, the latter can be determined by interpolation. The complete determination of the specific inductive capacity of the diamonds with a number of media was restricted to the two frequencies 800 and 2000 c./sec. and the two temperatures  $27\cdot8^{\circ}$  C. and  $54\cdot4^{\circ}$  C. For all other frequencies and temperatures air was employed as the immersion medium and the variation of the specific inductive capacity of the diamond was computed from the variation of the specific inductive capacity of the diamond-air mixture. Tests were made in a thermostat and continued until constant results were obtained, a period of several hours usually being required. The range of the investigation covered frequencies from 50 c./sec. to 1·6 Mc./sec. and temperatures from  $-65^{\circ}$  C. to  $80^{\circ}$  C.

*The condenser equipment.* For rapidity, and to minimize the effect of any small changes in the medium and in the test conditions, the condenser system was arranged so that the specific inductive capacity of both the mixture and the immersion medium could be measured simultaneously. Since dismantling and reassembly for the purpose of inserting the solid were necessary operations between measurements, it was essential that the main condenser should permit assembly to a high degree of accuracy.

The construction of the composite condenser is evident from figure 2. The bottom plate formed the high-voltage electrode while the middle plate, mounted concentrically within a guard ring, formed the low-voltage plate of the main diamond condenser. The separating washers were of accurately ground glass, fitted into recesses in the plates, and were of such thickness as to allow the guard ring to form a boundary for the diamonds. The uppermost plate provided the high-voltage electrode of the auxiliary condenser for the determination of the specific inductive capacity of the media, the other electrode being the middle plate. The spacing washers in this case were of mycalex and were separated by nuts in order to split the leakage path. With the exception of the top plate, which was of brass, the condenser components were of stainless steel. A cylinder of sheet copper and the electrode which was surplus to each condenser provided the requisite electrostatic screening. The diamonds were packed as tightly as possible in a single layer, giving a volume ratio of 0·334.

*Immersion media.* The liquid media consisted of either castor oil or mixtures of castor oil and nitrobenzene in varying proportions.\* The power factor of the castor oil was low—of the order of 0·2 per cent at  $27\cdot8^{\circ}$  C. and 0·9 per cent at  $54\cdot4^{\circ}$  C.—and remained stable for measurements made at 800 c./sec. With the mixtures of

\* The castor oil used was of pharmaceutical quality and the nitrobenzene of analytical quality.

castor oil and nitrobenzene the initial power factors were appreciable and progressively increased with time, particularly at the higher temperature.

The two liquids were de-aerated in a separating funnel and shaken together in vacuo. The mixture was then admitted slowly into the bottom of the previously evacuated desiccator containing the condenser through a glass dropping-tube. Evacuation was continued until all bubbles were removed.

After each test the condenser and diamonds were thoroughly washed with alcohol and dried.

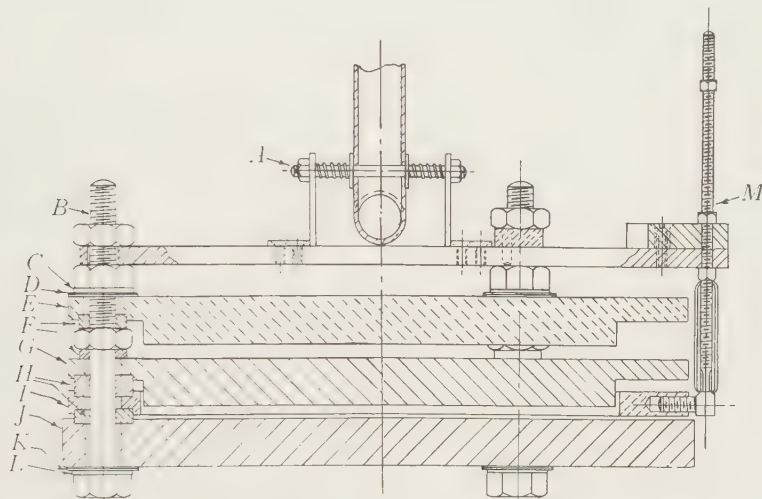


Figure 2. Construction of test condenser for the determination of the specific inductive capacity of diamonds. *A*, brass clamp for glass tube; *B*,  $\frac{1}{4}$ -in. B.S.F. bolts (3 at  $120^\circ$  apart); *C*, stainless steel washers; *D*, mica washers; *E*, high-voltage brass electrode; *F*, mycalex washers; *G*, low-voltage stainless steel electrode; *H*, glass washers; *I*, stainless steel guard ring; *J*, high-voltage stainless steel electrode; *K*, mica washers; *L*, stainless steel washer; *M*, rigid clips on 2 B.A. screws displaced at  $15^\circ$  with respect to each other. Low-voltage connexion screened by copper tubing connected electrically to guard ring.

*Measurement of capacity.* The audio-frequency measurements were made by substitution in a low-voltage Schering bridge employing as detector either an amplifier and telephones or a vibration galvanometer, the guard ring of the condenser and all screens being connected to the Wagner earth arm. The air capacity of the main condenser determined at 800 c./sec. together with the subsidiary and stray capacities are shown in table 2. Corrections for the latter were made where necessary, and a correction was made for the slight overestimation of the specific inductive capacity of the medium by the upper condenser.

The radio-frequency measurements were made only on the lower condenser. This can be considered as an equivalent delta network where  $C_x$  and  $C_z$  are the capacities of the guard ring (including the screens) to the low-voltage and high-voltage plates respectively and  $C_y$  is the required capacity between the low-voltage and high-voltage plates. If each capacity is short-circuited in turn, the sum of the

other two capacities is obtained, whence  $C_y$  is given by

$$C_y = \frac{1}{2} \{(C_x + C_y) + (C_y + C_z) - (C_z + C_x)\}. \quad \dots\dots(1)$$

These composite capacities were determined by substitution in the tuned circuit of a radio-frequency oscillator containing a variable precision condenser arrangement. An auxiliary oscillator loosely coupled to the main oscillator served as an indicator of tuning, the beat frequency being adjusted to 800 c./sec. by beating with a standard 800-c./sec. signal. The leads connecting the test condenser and auxiliary apparatus to the oscillator were screened, the screens being connected to the screens and guard ring of the test condenser which were always connected to the earthy side of the oscillator.

Table 2. Air capacity of condenser components measured at 800 c./sec.

Capacity measured	Value ( $\mu\mu F.$ )
High-voltage to low-voltage electrode of main condenser	$34.4 \pm 0.2$
Stray capacity over edge of guard ring	$0.74 \pm 0.03$
Leads to bottom condenser	$0.57 \pm 0.03$
Leads to top condenser	$1.02 \pm 0.03$

It is to be observed that the values of  $C_x$  and  $C_z$  were considerably greater than  $C_y$ ,  $C_z$  being the larger. In order to obtain the maximum accuracy, therefore, a variable air condenser covering the range  $(C_x + C_y)$  was employed, the additional capacity for the other two measurements being supplied by a fixed screened mica condenser. In view of the cancellation of the latter capacity in the final calculation for  $C_y$ , its accuracy depended only on the accuracy of the air condenser and the stability but not the absolute value of the fixed capacity. As an alternative method the effective range of a standard 100- to 1200- $\mu\mu F.$  variable air condenser was reduced to the appropriate value by connexion in series with a fixed air condenser, the law of combination being expressible in a linear form which served to facilitate both calibration and interpolation.

### § 3. EXPERIMENTAL RESULTS

*Interpolation methods.* It is essential that any formula which purports to compute  $\epsilon_m$ , the specific inductive capacity of a mixture, in terms of  $\epsilon_s$  and  $\epsilon_l$ , the specific inductive capacities of the solid and liquid components respectively, should satisfy the condition

$$\epsilon_s = \epsilon_l = \epsilon_m.$$

Thus, if the experimental values of  $\epsilon_m/\epsilon_l$  and the values of  $\epsilon_m/\epsilon_s$ , calculated from some possible formula, are plotted against  $\epsilon_m$ , then the two curves obtained must intersect at the point where

$$\frac{\epsilon_m}{\epsilon_l} = \frac{\epsilon_m}{\epsilon_s} = 1.$$

This condition of intersection at a particular point substantially increases the accuracy to which the curves can be drawn and hence gives a greater accuracy of

interpolation than can be obtained directly from the curve for  $\epsilon_m/\epsilon_l$ . This applies even though the formula which has been employed in the calculation of  $\epsilon_m \epsilon_s$  is not completely valid. The absolute accuracy is then determined by the accuracy of interpolation and the authenticity of the interpolation curves in the region of intersection which depends on the accuracy of the experimental values of  $\epsilon_l$  and  $\epsilon_m$  and of the resulting computation of  $\epsilon_s$ . From these considerations the error in the absolute determination is estimated to lie well within 1 per cent.

In a preliminary investigation carried out with glass beads, special cases of Wiener's general formula\* were examined in respect of their applicability to the determination of the specific inductive capacity of the immersed solid, and were found adequate as a basis of interpolation although invalid for purposes of calculation. In the diamond tests a new type of approximation was employed which took into account the size of the solid units as well as the volume ratio, the diamonds being considered as small contiguous spheres resting on the lower condenser plate. The disturbing effect of a dielectric sphere of volume  $v$  can then be represented by a dipole at the centre of the sphere of moment

$$(3/4\pi) Ev \{(\epsilon - 1)/(\epsilon + 2)\},$$

where  $E$  is the normal field and  $\epsilon$  is the ratio  $\epsilon_s/\epsilon_l$ . In order to obtain correct boundary conditions at the electrodes these dipoles must be successively reflected in the electrode surfaces, while in order to take the mutual influence of different spheres into account each dipole must be successively inverted with respect to all the other spheres. For the first-order dipoles the simplest approximation is that obtained by assuming that their effect is similar to a uniform sheet of dielectric of the same volume but is multiplied by a factor  $\nu$ , less than 1, to take into account the finite spacing of the dielectrics, whence if  $P$  is the normal polarization

$$-\frac{\Delta P}{P - \Delta P} = \frac{3\nu nv}{d} \left( \frac{\epsilon - 1}{\epsilon + 2} \right) = 3\mu\nu \left( \frac{\epsilon - 1}{\epsilon + 2} \right),$$

where  $n$  is the number of particles per  $\text{cm}^2$ ,  $d$  the distance between electrodes, and  $\mu$  the volume ratio of solid to total space. It is assumed that the image dipoles without the electrodes have no effect on the field within and that a disturbing potential  $\Delta V$  is set up with negligible contribution of flux.

The inverted dipoles are multiplied in successive orders by  $-(\epsilon - 1)/(\epsilon + 2)$  and a function of the mutual distances, so that as a first rough approximation

$$\begin{aligned} -\frac{\Delta P}{P + \Delta P} &= \frac{\Delta V}{V} = 3\mu\nu \left\{ 1 - \nu \left( \frac{\epsilon - 1}{\epsilon + 2} \right) + \nu^2 \left( \frac{\epsilon - 1}{\epsilon + 2} \right)^2 \dots \right\} \left\{ \frac{\epsilon - 1}{\epsilon + 2} \right\} \\ &= 3\mu\nu \left( \frac{\epsilon - 1}{\epsilon + 2} \right) / \left\{ 1 + \nu \left( \frac{\epsilon - 1}{\epsilon + 2} \right) \right\} = f, \end{aligned}$$

whence

$$\epsilon_m/\epsilon_l = 1/(1-f). \quad \dots\dots(2)$$

\* The formula is as follows:

$$\frac{\epsilon_m - 1}{\epsilon_m + u} = \mu \left( \frac{\epsilon_s - 1}{\epsilon_s + u} \right) + (1 - \mu) \left( \frac{\epsilon_l - 1}{\epsilon_l + u} \right),$$

where  $\mu$  is the proportion of the total volume occupied by the solid and  $u$  is a form factor which takes into account the effect of the shape of the solid on its contribution to the specific inductive capacity of the mixture.

Taking  $\nu$  as 0·9 and  $\mu$  as 0·334, the error in the computation of  $\epsilon_s$  from formula (2) was not greater than 3 per cent over the range of liquid media employed, i.e. for values of  $\epsilon_s/\epsilon_l$  from 0·82 to 1·2. On the other hand, for large values of  $\epsilon_s/\epsilon_l$  such as obtain with gaseous media, the error in the calculation of  $\epsilon_s$  is so large as to render the method of computation unreliable. The above approximation would therefore appear to be satisfactory only in the cases in which the specific inductive capacity of the media approximates to that of the immersed solid.

Table 3. Interpolation results at low frequencies

Temperature ( $^{\circ}$ C.)		27·8							
Frequency (c./sec.)		300		800		2000		4000	
Experimental values of $\epsilon_l$ and $\epsilon_m$	$\epsilon_l$	$\epsilon_m$	$\epsilon_l$	$\epsilon_m$	$\epsilon_l$	$\epsilon_m$	$\epsilon_l$	$\epsilon_m$	
	6·45	6·24	4·6 <sub>6</sub> 5·7 <sub>5</sub> 6·4 <sub>6</sub> 6·8 <sub>6</sub>	4·9 <sub>5</sub> 5·7 <sub>2</sub> 6·2 <sub>1</sub> 6·4 <sub>6</sub>	4·6 <sub>6</sub> 5·7 <sub>5</sub> 6·4 <sub>6</sub> 6·8 <sub>6</sub>	4·9 <sub>7</sub> 5·7 <sub>2</sub> 6·2 <sub>4</sub> 6·4 <sub>6</sub>	6·45	6·26	
$\epsilon_s$ (interpolated)				5·66		5·71			
Temperature ( $^{\circ}$ C.)		54·4							
Frequency (c./sec.)		300		800		2000		4000	
Experimental values of $\epsilon_l$ and $\epsilon_m$	$\epsilon_l$	$\epsilon_m$	$\epsilon_l$	$\epsilon_m$	$\epsilon_l$	$\epsilon_m$	$\epsilon_l$	$\epsilon_m$	
	6·0 <sub>3</sub>	6·0 <sub>5</sub>	4·3 <sub>9</sub> 5·3 <sub>8</sub> 5·9 <sub>7</sub> 6·3 <sub>2</sub>	4·7 <sub>7</sub> 5·4 <sub>9</sub> 5·9 <sub>3</sub> 6·2 <sub>1</sub>	4·3 <sub>7</sub> 5·3 <sub>8</sub> 5·9 <sub>6</sub> 6·3 <sub>1</sub>	4·7 <sub>7</sub> 5·4 <sub>8</sub> 5·9 <sub>3</sub> 6·1 <sub>4</sub>	5·9 <sub>6</sub>	5·9 <sub>5</sub>	
$\epsilon_s$ (interpolated)				5·81		5·79			

*Audio-frequency measurements.* The experimental values of  $\epsilon_m$  and  $\epsilon_l$  are shown in table 3 together with the interpolated values of  $\epsilon_s$ . Figure 3 comprises a typical pair of curves showing the experimental values of  $\epsilon_m/\epsilon_l$  and for the values of  $\epsilon_m/\epsilon_s$  calculated from equation (2). The experimental results obtained for the higher frequency are rather less consistent than those obtained at the lower frequency. A change of frequency from 800 to 2000 c./sec. causes a change in  $\epsilon_s$  of less than 1 per cent, the variation being in opposite directions for the two temperatures, and probably attributable to experimental error. This is confirmed by the values of  $\epsilon_l$  and  $\epsilon_m$ , also shown in table 3, for check tests carried out at 300 and 4000 c./sec. with one of the liquid media. A change of temperature from 27·8° C. to 54·4° C. causes an increase in  $\epsilon$  at both frequencies: the variation of 2·6 per cent at 800 c./sec. and 1·4 per cent at 2000 c./sec. is too great to be accounted for by experimental error and appears to be an intrinsic effect.

Table 4 summarizes the results for the additional check tests made in air over an extended range of temperature and frequency. There appears to be no consistent variation of  $\epsilon_m$  either with frequency or with temperature, so that the discrepancies must be attributed to experimental error. It can be shown from equation (2) that,

where the medium is air, a given percentage change in the specific inductive capacity of the solid causes only about one-fifth as great a variation in the specific inductive capacity of the mixture. The possible variation of  $\epsilon_s$  with frequency or temperature is within the limits of uncertainty associated with the group of values, namely a standard error of 1.5 per cent from 300 to 3000 c. sec. or of 3.2 per cent from 50 to 5000 c./sec.

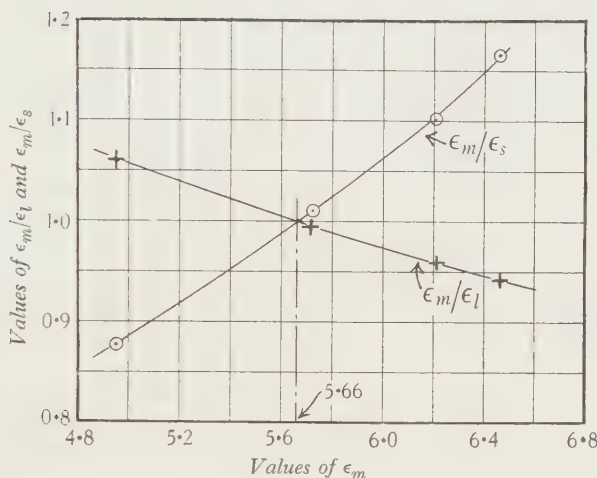


Figure 3. Experimental values of  $\epsilon_m/\epsilon_l$  and calculated values of  $\epsilon_m/\epsilon_s$  at  $27.8^\circ\text{C}$ . and  $800\text{ c./sec.}$

Table 4. Low-frequency check tests with air over extended range of temperature and frequency

Frequency (c./sec.)	$\epsilon_m$			
	-65° C.	28.8° C.	54.4° C.	80° C.
50*	1.590	1.592	1.563	
200*		1.563		
300*		1.587		
500		1.575		
800	1.578	1.575	1.584	1.575
2000	1.581	1.581	1.584	1.570
3000	1.581	1.581	1.592	
5000*		1.578	1.607	

\* These results are not very accurate owing to the lack of sensitivity of the detector at these frequencies.

*Radio-frequency measurements.* In order to eliminate the effect of change of capacity due to a change in the disposition of the diamonds between different series of tests, one determination of each series was always made at 800 c./sec. and was used as a standard of comparison. With the direct substitution method the results were corrected for residual inductance (about  $0.8\ \mu\text{H.}$ ) in the leads of the test condenser, while National Physical Laboratory calibrations at 1000 c./sec. and 1.6 Mc./sec. permitted the correction of small errors in the measuring condensers.

The ratios of  $\epsilon_m$  at various frequencies to  $\epsilon_m$  at 800 c./sec. are given in table 5. The standard deviation is of the order of 0.4 per cent, corresponding to a standard deviation in the specific inductive capacity of the diamonds of 2 per cent. The series-condenser method, owing to a different distribution of errors, does not lend itself to the same type of correction, so that the divergence from unity is, in general, greater than with direct substitution, although the results lie within the limits of experimental error for the particular test conditions. The random variation with frequency suggests that  $\epsilon_s$  is independent of frequency within a standard error of 2 per cent.

Table 5. Radio frequency measurements

Method of measurement	Ratio of $\epsilon_m$				
	800 c./sec.	Radio-frequency (kc./sec.)			
		35.5	175	308	600
A. Direct substitution	1.000 1.000	1.000*	1.003		0.999
B. Series-condenser method	1.000 1.000 1.000	1.006	1.017	0.983	1.000 0.995 1.003
Mean of B results	1.000		1.017	0.983	0.998 1.005

\* This value was obtained for a new disposition of the diamonds.

#### § 4. DISCUSSION OF RESULTS

The value 5.66 at 27.8° c. and 800 c./sec. compares closely with that obtained by Schmidt, namely 5.5, by the method of mixtures, but is higher than the values found by Robertson, Fox and Martin, whose method is, however, attended with great difficulties. These comparisons, nevertheless, definitely support the view that the specific inductive capacity is independent of frequency up to the order of some hundred megacycles per second.

Walter<sup>(8)</sup> made a careful determination of the refractive index of diamonds for the various Fraunhofer lines. The refractive index increased slightly with frequency as shown in figure 4, lying between 2.4 and 2.47. Peter<sup>(9)</sup> made up a diamond prism and deduced therefrom a limiting low-frequency refractive index of 2.38. Robertson, Fox and Martin give an index of 2.41 at  $\lambda 5461$ . These various values are indicated in figure 4 and may be said to agree with an extrapolated value of about 2.38. This corresponds on Maxwell's law to a specific inductive capacity of 5.67, which is in close agreement with the value measured.

Such extrapolations are always questionable, particularly in view of the infrared absorption bands studied by Robertson, Fox and Martin. However, the evidence is fairly strong for the view that the specific inductive capacity of diamonds is a constant of the diamond and arises from a polarization provided, as on the Lorentz theory, by electronic actions of the same type as those involved in the transmission of optical waves.

Table 6 summarizes the most representative modern values for data which were originally collected by Addenbrooke<sup>(1)</sup>, together with the present result, and indicates that Maxwell's law applies fairly closely for all the elements measured, even though the value of  $n^2$  employed in general is not extrapolated but corresponds to the  $D$  line.

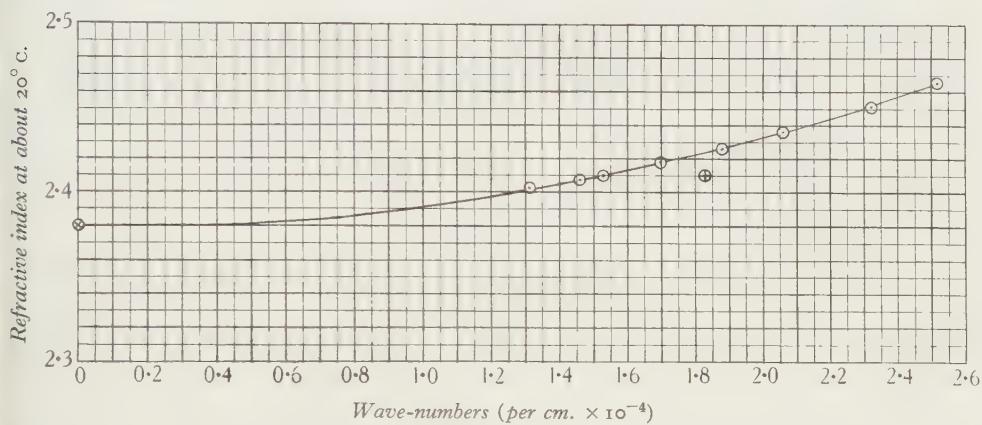


Figure 4. Refractive index of diamond.  $\odot$  Walter.  $\times$  Extrapolated value from Peter.  
+ Robertson, Fox and Martin.

Table 6. Comparison of specific inductive capacity with refractive index

Element		H	He	Ne	Ar	Kr	X	Cl	Br
Gases	$(\epsilon - 1) \times 10^6$	275	72	134	553	838	1353	—	—
	$(n^2 - 1) \times 10^6$	279	70	134	568	854	1404	—	—
Liquids	$\frac{\epsilon}{n^2}$	1.21	1.048	—	—	—	—	—	—
		1.21	1.048	—	—	—	—	—	—
Solids	$\frac{\epsilon}{n^2}$	—	—	—	—	—	—	1.97	3.12
		—	—	—	—	—	—	1.88	2.75

Element		I	O	S	N	P	C	Se	
Gases	$(\epsilon - 1) \times 10^6$	—	543	—	581	—	—	—	
	$(n^2 - 1) \times 10^6$	—	539	—	584	—	—	—	
Liquids	$\frac{\epsilon}{n^2}$	—	1.47	—	1.45	—	—	—	
		—	1.46	—	1.45	—	—	—	
Solids	$\frac{\epsilon}{n^2}$	4.00	—	4.00	—	3.85	5.66	6.14	
		3.70	—	4.00	—	4.14	5.67*	6.04	

\* Extrapolated value.

Cuthbertson<sup>(10)</sup> also arranged the molecular or, more appropriately in the present instance, the atomic polarization of the elements in the form of the periodic table. The atomic or molecular polarization is given by

$$P = \frac{\epsilon - 1}{\epsilon + 2} \frac{W}{d},$$

where  $\epsilon$  is the specific inductive capacity,  $W$  the atomic or molecular weight and  $d$  the density. He then found that certain simple ratios existed between consecutive elements in the same row or column. His data have more recently been revised by Dobieslaw Doborzynski<sup>(11)</sup> and mean values from the most recent observations lead to table 7, in which the value for carbon deduced from the present investigation on the diamond, namely 2·08, has been included.

The value for carbon gives exactly integral relations with hydrogen and helium and approximately simple relations with the other members of Group O. The atomic polarization of an element depends upon the distribution of electron orbits and the screening exercised by the inner orbits. The calculations made by Van Vleck and others become rather complicated when applied to elements of high atomic number. The present relations suggest that these effects are much simpler than the theory would, at first sight, seem to indicate.

Addenbrooke has gone further and has deduced certain relative electric attractions and relative energies from the specific inductive capacity and has compared these quantities with other constants such as the atomic number, melting and boiling points, and surface tension. Owing to the high subliming point of carbon the thermal comparisons do not appear valid for this element, a result which is to be anticipated since the infra-red absorption bands do not seem to be related to the specific inductive capacity whereas, on Lindemann's theory, these oscillation numbers should determine the melting point. As regards atomic number, Addenbrooke's curves for the elements will be unaffected, since although he used Schmidt's value, a slight arithmetical error caused his final result to agree actually with the value found in the present work.

There still remains, however, the question of the effect of temperature. In the method of mixtures the specific inductive capacity of the mixture is a function of the product of the specific polarization of the solid and its relative volume. This product does not change as a result of thermal expansion, so the negative temperature coefficient of the specific inductive capacity due to this cause should be absent. The thermal expansion of the apparatus should not have a primary effect since only ratios are involved between tests on the same apparatus.

Nevertheless, the change with temperature observed in the absolute determinations lay outside the apparent limits of experimental error. On the other hand, the relative tests over a wide range of temperature showed no consistent effect. It seems probable that the specific inductive capacity is substantially independent of temperature, as it should be on the Lorentz theory, and that the variation observed is due either to secondary effects or to a defect in the method of mixtures when the latter is applied to complex liquids not completely stable at the temperature of test. The secondary effects, if valid, are in any case small.

Table 7. Atomic polarizations in periodic table

Period	I Group	IV Group	V Group	VI Group	VII Group	O Group	Cuthbertson's relations*	
							$\frac{1}{2}$	I
I	H 1.04	C 2.08	N 2.20	O 1.96	F 1.45	He 0.52		
II	Si ?	P 8.98	N 4.08	S 8.08	Cl 5.6	Ne 1.01		
III		As ?		Se 11.7	Br 8.6	Ar 4.15	Ar Ne = 4.11	4
IV					I Cl = 2.50	Kr 6.31	Ar He = 1.52	6
	Mean ratios to O group	2.00	2.06	2.17	1.92	1.38	X 10.12	10
							X Ne = 10	
							X He = 19.5	
							I	

\* Ratio of periods to period I.

### § 5. CONCLUSIONS

(a) An accurate determination of the specific inductive capacity of diamonds in bulk indicates that the value is  $5.68 \pm 0.03$  at room-temperature and at frequencies from 500 to 3000 c./sec. The most accurate determination gave 5.66 at 800 c./sec. and 27.8° c. There appears to be a slight increase with temperature of the order of 1.5 to 2.5 per cent at about 60° c. This, however, is not consistent, and comparative observations indicate that the specific inductive capacity is, in general, constant to within 2 per cent from -65° c. to +85° c.

(b) The specific inductive capacity of diamonds has been shown to be independent of frequency to within a standard error of 1.5 per cent from 300 to 3000 c./sec., of 3.2 per cent from 50 to 5000 c./sec. and of 2 per cent from 800 c./sec. to 1.6 Mc./sec.

(c) The value so found agrees with Schmidt on single stones within the limits of error of the latter's measurement. It is higher than that found by Robertson, Fox and Martin, but the single stones employed by them introduced considerable difficulties of measurement. It is also in agreement with the optical refractive index on the basis of Maxwell's law.

(d) The specific inductive capacity of the diamond is thus probably a true constant of the crystalline element, in agreement with the hypothesis of Lorentz. The relationship with the atomic number and position in the periodic table envisaged by Addenbrooke and Cuthbertson is confirmed, but the connexion with other, particularly thermal, constants is open to doubt.

(e) The method of mixtures employed in the experiments offers possibilities of the accurate determination of the specific inductive capacity of solids in the form of small particles or powders, but it is unsafe to employ formulae for extrapolation from measurements on mixtures.

### § 6. ACKNOWLEDGEMENTS

The authors wish to renew the acknowledgements already made in the course of this paper and at the same time to thank those colleagues who assisted in the continuous operation of the tests throughout the period for which the diamonds were available. The thanks of the authors are also due to the Director of the British Electrical and Allied Industries Research Association for permission to publish this paper.

### REFERENCES

- (1) ADDENBROOKE. *Phil. Mag.* **47**, 945-65 (May 1924) and **50**, 225-43 (January 1926).
- (2) PIRANI. Dissertation, Berlin (1903).
- (3) SCHMIDT. *Ann. Phys., Lpz.*, **9**, 919 (1902) and **11**, 114 (1903).
- (4) ROBERTSON, FOX and MARTIN. *Philos. Trans. A*, **232**, 463 (1934).
- (5) ROSENHOLTZ and SMITH. *Amer. Min.* **21**, 115 (1936).
- (6) COHEN and OLIE. *Z. phys. Chem.* **71**, 385 (1910); *Commun. Phys. Lab. Univ. Leiden*, no. 113 (1911).
- (7) WIGAND. *Ann. Phys., Lpz.*, **22**, 64, 99 (1907).
- (8) WALTER. *Ann. Phys., Lpz.*, **42**, 505 (1891).
- (9) PETER. *Z. Phys.* **15**, 358 (1923).
- (10) CUTHBERTSON. *Philos. Trans. A*, **204**, 323 (1905).
- (11) DOBORZYNSKI. *Acta phys. polon.* **4**, 219 (1935).

## DISCUSSION

Mr G. L. ADDENBROOKE. My work on connexions between the specific inductive capacity of the non-metallic elements and their other properties has been referred to in the paper. It was in connexion with this that the uncertainty of the electrical data regarding carbon in the form of the diamond, and the desirability of obtaining completer and more accurate data became apparent, not only from a theoretical point of view, but also from the important part carbon plays in the constitution of so many insulating materials. It is now some six years since I brought this to the notice of Mr Wedmore, director of the Electrical Research Association, and obtained the offer of the Association to co-operate in the necessary work, the results of which are before you in this paper. Briefly the work covered by the paper divides itself under two headings: the first covers the theoretical considerations which must be taken into account when one is dealing with a mixture of substances, the other covers the methods of manipulation to be used in dealing with substances in granular form which require a number of experiments and need complete washing and drying between each set. I think Dr Whitehead has succeeded in putting in very convenient form the points which must be taken into account theoretically in dealing with mixed substances; and again I think much credit is due to Miss Hackett for the successful way in which she has carried out the experimental work without any loss from the 4000 stones which were involved in the experiments.

On p. 183 of the paper the authors have given a very neat table in which the specific inductive capacity of the non-metallic elements is compared with the square of the refractive index. This shows how closely Maxwell's law is obeyed and should, I think, be quoted in text-books in the future, as it puts Maxwell's law on a clear and solid basis. The law also covers a number of compounds in which hydrogen is united with the non-metallic element, but it fails when oxygen is included in the compound.

I was anxious in these experiments to see how carbon would fall in with the other elements, as its atomic volume 3·4 is so very small in comparison with theirs—for instance, that of iodine, which is about 27. Now the molecular polarization of carbon according to the formula  $\text{atomic volume} \times (E - 1)/(E + 2)$  is about 2·2 and thus falls into its proper place in a diagram representing atomic numbers as abscissae and the relative polarizations or attractions as ordinates. Such a diagram also shows how the inductive capacities of these elements vary with their atomic numbers and their positions in the periodic table.

It does not seem to be generally recognized what a fundamental property specific inductive capacity is. For instance, to give one of these non-metallic elements an electric charge is to store energy in it in accordance with its atomic number and weight, and its position in the periodic table. If, now, the temperature of the element is raised or lowered, there is hardly any change in the inductive capacity or in the energy stored, and this is the case down to the absolute zero of temperature. But heat is also a storage of energy, and though this storage per

degree does not vary much above ordinary temperatures, it falls off rapidly until it becomes negligible near the absolute zero of temperature.

It is true that the electrical storage of energy is effected by creating strains between the oppositely charged components of the atoms while the storage of heat, so called, is effected by increasing the motion of vibration of the atoms or molecules as wholes. This motion of the atoms or molecules of the substance itself is, however, brought about initially by production of strains due to electromagnetic radiations from the source which produce similar strains in the atoms to those set up by an ordinary electric charge and these by resonance cause a vibratory motion of the molecules which is dissipated in subsidiary radiations through the substance giving rise to heating, except when it is transparent, that is, when the radiations are propagated through the substance in an orderly manner and without irregular dissipation of their energy.

Dr D. OWEN. The principle of the mixture method employed by the authors in their capacity bridge determination of the dielectric constant of diamonds seems the only sound one to employ in a condenser method when the specimen is given in fragmentary form. Thring proposed a formula to deal with the calculation in the case of a mixture of a liquid and a solid dielectric, but there is no doubt that the formula is unsound. The true approach is to find a liquid whose dielectric constant is equal to that of the solid, or, as is shown in the present paper, by interpolation from a series of experiments using different combinations of two liquids miscible in continuously variable proportions, one of higher, the other of lower dielectric constant than that of the solid. The authors have succeeded in finding two suitable liquid media for the purpose, and there seems little reason to doubt the substantial accuracy of their final results.

Mr Addenbrooke is to be congratulated on his successful offices in making the present investigation possible, as well as on his fruitful work over many years on the subject of dielectrics. His suggestive papers provide a mass of data ready to the hand of the mathematical physicist. At his suggestion Miss A. I. Anderson made a determination of the dielectric constant of another pure element, bromine; this work is also published in the *Proceedings* of this Society. It is noteworthy that in that work, as also in the present work on the diamond, the results agree closely with those of Schmidt, obtained nearly forty years ago, using one of Drude's short-wave methods.

Dr L. HARTSHORN. It occurs to me on rereading the paper that the apparent increase of dielectric constant with temperature at about  $60^{\circ}\text{ C}$ . is almost certainly due to the conductance of the liquid. The measured capacitance of a mixture is proportional to the electrostatic energy stored in it for a given terminal voltage, and therefore depends on the potential distribution as well as on the dielectric constants of the constituents. It is a well-known principle in electrostatics that this energy has a minimum value for the electrostatic distribution of potential, that is to say, for that distribution which is obtained when there is no conduction current. It follows that any departure from this potential distribution arising from inequalities of conductance causes an increase in the measured capacitance. Strictly speaking,

the method of mixtures is only valid when the frequency is so high that the conduction current is negligible in comparison with the displacement current, in other words, when the power factors of all the materials are small.

In the present experiments the conductance of the liquid was clearly much greater than that of the diamonds, and increased with rise of temperature. The result was an increase of capacitance with rise of temperature, or an apparent increase of dielectric constant  $\epsilon_s$ . The lower the frequency the greater is the ratio of conduction current to displacement current, and therefore the greater the apparent increase of  $\epsilon_s$ . For the experiments over an extended range of temperature the diamonds were in air the conductance of which was too small to produce such an effect.

These considerations might suggest that the authors' results are all too high, but the evidence provided by the observations shows that apart from the apparent effect of temperature already discussed, the error due to conductance is not likely to be very important. For an error of this kind is necessarily associated with an apparent diminution of dielectric constant with rise of frequency, and although it is unfortunate that circumstances did not permit observations over a wider range of frequencies, the values in table 3 are sufficient to show that this effect, which is just noticeable at 54° C., is not detectable at 28° C. The main conclusion to be drawn is that one is justified in neglecting the apparent increase of dielectric constant at a temperature of about 60° C.

Dr A. E. MARTIN. Dr Whitehead has referred to the value of about 5.0 at 1 M./sec. for the specific inductive capacity of diamond, reported by Robertson, Fox and Martin in 1934. This result was obtained for single crystals of the two types of diamond which we had then recently discovered, no measurable difference being found for the two varieties.

More recently Dr Groves and I have repeated the measurements with improved apparatus and have found the value 5.26, which is considerably lower than Dr Whitehead's determination. A possible reason for the lowness of our figure is as follows. In our measurements the diamond in the form of a cleavage plate, several millimetres thick, is sandwiched between electrodes and the capacity measured. Owing to imperfections in the diamond and electrode surfaces small air gaps must necessarily be present and these will cause the value obtained for the specific inductive capacity to be low. For example, it can be shown that a uniform air space equal to 1 per cent of the diamond-thickness would lead to a value nearly 5 per cent low. Such a large air gap as this we believed to be unlikely, and since our method gave for fused silica discs, similar in size to the diamonds, the value 3.69, in agreement with the comprehensive measurements of Jaeger\*, we concluded that no appreciable error arose from the slight air gaps present.

I think it would be worth while if Dr Whitehead could make measurements on fused silica (in small pieces) with his apparatus and see that the same value is obtained as for fused silica in sheet form.

AUTHORS' REPLY. We thank Mr Addenbrooke for his kind remarks and are glad that, even though after some delay, we were able to implement his suggestions. The

\* Jaeger, *Dissertation*, Berlin (1917).

validity of Maxwell's law depends upon the frequency at which the comparison is made and it is necessary for exactitude to extrapolate the refractive index to zero frequency. Accordingly it is truer to say that the specific inductive capacity of these elements obeys classical theory and that the infra-red spectrum has little effect outside its immediate neighbourhood. If frequencies in the neighbourhood of the ultra-violet absorption were considered, the results would be much more complicated. The table of atomic polarizations shows, we think, that to a first approximation, the theory of electric displacement or electronic deformation in elements is much simpler than the mathematical theory so far suggests, since it can be seen that simple integral relationships roughly hold. However, the deviations from these relationships are appreciable and indicate the existence of complicated correction terms.

We agree with Dr Owen that the use of a liquid of equal specific inductive capacity is the best method for powders and fragments. It would, however, have been too laborious to obtain an exactly equivalent liquid, on account of the time necessary for stability, so that we were led to an interpolation method which should not introduce any material errors, since the differences in specific inductive capacities were small. The value for bromine found by Miss Anderson was used in preparing the tables for other elements in the paper.

Preliminary experiments were made on glass beads of dimensions similar to those of the diamonds employed. Only an indirect comparison could be made from a knowledge of the composition and properties of the glass, but this indicated that the method was satisfactory. We hope, nevertheless, to make later a more exact comparison as Dr Martin suggests, but feel that no very considerable error can affect our results.

Dr Hartshorn raises what is perhaps the greatest difficulty in our method, namely, the fact that unless all the electrical properties of solid and liquid are the same, the two are not strictly equivalent. If field-distortion is ignored then it is possible to calculate the error due to the power factor or loss angle  $\delta$  of the liquid and the following correction factor is arrived at:

$$\{1 - (3\alpha - 2\beta) - \frac{2}{3} \tan^2 \delta\},$$

where  $\alpha$  and  $\beta$  are corrections to the bridge equations arising from the same cause. The value of this correction is of the requisite order for the media of highest specific inductive capacity but it cannot exceed 0.8 per cent, in the neighbourhood of interpolation, and is probably a good deal less. Accordingly, the anomalous effect of temperature cannot satisfactorily be explained in this way, although it is still possible that the error as estimated is exaggerated in reality on account of the distorted nature of the field and the additional interpolation error due to the fact that the experimental curves are incorrect in shape. Unfortunately it is not possible to calculate these effects from the data available, but we intend to pursue this point when an opportunity presents itself and may be able to explain the discrepancy. In any case we agree with Dr Hartshorn that the interpolation results at 54° C. should not be taken as implying a true change in the specific inductive capacity of diamonds, unless subsequently they are otherwise confirmed.

## REVIEWS OF BOOKS

*Ions, Electrons and Ionizing Radiations*, by J. A. CROWTHER. 7th edn. Pp. xi + 348. (London: Edward Arnold and Co., 1938.) 12s. 6d. net.

There is probably no text-book in any branch of physics which is more widely recommended to science degree students in British universities than this well-known volume of Prof. Crowther. It is now nearly twenty years since the first edition was published and a generation of students has found in it a wealth of information clearly expressed and well illustrated. Progress in this field has been so rapid during the four years since the last edition appeared that teachers and pupils will welcome the additions to the text that have been made, not only in re-written chapters but also from point to point throughout the volume.

Readers will naturally turn to the chapters dealing with modern atomic and nuclear physics. Here they will find a most admirable selection of the old and the latest material, full but not overloaded. One would perhaps have preferred an order of presentation which postponed a description of artificial and induced radioactivity until after the law of radioactive change had been enunciated, but this is only a minor point.

In the reviewer's opinion the earlier chapters are less happy because here the revising pen has not been sufficiently used. For instance, the majority of physicists would not now accept the early explanation of spark discharge given in chapter v if Townsend's  $\beta$  is related to the ionization of gas atoms by the impact of positive ions. Perhaps it is personal prejudice which makes the reviewer wish to see the section on mobility rewritten. Amongst other things he would like to see the method of Tyndall and Powell published in 1930 substituted for that of Tyndall and Grindley which it quickly superseded; it is also much simpler for students to understand.

These minor criticisms may serve to introduce a suggestion that the reviewer wishes to make, namely, that in the next edition, which must again follow within a few years, some of the subject-matter of the book should be re-arranged as well as re-edited. There has been a great change in the relative importance of different parts of the subject during the past twenty years. In its general form the book follows the traditional order first adopted by J. J. Thomson in his early treatise. Subjects such as mobility, recombination and spark and glow discharge loomed large in the researches of that period. To-day they must take, in their details, a second place in a student's curriculum, partly because they are now less important and partly because information on them is still comparatively unprecise. To emphasize this we have only to compare our present knowledge of the action of a thermionic valve with that of a Geissler tube, which was the show piece of an earlier period. There is, therefore, much to be said for abandoning the historical introduction to the subject and discussing in the first place phenomena at low pressures, from which one can then proceed to the more complicated problems brought about by the addition of gas. Such changes in the presentation would make more demands on the time of the author in a busy life; but if they were undertaken the value of the book, already obvious, would be enhanced.

A. M. T.

*Electron and Nuclear Physics*, by J. BARTON HOAG, Ph.D. Pp. ix + 502. (London: Chapman and Hall, Ltd., 1938.) 20s. net.

Designed to bridge the gap between elementary and advanced physics, this book aims "to present the experimental evidence for those concepts which lie in the domain of electron and nuclear physics". It consists of a survey of modern atomic physics treated

from a strictly practical point of view. The electron is discussed in all its aspects, and x rays, nuclear phenomena and cosmic rays are all considered. A section on laboratory technique is included. The subject matter is of great interest, and the gathering together of such a store of information in one book represents a useful service, especially as numerous references are given to original papers. In view of this, it is a pity that the book is written in a loose and often inaccurate fashion. Thus, speaking of the Compton effect, the author says: "However, most of the energy of these deflected rays are found to have a small but definitely longer wave-length." Again, the definition of the röntgen is inaccurately given and loose statements of various kinds crop up continually. The book in its present form certainly fails to do justice to the considerable amount of work which must have gone towards its compilation.

J. T.

*Fluorescence and Phosphorescence*, by E. HIRSCHLAFF, Ph.D. Pp. vi + 130. (London: Methuen, 1938.) 3s. 6d. net.

This recent addition to Methuen's well-known series of physics monographs can be thoroughly recommended to honours and post-graduate students in physics and physical chemistry, and especially to those who wish to know something of the spectroscopic basis and the modern technical applications of fluorescence. In twelve short chapters the author deals admirably with such matters as experimental methods, fluorescence spectra of atoms and molecules, quenching of fluorescence, collision processes, photochemical aspects, fluorescence in liquids and solutions, fluorescence and phosphorescence in solids, details of the absorption and emission process in phosphors, cathodo-luminescence in solids, liquids and gases, technical applications. The text is adequately illustrated with 42 line diagrams, such as atomic and molecular energy-level diagrams, intensity-distribution curves, etc., and a short bibliography is given at the end of every chapter.

W. J.

*Modern Atomic Theory*, by J. C. SPEAKMAN, M.Sc., Ph.D. Pp. 208. (London: Edward Arnold and Co., 1938.) 6s. net.

There will be wide agreement with the author in his belief that a logical rather than an historical treatment of modern atomic physics is now not only possible, but also, for teaching purposes, desirable. In this excellent little book the author has attempted such a treatment with as little compromise as possible, and the attempt appears to be very successful indeed. The book is intended to supplement ordinary text-books of Physics and Chemistry for students in the universities and colleges and also in the higher forms of schools. One might go so far as to say that every student of Physics and Chemistry should read it as soon as possible after his Intermediate Science examination as a prelude to his study of larger works on atomic structure.

When a second edition is called for, as it surely will be, attention might be given to the use of parentheses with the solidus in a few expressions, such as those for the mass of the proton (p. 39, fifth line) and a de Broglie wave-length of cathode rays (p. 61, seventh line). To be strictly accurate it should be stated that the velocity and wave-lengths quoted on p. 52 are in vacuo, and that much of the important work on the isotope effect in band spectra (p. 147) was done before, as well as since, 1929.

W. J.

*A Course in Chemical Spectroscopy*, by H. W. THOMPSON, B.Sc., M.A., D.Phil. Pp. vii + 86. (Oxford University Press, Humphrey Milford, 1938.) 6s. net.

In view of the use of the word "chemical" in this title it would be well to point out at once that the book is concerned not with the spectrographic analysis of materials but with the analysis of atomic and molecular spectra in accordance with the quantum theory.

The book is based on a laboratory course introduced by the author for undergraduates reading the Final Honour School of Chemistry at Oxford, but will be equally suitable for physics students. The course consists of eight well chosen experiments or groups of observations, each of which brings to the student's notice an important section of spectral theory. The equivalent of a chapter of the book is devoted to a description of each experiment or group, its underlying theory, the apparatus to be used and the procedure to be followed, with tables, diagrams, plates of spectrograms and references to other spectroscopic works. The interweaving of theory and practice is one of the valuable features of the book. The student is guided through instructive exercises based on observations of typical atomic, diatomic and polyatomic spectra, some in emission and some in absorption. Some of these exercises are a graphical determination of the Rydberg constant, the identification of series of atomic lines, the construction of Grotrian diagrams of atomic terms, analysis of the vibrational structure of an electronic band system, analysis of the rotational structure of an electronic band of simple type, the recognition and significance of predissociation, the spectroscopic determination of dissociation energy, the plotting of potential energy curves of a diatomic emitter, and a study of the alternating intensities in an infra-red absorption band of acetylene. Could a course be more instructive than this?

W. J.

*The Elements of Physics*, by A. W. SMITH. Fourth edition. Pp. xix + 790. (McGraw Hill Publishing Co., 1938.) 21s.

A book which passes into its fourth edition has found for itself a secure place in the literature of science. The author in his present revision has made changes and additions which were suggested as desirable by users of the book. He states that increased emphasis has been placed on the importance of physics in the other sciences and in the industries. It has been found necessary to rewrite some of the paragraphs relating to modern physics, and to introduce a separate chapter on nuclear physics.

The ground covered is surprisingly large. One finds a concise account of x rays and crystal structure, series in optical spectra, radioactive substances, the thermionic valve, and the cyclotron, to mention but a few. A chapter is devoted to astrophysics and gives a clear impression of the applications of physics in modern astronomy. At the present day it requires some courage to attempt to compass within a single volume the range of subjects embraced by the word "physics"—one recalls the massive size of Ganot's *Physics*—but the author has been very successful in his efforts to select the material which is likely to be of importance to the present-day student. The book is an attempt to lay the basis for correct scientific thinking, and little attention is given to historical developments.

The illustrations include a number of coloured plates.

E. G.

*A Textbook of Electricity*, by H. G. MITCHELL, M.A., B.Sc.  $7\frac{1}{2}$  in.  $\times$  5 in. Pp. xiii + 525, 357 diagrams. (London: Methuen and Co., 1938.) 10s. net.

This book is intended to provide a complete course in electricity and magnetism for Higher School Certificate, Intermediate and University Scholarship candidates, and also to meet the main requirements of students preparing for pass degrees and examinations such as the Cambridge Tripos, part I.

The appearance of a new text-book on this subject, of the standard indicated, is a matter of no little interest. The speed of growth of this side of physics demands new renderings of its subject-matter, and any fresh and balanced treatment, such as that of the present book, is to be welcomed. The author has worked out his own line of treatment;

he generally singles out the points of real physical interest, and smoothes the places usually presenting difficulties to the first-time reader. The portions relating to electro-chemical actions (chapters, vi, vii and xix) are notably well and fully treated. In chapter viii the subject of the magnetic field is introduced on the basis of electrodynamic action, the idea of magnetic pole following as a secondary mode of treatment. This is admittedly a logical procedure, but it is not easy to put it into execution, and many teachers will question its advisability, though it should not be shelved without a trial.

A few points of criticism may be of service. The argument of § 27 (following on Gauss' theorem) is hardly cogent, as the sign of  $E$  is not shown to be the same at all points of the closed surface. In the same chapter the terms polarization, displacement and induction might be more clearly distinguished: the term "polarization" as applied to electrically strained media has unfortunately been used in different senses by some distinguished writers. In § 43 the electrolytic condenser is described, but it is not quite clear that its use is limited to cases where the applied voltage is unidirectional. Figure 102 (magnetic field of helix) needs some emendation. In chapter xi Schuster and Smith's determination of  $H$  is described, and we are informed that a "fairly accurate" value may be calculated: this is a considerable understatement of the value and importance of this method. In § 180 the laborious method of successive approximations in order to convert "platinum degrees" into degrees Centigrade seems unnecessary, as the correction can be read from a simple graph. On p. 314 some of the statements in regard to paramagnetic and ferromagnetic substances need a little revision, and there is a contradiction between one of these and a later statement in the first paragraph of § 215. In describing the magnetometric method of obtaining the magnetization curve a vertical solenoid might with advantage be substituted for a horizontal one. These critical suggestions are included in no spirit of detraction from the general excellence of this text-book, which can be heartily recommended to teachers and students.

D. O.

*Moderne Mehrgitter-Electronenröhren*, von Dr M. J. O. STRUTT. (Eindhoven. Vol. I, pp. vi + 143, 1937; Vol. II, pp. viii + 129, 1938; Berlin: Julius Springer. Vol. I, RM. 12.60; Vol. II, RM. 13.50.)

The first volume of this book deals with the construction, modes of application, and the characteristic properties of the multi-grid thermionic tubes used in wireless receiving circuits. The competent knowledge of physics and mathematical equipment which the author brings to his task are supplemented by practical experience gained in his own researches on the behaviour of electron tubes. Attention is directed to recent developments, through tetrode, pentode and so on up to octode.

This volume is divided into three sections: the first dealing with high-frequency amplifiers, over wave-lengths down to one metre; the second with frequency-changers; the third with low-frequency power amplifiers. Studies of special phenomena, such as secondary emission and electron beams, also find a place. The author presents a thorough treatment of the various effects involved, and of problems such as the measurement of the characteristic admittances, which should be of great assistance to the designer who aims at the improvement and further development of multi-grid tubes in their various possible applications. At the end a list of references is given to 227 original papers.

The second volume treats more intimately of the actions in the different regions of the various types of tubes. The problem of the motion of an electron in electric and in magnetic fields, and in combinations of these, is first treated. Then in due course the movement of electrons in the tubes, transit times, the actions in the space from screen-grid to anode, are subjected to detailed consideration. Electrostatic theory is applied to the calculation

of inter-electrode capacitances; and the effect of space-charge, leading to the "dynamic", values, is determined. This volume includes a list of references to a further 68 papers.

In both volumes ample specific data are supplied, and examples of theoretical calculation and application to tubes of which the constructional data are given, and the results of practical measurements, are clearly set forth. Both volumes are fully illustrated with diagrams and photographs. The specialist should find the contents of this book of great value over the whole range of multi-grid electron tubes.

D. O.

*Applied Geophysics in the search for Minerals*, by A. S. EVE and D. A. KEYS. Third edition. Pp. x+316. (Cambridge University Press.) 16s.

This third edition follows the lines of the previous editions and is primarily concerned with electrical and electro-magnetic methods of prospecting for minerals. In this branch of applied geophysics the book maintains its established reputation, but in other respects the new edition is disappointing. There is no adequate treatment of the very great progress in gravitational and seismic methods during the five-year interval since the previous edition. It is true that one finds a new chapter on "Recent advances", but in this only two pages or so are devoted to the seismic reflection method, and there is no mention at all of the recently developed static gravimeters of remarkable sensitivity, which have so greatly accelerated the rate of gravitational surveying. As a general treatise on applied geophysics the book thus remains unbalanced, and meagre in its information regarding those branches which are of the widest practical application in the search for oil.

The arrangement of the subject-matter is generally good, except in the chapter entitled "Radio-active and other methods". Here one finds unexpectedly an odd assortment of sections with sub-titles such as "Salt domes", "Geophysical exploration in Australia", "Brief notes on diamond drilling", and the like, which seem to be inappropriately placed. The text is pleasant to read, and the authors evidently believe in a mixture of fun and sober truth, for they frequently adopt the gay manner, and more than once emphasize the wit with exclamation marks.

Readers interested in appendix IV should note an error which apparently escaped revision, and rather spoils the elegance of Dr L. V. King's proof. The velocity  $v_0$  is not the surface velocity as stated, but that at the point of greatest penetration of the ray.

A. O. R.

*The Phase Rule and Phase Reactions*, by SYDNEY T. BOWDEN, D.Sc., Ph.D., F.I.C. Pp. 290. (London: Macmillan and Co., Ltd., 1938.) 10s.

This book should appeal to a wide variety of readers. The treatment is clear and simple enough for the student to whom the subject is new, yet sufficiently ample to interest the more expert reader. There are copious descriptions of experiments and a wealth of excellent diagrams to illustrate the theory, but only few references to original experimental data. At the end of each chapter is a selection of examination questions of standard varying from that of the Higher School certificate to that of the tripos.

The single-component systems described include  $D_2O$ ,  $CO_2$ , Sn, C as well as the more usual ones. As is natural, about two-thirds of the book is devoted to systems of two components. There is a clear elementary description of the theory of a simple distillation of a mixture in the absence of a fractionating column. The description of fractional distillation omits the most important point, that the process occurring in the fractionating column is effectively a large number of successive simple distillations. The statement on p. 119 that "the process of fractional distillation can be used only for the separation of

zeotropic mixtures" is inexact and contradicts the correct statement on p. 114; it can become true if for "separation" one reads "complete separation" and transposes the word "only". The description of ideal solutions is brief but accurate. That of other solutions is less satisfactory. There is an irrelevant reference to "internal pressure" which is not even defined. The curves in figure 75, illustrating deviations from Raoult's law, are impossible; the correct shapes should resemble the middle curve in figure 76, showing an approach to Raoult's law for an almost pure component. In discussing optical isomers the author states that according to wave mechanics the d- and l- forms of a component must differ slightly in energy and rotatory power. This is impossible and the author must have been misinformed. The last chapter of the book gives an interesting summary of the properties of anisotropic liquids. Some of the stated derivations of words are inaccurate or obscure. In particular "azeotropic" is stated to be derived from the Greek meaning "privative, to boil"; the correct meaning is surely "not changing on boiling". Again, "eutectic" means "well-melting", not "easy melting". The book concludes with an appendix which is an amplification of a letter to *Nature* by the author. It would take too much space to discuss the views put forward. In the reviewer's opinion they are inaccurate and misleading.

In spite of such small defects as those enumerated the book is an enjoyable one to read and a useful one to possess.

E. A. G.

*A Text-book on Thermodynamics*, by F. E. HOARE, Ph.D., M.Sc., A.R.C.S., D.I.C.  
Second Edition. Pp. xii + 302. (London: Edward Arnold and Co., 1938.) 15s.

In the second edition of this book there have been few alterations in the text, and it remains as valuable a treatise for students of thermodynamics as was the first edition which was given so good a reception by its various reviewers six years ago. The most extensive alteration is that of bringing the symbols used throughout the text into line with the recommendations of the joint committee of the Chemical Society, the Faraday Society and the Physical Society. To the text some eight to ten pages of new material have been added. There have also been added two appendices and a collection of representative and useful examples. The first appendix deals with the recommendations with regard to symbols, and the second gives the adopted and most probable values (after Birge) of some fundamental constants. In addition to extensions to the text certain other modifications have been made, as for example in the section dealing with the Stefan-Boltzmann law and in the discussion of the quantum theory of the specific heats of gases, which latter has also been slightly extended. Further modifications might perhaps be made with advantage; for instance, from the second paragraph on p. 22 in the treatment of the first law it would appear "from the foregoing discussion" on pp. 21 and 22 that it is to be concluded that the internal energy is a single-valued function of any two of the variables defining the state of the substance. This fact has, however, been assumed in formulating equations 12 and 13 at the beginning of the discussion, and might well be mentioned at that stage. The method of approach to the definition of entropy, in the first part of § 27, is perhaps a little unfortunate and is liable to start that entropy complex which is characteristic of the outlook of so many students of thermodynamics. Could not the appearance of a new single-valued function of the variables defining the state of the substance in the last equation of § 26 be made the basis of the entropy definition? The fact that the entropy is such a single-valued function does not re-emerge till the second paragraph of § 27. Further, there is still no mention of that important aspect of entropy—its correlation with the probability of a system existing in a given state.

Lastly it seems strange that the author, who was once one of Callendar's pupils, should not have found place in his book for some reference to Callendar's work on the nature of

the  $PV$   $P$  isothermals in the neighbourhood of the critical point as illustrated by the  $H/P$  isothermals in figure 2 of Callendar's last paper.\* Instead, as in figure 6 of the present book, the saturation lines are shown to be parabolic without comment. Callendar once remarked that there is a time lag of about twenty-five years before mention of such work is likely to be made in text-books, so there is another fifteen years to go! Table V on p. 112 giving values of the saturation pressure for steam up to  $200^{\circ}\text{C}.$ , which has been taken from the 1920 edition of Callendar's *Properties of Steam*, is rather out of date, as data up to the critical point have been available for some ten years.

With regard to the presentation of the subject-matter it seems a pity that such thick lines should have been used for some of the diagrams, which in many cases look like linocuts. Figure 18 in fact looks, inappropriately enough, more like the announcement of a bereavement. In the reviewer's copy the printing on pp. 129 to 131 has not been very carefully done. The points of criticism which have been made are not, perhaps, of great importance, and a second edition of a book of such obvious use to honours students is to be welcomed. A third edition will, however, be looked forward to, and it is to be hoped that these criticisms, if they are sufficiently well founded, may receive more consideration in the writing of the third edition than do the "minor matters" raised, in the review of the first edition,† appear to have received in the second.

W. B. M.

*Stellar Dynamics*, by W. M. SMART. Pp. viii + 434. (Cambridge University Press, 1938.) 30s.

After his magnificent *Spherical Astronomy*, it is not surprising that Dr Smart has been able to produce a readable, though mathematical, book on the general subject of stellar dynamics, in which he includes stellar kinematics. The theories of the single and double star streams are vaguely familiar to many who are not astronomical specialists, and here is a very pleasant account of what the theories are, how they are tested, and what their further interpretation may be, written by a specialist with due regard to the needs of his fellow specialists. Such matters as the change from one set of co-ordinates to another are considered in full detail, and doubtless add much to the value of the book for the specialist, since all his reference formulae lie within one pair of covers. On the other hand, those who care to skip such passages will find that they can follow the threads of the main story quite easily, and the book is a far better account, for those seriously interested, than most of those specially written for popular consumption. It deals in turn with star drifts and the ellipsoidal theory of Schwarzschild, statistical parallaxes, space distribution of stars, star clusters and the most general theories of stellar dynamics. Scattered through the book is a large amount of work on the statistical treatment of observations, which is probably unknown to most statisticians and workers in fields outside that of which this book treats.

J. H. A.

*Introduction to Bessel Functions*, by F. BOWMAN. Pp. ix + 135. (Longmans, Green and Co., 1938.) 10s. 6d.

This little text-book forms an admirable introduction to the use of Bessel functions for a student. It will probably also prove useful to the research worker as a handy compendium of the simpler formulae and results. It contains seven chapters, of which the first five deal with the function of zero order only. The function  $J_0$  is first defined from its power series. Thus the differential equation is obtained, and the function  $Y_0$  is deduced as the second solution. The simpler integrals involving  $J_0$  are then discussed, the expansions of Fourier-Bessel and Dini of zero order are treated, and the arrangement of the

\* *Proc. Roy. Soc. A.* **120**, 460 (1928).

† *Proc. Phys. Soc.* **44**, 615 (1932).

zeros of  $\mathfrak{J}_0$  is dealt with. Applications to vibration of membranes, oscillation of chains and conduction of heat are next mentioned. The modified functions of zero order,  $I_0$  and  $K_0$ , are then introduced and developed by the same methods as  $\mathfrak{J}_0$  and  $Y_0$ . Their application to problems of flow of heat and of alternating electric currents is dealt with, and Kelvin's ber and bei functions are defined. Next follows a chapter on definite integrals involving  $\mathfrak{J}_0$ , such as Lipschitz's and Weber's integrals. Then Hankel's contour integral is introduced, and thus are found the asymptotic expansions for all the functions of zero order.

Now the functions of any real order are introduced; they are defined in the same way as those of zero order, and it is shown that they obey the appropriate differential equation. The recurrence formulae are proved, Sonine's first finite integral is deduced, and the occurrence of zeros and the behaviour of the functions for high values of the argument are discussed. Lastly a number of transformations of the differential equation are given. Applications to the problems of planetary motion, critical length of a vertical rod, and the vibration of circular membranes are then treated.

A considerable number of informative examples are given throughout the book, in particular the reviewer notes that the useful Struve function is defined and its asymptotic expansion is given in examples. The subject of one example is the monotonic function  $H_0 - Y_0$ , which has important physical applications in hydrodynamics.

A short table is given at the beginning of the book—not at the end as stated on p. 15—showing the course of the function  $\mathfrak{J}_0$  and  $\mathfrak{J}_1$  and also giving a few of the smaller zeros of  $\mathfrak{J}_2$ ,  $\mathfrak{J}_3$ ,  $\mathfrak{J}_4$  and  $\mathfrak{J}_5$ . A very short but useful index is given, and the general printing and appearance of the book are excellent. A number of references appear for the reader who desires further information.

C. W.

*Funktionentafeln—Tables of Functions*, by E. JAHNKE and F. EMDE. Pp. xii + 305. (B. G. Teubner, Leipzig, 1938.) RM. 15, less 25% abroad.

A book of mathematical tables is of use to any particular user, if (a) it tabulates the function in which he is momentarily interested, (b) over the range which he is concerned, (c) to a sufficient number of significant figures, and if (d) the entries can be relied on as accurate. It is also desirable (e) that the interval of the argument should permit of easy interpolation and (f) that the meaning of any devices used to economize space should either be evident at first glance, or prominently explained.

When Jahnke and Emde's book first appeared in 1909 it came nearer than any other to fulfilling requirement (a), and even the first edition still stands among the first three books from this point of view. It opens, for example, with tables of  $x^{-1}\tan x$  and  $x \tan x$  and contains a very wide collection of tables relating to Bessel and elliptic functions. Since the authors were not publishing original calculations but only collecting and so making available the work of others, they could not be blamed for any failure to comply with requirements (c), (d) or (e), though such failures were fairly common. Thus, a section of the table of  $x \tan x$  mentioned above is reproduced in table I, and it will be seen that the intervals are too great for easy interpolation.

Table I

$\pm x$	$x \tan x$
1.2	3.0866
1.3	4.8627
1.4	8.2627
1.5	21.1523
$\pi/2$	$\infty$

The present edition is the third, and has been very considerably enlarged. A feature is the large number of graphs, many of them perspective drawings of three-dimensional figures, showing the behaviour of many of the functions dealt with. Another point is the consistent use of English as well as German in the text, and even in the contents, prefaces, index and list of figures. The page is somewhat taller, but contains no more printed matter. The fount used gives rather a heavy impression, but the size is such that this makes for easy reading and little or no eye-strain.

As regards the actual contents, the tables relating to trigonometrical and hyperbolic functions have been omitted, and it is stated that a second volume containing them will appear shortly. In any case, several convenient books of tables are now available which include them. Although the elementary functions have been omitted, the book is more than 100 pages longer than the first edition, partly on account of the illustrations and partly owing to the inclusion of new tables. The table of contents groups them into eleven sections; the sine, cosine and logarithmic integrals, the factorial function, the error function, the theta function, elliptic integrals, elliptic functions, Legendre functions, Bessel functions, the zeta function, the confluent hypergeometric functions and the Mathieu functions. In every case there is an introductory section giving the main properties of the functions, and references to tables which have been published elsewhere.

It is manifestly impossible to examine the book throughout for accuracy, though experience with the first edition suggests that on the whole it is very reliable. The one table which has been examined with care is disappointing in this respect, though probably not typical.

It is the table of  $C(u)$ , the cosine integral  $\int_0^u \cos \frac{1}{2}\pi u^2 du$ . Since the first edition appeared, the table of  $C(u)$  has been recalculated by Lash, Miller and Gordon, and there are seven places where their table differs from that of the first edition. In the third edition, one of these entries has been altered to agree with Lash, Miller and Gordon, but the other six have not. The values concerned are set out in table 2.

Table 2. The cosine integral

$u$	1st edition	Lash, Miller and Gordon	3rd edition
0.1	0.0999	0.1000	0.0999
0.8	0.7230	0.7229	0.7230
1.1	0.7648	0.7638	0.7648
1.8	0.3363	0.3337	0.3337
4.5	0.5258	0.5260	0.5258
5.1	0.4987	0.4998	0.4987
7.3	0.5393	0.5190	0.5393

The first two cases are not very important, whilst an inspection of the differences of the 4th or 5th order leaves no doubt that the correct value in the next entry is 0.7638. I have found by calculating  $\int_{5.0}^{5.1} \cos \frac{1}{2}\pi u^2 du$  by Simpson's rule (using 21 ordinates and checking with 11 ordinates) that the true value at  $x = 5.1$  is 0.4998. Again, a series expansion requires only two terms to verify that  $C(0.1)$  is 0.1000 and not 0.0999, whilst five terms suffice to show that the value of  $C(0.8)$  is nearer 0.7229 than 0.7230. There is thus no doubt that at least four, and possibly six, of the values in the table in the third edition are wrong.

One other criticism is possible, in respect of the abbreviations. The table of  $x!$  on p. 14 ends thus:

$$x! = \Pi x = \Gamma(x+1)$$

$x$	0	1	2	3	4	5	6	7	8	9	$d$
0,0	0,9	—	943	888	835	784	735	687	642	597	555
1		514	474	436	399	364	330	298	267	237	209
2		182	156	131	108	085	064	044	025	007	*990
3	0,8	975	960	946	934	922	912	902	893	885	879
4		873	868	864	860	858	857	856	856	857	859
5		862	866	870	876	882	889	896	905	914	924
6		935	947	959	972	986	*001	*017	*033	*050	*068
7	0,9	086	106	126	147	168	191	214	238	262	288
8		314	341	368	397	426	456	487	518	551	584
9		618	652	688	724	761	799	837	877	917	958
1,0	1,0	000	043	086	131	176	222	269	316	365	415
1		465	516	568	621	675	730	786	842	900	959
2	1,1	018	078	140	202	266	330	395	462	529	598
3		667	738	809	882	956	*031	*107	*184	*262	*341
4	1,2	422	503	586	670	756	842	930	*019	*109	*201
5	1,3	293	388	483	580	678	777	878	981	*084	*190
6	1,4	296	404	514	625	738	852	968	*085	*204	*325
7	1,5	447	571	696	824	953	*084	*216	*351	*487	*625
8	1,6	765	907	*051	*196	*344	*494	*646	*799	*955	**113
9	1,8	274	436	600	767	936	*108	*281	*457	*636	*816
2,0	2,	000	019	037	057	076	095	115	136	156	177
1		198	219	240	262	284	307	330	353	376	400
2		424	448	473	498	524	549	575	602	629	656
3		683	711	740	768	798	827	857	888	918	950
4		981	*013	*046	*079	*112	*146	*181	*216	*251	*287
5	3,	323	360	398	436	474	513	553	593	634	675
6		717	760	803	846	891	936	981	*028	*075	*122
7	4,	171	220	269	320	371	423	476	529	583	638
8		694	751	808	867	926	986	*047	*108	*171	*235
9	5,	299	365	431	499	567	637	707	779	851	925
3,0	6,	000	076	153	231	311	391	473	556	640	726
1		813	901	990	*081	*173	*267	*362	*458	*556	*656
2	7,	757	859	963	*069	*176	*285	*396	*508	*622	*738
3	8,	855	975	*096	*219	*344	*471	*600	*731	*864	*999
4	10,	136	275	417	561	707	855	*005	*158	*314	*471
5	11,	632	795	960	*128	*299	*472	*648	*827	**009	**194
6	13,	381	572	766	962	*162	*366	*572	*782	*995	**211
7	15,	431	655	882	*113	*348	*586	*829	**075	**325	**579
8	10 × 1,	784	810	837	864	891	920	948	977	*006	*036
9	10 × 2,	067	098	129	161	194	227	260	294	329	364

This form is such as to leave some doubt as to the precise meaning, although actually it is correct. Expanded, the table would run:

$x$	0	1	2	...
3·6	13·381	13·572	13·766	...
3·7	15·431	15·655	15·882	...
3·8	17·84	18·10	18·37	...
3·9	20·67	20·98	21·29	...

Again the entry  $1^{12}275$  is difficult to interpret as  $1 \cdot 275 \times 10^{12}$  until one finds a general explanation of the notation, in a rather obscure position on p. xii. A reference to it by footnote would be distinctly useful.

The last part of this review, dealing with blemishes on the book, is not to be taken as implying a general condemnation. The faults are mentioned since they are likely to be of use to readers, and as suggestions for a future edition. The book can be recommended for every college library and for the private libraries of all who do much calculation, though users must be on the look-out for possible errors here and there.

J. H. A.

*Comité International des Poids et Mesures, Procès Verbaux des Séances, 2e Série, Tome XVIII. Pp. 310. (Paris: Gauthier-Villars, 1937.)*

This volume contains full reports of the proceedings at the meetings of the International Committee for Weights and Measures, and of its Consultative Committees for Electricity and Photometry, held in June 1937. The first fifty pages contain accounts of the work of the Committee and of the Bureau International for the period September 1935 to May 1937. The report of the Commission des Travaux, pp. 56–63, contains two resolutions, of which the first is a recommendation to the various national laboratories to undertake further studies of sources, in particular cadmium and krypton, of monochromatic radiation suitable for use in the determination of standards of length, and the second is a decision to undertake a recomparison of the international kilogramme with its *témoins*—an operation which has not been carried out since the international standards were originally established in 1889.

We learn on p. 79 that the Committee agreed to set up a new Consultative Committee for Thermometry, with a constitution parallel to those of the Consultative Committees for Electricity and Photometry.

The report of the Consultative Committee for Electricity carries one stage further the proposal to substitute the practical absolute system of electrical units for the existing international system, on and from 1 January 1940. Provisional mean values for the relationships of the present to the new units were adopted, and are as follows:

$$1 \text{ ohm}_{\text{int.}} = 1 \cdot 000 \, 48 \text{ ohm}_{\text{abs.}}$$

$$1 \text{ volt}_{\text{int.}} = 1 \cdot 000 \, 36 \text{ volt}_{\text{abs.}}$$

The report is accompanied by fifteen appendices giving details of work effected and methods employed, at the Bureau International and at various national laboratories, in connexion with electrical units.

The report of the Consultative Committee for Photometry, now constituted independently of the Consultative Committee for Electricity, which formerly dealt with both subjects, contains an important resolution, p. 223, setting up, as from 1 January 1940, a new standard of luminous intensity to be called the "new candle", and defined as such that the brightness of a black-body radiator, at the temperature of solidification of platinum, shall be 60 new candles per square centimetre. The new candle is thus approximately 1 part in 60 smaller than the international candle at present employed in France, Great Britain and America. Further resolutions deal with the question of colour temperature and the intercomparison of standards. This report is accompanied by six appendices.

The volume concludes with obituary notices of four former members of the International Committee: Sir John Cunningham McLennan, Canada; Louis Bodola de Zágon, Hungary; Leonardo Torres y Quevedo, Spain; and Paul Janet, France. J. E. S.



# REPORTS ON PROGRESS IN PHYSICS

VOLUME V (1938)

445 pages: illustrated

20s. post free

Bound in cloth

## A COMPREHENSIVE REVIEW

by leading physicists and under the general editorship of Prof. Allan Ferguson.

THE CONTENTS INCLUDE CHAPTERS ON

ABSOLUTE ELECTRICAL MEASUREMENTS	ATOMIC PHYSICS
PLASTICS IN INDUSTRIAL PHYSICS	SOUND
AIDS FOR DEFECTIVE HEARING	ASTRONOMY
TEACHING OF PHYSICS IN SCHOOLS	METEOROLOGY
X-RAYS AND $\gamma$ -RAYS IN MEDICINE	HEAT
ELECTRIC WAVE FILTERS	OPTICS
THE GEIGER COUNTER	SPECTROSCOPY
QUANTUM MECHANICS	ELASTICITY
THE LIQUID STATE	SURFACE TENSION
SOFT X-RAY SPECTROSCOPY OF THE SOLID STATE	VISSOCISITY

VOLUME IV (1937)

389 pp. 20s. post free

VOLUME III (1936)

390 pp. 20s. post free

“...The present Reports are indispensable in any science library and readers are heavily indebted to the many individual contributors who have had to sacrifice some of their research effort to carry out the arduous task of digesting hundreds of research papers.”

NATURE

“...The Reports are indispensable to physicists, chemists, and metallurgists. I recommend them to students in physics and to their examiners. The price of this well-written, well-printed, and nicely-bound Report is extremely reasonable.”

JOURNAL OF THE INSTITUTE OF METALS

“As we said of Vol. III last year: No physical research laboratory is completely equipped if it lacks this Volume and its precursors.”

INSTRUMENTS

Orders, with remittance, should be sent to

THE PHYSICAL SOCIETY

1 Lowther Gardens, Exhibition Road, London, S.W.7

or to any bookseller

# Moulders to the Trade since 1899

MOULDINGS  
IN BAKELITE,  
BEETLE, RESIN  
"M" and other  
SYNTHETICS

PLASTIC  
MOULDINGS  
in grades to  
resist Water, Acid,  
Heat, Alkali  
and Oil.

Mouldings in Bakelite and other synthetic resins, also in EBONESTOS plastic compositions, as used in the manufacture of electrical and other scientific instruments.

Since 1899 we have supplied many customers whom we are still serving satisfactorily. Such long continued business is the result of two things—the excellent QUALITY of our mouldings and our unfailing DELIVERY SERVICE. The services of our Technical Staff are available for advice on any matters relating to design, etc.

Let us know your requirements. Telephone, and one of our trained representatives will call to discuss with you any questions you may have regarding mouldings of any description or quantity—we can quote special mass-production prices.

**EBONESTOS**  
INDUSTRIES LIMITED

EXCELSIOR WORKS, ROLLINS STREET, LONDON, S.E.15

Telephone: NEW CROSS 1913 (6 lines)

*Moulders to the General Post Office, Admiralty, Air Ministry and other Government Departments*